SEISMOLOGICAL STUDIES OF THE NW HIMALAYA BASED ON EARTHQUAKE DATA RECORDED IN THE GARHWAL HIMALAYA

A THESIS

submitted in fulfilment of the requirements
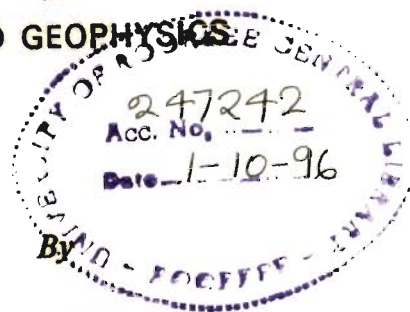*for the award of the degree*
of

DOCTOR OF PHILOSOPHY

in

APPLIED GEOPHYSICS

By

SUSHIL KUMAR

DEPARTMENT OF EARTH SCIENCES
UNIVERSITY OF ROORKEE
ROORKEE-247 667 (INDIA)

AUGUST, 1994

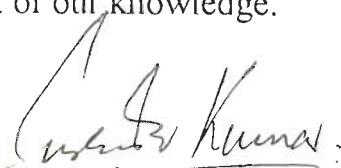Gratis

CANDIDATE'S DECLARATION

I hereby certify that the work, which is being presented in the thesis entitled **"SEISMOLOGICAL STUDIES OF THE NW HIMALAYA BASED ON EARTHQUAKE DATA RECORDED IN THE GARHWAL HIMALAYA"** in fulfillment of the requirements for the award of the Degree of Doctor of Philosophy, submitted in the Department of Earth Sciences, University of Roorkee, is an authentic record of my own work carried out during a period from August, 1986 to August, 1994 under the supervision of **Prof. Ramesh Chander** and **Dr. Surendar Kumar.**

The matter embodied in this thesis has not been submitted by me for the award of any other degree.

Date : August 20, 1994

(SUSHIL KUMAR)

This is to certify that the above statement made by the candidate is correct to the best of our knowledge.

(SURENDAR KUMAR)

Scientist E-II
Wadia Institute of Himalayan Geology
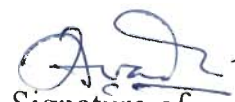33 General Mahadeo Singh Road
Dehra Dun - 248 001, INDIA

(RAMESH CHANDER)

Professor
Department of Earth Sciences
University of Roorkee
Roorkee - 247 667, INDIA

The Ph.D. Viva-voce examination of **Mr. Sushil Kumar**, research Scholar, was held on 16 June 1995

Signature of
Supervisor

Signature of
Supervisor

Signature of
External Examiner

ABSTRACT

This thesis is based on analysis of seismological data recorded with portable seismograph arrays operated during 1984-86 in the Garhwal segment of the northwest Himalaya. The arrays were operated to monitor the local small and micro-earthquakes of the Garhwal region. The first and main part of the thesis is a report on the analysis of these data. The arrays also picked up earthquakes occurring in the Hindu Kush region of Afghanistan about 900 km to the north-west. The second and smaller part of the thesis in an analysis of the travel times of P waves from 22 Hindu Kush earthquakes as recorded in the Garhwal Himalaya during 1985-86 season.

SEISMICITY AND FAULT PLANE SOLUTION STUDIES

In all data from 152 small and micro-earthquakes of the Garhwal Himalaya picked up by the seismograph arrays during 1984-86 have been analysed. The work involved examination of seismograms, picking of phases and their collation to identify earthquakes whose hypocentres could be located from the available readings. Subsequently the locations were also carried out using a program prepared for the purpose in the Department during an early study. The results of these analyses were combined with the previously available results for 193 small and micro-earthquakes recorded during 1979-80 in an adjoining segment of the Garhwal Himalaya. The 345 earthquakes define a relatively narrow belt of earthquake epicentres which straddles the Main Central Thrust in the Garhwal Himalaya. This belt coincides with the belt of moderate and small earthquakes located using teleseismic data. The focal depth of these earthquakes range between 0 and 30 km, though a vast majority of them (85%) occur within the upper 16 km.

Three composite fault plane solutions were determined from reliable first P motion data. The first composite is a strike-slip solution with nodal planes oriented north-south and east-west. The second fault plane solutions is of the reverse/thrust type

with nodal planes striking subparallel to the local strike of the Himalaya. The nodal plane dipping at 60° towards N42° is picked as the fault plane. The third fault plane solution has nodal planes striking north-south and showing normal fault type slip on them. This fault plane solution has affinity with the fault plane solution of the Kinnaur earthquake of January 15, 1975 with a M_s of 6.0.

The reverse/ thrust solution is interpreted as suggesting that the Higher Himalaya are currently rising relative to the Lesser Himalaya across a fault zone defined by the seismicity belt. The strike slip solution is considered to be evidence for lateral horizontal adjustments within the Garhwal Himalaya. The normal fault solution appears to represent concurrent extensional tectonics in the region. But overall, the data support the view that the earthquakes are occurring in response to the under thrusting of the Indian Shield material beneath the Himalayan rocks due to the convergence of Indian and Eurasian plates.

TRAVEL TIME STUDY

The 22 Hindu Kush earthquakes had focal depths in the range of 50 to 245 km. The 154 P travel time readings obtained from them were interpreted using a computer program based on least squared inversion and written specifically for the purpose. The upper mantle P wave speed along the north-west Himalaya obtained from this study has a value of 8.1 km/s. It appear to persists upto a depth of about 100 km. Below that level, it appears to increase to 8.35 km/s. The upper mantle P wave speed is found to be compareable to that obtained along a DSS profile in Kashmir. However it is lower by 0.35 km/s. from the value estimated by Ni and Barazangi in 1982.

ACKNOWLEDGEMENTS

my lovely nephews Mohit, Swati and Shubham for keeping the atmosphere healthy with their sweet laughing and naughty actions which remains helpful in the last days of tension.

I shall be out of my duties if I do not express my thanks to respected Mrs. Chander for her blessings to complete this work.

My thanks are also due to my room sharers Shri Anil Symwal, Shri Nepal Singh, Miss Anupma Rastogi, Miss. Vasundhra and my friends Shri R.S. Jadoun, Dr. R.S. Anand, Shri Subhash Verma, Shri Kailash Rathor, Dr. R.A.Gupta, Shri A.N. Mishra as all of them helped and encouraged me at every moment of the work.

It gives me pleasure to acknowledge with thanks for the exchange of ideas and valuable help, assistance and moral support provided me by Shri Sameer Walia, Shri Abid Hassan, Shri Vineet Gahalaut, Mrs. Kalpna, Shri S.C. Gupta, Dr. (Mrs.) S. Mukhopadhyaya, Shri P.K.S. Chauhan, Shri Satish Sangode, Shri V. Sriram, Dr. M. L. Sharma, Dr. K.N. Khanal, Shri A.K. Bansal, Shri Ravinder Singh and Shri S.K. Chabak.

My special thanks to Shri Bahar Alam who helped me a lot in different stages of computer programming.

My thanks to the staff of Computer Center, University of Roorkee, who helped me during computational work.

Lastly but not the least, I would like to express my sincere thanks to all of them who have helped me directly or indirectly towards the making of this dissertation.

SUSHIL KUMAR

CONTENTS

CONTENTS

LIST OF
FIGURES & TABLES

PART-1

SEISMICITY AND FAULT PLANE SOLUTION STUDIES

1

INTRODUCTION

Earthquakes come and go as they please, leaving behind them trails of destruction and casualties. Although their occurrence is little affected by what we do or think, it is the task of Earth Scientists to keep studying them from all possible angles to accumulate knowledge about the effects of earthquakes, their geographic patterns, the waves emitted by them, and the internal constitution of the earth, until ways and means are found to divert, forecast, and eventually control them.

1.1   GENERAL

The Himalaya (Fig. 1.1) have been a source of irresistible fascination for the people of India since times immemorial. But objective, quantitative information about these mountains has accumulated gradually over the past two centuries. This in turn has inspired further wonder and interest among the lay people and thrown up numerous riddles for scientists and other serious thinkers. The pace of accumulation of knowledge about the Himalaya has accelerated over the past few decades.   This is partly because scientists worldwide in increasing numbers are turning their attention to the Himalaya as an important frontier for earthscience investigations. Moreover, the governments of the countries exercising suzerainty over the Himalaya have been persuaded albeit reluctantly that a thorough understanding of the structure, origin and ongoing geodynamic processes of these mountains is necessary for safe and rapid exploitation of their resources. The present thesis can be regarded as a part of both these enterprises.
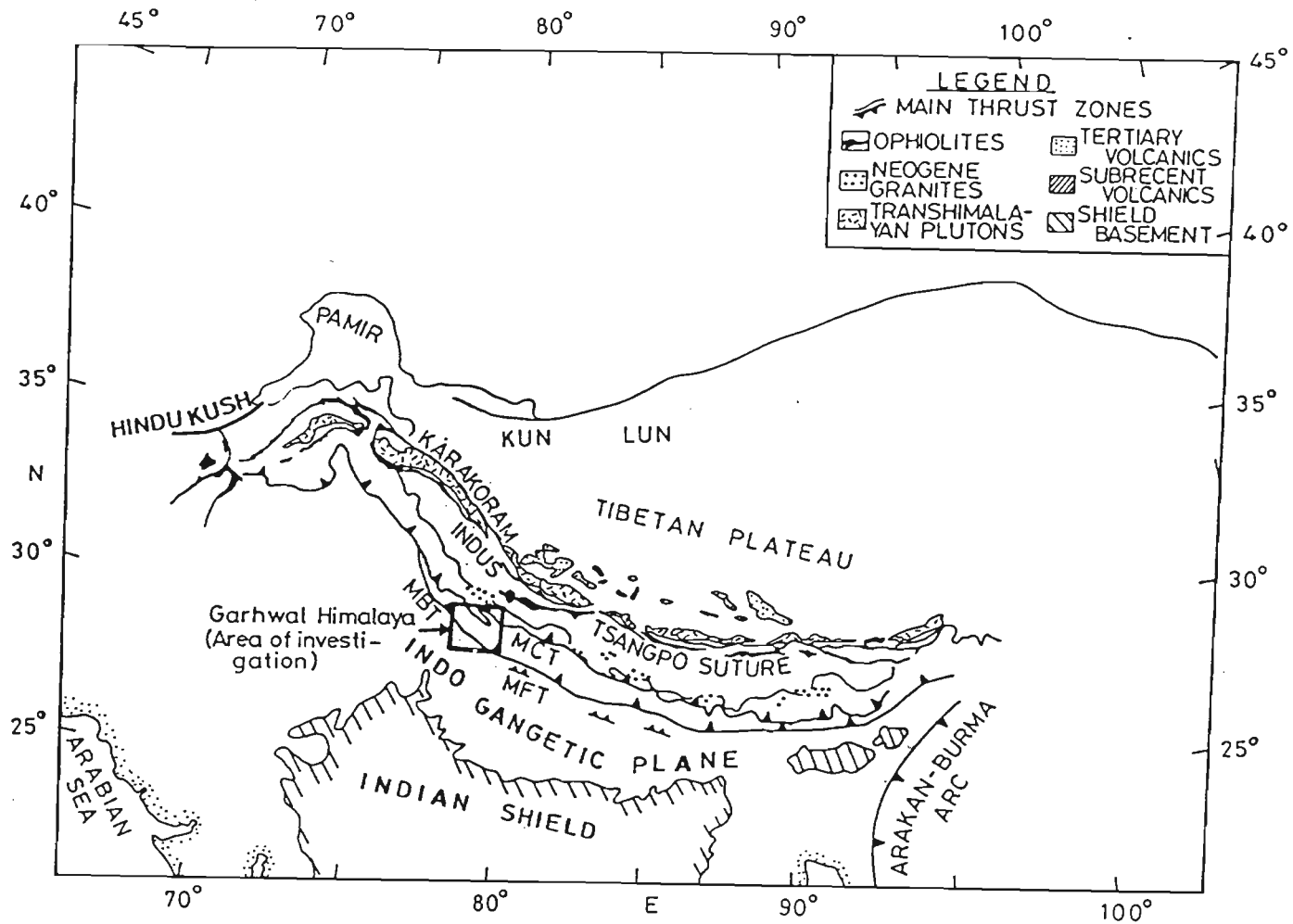
Figure 1·1   Himalayan arc bounded on the north by the Indus-Tsangpo Suture and in the south by the Main Frontal Thrust (MFT). The Himalaya lying west of 80·5°E longitude have been called the NW Himalaya. Main Boundary Thrust (MBT) and Main Central Thrust (MCT) are shown. The Garhwal segment of the NW Himalaya is shown by the rectangle. (After Gansser, 1964)

1.2   TERMINOLOGY

The Himalayan mountain ranges extend over a distance of about 2500 km along a broadly east-west, southwardly convex arc between 74^0 E and 95^0 E longitudes (Fig. 1.1). The segment lying west of the India-Nepal border at about 80.5^0 E longitude (Fig. 1.1) is frequently referred to as the NW Himalaya. The Garhwal segment (Fig. 1.1) stretches within the NW Himalaya for about 200 km from west of 78^0 E longitude to about 79.5^0 E longitude. This segment will be called the Garhwal Himalaya in the sequel.

1.3   STUDY OF SMALL AND MICRO-EARTHQUAKES OF THE GARHWAL HIMALAYA

Drained by the Tons, Yamuna, Bhagirathi and Alaknanda rivers and their tributaries, the Garhwal Himalaya (Fig. 1.2) have vast hydro-electric potential. An ambitious scheme entailing construction of many dams, of which the Tehri dam (Fig. 1.2) is the most important and controversial, has been formulated for hydro-electric power generation, irrigation and flood control. Also a rapidly growing but chronically poor and backward population is awakening and clamouring for rapid development. Earthquakes pose a grave threat to the people and developmental activates of the region.

The Uttarkashi earthquake of October 20, 1991, is only too fresh in the memory of the people of Garhwal. It had a surface wave magnitude (M_s) of 7.0 according to the US Geological Survey. More than 900 people died and 42,000 houses were destroyed. We have no doubt that earthquakes of M_s greater than 8.0 also occur in the region, though some conservative civil engineers engaged in the design of dams deny the possibility. For, in fact, the NW part of the Garwhal Himalaya comprising of Dehra Dun, Tehri and Uttarkashi districts was at the southeastern end of the meizoseismal region of the great Kangra earthquake of 1905 with a magnitude of 8.6 (Richter, 1958) (Fig. 1.3). The remaining, southeastern part of the Garhwal Himalaya is a part of a nearly 700 km long seismic gap between the rupture zones of the 1905 and 1934 earthquakes (Fig. 1.3). The latter earthquake, known popularly as the great Bihar-Nepal earthquake, was assigned
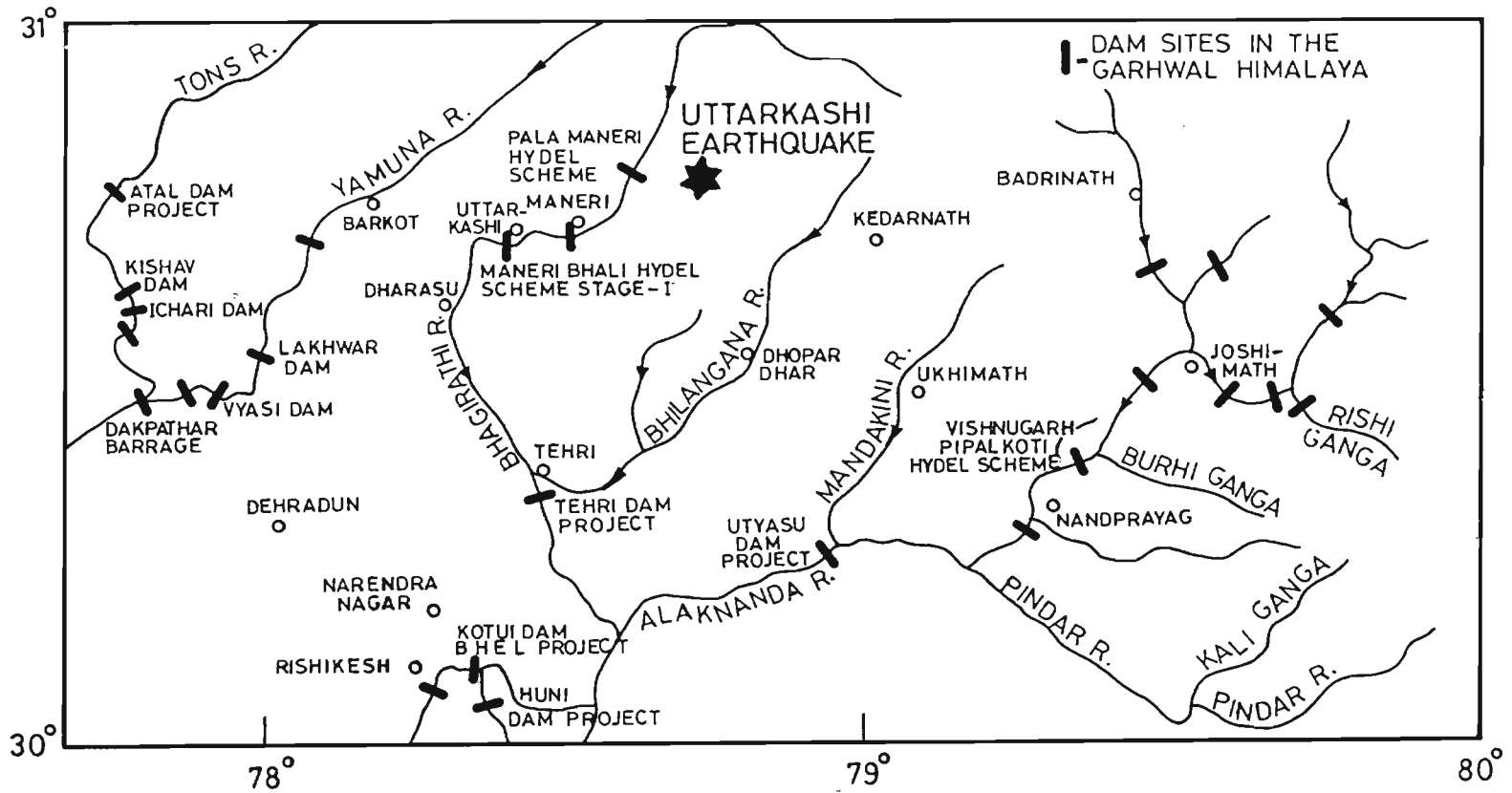
Figure 1·2 Various dams proposed to be setup in the Garhwal Himalaya to exploit the hydroelectric and irrigation potential.

a magnitude of 8.4 (Richter, 1958).

Although seismological investigations of the Garhwal Himalaya began about two decades ago, a motivated and systematic programme of field recording of small and micro-earthquakes of the region using arrays of portable seismographs was begun by the Department of Earth Sciences, University of Roorkee, in 1979 with funds from the Department of Science and Technology, Government of India. We report in this thesis our analyses of local and some regional earthquake data recorded during 1984-86 under that programme. There are two principal parts of this work. In the first part reliable hypocentral locations of 152 small and micro-earthquakes of Garhwal Himalaya are reported here for the first time. The vast majority of the earthquakes occurred between Bhagirathi and Alaknanda valleys (Fig. 1.2). They add to reliable hypocentral locations of 193 small and micro-earthquakes occurring between the Tons and Bhagirathi valleys of the Garhwal Himalaya (Sarkar 1983, Gaur et al 1985) (Fig. 1.2). The results of the two studies are generally similar and spatially complementary. Also first P motion data for many of the newly reported earthquakes contribute to three distinct composite fault plane solutions. A strike-slip type composite fault plane solution had been reported by Sarkar (1983) and Gaur et al (1985). Some of the new first P motion data are consistent with this fault plane solution. But most of the new data yield a reverse/thrust fault type and a normal fault type composite solutions. The implications of these solutions are examined here.

1.4 UPPER MANTLE P WAVE SPEED MODEL FOR THE NW HIMALAYA

In addition to local earthquakes many regional earthquakes, especially from the Hindu Kush mountains (Fig. 1.1) of Afghanistan, were also picked up by the instruments of the above arrays. We report in the second part of the thesis observations of P travel time data and their analyses for upper mantle structure under the NW Himalaya lying between the earthquake sources in the Hindu Kush at around 72° E and 36° N approximately and the recording stations in the Garhwal Himalaya. This study is pure

5
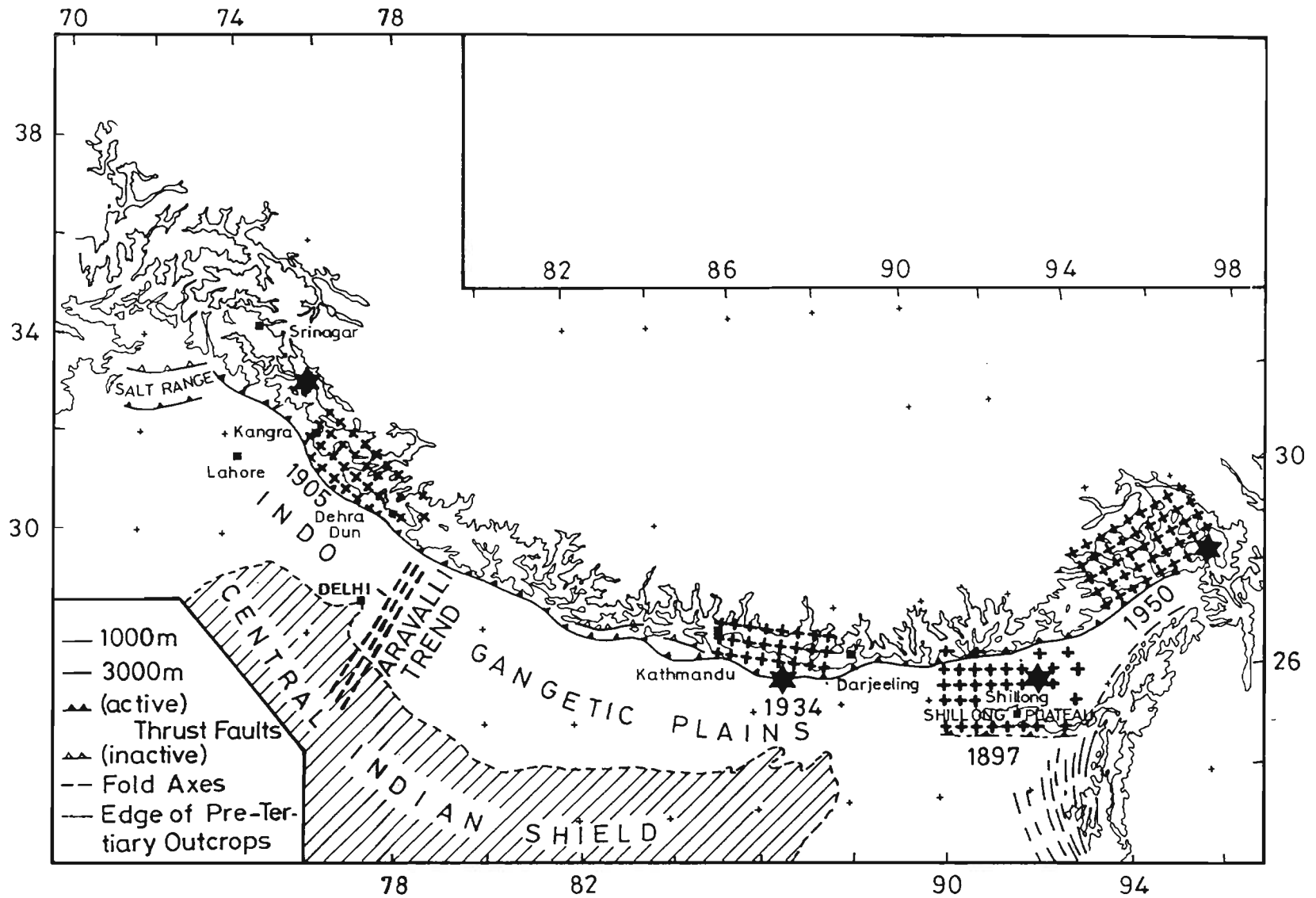
Figure 1·3   The Himalayan arc along with the inferred rupture zones (shown by crosses) for the four great earthquakes of the last 100 years. Aravalli trend marks the position of Precambrian Aravalli mountains of Rajasthan. (After Molnar and Pandey, 1989)

bonus in the sense that the data were recorded automatically through instruments set up for a different purpose.

The two studies, namely, investigations of small and micro-earthquakes of the Garhwal Himalaya and the travel time study, together constitute the seismological investigations of the NW Himalaya mentioned in the title of the thesis.

2

ON THE EARTHQUAKES OF THE GARHWAL HIMALAYA

2.1 GEOLOGICAL SETTING

The earthquakes of the Garhwal Himalaya cannot be discussed comprehensively without a brief reference to the geologic and tectonic setting of the region. Thus, as in other segments of the Himalaya, the Garhwal Himalaya too may be subdivided into four broad units, which, proceeding northwards from the Indo-Gangetic plains, are the Outer, Lesser, Higher and Tethys Himalaya (Fig. 2.1). The boundary between the sediments of the Indo-Gangetic plains and the Outer Himalaya is marked by the Main Frontal Thrust (MFT) and that between Outer and Lesser Himalaya by the Main Boundary Thrust (MBT). The boundary between the Lesser and Higher Himalaya is marked by the Main Central Thrust (MCT). The precise nature of the contact between the Higher and Tethys Himalaya is a matter of debate (Gansser, 1964 and Valdiya, 1980). The views range between unfaulted contact and a low angle normal fault type contact. The boundary between the Tethys Himalaya and Trans Himalaya is marked by the Indus-Tsangpo Suture Zone (ITSZ).

Besides the above bounding intra-crustal faults, a large number of lesser thrusts are mapped in the Garhwal (Fig. 2.1) as well as in the other parts of the Himalaya. The dips of these thrusts are northerly in overwhelming number of cases, but thrusts dipping

8
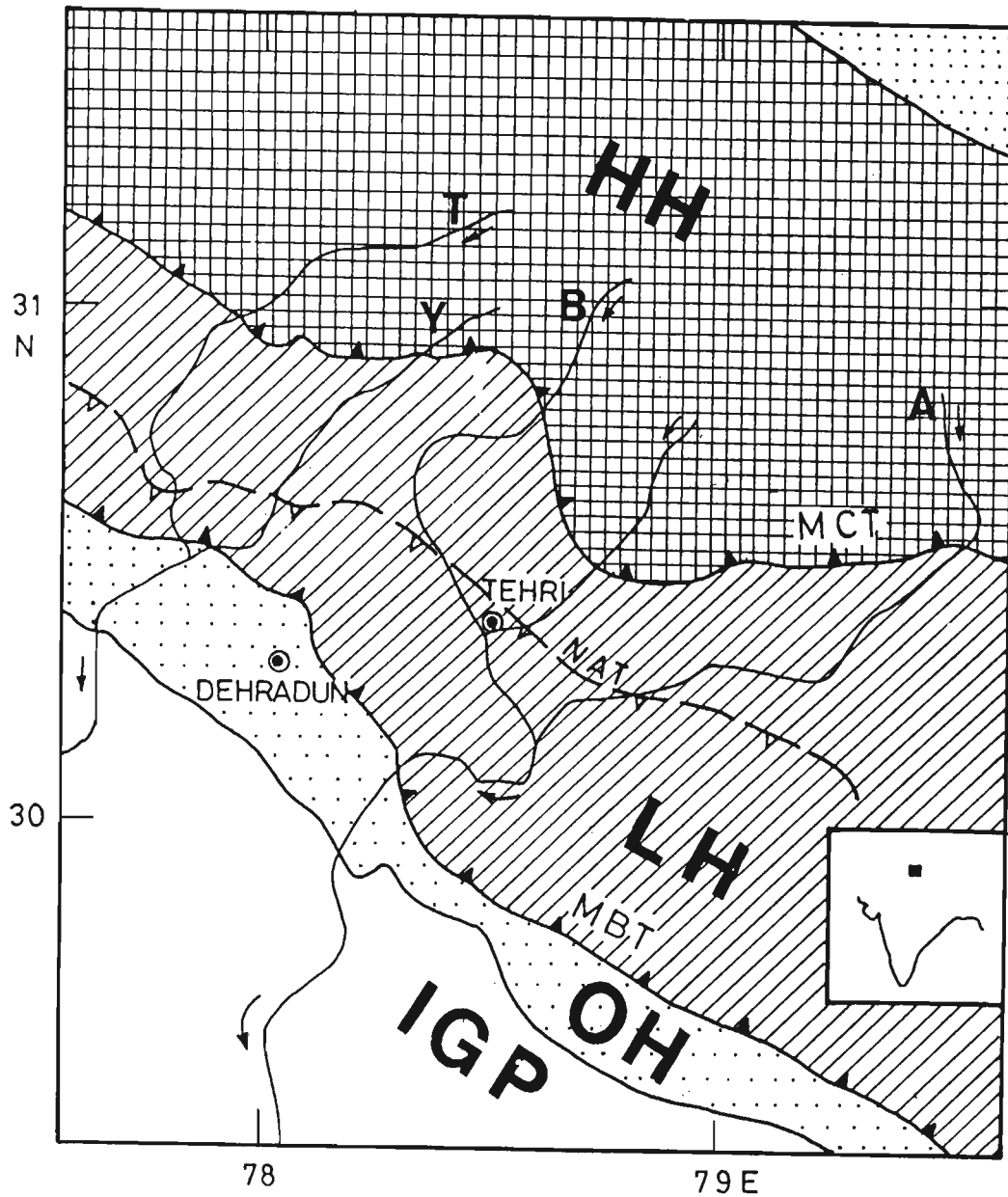
Figure 2·1 Broad scale geology of the Garhwal Himalaya.
HH, LH and OH represent the Higher, Lesser
and Outer Himalaya. T, Y, B and A represent Tons,
Yamuna, Bhagirathi and Alaknanda rivers. (Partly
after Gansser, 1964). NAT: North Almora Thrust.

southward, at least at the surface, are not unknown (Fig. 2.1). It is commonly held that the thrusts are listric and flatten at depth.

In the geologically complex environment of the Himalaya, the possibility of normal and strike-slip faults should not be ruled out also. But the evidence for these is accumulating slowly. The possibility of normal fault contact between the Higher and Tethys Himalayan rocks has been mentioned. Evidence for extensional tectonics south of the Higher Himalaya is being mooted (Jain, personal communication, 1994).

However the evidence for strike-slip faults in the Himalaya is relatively more abundant. Valdiya (1976) has documented strike-slip faults transverse to the general trend of the Himalaya. Jain (1987), from a study of lineaments of the Garhwal Himalaya, has identified several sets of dextral and sinistral strike-slip features of varying importance and linear extent.

The Outer Himalaya are composed mainly of Miocene and younger sedimentary rocks which are folded and faulted. The Lesser Himalaya are composed of Paleozoic and older metasedimentary rocks which are mainly unfossiliferous. These rocks are tightly folded and thrusted. The Higher Himalaya are composed of high grade metamorphic rocks which have been intruded by granitic bodies. The Tethys Himalayan rocks are mostly of marine origin and they are abundantly fossiliferous.

2.2   THE SEISMOLOGICAL SCENE IN THE GARHWAL HIMALAYA IN 1979

At the time of the initiation of above mentioned recordings of small and micro-earthquakes in the Garhwal Himalaya, the knowledge about earthquakes of the region was very limited indeed. It was acknowledged of course that, as in other parts of the Himalaya, earthquakes occur in this region also. But a commonly held view was that seismicity occurs mainly along the MBT.

Historical records of past great earthquakes of the region are virtually non-existent. Early British explorers tried to compile lists of earthquakes from local enquiries. But, in

our opinion, little credence can be given to such lists. The first specific and documented case of a great earthquake of the region is that of the 1905 Kangra earthquake, to which a magnitude of 8.6 (Richter, 1958) has been assigned. It was investigated by Middlemiss (1910) who drew an isoseismal map (Fig. 2.2) in which the Rossi-Forel (RF) VII isoseismal marking the limit of perceptible damage was elongated along the trend of the NW Himalaya and included substantial areas of the Himachal and Garhwal Himalaya. Middlemiss drew two separate RF VIII isoseismals, one around Kangra in the Himachal Himalaya and the other around Dehra Dun in the Garhwal Himalaya (Fig. 2.2). Intensities of RF IX and X were observed around Kangra only. An active role of the MBT in the occurrence of this earthquake was envisaged by many earth scientists (e.g. Middlemiss, 1910).

In 1979, teleseismically recorded moderate earthquakes were being located by US Geological Survey and the International Seismological Center. But, due to a lack of close in seismograph stations, the depth control was very poor. Still the view advocated, for example, by Richter (1958) that intermediate focal depth earthquakes occur only in the Hindu Kush and the Burmese mountains and not in the Himalaya was prevalent.

Fitch's (1971) study of a few fault plane solutions of moderate Himalayan earthquakes, none of which was from the Garhwal Himalaya, suggested that, in accord with the plate tectonics view, such earthquakes may occur on low angle thrust faults dipping under the Himalaya.

The Kinnaur earthquake of 1975 had occurred in the Sutlej valley (Fig. 1.3). Although it does not belong to the Garhwal Himalaya strictly, it deserves mention because of several reasons. Firstly, it occurred reasonably close to the region of interest. Secondly, it had a magnitude (M_s) of 7.0, was well located, and was followed by numerous aftershocks. Thirdly, a normal-fault type individual fault plane solution has been determined. There appears to be considerable similarity between this fault plane solution and our normal fault type composite solution.

11
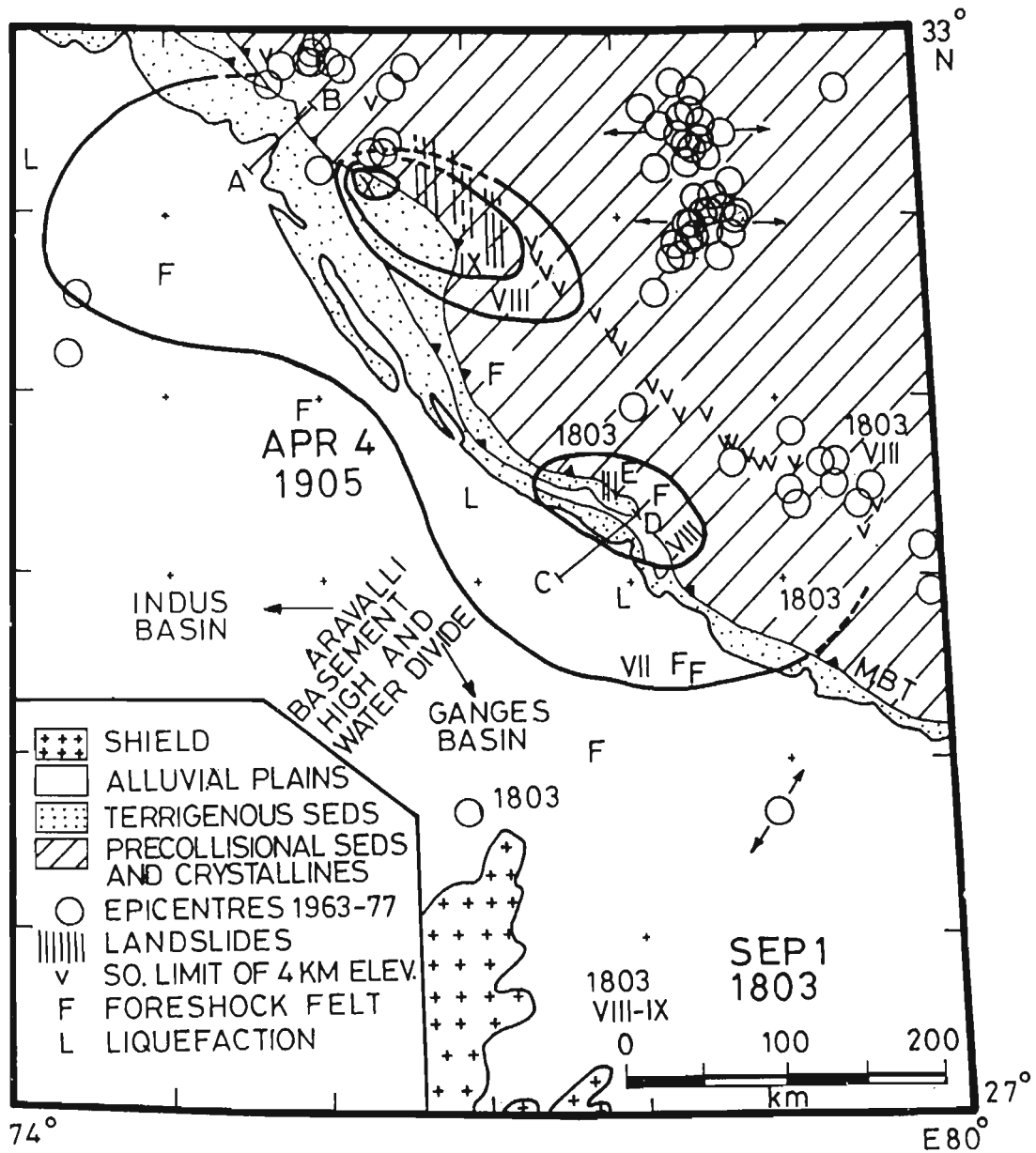
Figure 2·2   Isoseismals of the Kangra earthquake of 1905.
Background information according to Seeber
and Armbruster (1981).

There was no reliable information about small and micro- earthquakes of the Garhwal Himalaya in 1979 although four observatory type instruments had been set up in the region by the India Meteorological Department (Srivastava et al, 1986).

2.3 CURRENT SEISMOLOGICAL SCENE IN THE GARHWAL HIMALAYA

Although the data from the Garhwal Himalaya analysed and reported here were collected in the period 1984-86, we summarize here the evidence about the Garhwal earthquakes at the time of present writing. Only the evidence obtained by us is left out for detailed discussion in the following chapters.

2.3.1 A model for Himalayan seismicity

One of the more important event of the past fifteen years in connection with our understanding of Himalayan seismicity has been the proposal of a tectonic model (Fig. 2.3) by Seeber and Armbruster, (1981). It is envisioned in this model that Indian Shield rocks underthrust rocks of the Outer, Lesser, and Higher Himalaya along a detachment surface or simply detachment. The Shield rocks also underlie the sediments and sedimentary rocks of the Indo-Gangetic Plains but the two are coupled, i.e., there is no relative motion between them (Fig. 2.3). However, relative slip occurs above and below the detachment episodically and/or continuously in different dipwise sections. The detachment has a gentle dip under Outer and Lesser Himalaya, a ramp-like steeper dip under the MCT and a gentle dip again to the north (Seeber and Armbruster 1981) (Fig. 2.3).

Seeber and Armbruster (1981) postulated that great earthquakes occur by thrust type slip along the detachment under the Outer and Lesser Himalaya (Fig. 2.3). They also argued from the extended sizes of areas of perceptible damage during the four great earthquakes of the past hundred years along the Himalayan seismic belt that these earthquakes had comparably large extents of ruptures within the detachment (Fig. 1.3). Thus, for the above mentioned Kangra earthquake of 1905, they estimated the size of
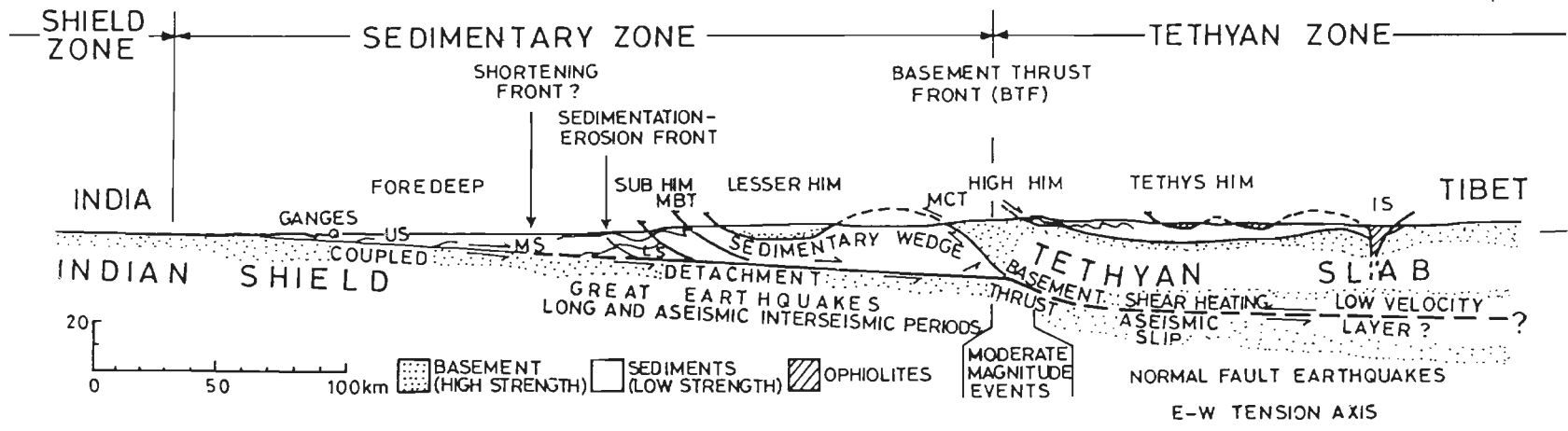
Figure 2·3   The plate tectonic model for the Himalaya proposed by Seeber and Armbruster (1981).

the rupture zone, i.e., the surface projection of the buried causative rupture in the detachment, to be approximately 300×100 km^2. The longer dimension is along the local strike of the Himalaya.

Seeber and Armbruster (1981) also suggested in their tectonic model that moderate magnitude Himalayan earthquakes occur along the ramp in the detachment that coincides with the MCT in the map view (Fig. 2.3). Proceeding northward in the Himalaya, there is a noticeable increase in average slope of the topography across this boundary (Fig. 2.3).

Thus Seeber and Armbruster (1981) ascribed great and moderate earthquakes of the Himalaya to thrusting motion along the detachment whereby the Indian Shield and hence the Indian lithospheric plate slips under the Himalaya.

2.3.2. Studies of the 1905 Kangra earthquake

2.3.2.1 General

Ever since the publication of Middlemiss's (1910) report on the 1905 Kangra earthquake, a controversy has raged as to whether it was one earthquake or two. This stems partly from the fact that Middlemiss identified two separate areas of high intensity about 100 km apart (Fig. 2.2). Also, estimates of the time of occurrence of this earthquake as reported to Middlemiss would suggest that the earthquake occurred simultaneously at Kangra and Dehra Dun as well as at intermediate places such as Simla.

Richter (1958) has discounted the two earthquake theory and suggested that confusion about the nearly same time of occurrence reported from widely separated localities is due to poor standard of time keeping prevailing in India at the time.

Molnar (1987) has re-examined the intensity reports cited by Middlemiss and argued that perhaps the two RF intensity VIII isoseismals could in fact have been connected in a single albeit highly elongated contour. It is to be mentioned however that this is not a feature of this Himalayan earthquake alone. Dunn et al (1939) identified three widely separated regions where intensity reached Mercalli IX and X levels during the

1934 Bihar-Nepal earthquake.

Molnar (1987) agreed with Seeber and Armbruster (1981) that the earthquake occurred by extended rupture in a low angle thrust fault. But rather than identifying this fault as the detachment, Molnar considered that the earthquake occurred on deeper, flatter section of a listric MBT.

Moreover, Molnar (1987) proposed three possible models about the length of the rupture zone of this earthquake. Thus, firstly, he suggested that there could have been a single rupture zone extending from the vicinity of Kangra to the vicinity of Dehra Dun. Secondly, he surmised that there could have been two separate rupture zones, namely, between Kangra and Mandi (Fig. 2.3) in the northwest and around Dehra Dun in the southeast. Thirdly, he speculated that there might have been just a single rupture zone between Kangra and Mandi.

2.3.2.2 Geodetic levelling observations

In the annals of geodetic observations in India, the Kangra earthquake is the only one for which pre- and post-seismic geodetic observations are available and have a modicum of reasonableness about the number of stations, their location relative to region of interest, and the magnitude of the effects observed at those stations.

Thus, near the southeastern edge of the meizoseismal area of this earthquake, a set of levelling bench marks had been set up in 1861-62 (Middlemiss, 1910) from Saharanpur in the Indo-Gangetic plains via Dehra Dun in the Outer Himalaya up to Mussoorie in the Lesser Himalaya (Fig. 2.4). The total length of the line in a projection along the NE-SW direction, sub-normal to the local trend of the Himalaya, was about 80 km. The line was partly re-surveyed in 1903-04 between Dehra Dun and Mussoorie. Then the Kangra earthquake occurred in 1905. The entire line from Saharanpur to Mussoorie was relevelled in 1905-07. Assuming that the reference bench mark at Saharanpur had not been affected by the earthquake, it was observed that heights of most other bench
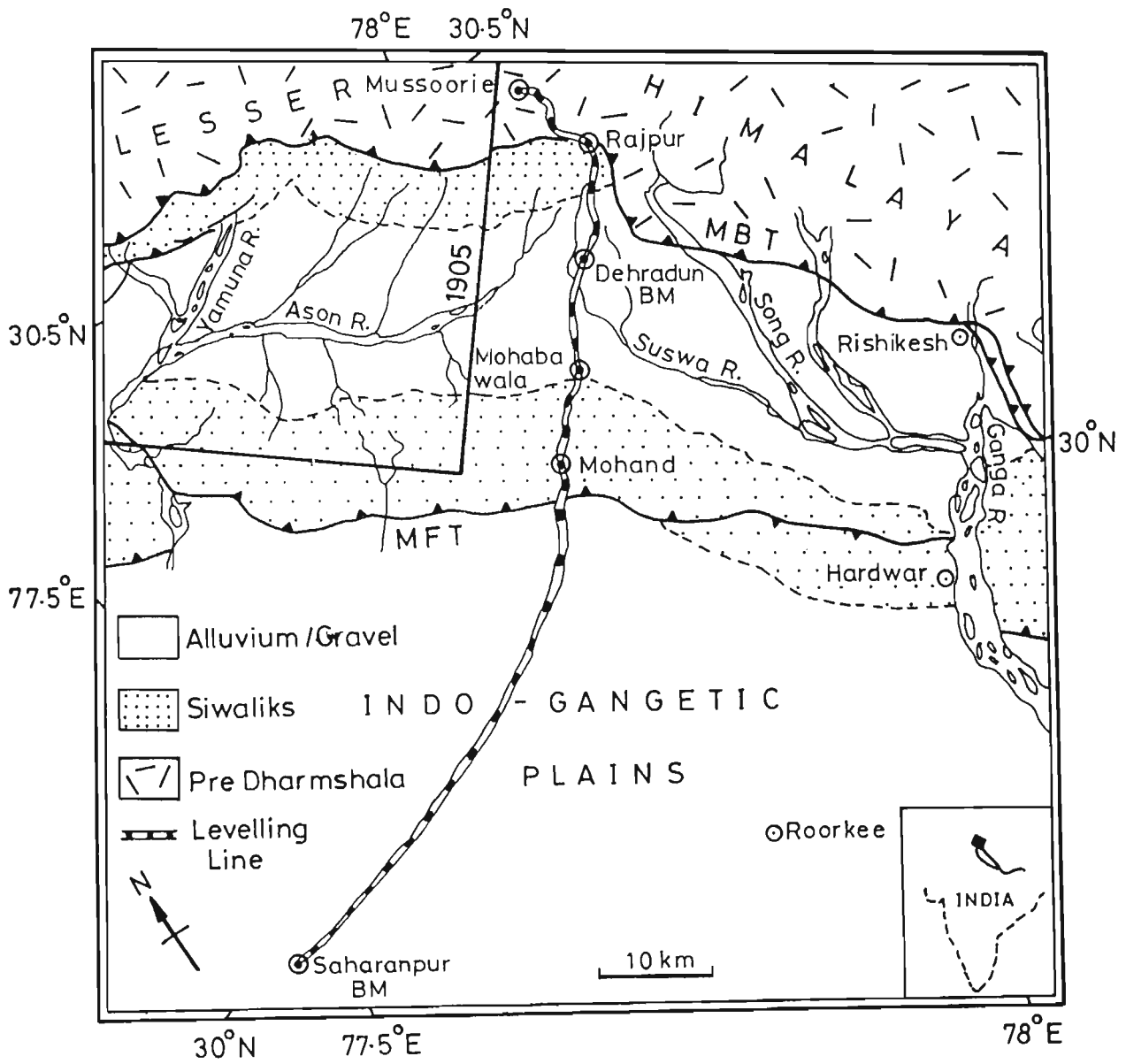
Figure 2·4 Route of the levelling line between Saharanpur and Mussoorie. (After Rajal et al 1986 and Ghalaut and Chander, 1992).

17

marks had increased by varying amounts upto 14 cm.

Middlemiss (1910) commented upon the difficulties of observations and the precautions taken in observations along the mostly hilly course. But he ascribed the observed elevation changes to Kangra earthquake without making an effort to interpret them further. The view was repeated by Seeber and Armbruster (1981) and Rajal et al (1986).

Chander (1988), Gahalaut and Chander (1992) and Yeats and Lillie (1991) interpreted the elevation changes using formulas of elastic dislocation theory that predict permanent displacements of medium particles in response to a dislocation source. They thus obtained various non-unique models of the causative fault, the causative rupture within it, as well as the amount of slip on the fault during the earthquake. Chander (1988) simulated the causative fault as a planer thrust dipping under the Himalaya. Gahalaut and Chander (1992) considered listric thrust models. The total extent of rupture zone considered by these investigators was 280 x 80 km^2 .

Thus it transpires that the observations of coseismic elevation changes during the Kangra earthquake are consistent with the plate-tectonics based model of Seeber and Armbruster (1981), namely, that great Himalayan earthquakes occur along the detachment at a relatively shallow depth. In the models of Chander (1988) and Gahalaut and Chander (1992), the maximum depth of the detachment considered was 17 km under the surface trace of the MCT in the Garhwal Himalaya. The magnitude of thrust type slip was estimated to be 3 to 5 m.

Chander (1988) argued from the levelling observation that the MBT was not involved in the occurrence of the Kangra earthquake atleast in the Dehra Dun region.

Yeats and Lillie (1991) regarded the Kangra earthquake as a large fold related earthquake. Gahalaut and Chander (1992) argued that the elevation change observations are consistent with models in which the causative fault does or does not outcrop near the local southwestern limit of the Himálaya. Still the weight of evidence is in favour of a buried
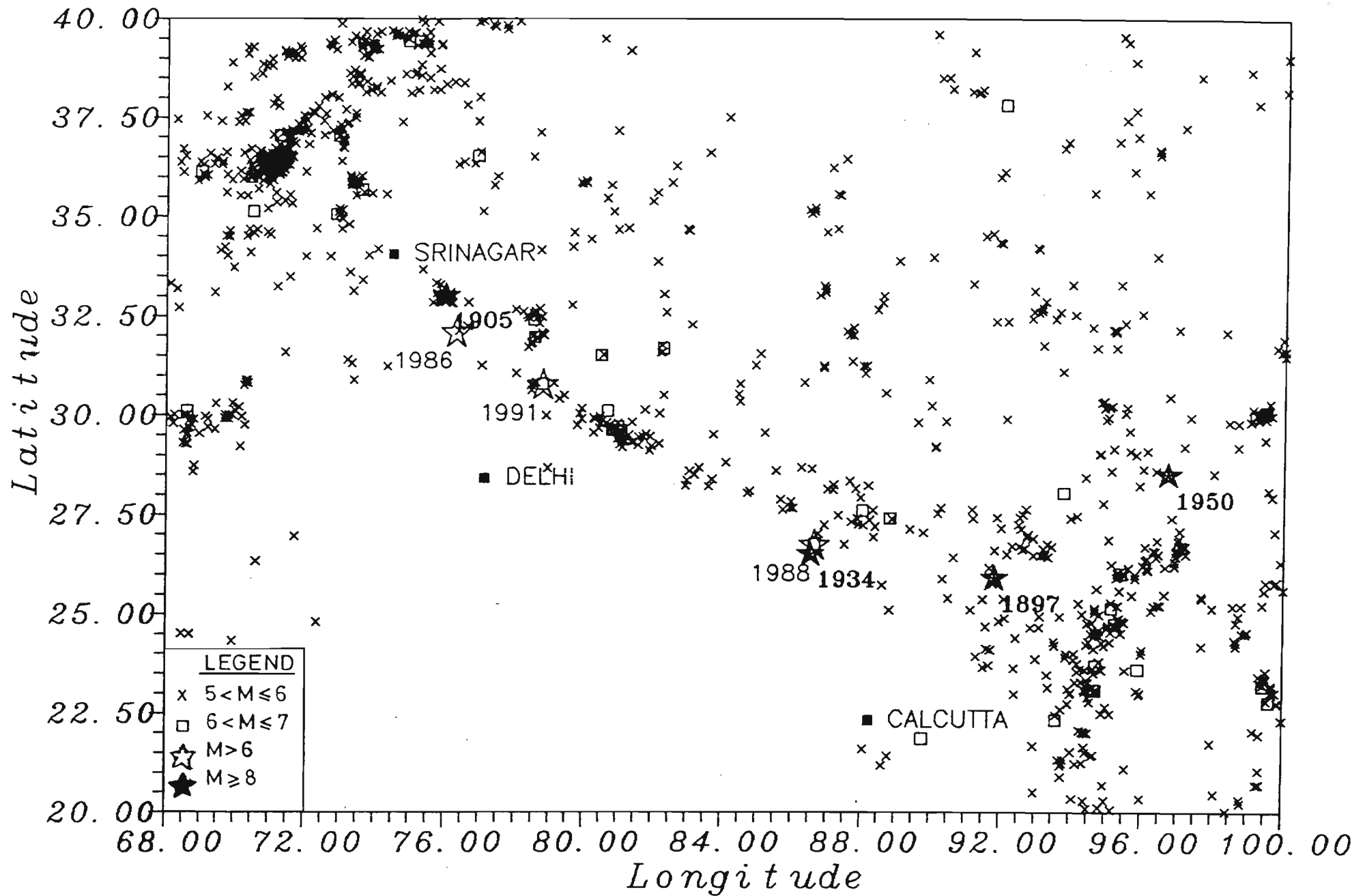
Figure 2·5 Epicentres of recent earthquakes along the Himalaya and Tibet.

rupture.

2.3.2.3 Epicentre

An intriguing situation exists regarding the epicentral location of the Kangra earthquake. Gutenberg and Richter (1952) have estimated the epicentre in southeastern Kashmir about 100 km outside the meizoseismal area and the rupture zone estimated by Chander (1988) and Gahalaut and Chander (1992) (Fig. 1.3). Two possibilities exist. Firstly, the epicentre is well located and the estimates of the extent of the rupture zone should be enlarged. Secondly, the epicentre is mislocated. Although the question is unresolved, Chander (1988) has suggested that, if the epicentre is assumed in the Garhwal Himalaya, northeast of Dehra Dun, then the high intensities around Kangra could be ascribed partly to rupture propagation in the northwestward direction.

2.3.2.4 Interseismic elevation changes in the Outer and Southern Lesser Himalaya

Although the topic is not related to earthquakes directly, yet it is not too far removed also. Repeat levelling of the above mentioned bench marks between Saharanpur and Mussoorie in 1925-26 and 1974-76 (Rajal et al 1986) show that the Outer and southern Lesser Himalaya experienced uplift even in the period since the Kangra earthquake. This indicates that aseismic strain release and slip are also occurring on the detachment.

2.3.3 Moderate earthquakes of the Garhwal Himalaya

2.3.3.1 Epicentres

It is worthwhile to begin by recalling that Seeber and Armbruster (1981) regarded the moderate earthquake epicentres in the Himalaya (Fig. 2.5) to be spatially related to the topographic break between the Lesser and Higher Himalaya (Fig. 2.3). They suggested that the hypocentres lie on a ramp in the detachment partly downdip of the MCT The teleseismically located epicentres of moderate Himalayan earthquakes were examined further by Ni and Barazangi (1984). They inferred that the epicentral belt is about
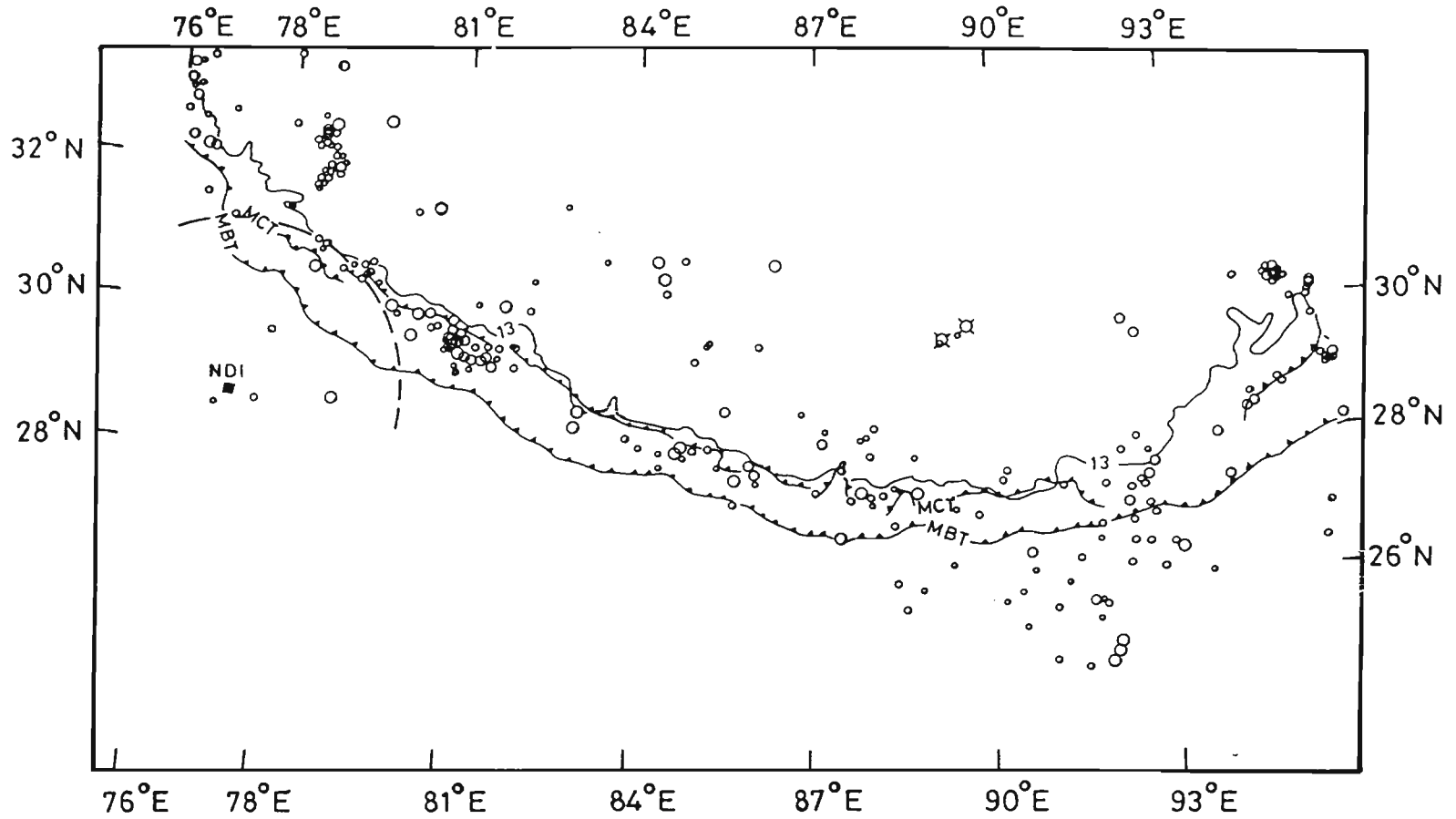
Figure 2·6 Relationship of epicentres of moderate Himalayan earthquakes and the Main Central Thrust (MCT) in the Himalaya (After Ni and Barazangi,1984).

50 km wide and lies between the MCT and MBT but closer to the former rather than the latter (Fig. 2.6).

Fig. 2.7 is display of the moderate earthquake epicentres of the Garhwal Himalaya as located by the US Geological Survey. The belt is seen to lie astride the MCT. We have to point out that there is some controversy in the geological literature regarding the precise geographic location of the MCT. The modern trend is to consider several faults as MCT and differentiate them as MCT1, MCT2, etc. But we follow Gansser (1964) for specificness as his book is internationally accessible.

Accuracy of epicentral locations :

With passage of time, there has been a progressive decrease in the magnitudes of standard errors of epicentral longitudes and latitudes of moderate Himalayan earthquakes. Today errors of ± 1 to ± 2 km are reported routinely. But the following case history is notable. The moderate earthquake of December 28, 1979, was picked up by teleseismic stations as well as a local seismograph array set up by our Department (see below). The estimates of epicentral location from the two sets of observations are approximately 23 km apart (Sarkar et al 1987). The locally estimated epicentre fell within the recording array and is more credible in our opinion.

2.3.3.2 Focal depths

Focal depth estimates for moderate Himalayan earthquakes based exclusively on teleseismically recorded data have been a cause of concern for decades. USGS has routinely reported "normal" focal depths of 33 km until about 1990. Subsequently availability of depth phase readings appears to have become relatively more abundant and shallower focal depth estimates have started to appear more frequently. But, "normal" focal depths are still not a thing of the past. International Seismological Centre (ISC) bulletins have reported focal depth estimates for moderate earthquakes of Garhwal
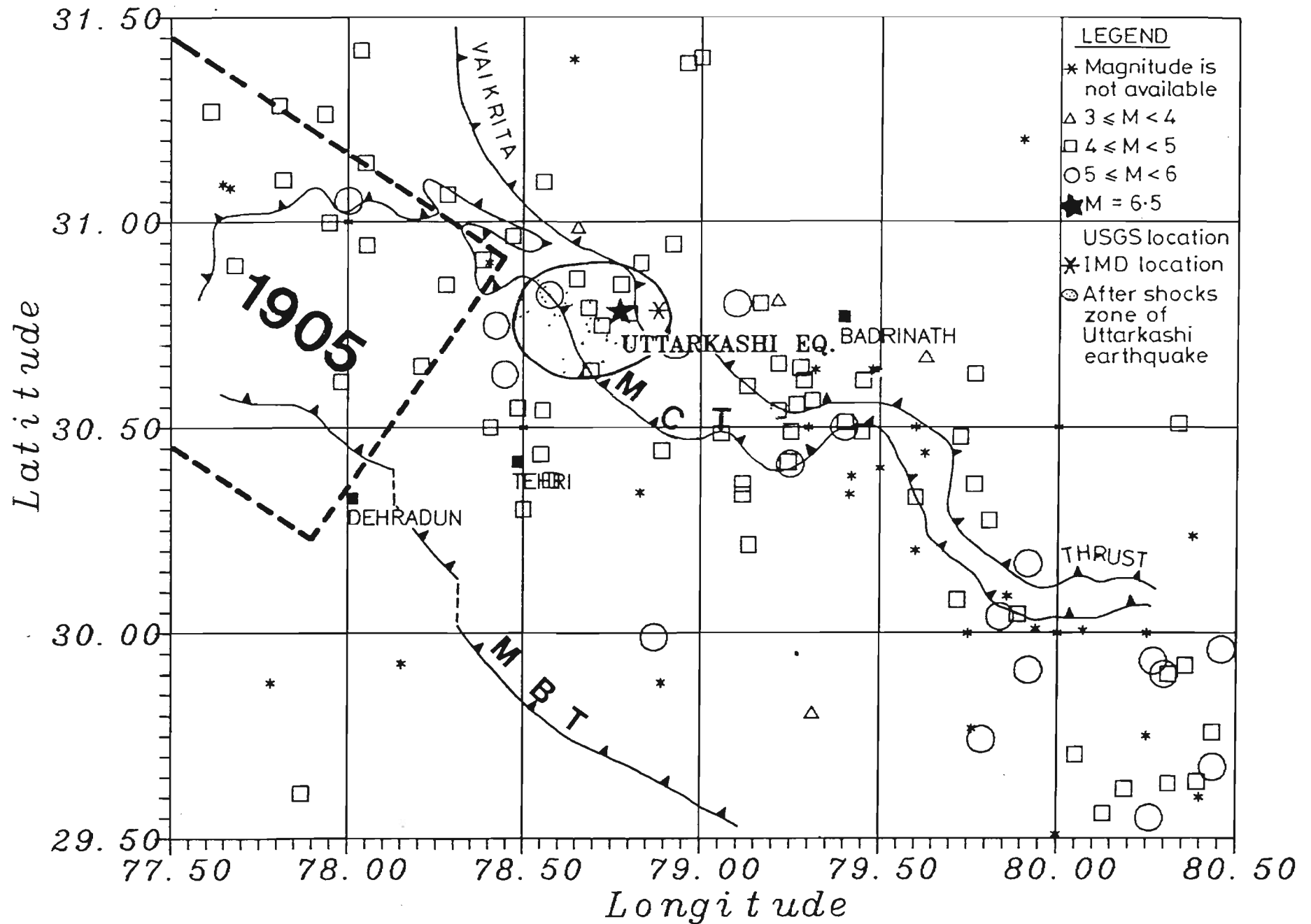
Figure 2·7   Epicentres of important earthquakes of the Garhwal Himalaya.
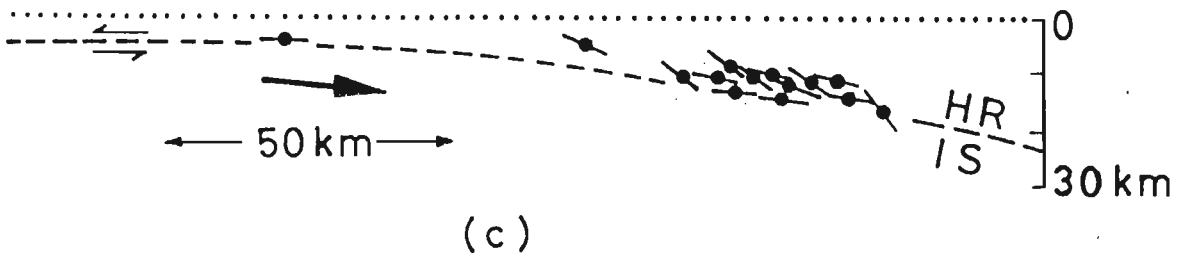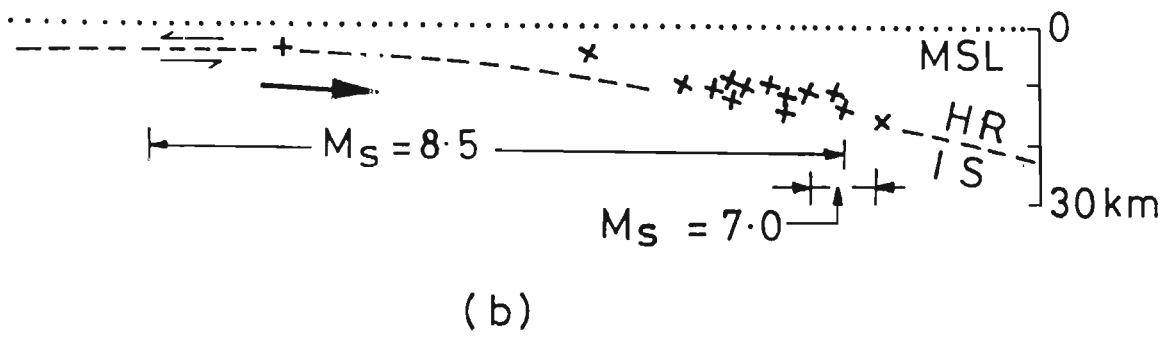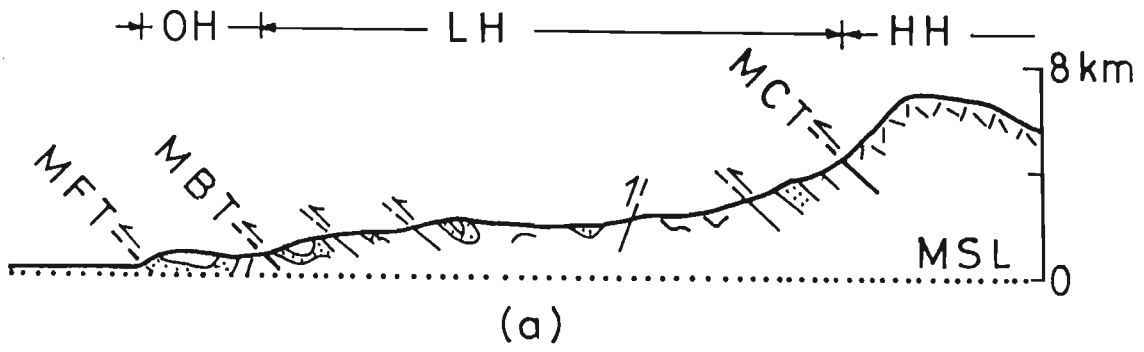
Figure 2·8   Hypocentres and fault plane solution information
for moderate Himalayan earthquakes.(After Ni and
Barazangi, 1984).

Himalaya in the range of 3 to 100 km.

Ni and Barazangi (1984) compiled a list of moderate Himalayan earthquakes for which focal depth estimates based on depth phases and/or wave form synthesis were available. These estimates range between 10 and 20 km consistently. Ni and Barazangi plotted projected locations of these hypocentres on a single plane normal to the trend of the Himalaya, taking the arcuate shape of the mountains into due account (Fig. 2.8). It transpires that the plotted hypocentres define a vertically narrow zone and make it plausible that they define the detachment under the Lesser Himalaya (See below).

Relatively more precise focal depth estimates are available for four moderate earthquakes of the Garhwal Himalaya. Thus, for the moderate earthquake of December 28, 1979, mentioned in the preceding subsection, local array data yielded an estimate of 15 km, compared to the "normal" focal depth of the US Geological Survey. Molnar and Lyon-Caen (1989) report a focal depth estimate of 13 km for the moderate earthquake of 16 June, 1986, based on waveform syntheses. Finally USGS has reported focal depths of 18 and 10 km based on depth phases, for the earthquakes of December 18, 1990 and October 19, 1991 (See below). The sample is too limited. But if it is reflective of a general trend, then moderate earthquakes occur in the Garhwal Himalaya at slightly shallower depths than elsewhere in the Himalaya.

2.3.3.3 Fault Plane Solutions

Molnar (1990) compiled a list of 16 moderate Himalayan earthquakes for which fault plane solutions are available based on waveform syntheses (Fig. 2.9). In every solution, one nodal plane strikes sub-parallel to the local trend of the Himalaya and dips gently under the Himalaya. The other nodal plane also has a similar strike generally but it dips toward the adjoining plains at a steep angle. Motion is reverse slip on each nodal plane, strike slip component being negligible in most cases. The only exception is a strike-slip solution in the Sikkim Himalaya (Ni and Barazangi 1984) (Fig. 2.9) but it does not

25
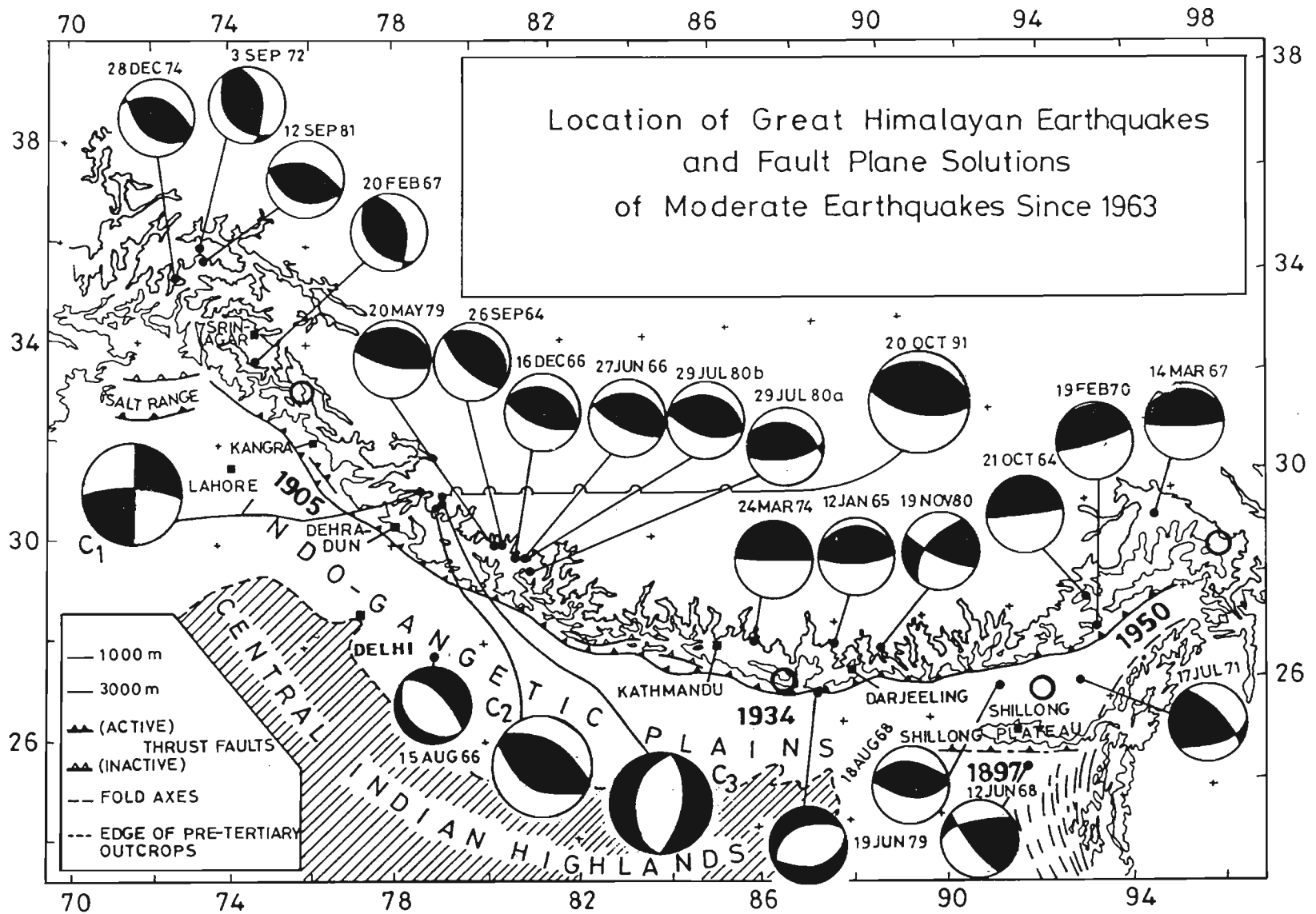
Figure 2·9 Locations of great Himalayan earthquakes and fault plane solution of moderate earthquakes. Lower hemisphere projections of the focal spheres, with blackened quadrants showing those with compressional first motions, were taken from Molnar et al (1977), Baranowski et al (1984), and Ni and Barazangi (1984). Bigger beach balls represents composite fault plane solutions (C) obtained by us in this study. Circles show epicentral locations of Great Himalayan earthquakes.

concern us here.

If the gently dipping nodal planes of the solutions are regarded as the corresponding fault planes, then the concept is reinforced that an active thrust type detachment exists under the Himalaya at least in the region of the epicentral belt of moderate earthquakes.

So far only one fault plane solution for a moderate earthquake of the Garhwal Himalaya is based on waveform synthesis. It is the earthquake of 16 June 1986 mentioned already.

2.3.3.4 Summary

When these results about moderate earthquakes are combined with those previously quoted for the Kangra earthquake then the picture emerges that detachment under the Lesser Himalaya but close to the MCT is active quite frequently due to moderate earthquakes. But under the Outer and southern Lesser Himalaya it is active also and releases strain episodically in great earthquakes. During intervals between great earthquakes some slip occurs on the detachment aseismically.

2.3.4 Small and micro-earthquakes of the Garhwal Himalaya : *Previous work*

This is a major theme of the present work also. But we summarize here the results of a previous study based on recordings carried out in 1979-80 in the Garhwal region (Gupta 1980, Sarkar 1983, Gaur et al 1985).

2.3.4.1 Activity along the MBT

The survey using portable seismographs was begun by installing an array astride the MBT in southeastern Garhwal Himalaya. It was apparent within a few weeks that no earthquakes were originating along the surface trace of the MBT (Gupta 1980). But many earthquakes were occurring 30 to 40 km to the north, though they could not be well located due to the short aperture of the array. This was significant evidence about

the current tectonic status of the MBT. It gains importance in light of above evidence on the MBT through analyses of elevation changes due to the Kangra earthquake. However, geologists frequently cite evidence of neotectonic activity along the MBT even within the Garhwal Himalaya. Thus the current tectonic status of the MBT bears further scrutiny through paleoseismic studies along the MBT as well as through seismicity observations using short arrays of sensitive seismographs.

2.3.4.2 Activity around the MCT

In the next phase of field recording a relatively large array with maximum dimension of about 100 km was operated in the Garhwal Lesser Himalaya (station shown by squares in Fig. 2.10). It was observed that a moderate intense source of small and micro-earthquakes existed a short distance to the northwest of the stations (Dunda and Bhatwari) in the Bhagirathi valley (Fig. 2.10). Hence the array configuration was readjusted in an attempt to encircle this source region with available seismographs. An array of maximum dimensions of 45 km was operated between December 1979 and June 1980 (Fig.2.10). The analyses of these data have been reported by Sarkar (1983) and Gaur et al (1985).

Epicentres:

It was clear that earthquakes occurring within the array were well located and defined a narrow belt of seismicity about 20 km south of the MCT between Yamuna and Bhagirathi valleys (Fig. 2.11). Due to paucity of data in the initial stages, many earthquakes outside the array were also considered. The scatter in epicentres was greater in these cases. But it could not be ascertained from the recorded data whether this was due to lack of constraints on observation or to the actual nature of seismicity in the region.

Focal depths:

For earthquakes occurring within the array, estimated focal depths turned out to be
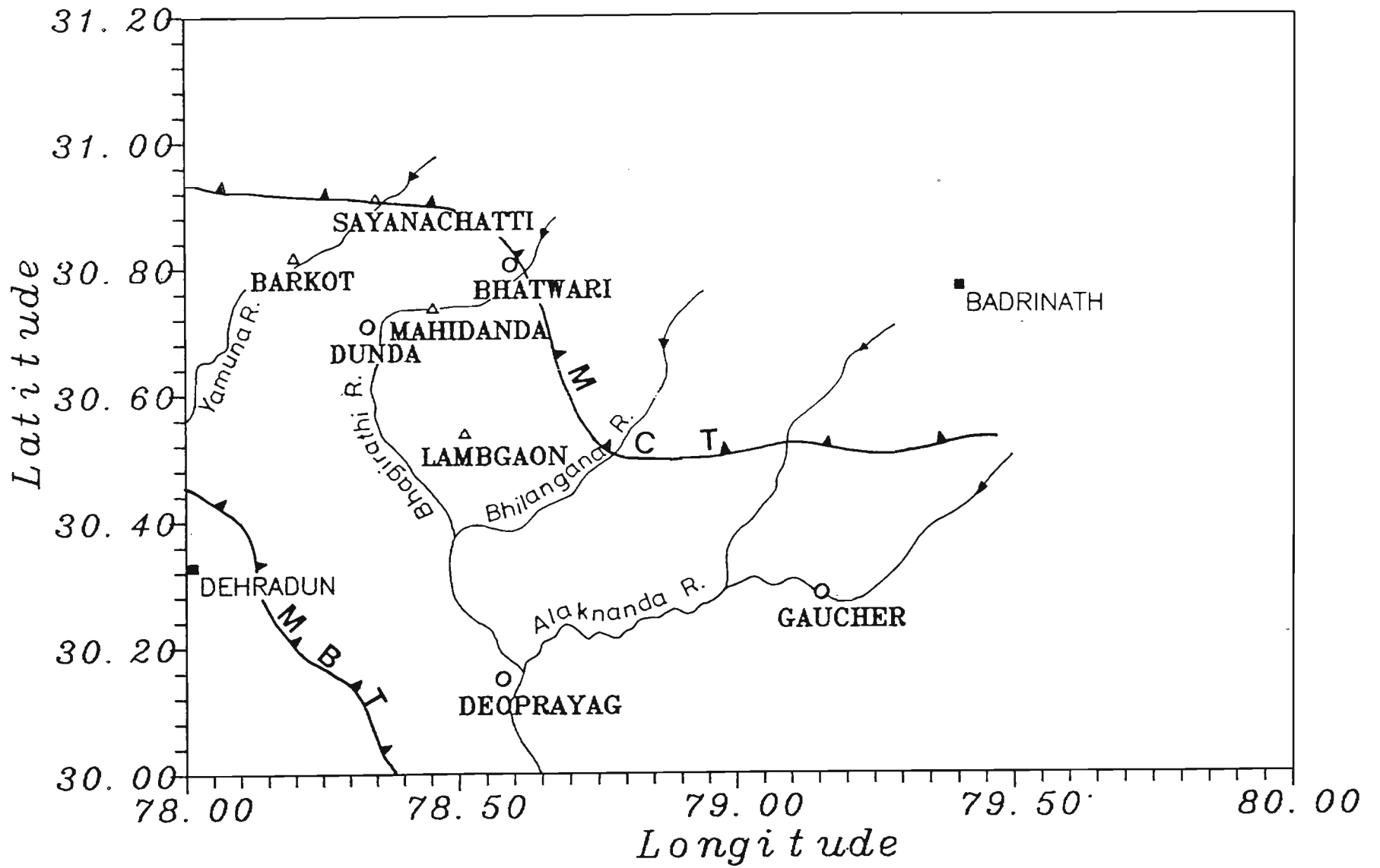
Figure 2·10   Recording stations for local seismicity study operated in 1979 and 1979–80. Bhatwari and Dunda stations were operated in 1979-80 also.
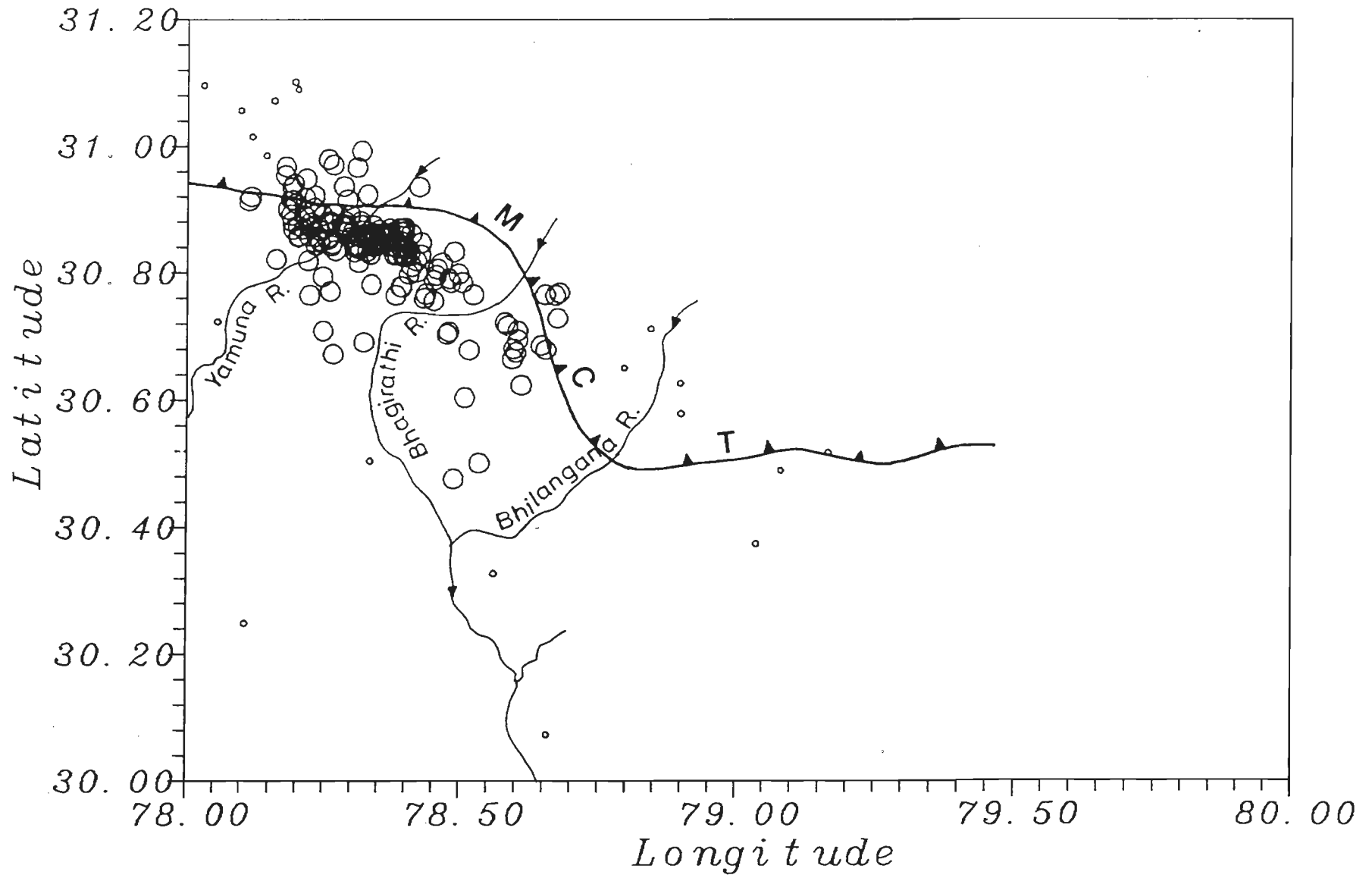
Figure 2·11   Epicentres of earthquakes recorded by the array shown in Fig. 2·10.

relatively shallow, being in the range of 0 to 23 km. There were many more earthquakes at depths shallower than 10 km. For earthquakes outside the array greater depths were observed. However, assuming the possibility that the earliest recorded P waves from many of these earthquakes were head waves along the base of the upper crustal layer it could be argued that these earthquakes too could have had shallow focal depths. But the case could not be established more strongly.

Fault Plane Solution:

A composite fault plane solution was obtained using the most reliable readings of P wave first motion (Fig. 2.12). It turned out to be a strike slip solution with nodal planes striking north-south and east-west. The former was better constrained and dipped vertically. The dip of the latter plane could be constrained only to the extent that it could be between 65° to the north and 90° (see below).

Major conclusion:

The small and micro-earthquake data recorded in the first phase of the field work in the Garhwal Himalaya indicated that in the vicinity of the MCT there was well defined seismic activity within the upper crustal layer. But further observations were needed. The analyses of observations in the second phase of recording is described in the following chapters.

2.3.5 The Uttarkashi Earthquake of 1991

While the analyses for the present thesis were proceeding at a slow pace because the author had to seek employment to make both ends meet, a relatively severe earthquake occurred in the Garhwal Himalaya on October 19, 1991 (Fig. 1.3). Unfortunately again the equipment with which the present data were acquired had been demobilised and the field assistants sacked because the funds for research had been stopped. Hence a golden
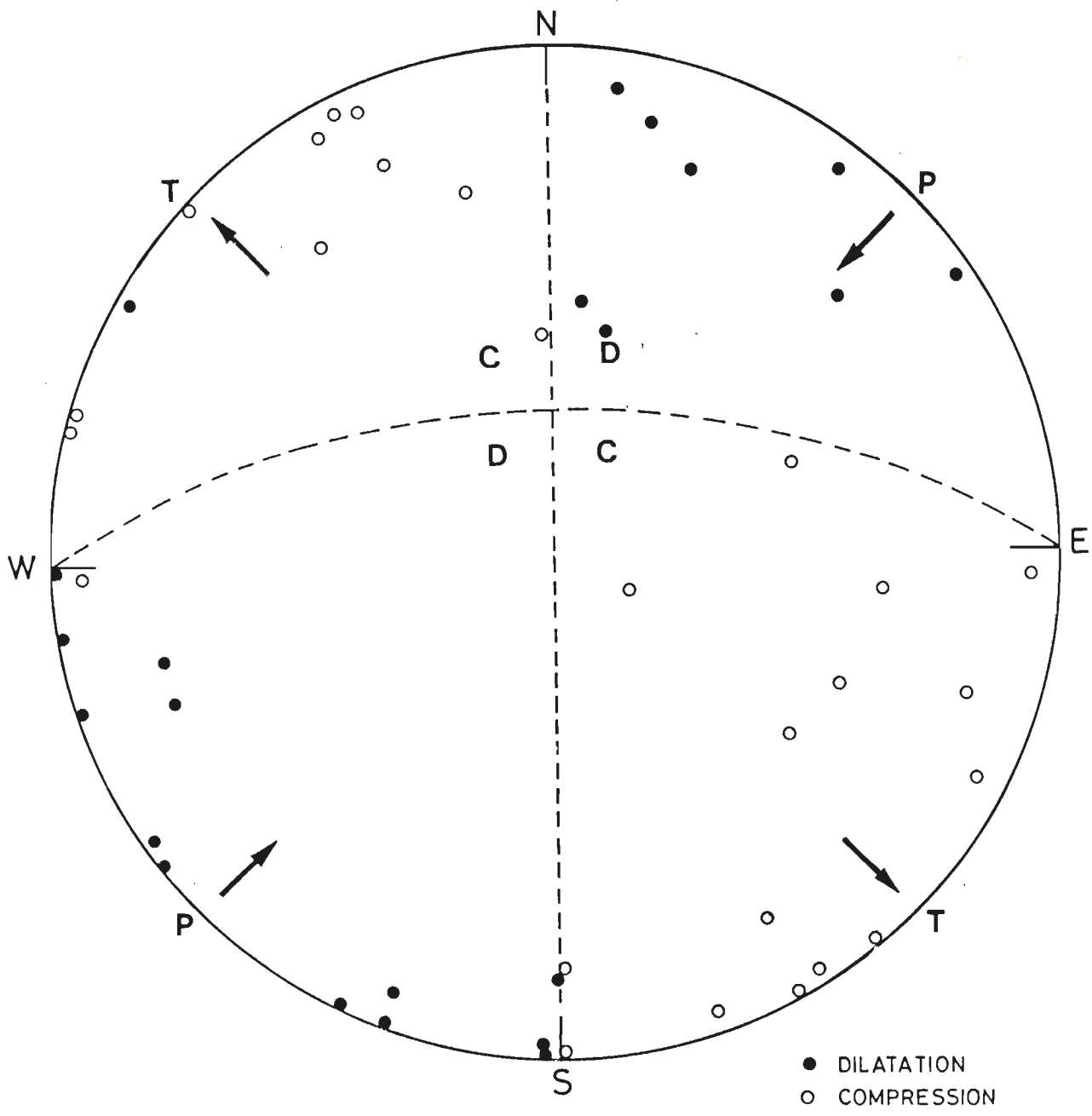
Figure 2·12 Composite fault plane solution reported by Gaur et al (1985).

opportunity to record aftershocks in the Himalaya and analyse their data uniformly in the pattern of pre-earthquake data was lost. It is not to say that other government agencies did not go into the epicentral tract and set up portable seismographs. But there was lack of uniformity in equipment and inadequate control on time marks. Although some results have been prepared, we do not have full access to them and there are doubts about their quality. The following remarks are based on limited published data.

2.3.5.1 Main Shock

The U.S. Geological Survey estimated the epicentral coordinates as $30.780°N$ and $78.774°E$. The focal depth based on depth phases was estimated to be 10.5 km. The m_b and M_s were 6.5 and 7.0 respectively. The P wave fault plane solution was not well constrained but thrust motion on a fault dipping $5°$ along $N16°$ could be assumed.

The earthquake caused more than 900 deaths and led to total and partial destruction of 42,000 houses. The property losses were ascribed to poor quality of construction of houses as also to the fact that many houses were built on river terraces. The lives lost were ascribed to these factors as well as occurrence of the earthquake in the middle of the night in the part of the year when the severe mountain winter was setting in.

The earthquake set off many landslides. There were reports of light and sound. But these have not been scientifically considered.

The India Meteorological Department gave out several estimates of the epicentral location of the main shock. The first estimate was so wrong that initial relief parties were misled grossly. Eventually the epicentral estimates converged towards the USGS determination. This was due to inclusion of more readings from the Indian national seismograph network.

2.3.5.2 After Shocks

Fig. 2.13 is a display of after shock epicentres determined by India Meteorological
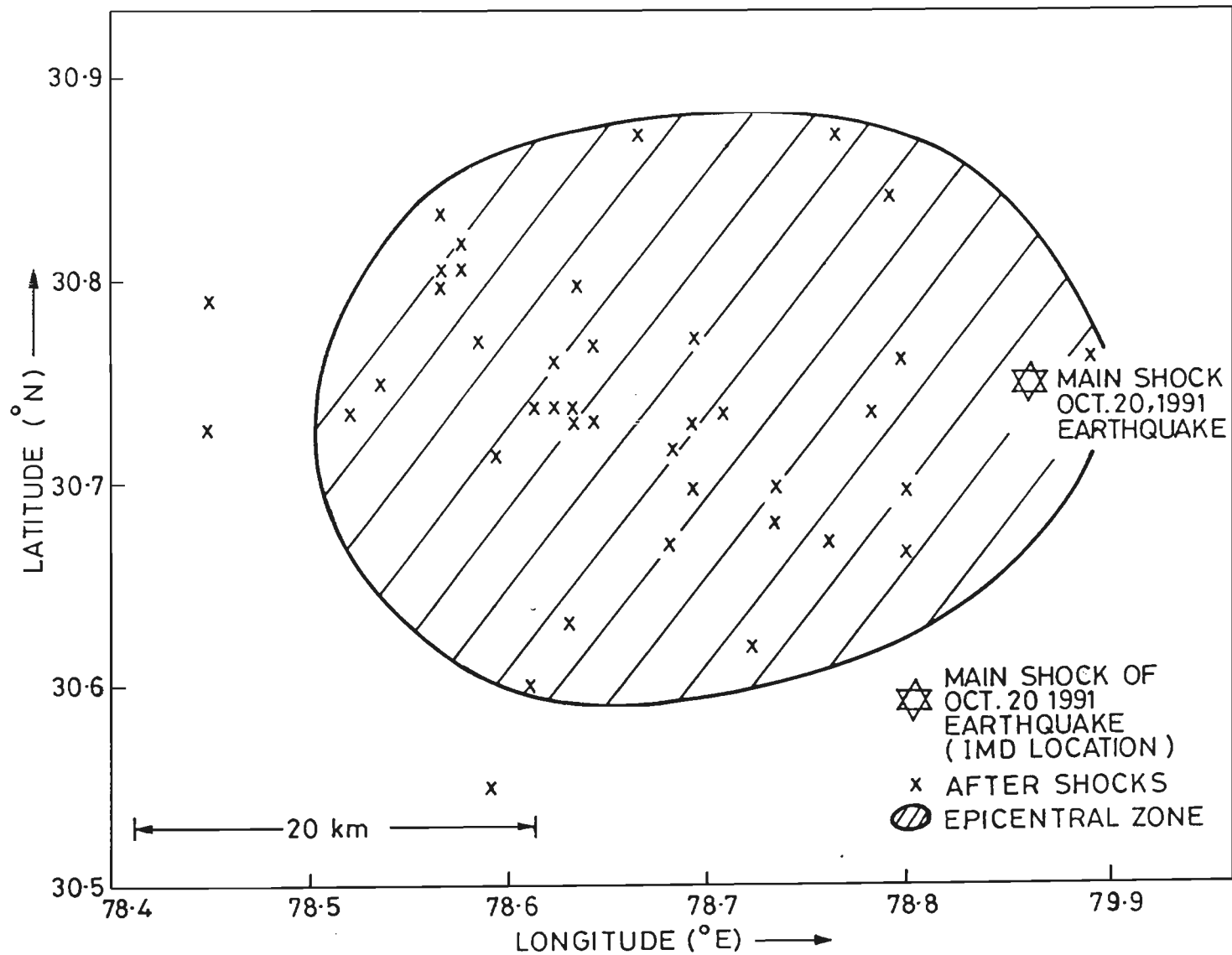
Figure 2.13   Aftershocks epicentres of the 1991 Uttarkashi earthquake (Anonymous, 1992).

Department (Anonymous, 1992). We shall argue that the main shock as well as most of the aftershocks lie well within the seismic belt traced from local recordings of small and micro-earthquakes prior to the Uttarkashi earthquake.

2.4 SUMMARY

Thus the Garhwal Himalaya are seismically active. Within this century there has been an earthquake of magnitude greater than 8.0 and another of about 7.0. Moderate and small earthquakes are occurring routinely. Evidence of frequently occurring micro-earthquakes has already been obtained to some extent and is described further in the following chapters. The attempt has been, is and should be to understand this seismicity as far as possible.

3

METHODS OF DATA ACQUISITION AND ANALYSIS

3.1 DATA ACQUISITION

The author was not directly involved in the field acquisition of the Garhwal Himalayan data interpreted here. However, he has been associated with acquisition of similar data in northeast India using identical equipment and procedures. Hence the following paragraphs of this section still have the stamp of considerable personal knowledge and first hand experience.

3.1.1 Equipment

The field recording in the Garhwal Himalaya was carried out using portable seismograph equipment. The sensor was Teledyne-Geotech S-13 seismometer operated in the vertical mode at all stations except, in one season at one station (Ukhimath) (Fig. 3.1), where it was operated in the horizontal mode. The recorder was the Teledyne-Geotech portacorder with provision for recording on smoked paper. A commercial radio receiver was available at each station to receive standard time signals and calibrate instrumental clock regularly. Power for station operation was provided by two car batteries of 120 ampere-hour rating. After one pair of batteries were run down,
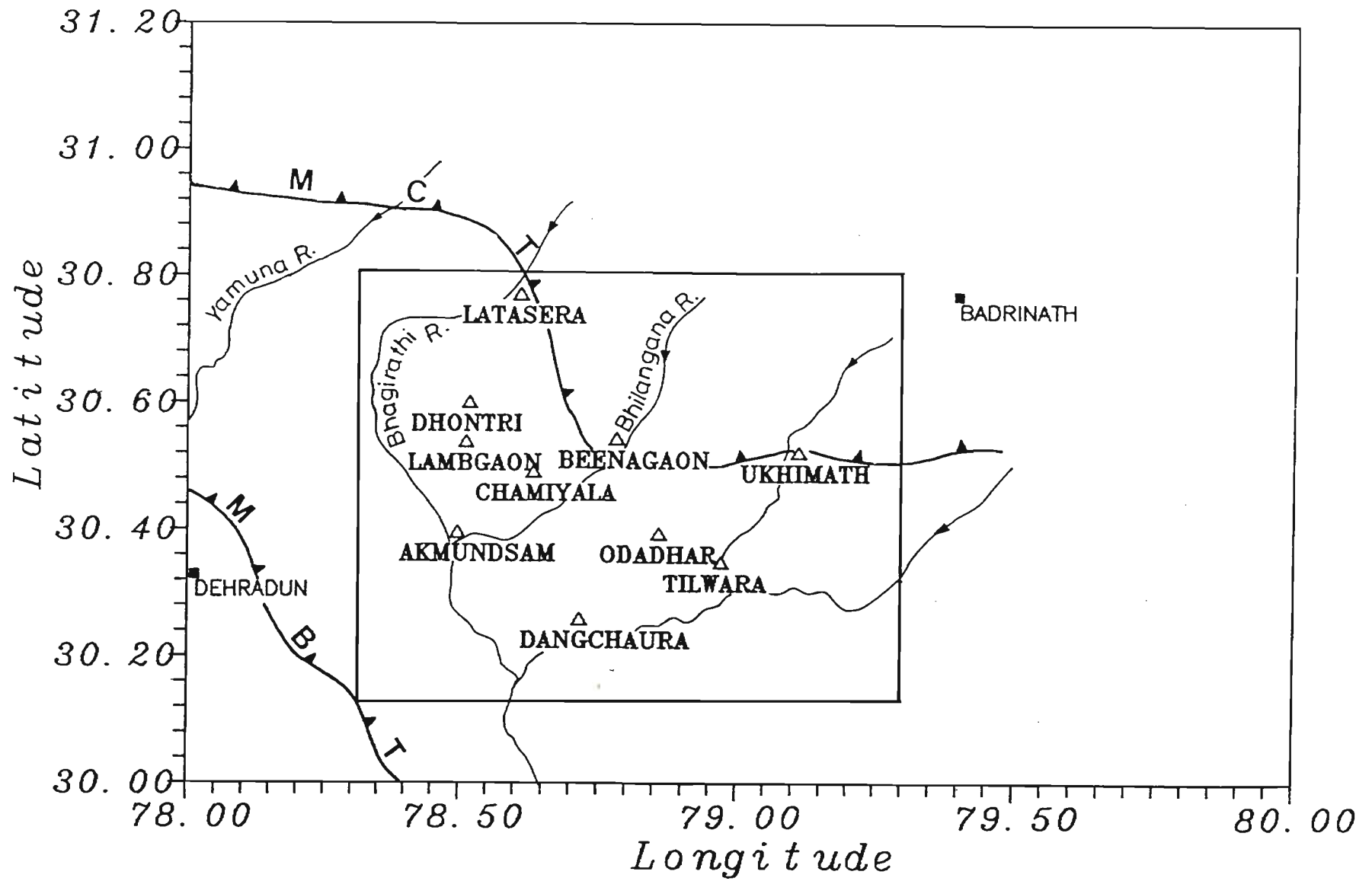
Figure 3-1 Portable seismograph stations operated during 1984-86

a spare pair was substituted and the run-down batteries were taken for recharging. Thus station down time due to this cause was minimized.

3.1.2 Station arrays and station sites

Throughout the field work, for which data are analyzed, the seismograph array consisted of a minimum of five and maximum of seven stations. Each station was manned by a person trained in basic, practical electronics at an industrial training institute. Seismological motivation of these persons being limited, regular checks were kept on their work to see that filter settings, recording speeds, battery charge levels and daily time checks were conducted as per instructions. Logistic constraints in the Garhwal Himalaya are severe. Station sites were picked in remote areas of Garhwal keeping in mind the local noise conditions at top priority and daily accessibility on foot by the station operator at a marginally lower level of priority. Stations were invariably on valley sides in those valleys of Garhwal where motorable roads existed to transport equipment from Roorkee. Equipment and batteries were carried on mule backs from road heads to station sites. Reasonable interstation spacing was sought and the maximum array size could be maintained between 45 and 70 km (Fig. 3.1).

3.1.3 Station Operation

Filter settings and instrumental attenuation settings were controlled by local site conditions. But a frequency passband of 5 to 15 Hz and recorder magnification in the range of 60 to 78 db were maintained at all times.

Recorder speed of 60 mm/min was maintained. Daily change of record was mandatory for ease of analyses of seismograms. However, closer trace spacing was resorted to when the operator had to be away for more than a day. Efforts were made to limit such instances.

Clock check at the beginning and end of each record was required from the

TABLE 3.1 GEOGRAPHICAL LOCATION OF STATIONS OPERATED IN THE GARHWAL HIMALAYA

DURING 1985-86 BY THE DEPARTMENT OF EARTH SCIENCES, UNIVERSITY OF ROORKEE.

| S. NO. | STATION NAME WITH CODE | LOCATION | | ELEVATION (METERS) |
		LATITUDE (^{0}N)	LONGITUDE (^{0}E)	
1.	Akmundsum (AKM)	30^0 23.76'	78^0 29.76'	0850.00
2.	Chamiyala (CHA)	30^0 29.46'	78^0 37.98'	1500.00
3.	Beenagaon (BNA)	30^0 32.58'	78^0 46.86'	1500.00
4.	Dangchaura (DAG)	30^0 15.54'	78^0 42.96'	1300.00
5.	Odadhar (ODA)	30^0 23.64'	78^0 51.42'	2000.00
6.	Tilwara (TIL)	30^0 20.94'	78^0 58.26'	0700.00
7.	Ukhimath (UKH)	30^0 31.32'	78^0 06.54'	2800.00
8.	Lambgaon (LAM)	30^0 32.34'	78^0 30.60'	1640.00
9.	Dhontri (DHO)	30^0 36.06'	78^0 30.96'	2500.00
10.	Latasera (LAT)	30^0 46.26'	78^0 36.42'	1350.00

operators and was obtained on a fair number of days. Weather conditions and limited duration of broadcast for the standard time imposed constraints.

At most stations, cultural noise during day time impaired record quality. Night time recording was superior invariably.

3.1.4 Time checks

The standard time broadcast available in the Garhwal Himalaya was that from station ATA on frequencies of 5, 10 and 15 MHz. The atomic clock preferred in these broadcasts is kept at National Physical Laboratory in New Delhi. During the period of interest here, time broadcasting ceased at night and on Sundays and national holidays. Occasionally, atomic time broadcasts from China interfered.

Instrumental clock was adjusted visually by synchronization of second marks generated by the instrumental and atomic clocks.

We judge that the arrangement worked in the medium to good range mostly, interspersed with brief periods of good to very good and fair to medium.

3.2   ESTIMATION OF STATION LOCATIONS

Station coordinates were read from the Survey of India topographic sheets of 1:250,000 scale in most cases and 1:500,000 scale in a few cases after plotting station positions on the sheets. Considerable difficulty was encountered. Some times the toposheets were several decades old and did not reflect increasing population and increase in the number of roads. Errors of more than ± 1 km in each of station latitude and longitude cannot be ruled out.

3.3   DATA ANALYSIS

3.3.1   Record Reading

Plate 3.1 is taken from one of the records obtained to show a locally recorded micro-
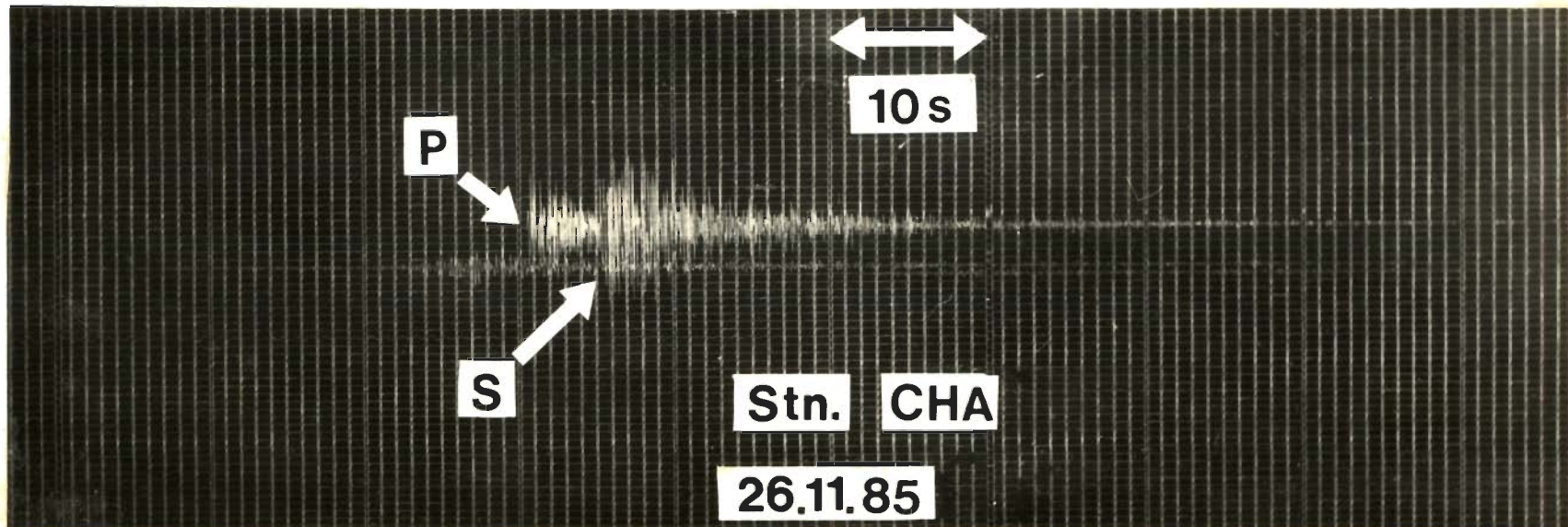
Plate 3.1. Part of the vertical component seismogram from Chamiyala (CHA) station showing clear P and S phases from a microearthquake occurring in the Garhwal Himalaya on November 26, 1985.

earthquake. All the relevant seismograms were read by the author personally. The entire process was manual. Clock correction was applied by linear interpolation using the nearest time checks before and after the concerned earthquake. Times were read using an engine divided plastic scale. A small magnifying glass was used to facilitate picking of phases on the seismograms and reading the first motion of P where possible.

Objectivity in reading P and S times and first P motion was exercised. Still the records were reexamined as many times as necessary during hypocentral locations and determinations of fault plane solutions.

Although it is tempting, reading accuracy of phase arrival times to better than about ± 0.5 s is difficult to claim in most cases.

3.3.2 Computer Program for Hypocentral Location

Sarkar (1983) and Sarkar et al (1987) describe a computer program for hypocentral location that was developed at the Department of Earth Sciences, University of Roorkee, to meet the task at hand. Important features of the program are as follows. Firstly, the hypocentral parameters of latitude, longitude, focal depth and origin time are estimated from observed arrival times of P and S phases for a single earthquake at a time. A minimum of five such readings are required. Secondly, the wave speed model can have layers of uniform speed and plane interfaces of arbitrary dips and strikes in three dimensional space. However, more than one interface was never considered in the present analysis. Thirdly, the program incorporates an iterative variational scheme (Chander, 1977) to trace rays between the assumed hypocentre and stations with specified coordinates. Fourthly, a least squared error procedure is used to minimise differences between observed and computed arrival times of P and S phases. Fifthly, a penalty function approach is used to guide the search for optimum values of hypocentral parameters. Sixthly, the Newton-Raphson procedure is used to compute increments in hypocentral parameter estimates so that the solution moves in the direction of the nearest

local minimum in successive iterations. Lastly, a joint confidence region for hypocentral parameters is estimated in the error analysis.

The program was investigated and re-evaluated by us using synthetic data. But further details of the program and synthetic data used are omitted because the former was not written by us and the revalidation required a small amount of time compared to that expended in other activities related to this thesis. A copy of this program is attached for record (appendix - I). The limited changes introduced by us to facilitate operation and use of the program are indicated.

3.3.3 Wave speed model used for hypocentral location

Based on data recorded during the first phase of recording in 1979-80 in the Garhwal Himalaya, Chander et al (1986) estimated a P wave speed of 5.2 km/s in the upper crustal layer. Similarly Kumar et al (1987) estimated a P wave speed of 6.0 km/s in the second crustal layer of the region using earthquake generated head waves from the top of the layer. A thickness of 17 km for the upper crustal layer was assumed based on the estimated depth of the detachment under the MCT (Ni and Barazangi 1984, Chander 1988). The interface between the two layers was assumed horizontal. This wave speed model was used to determine hypocentral parameters of earthquakes reported in the next chapter. Since only 25 out of 152 earthquakes had estimated focal depths below 17 km, these were the only earthquakes for which there was need to consider this two layered model.

3.3.4 Coda magnitudes

3.3.4.1 General

There are two approaches to calculate the magnitude of micro-earthquakes. One approach is to calculate the ground motion from the recorded maximum amplitude, and from this compute the response expected from Wood Anderson seismogram. Another

approach is to use signal duration instead of maximum amplitude. The idea has gained a measure of popularity in analyses of micro-earthquake data recorded with portable seismographs with analogue recorders were possibility of clipping of traces is considerable.

The definition of signal duration is not very critical because the magnitude is also a rough estimate of the size of an earthquake. The total signal duration of an earthquake has been defined on the duration of both the body and surface waves. But a lot of difference exists in reading the end of the seismogram of the event. Different authors (e.g. Lee et al 1972 and Real, 1973) define coda lengths in different ways.

Here we have used the definition of Real (1973) in which coda length is the time interval between onset of first arrival and the point where signal falls below the background noise level. The advantage of this is that background noise makes the duration somewhat independent of the instrumental gain, since, increasing gain would amplify both the signal and background noise.

3.3.4.2 Methodology

We have used the above criteria to define coda lengths and used the empirical formula of Lee et al (1972) for estimating the magnitude (M_c) i.e.

$$M_c = C_1 + C_2 \log (T) + C_3 \Delta \qquad ...(1)$$

Where
M_c = Coda Magnitude
C_1 = -0.87
C_2 = 2.0
T = Signal duration (seconds)
C_3 = 0.0035
Δ = Epicentral distance in kilometers

We also estimated the local magnitude using the formula of Singh et al (1976) given for Garhwal region.

$$M_l \quad = \quad -4.3 + 3.25 \log(T) \qquad\qquad ...(2)$$

3.3.5 Composite fault plane solutions

The number of recording stations in the arrays operated being relatively small, individual fault plane solutions of earthquakes could not be determined. Composite faults plane solutions offer a distant second best option. But we adopted it perforce. Since the number of earthquakes with estimated foci in the second layer of the above wave speed model was a very small percentage of the total number of relevant earthquakes, fault plane solutions were carried out assuming a uniform medium between hypocentres and respective recording stations for all earthquakes for which first P motion data could be read reliably on the seismograms.

The analyses were carried out manually using Wulff's equal area projection net.

3.4 CLOSURE

It is a matter of some regret that computer facilities available to us were limited. Hence many of the analyses had to be carried out manually. But every effort was made so as not to compromise further on accuracy of the results reported using the data and analysis procedures described above.

4

SEISMICITY RESULTS

4.1 GENERAL

Field recording of earthquakes in the Garhwal Himalaya was undertaken at the Department of Earth Sciences, University of Roorkee, to increase our information about regional seismicity. Recording of small and micro-earthquakes would complement information obtained from teleseismic observations of moderate and stronger earthquakes of the region. Overall errors of hypocentral locations would be reduced and association of observed local earthquakes with specific tectonic features might be attempted.

As mentioned above, field observations were initiated with very limited information in 1978. By December 1979, a reasonably planned array was in place. Within a few months, by June, 1980, a substantial amount of data had been obtained. Their analyses (chapter 2 and 6) suggested an association between current seismicity and the MCT region. Hence when the field recording was resumed in 1984 with fresh research funds, the target was well formulated, namely, to shift the recording array along the trend of the MCT and examine this association of earthquakes further. A natural choice, keeping the logistics in mind, was to move southeastward from the previous array site in Yamuna and Bhagirathi valleys (Fig. 2.10 and 3.1). By June, 1986, the region from the Bhagirathi

valley to northwest of Alaknanda valley had been given a first look. We present the seismicity results in this chapter and fault plane solutions in the following chapter.

4.2   ARRAYS

Table 4.1 gives a list of stations occupied in the 1984-86 period. Referring to this table and Fig. 3.1, stations Akmundsam, Chamiyala, Lambgaon/Latasera, Beenagaon, and Dhontri were occupied in the 1984-85 season and gave information about the region immediately southeast of Bhagirathi valley. In the next field season, seven stations, namely, Akmundsam, Chamiyala, Beenagaon, Odadhar, Dangchaura, Tilwara and Ukhimath were operated and the regions still further southeastward upto Alaknanda valley were investigated.

The station at Ukhimath was operated in the horizontal mode with a view to test whether this would lead to better recording of P and S phases. The improvement was not very remarkable and this mode of operation was discontinued in subsequent work.

4.3   NUMBER OF EARTHQUAKES INVESTIGATED

Table II.1 of Appendix II gives a chronological list of recorded arrival times of P and S phases at various stations that enabled hypocentral locations of 152 earthquakes to be determined. The choice of earthquakes to be considered was made on the following bases. The earthquake should yield;

i)   P phases readings from a minimum of 5 stations;

ii) P phase readings at 4 stations and S phases readings from at least one of these stations;

iii) P phase readings at 3 stations and S phase readings from at least 2 of these stations.

The second and third options were to cope with cases where a small earthquake was not recorded at all the stations of an array. A restriction was also placed that difference in
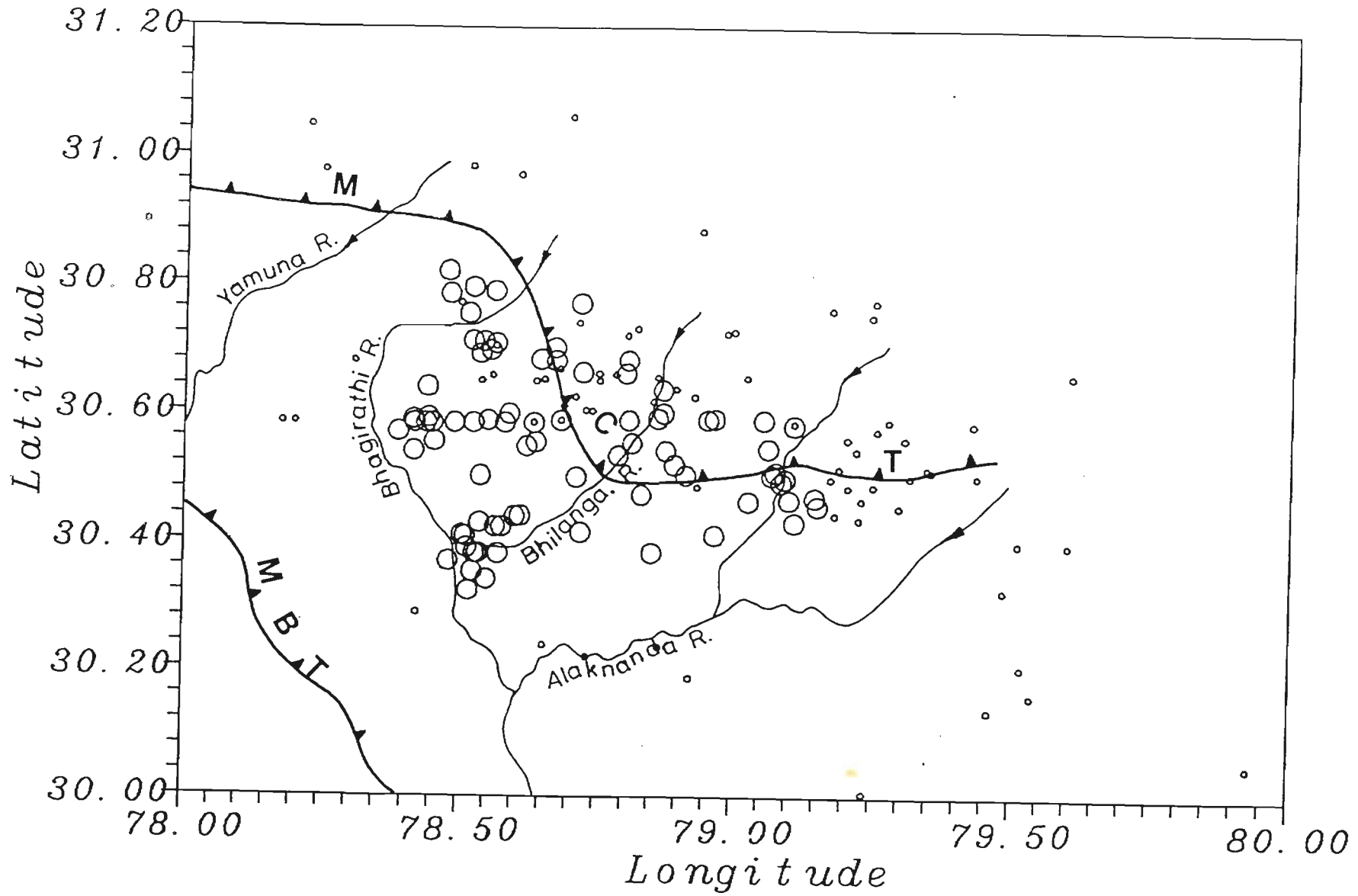
Figure 4·1   Epicentres of earthquakes recorded during 1984-86

48

arrival times of P and S phases at none of the stations should exceed 10s. The aim was to improve the chances that first arriving P waves would be direct waves from the hypocentres. However in eleven cases earthquakes yielding differences in P and S arrival times up to 19s were included and analysed on the assumption that the first arriving waves were head waves from the top of the second crustal layer.

4.4 SOURCES OF ERRORS IN HYPOCENTRAL PARAMETER ESTIMATES

The hypocentral parameter estimates obtained for various earthquakes are subject to errors from a number of sources.

i) Errors in reading the arrival times of P and S phases from the seismograms;

ii) Errors in synchronization of the instrument clocks with the standard radio time signals;

iii) Drift of instrumental clocks and irregularities in time keeping arrangements within the instrument such as irregular rotation of the recording drum, etc.

iv) Errors in determining the exact locations of the recording stations.

Each of the first three sources leads to random and systematic errors, while there are systematic errors, due to adoption of specific estimates of station location. At the time when the present analyses were started, it was not possible to perform experiments and make estimates of the systematic errors. The random errors were assumed to be normally distributed with zero mean and unit variance and hypocentral parameters estimates were obtained using the least square error procedure accordingly.

4.5 RESULTS

4.5.1 Epicentral locations

4.5.1.1 Maps and tables

Table II.2 (Appendix II) is a list of the estimated hypocentral parameters of the 152 earthquakes Fig. 4.1 is a display of located epicentres. In all 52 of these earthquakes

were recorded in the 1984-85 season and 100 in the next season. Since greater confidence can be attached to epicentral locations falling within and close to the recording array, they are shown with larger symbols. Epicentres falling relatively further away from the array are shown with smaller symbols. The distinction is somewhat arbitrary and this is reflected to some extent in the figure especially near longitude 79.3º E. 92 earthquakes were considered as occurring within and sufficiently near the recording array to be allotted the bigger symbol. The remaining 60 earthquakes were allotted the smaller symbol.

The surface traces of the MCT and MBT as taken from the tectonic map of the Himalaya by Gansser (1964) are plotted along with the major rivers and tributaries in Fig. 4.1 for background information.

4.5.1.2 Estimates of standard errors in epicentral coordinates

As seen from Table II.2, the worst values of standard errors in latitude as well as longitude estimates of epicentral locations turnout to be ± 6.4 km though in most cases the errors are considerably less.

4.5.2 Focal depths

4.5.2.1 Distribution of focal depths in different depth intervals

The estimated focal depths of the 152 earthquakes are also listed in Table II.2. They range from 0 to 30 km. Fig.4.2 is a plot of the number of earthquakes per km depth interval at different depths. It is seen that the distribution is unimodal with maximum frequency in the depth range of 10-12 km. 129 earthquakes or approximately 85% of the total population fall within the top 16 km with the remaining 23 distributed more or less evenly up to a depth of 30 km.

4.5.2.2 Depth sections

Figure 4.3 is a depth section displaying hypocentral locations plotted on to a
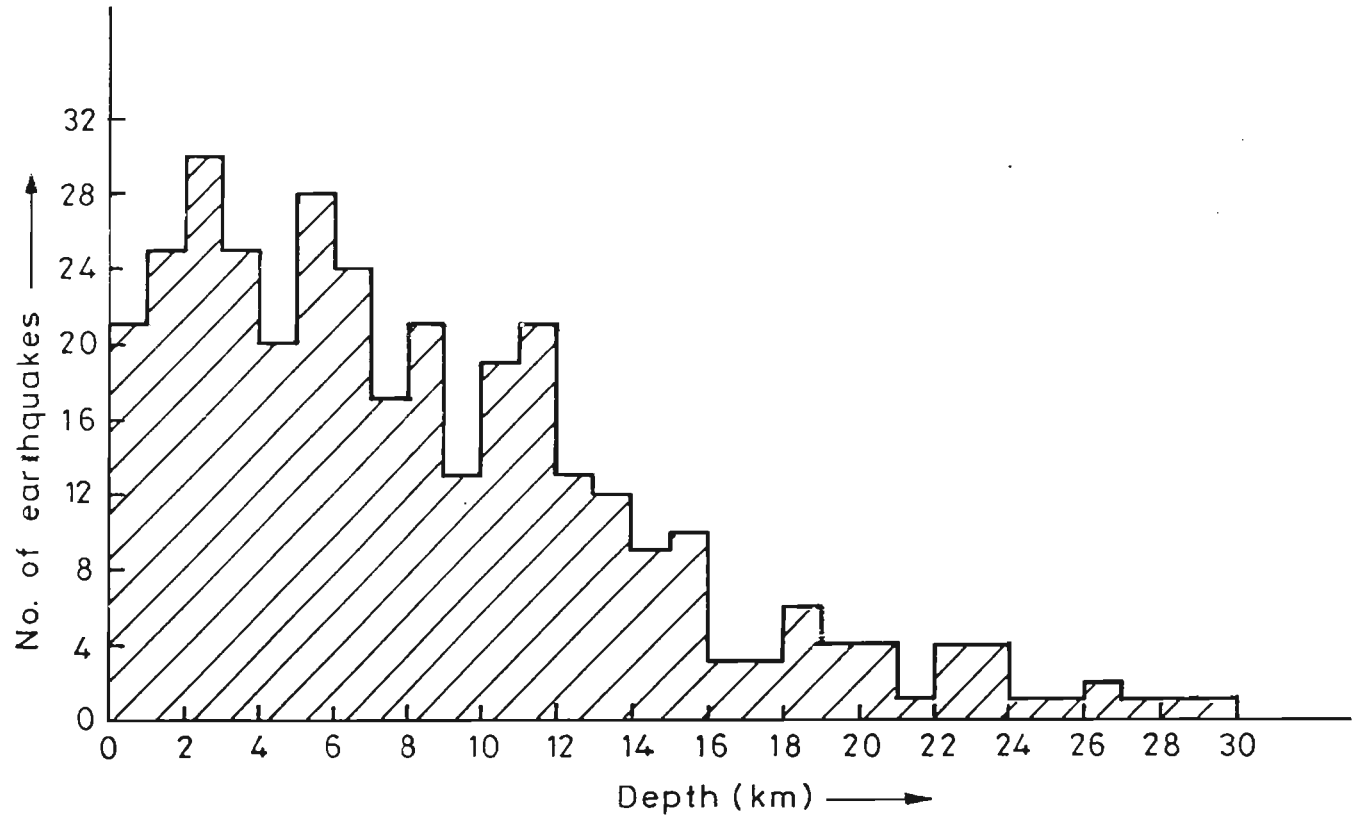
Figure 4·2   Histogram of focal depths of earthquakes shown in Fig. 4·1.

single vertical plane parallel to the estimated overall trend of the MCT across the Garhwal Himalaya. The fall in the number of earthquakes beyond about 125 km on this depth section indicates a fall in the detection capability of the recording array operated in 1985-86 for small and micro-earthquakes occurring to the southeast.

Since the direction normal to the trend of Figure 4.3 is also the general direction in which various geologically mapped thrusts of the region would appear in section, therefore depth sections representing four slices (Figure 4.4) were considered in the hope that association of earthquake hypocentres with specific faults might be attempted. But they were belied. These depth section results are shown in Figs. 4.4 to 4.12.

Figs. 4.5 and 4.6 pertain to the large rectangular slice A enclosing epicentres in the northwestern part of Fig. 4.4. Figures 4.7 and 4.8 pertain to only the B slice of Fig. 4.4. Slices C and D of Fig. 4.4 are similarly considered in Figs. 4.9 and 4.10 and Figs. 4.11 and 4.12 respectively. Although some northeasterly trends in these hypocentral plots tend to be prominent, we hesitate to consider that specific faults have been identified in the sections of Figs. 4.6, 4.8, 4.10 and 4.12. This is partly because of the errors in depth estimates discussed in the following subsection as well as the fact that independent subsurface mapping of faults in the region is nonexistent.

4.5.2.3 Errors in depth estimates

A glance along column 10 of Table II.2 (Appendix - II) indicates that the estimated standard error in focal depth estimate has maximum value of ± 8.2 km. Even the number of entries showing standard error of ± 5.0 km also is not significant.

4.6   CODA MAGNITUDE RESULTS

In order to get rough estimates of the relative magnitudes of earthquakes which we have analysed for hypocentral locations we have used the empirical formulas (1) and (2) above. The cut off for reading the coda length being the background noise level, we read
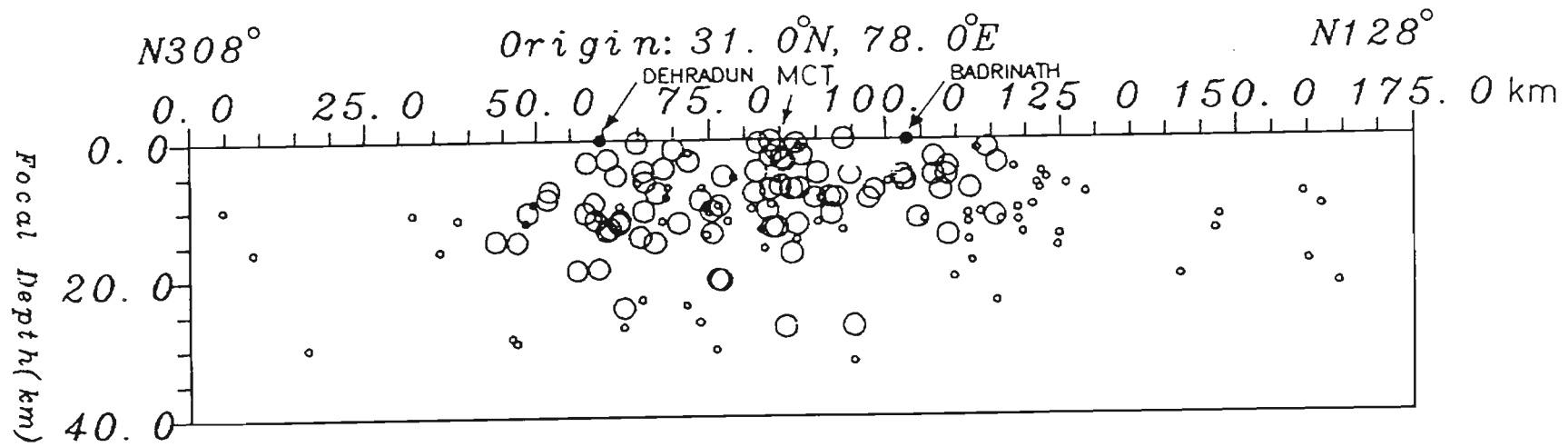
Figure 4·3   Depth section for earthquakes of Fig. 4·1.
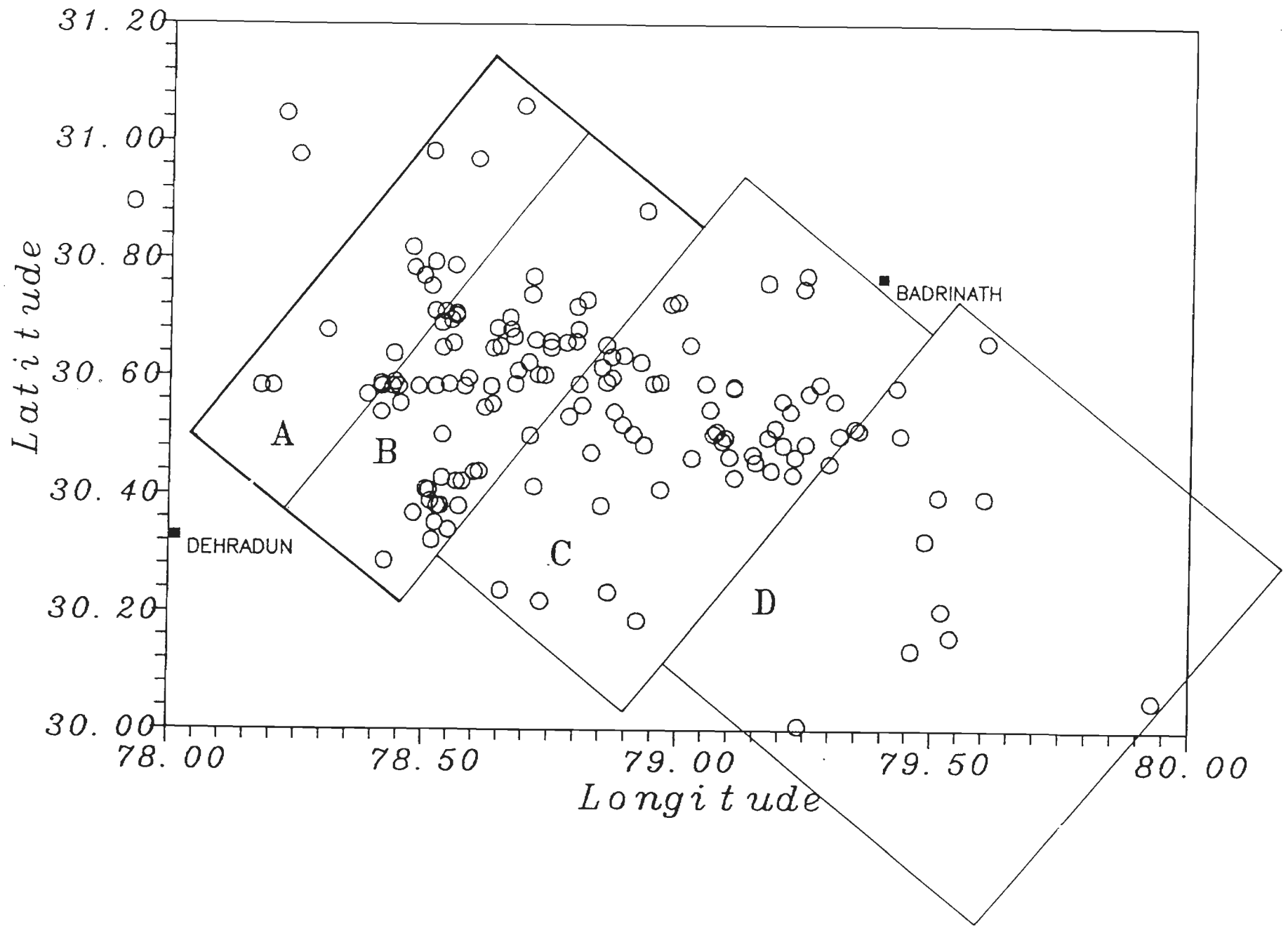
Figure 4·4   Division of earthquake epicentres for transverse depth sections.
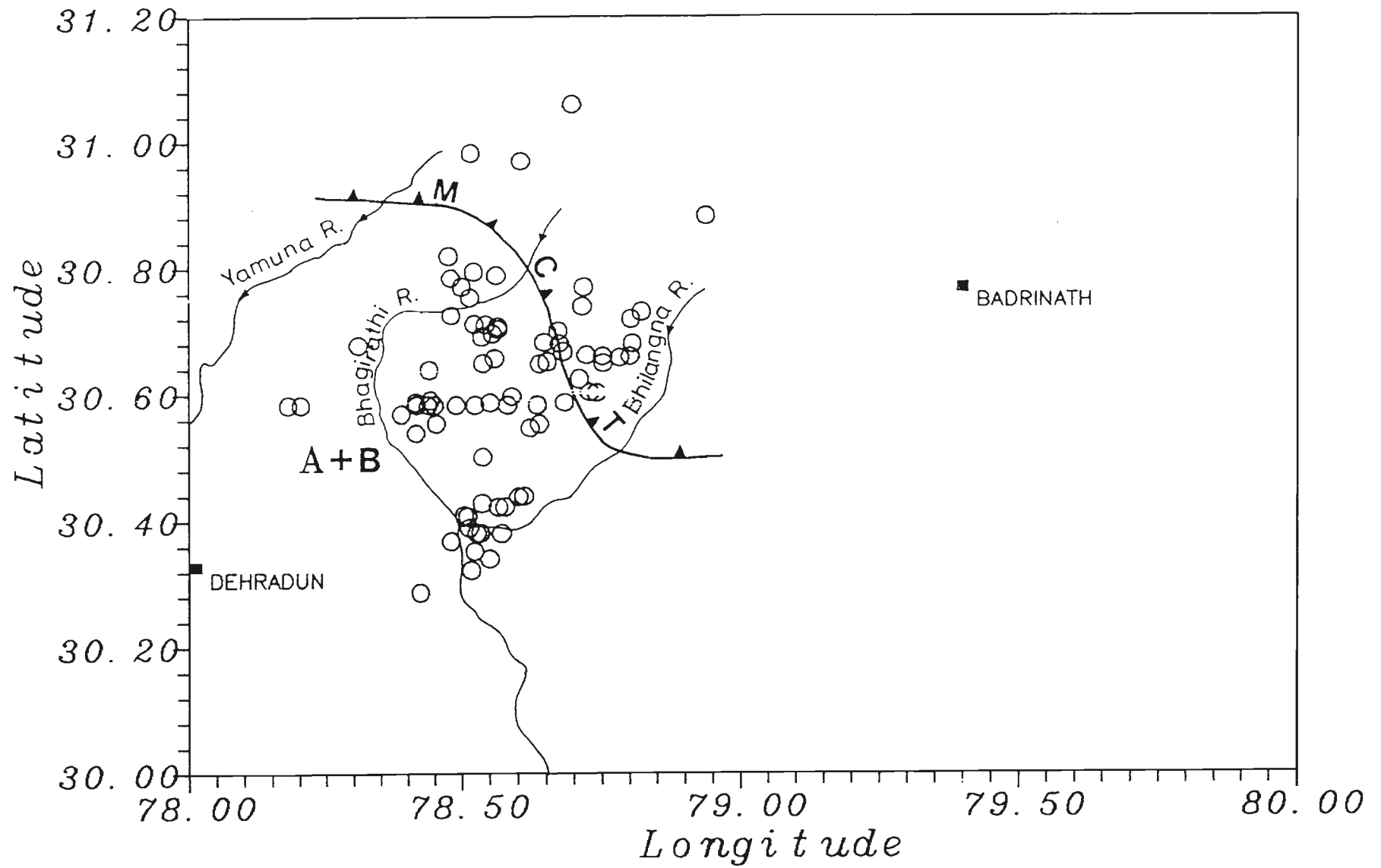
Figure 4·5   Epicentres of earthquakes whose depth section is shown in Fig. 4·6.
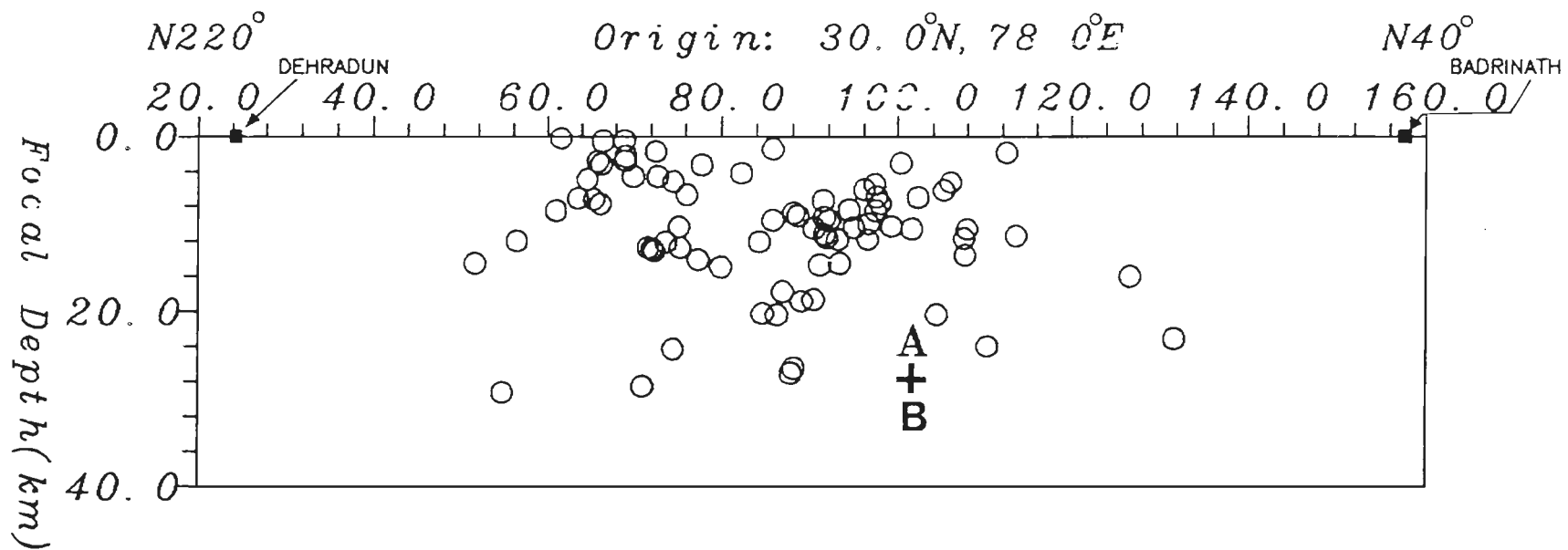
Figure 4·6 Transverse depth section for epicentres of Fig. 4·5.
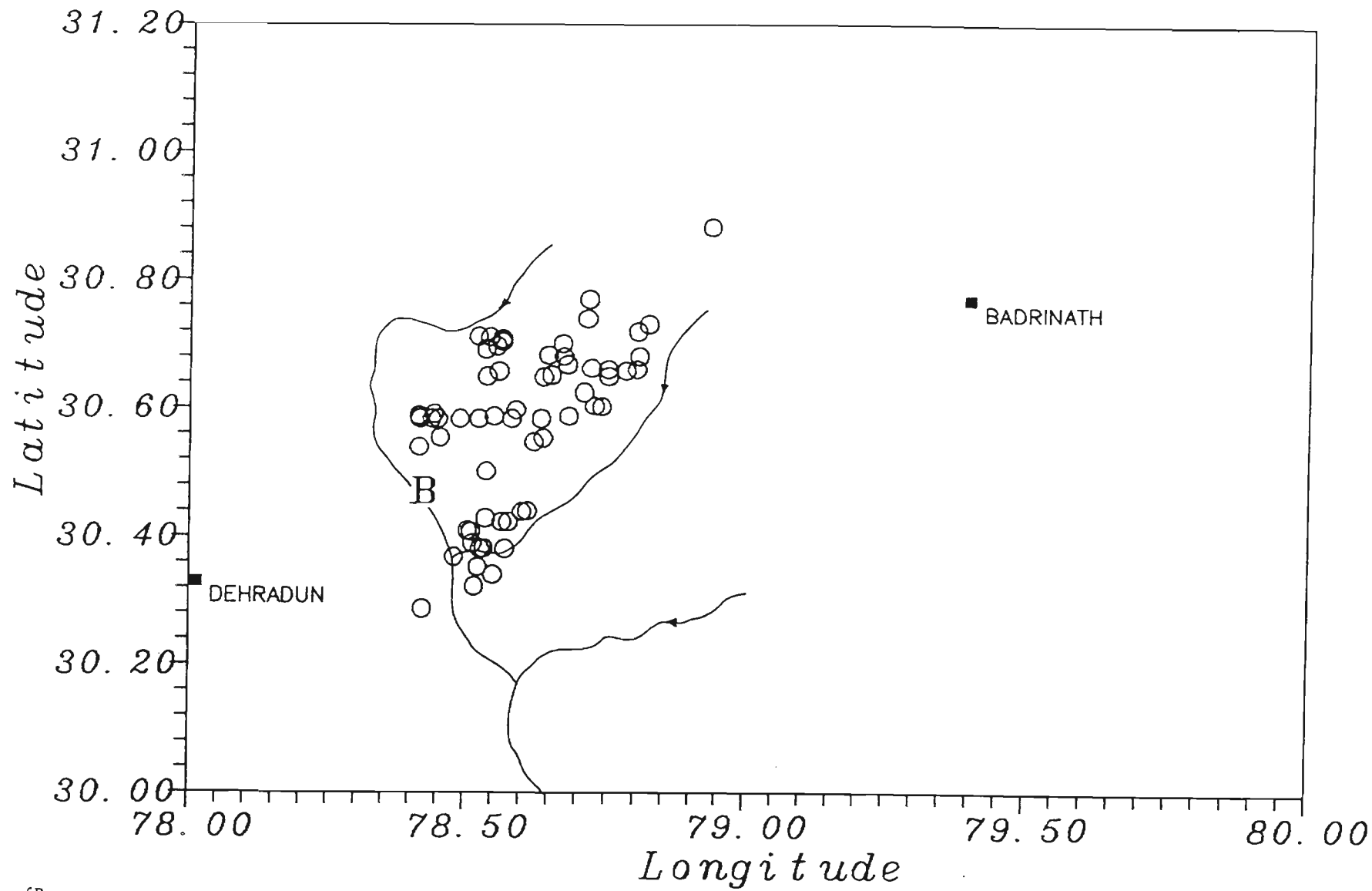
Figure 4·7   Similar to Fig. 4·5 for depth section of Fig. 4·8.
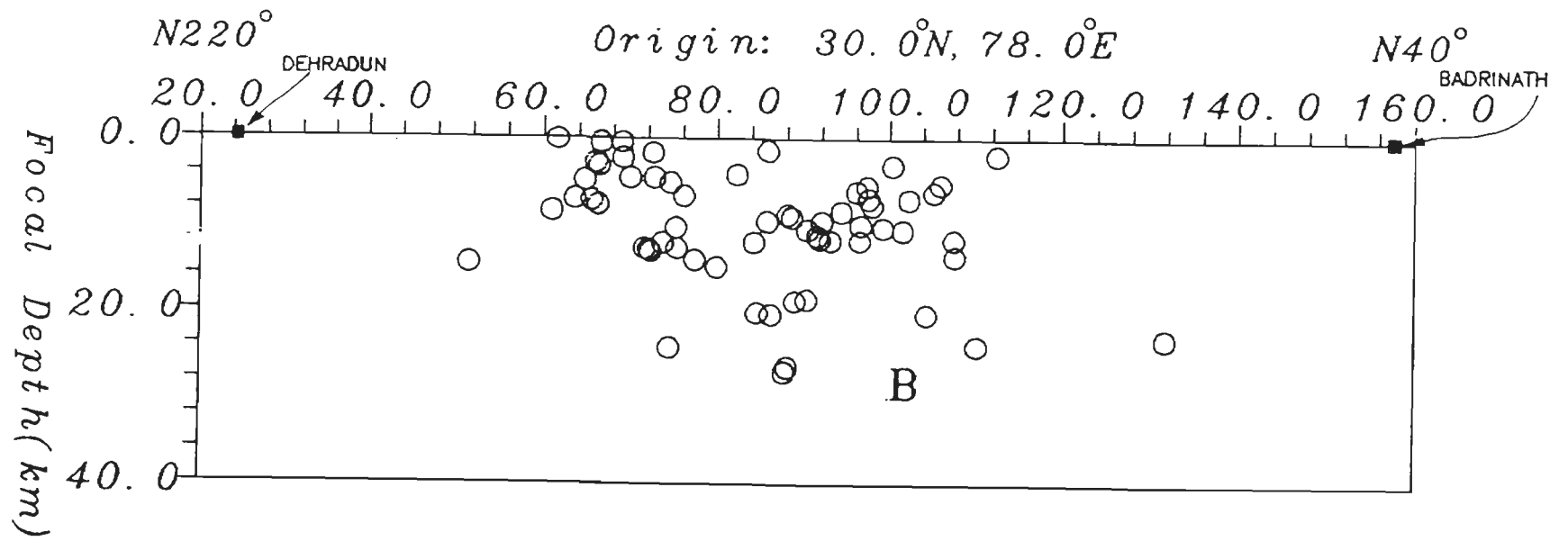
Figure 4·8   Transverse depth section for epicentres of Fig. 4·7.
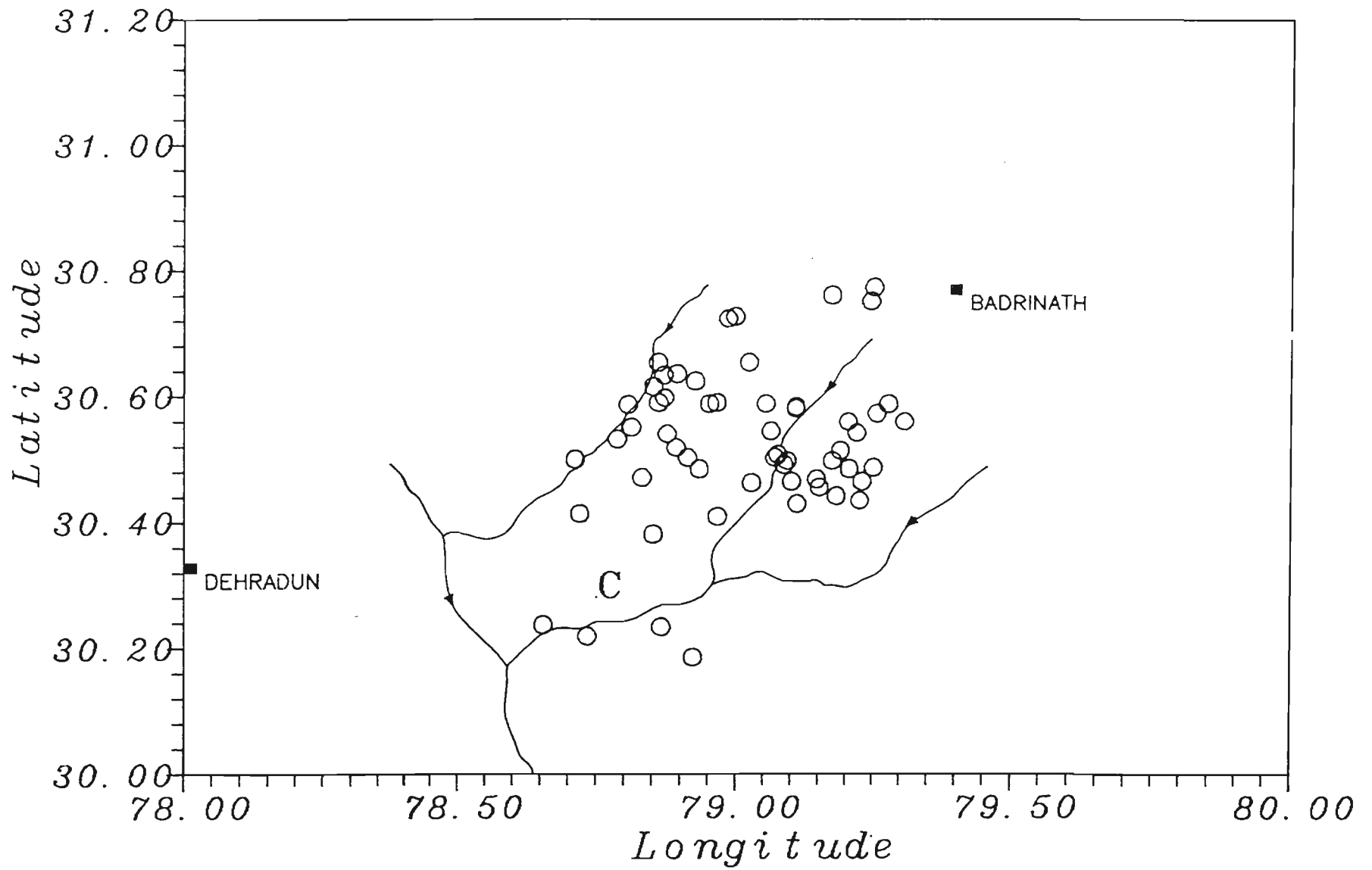
Figure 4·9 Similar to Fig. 4·5 for depth section of Fig. 4·10.
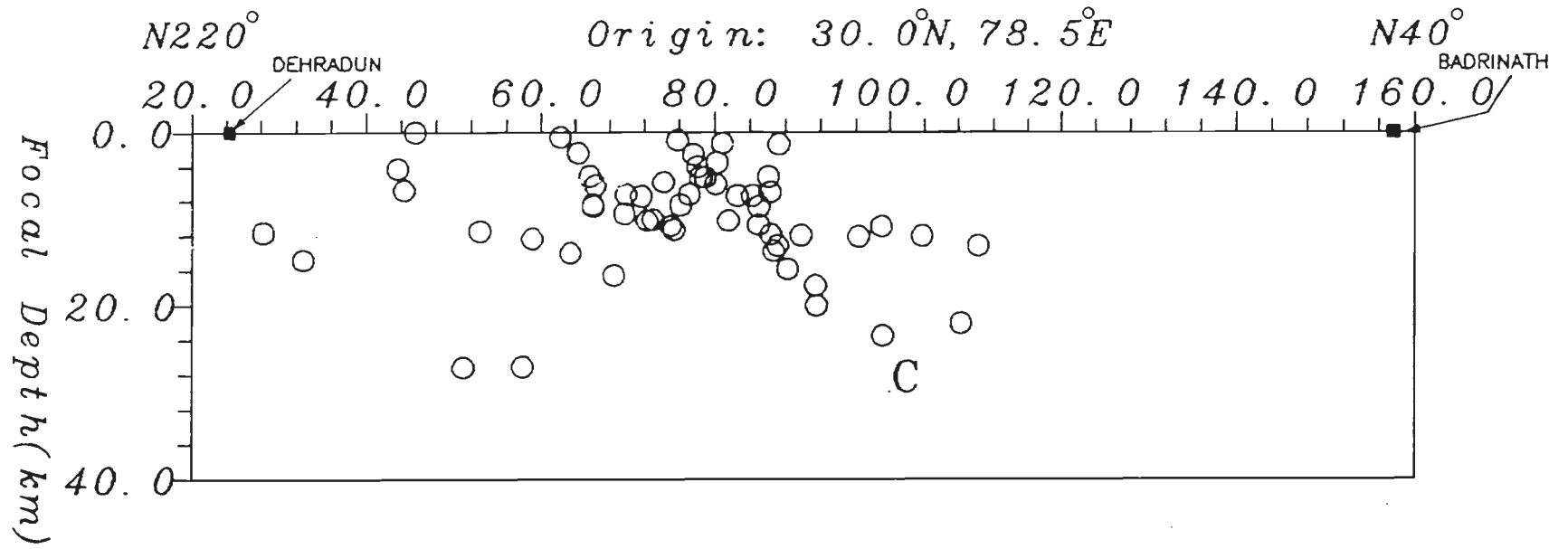
Figure 4·10   Transverse depth section for epicentres of Fig. 4·9.
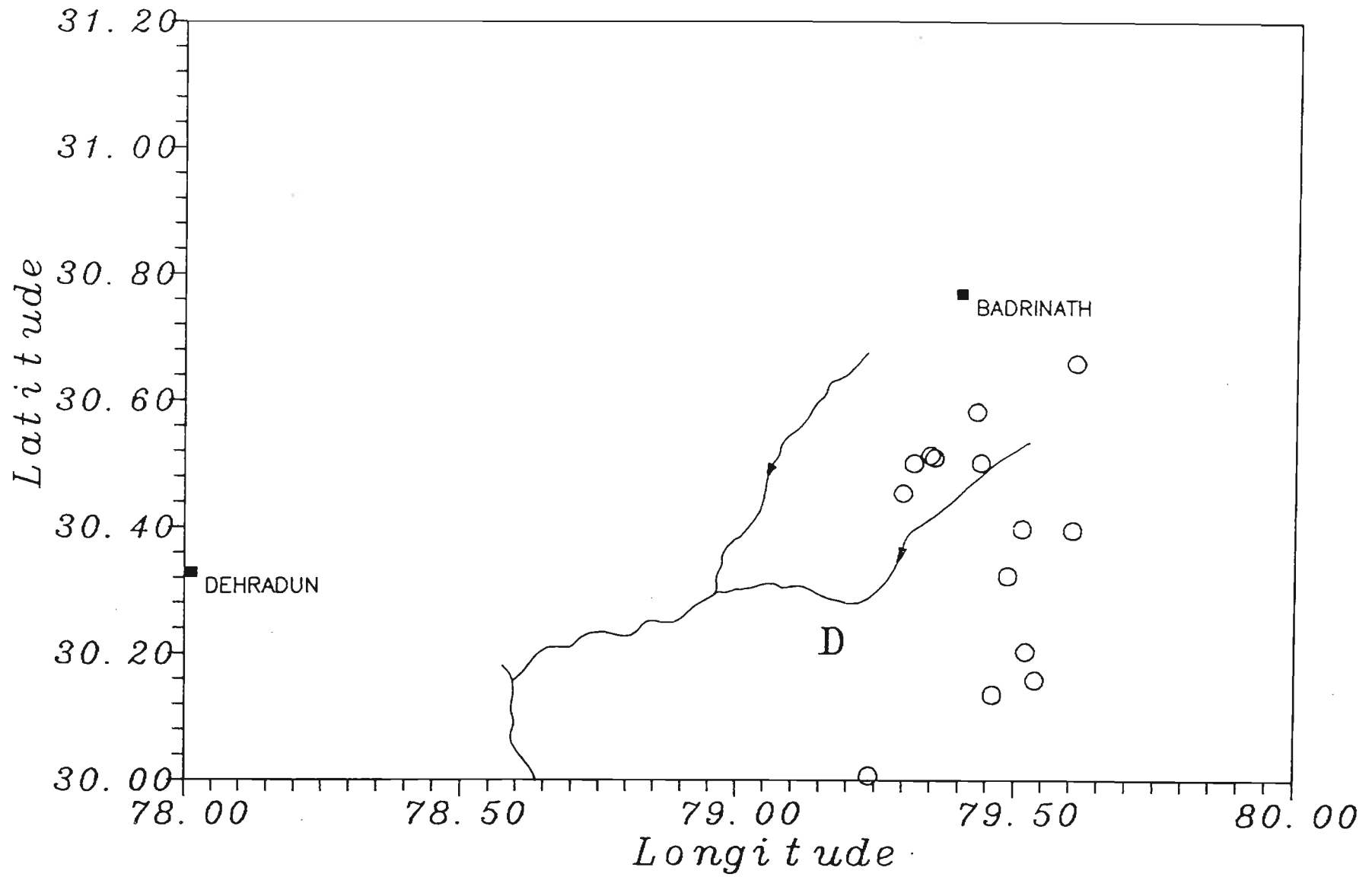
Figure 4·11   Similar to Fig. 4·5 for depth section of Fig. 4·12.
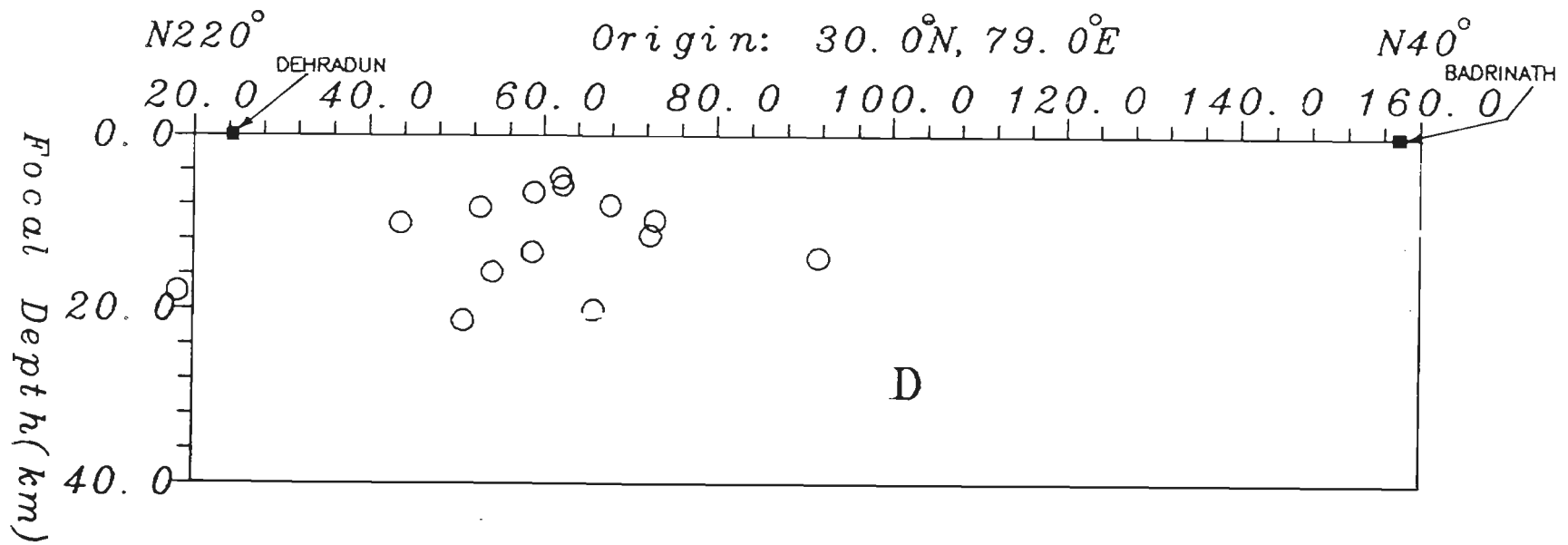
Figure 4·12 Transverse depth section for epicentres of Fig. 4·11.

the coda lengths to our best judgement. The coda magnitude was computed for each station, and the average of the station magnitudes was taken as the earthquake magnitude. The results are shown in Table II.3.

It is observed that the magnitudes of these 152 earthquakes were in the range of 1.0 to 4.2 using Lee (1972)'s formula and -1.4 to 3.5 using Singh (1976)'s formula. Using the results of calculations according to Lee (1972)'s formula, the maximum number of earthquakes appear to have been in the magnitude range of 1 to 3. A lesser number of earthquakes with magnitude 3 to 4 were recorded. There was only one earthquake with magnitude greater than 4 in this lot.

This justifies to some extent our use of the phrase small and micro-earthquakes of the Garhwal Himalaya.

4.7   CLOSURE

Interpretation of the results presented here is taken up in chapters 6 and 7 below.

5

COMPOSITE FAULT PLANE SOLUTIONS

5.1 INTRODUCTION

Fault plane solutions of earthquakes have played an important role in seismology in the understanding of earthquake source process. The first fault plane solution was prepared by Byerly in 1926 using limited data available from the relatively small number of seismograph stations operating at that time. Great progress has been made since then in this field in many different directions. Firstly, stereographic projection was used to portray readings on the focal sphere initially. Currently the use of Wulff's equal area projection is considered desirable. Secondly, there has been improvement brought about in the fault plane solution studies due to improvements in instrumentation. During early days of this endeavour data from short period seismographs had to be used. But, with the availability of WWSSN short and long period seismograms, comparative studies have demonstrated clearly that the use of long period P wave observations yields considerably more consistent solutions. Thirdly, in the early stages, seismograms of a given earthquake had to be either collected through a slow process of exchange or readings provided by different observers had to be used. Again it has been demonstrated that a single observer reading long period WWSSN seismograms obtains solutions with very few or no inconsistent readings. Fourthly, Byerly interpreted the fault plane solution using

the single couple model, whereas today it is more customary to use the double couple model in interpretation of fault plane solutions. Fifthly, these days fault plane solutions based on synthesis of body waveforms are preferred to those based solely on first motion of P waves. Sixthly, the use of S waves to constrain the solutions has been in use for about three decades. Lastly, with the increase in the number of stations worldwide, use of probabilistic techniques to draw the nodal planes has gained favour among the seismologists (e.g. Bullen and Bolt 1985).

It is gratifying that the USGS is providing fault plane solutions based on first P motion data for increasing number of earthquakes every year. However since these solutions make use of observations made by different observers the number of inconsistent readings is large.

The number of such individual fault plane solutions for earthquakes from the Garhwal Himalaya is just two.

In view of the bearing of fault plane solutions on investigations of the active tectonics of a region we have undertaken considerable pains to obtain composite fault plane solutions from the limited short period readings available to us. By exercising restraint in accepting only unambiguous first P motion readings, the number of inconsistent readings has been reduced considerably but not eliminated.

Finally, due to constraints on computer time available we have been forced to use manual methods for drawing nodal planes rather than adopting the probabilistic approach mentioned above.

5.2   OBSERVATIONS AND METHOD OF ANALYSIS

A total of 328 first P motion observations for 115 earthquakes were analyzed. Two special features of the analysis procedure are now mentioned. Firstly, the wave speed model adopted for hypocentral locations is comprised of just two layers, with the upper layer having a thickness of 17 km. Also 85% of the earthquakes considered had focal

depths less than 16 km. Therefore plotting of observations on the Wulff net was on assumption that the ray paths between the hypocentres and the stations were straight lines. Secondly, the relative disposition of hypocentres and recording stations is such that the use of upper hemisphere projection is logical. However, since lower hemisphere projection of focal spheres are by far the most common, therefore we display our results through lower hemisphere projections.

5.3   RESULTS

As noted above the available first P motion data appear to satisfy three composite fault plane solutions.   These will be described in this section.   .

5.3.1 Strike slip solution

A strike slip type composite fault plane solution (Fig. 2.12) has been reported by Sarkar (1983) and Gaur et al (1985) using first P motion observations mainly from earthquakes occurring between the Tons and Bhagirathi valleys. First P motion data from 115 earthquakes of this study were superimposed, one earthquake at a time, on this fault plane solution. First P motion data for only 19 of these earthquakes were seen to be consistent with this fault plane solution. Fig. 5.1 is a epicentral map of these 19 earthquakes. Fig. 5.2 is a display of the composite fault plane solution in which the first P motion data of the earthquakes is plotted. The nodal planes shown in this figure are taken from Fig. 2.12. There are a total of 9 inconsistencies out of a total population of 74 first P motion data. The east-west nodal *plane* would have sinistral slip were it to be the fault plane. The north-south nodal plane would have dextral slip similarly. The east-west striking nodal plane had been picked as the fault plane by Sarkar (1983) and Gaur et al (1985) on the basis of parallelism with local epicentral belt located by them between Bhagirathi and Yamuna valleys. This cannot be offered as a reason for choosing the same nodal plane from the new data as the epicentres have a more NW-SE trend (Fig. 5.1). Jain
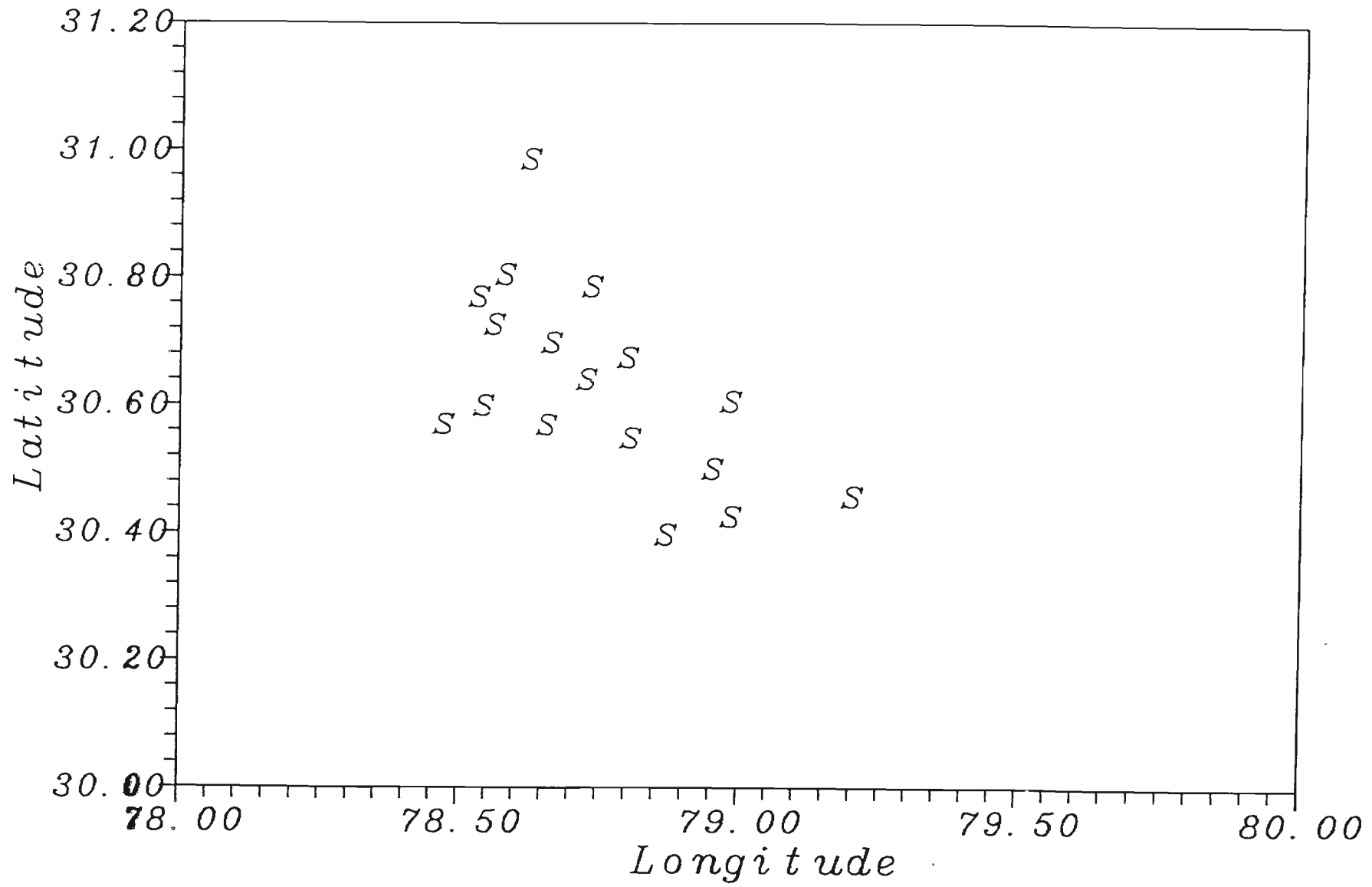
Figure 5·1   Epicentres of earthquakes contributing to strike-slip fault plane solution of Fig. 5·2.
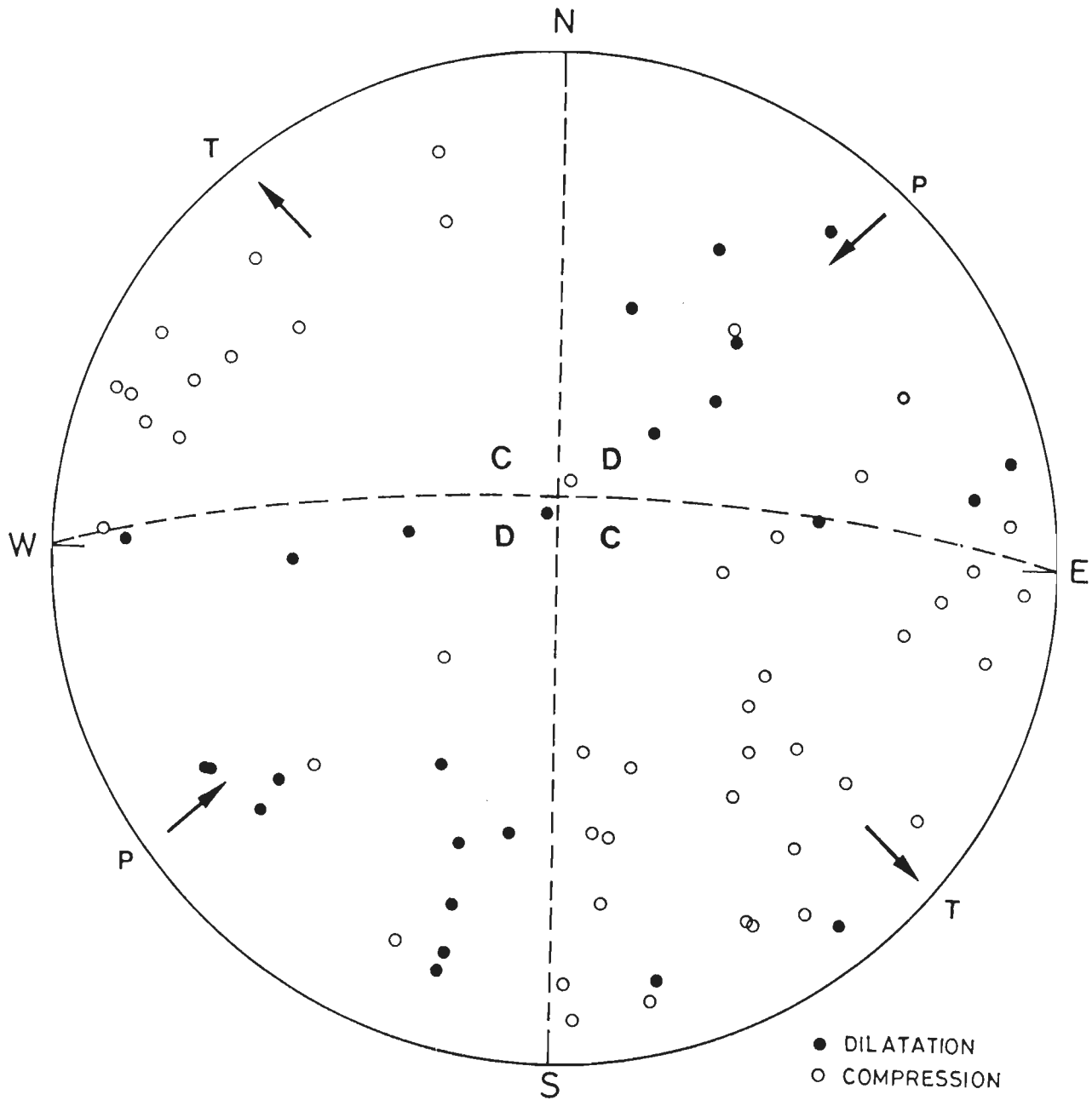
Figure 5·2 Composite fault plane solution for earthquakes of Fig. 5·1.

(1987) observed EW sinistral and NS dextral slip features in his study of lineaments of the Garhwal Himalaya. These are consistent with the sense of slip on the nodal plane of Fig. 5.2. Hence the possibility exist either one of the nodal plane could be a fault plane in all these earthquakes, or one nodal plane could be the fault plane for some earthquakes and the other nodal plane could be the fault plane for the remaining earthquakes. Table III.1 of Appendix III gives first motion informations of each earthquake at stations operated.

5.3.2 Reverse/Thrust type fault plane solution

Fig. 5.3 is a display of epicentres of 60 earthquakes yielding 181 first P motion data which contributed to the fault plane solution shown in Fig. 5.4. It transpires that the nodal planes shown lead to only 18 inconsistent readings. The distribution of dilatation and compression is such that the slip would be of the reverse type on both planes. One nodal plans dips along N222° at 30° and would be a thrust fault. The other nodal plane dips along N42° at 60° and would be a reverse fault. The strikes of both these nodal planes are identical and are subparallel to the local trend of the Himalaya.

Numerous thrust faults have been mapped in the Himalaya generally and also in the Garhwal Himalaya. Due to difficulties of field observations, the dips of these faults have not been measured reliably in general. Still the impression remains that these are generally high angle faults at the surface. Thus it is logical to some extent to choose the nodal plane dipping steeply in the N42° direction at 60° as the fault plane for these earthquakes. Molnar (1990), as also Baranowski et al (1984), have shown that in the individual fault plane solutions based on teleseismic data for moderate Himalayan earthquakes, the nodal plane picked as the fault plane dips gently under the Himalaya and is of the thrust type. Details about the dips and strikes of these nodal planes are given in Table 5.1. Table III.2 of Appen lix III gives first motion informations of each earthquake at stations operated.

A preference for a nodal plane to be regarded as the fault plane has been given

TABLE 5.1 NUMERICAL DATA FOR THE REVERSE / THRUST SOLUTION OF FIG.5.4

S. No.		STRIKE	DIP
1.	Nodal plan 1	N 48°W - S 48°E	60° along N 42°E
2.	Nodal plan 2	N 48°W - S 48°E	30° along S 42°W
		Trend	Plunge
3.	Pressure axis	N 42°E - S 42°W	15° along N 42°E
4.	Tension axis	N 42°E - S 42°W	75° along S 42°W
5.	b axis	N 48°W - S 48°E	Nil
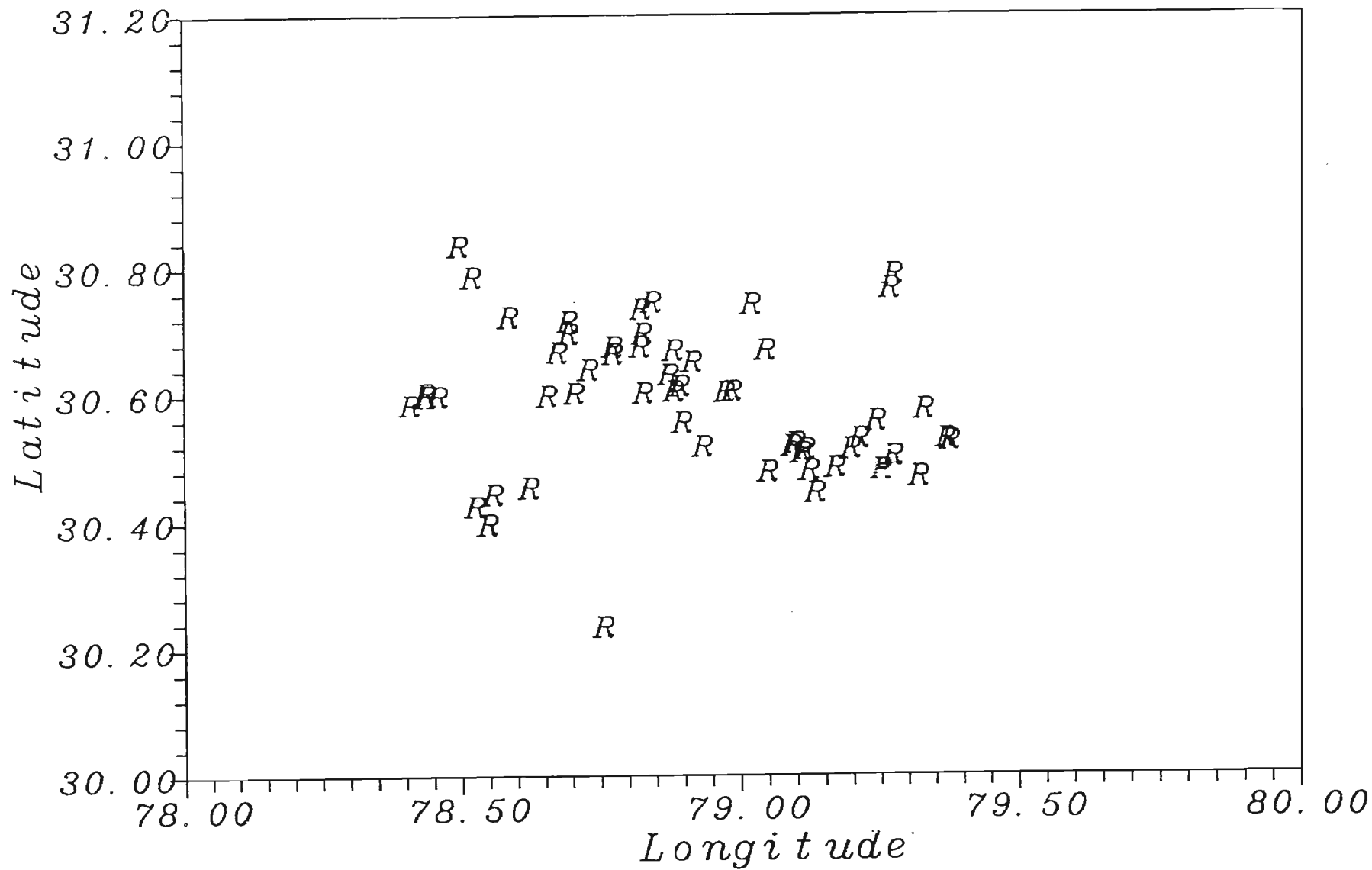
Figure 5·3 Epicentres of earthquakes contributing to Reverse/Thrust fault plane solution of Fig. 5·4.
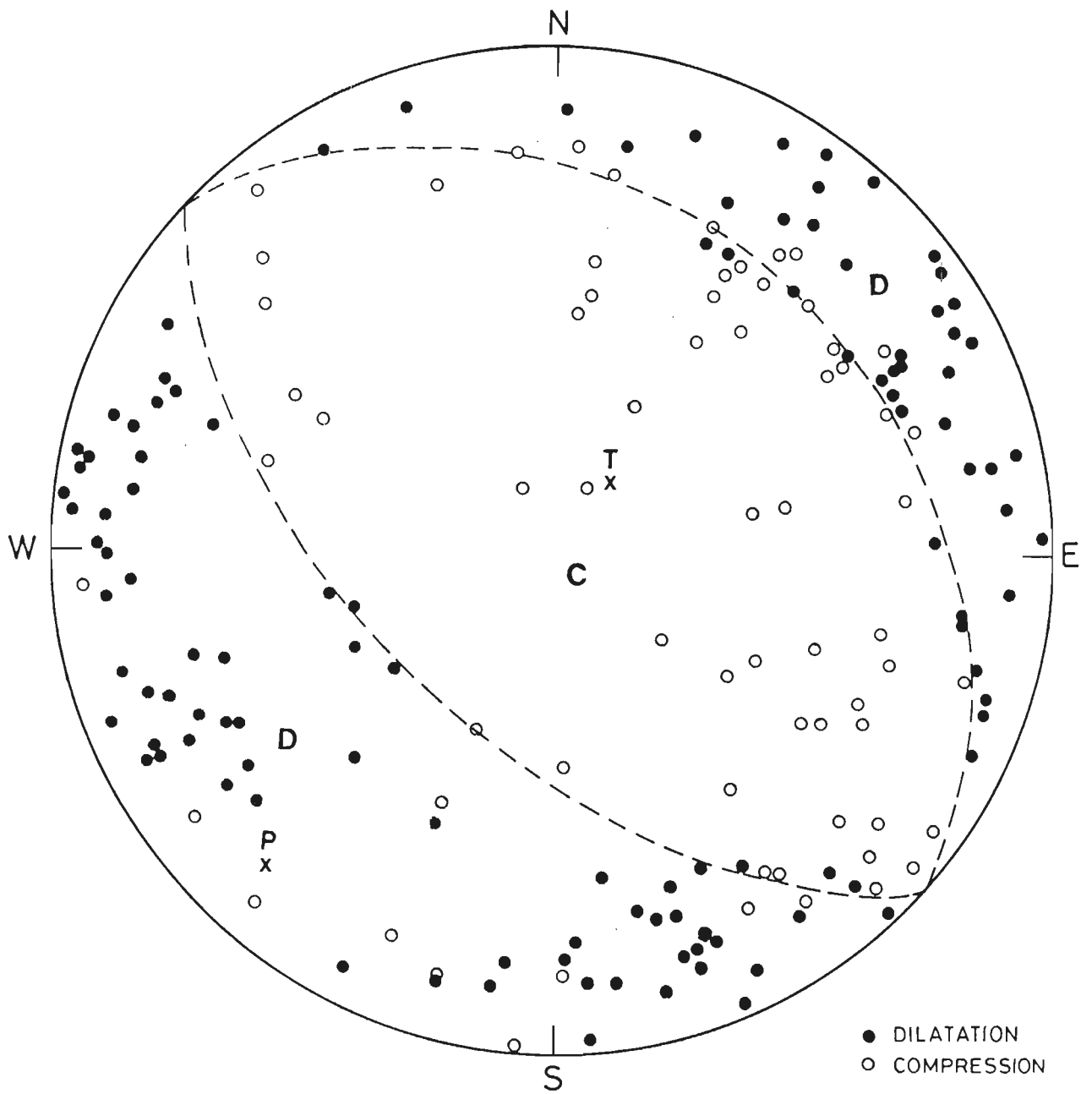
Figure 5·4 Composit fault plane solution for earthquakes of Fig. 5·3.

for the solution shown in Fig. 5.4. We shall argue in Chapter 7 that this choice of nodal planes as the fault plane could be interpreted as supporting the view that the Higher Himalaya are rising relative to the Lesser Himalaya currently.

5.3.3 Normal fault type composite solution

Fig. 5.5 is a plot of epicentres of 36 earthquakes which yielded 73 first P motion data contributing to the composite fault plane solution shown in Fig. 5.6. The distribution of compressions and dilatations is such that reasonably constrained nodal planes striking north-south can be drawn Motion would be pure dip-slip with hanging wall moving down in the both cases. One nodal plane dips east at 30^0 and the other west at 60^0. There are no clues in the local geology, tectonics and seismicity to choose one nodal plane as the fault plane. However the steeper dipping plane could be preferred because such faults could be oriented favourably for reactivation under east-west directed tensional stresses.

A very remarkable feature of this fault plane solution in that the strikes of its nodal planes are comparable to those of the nodal planes for the fault plane solution of the 1975 Kinnaur earthquake (Fig. 1.3 and Fig. 5.7). The west dipping nodal plane has a dip amount of 50^0 (Molnar and Lyon-Caen 1989) for Kinnaur earthquake and 60^0 for the composite solution of Fig. 5.6. Table III.3 of Appendix III gives first motion informations of each earthquake at stations operateu.

Hence it seems desirable to give importance to this solution as it implies tectonic affinities across the Higher Himalaya.

5.4 IMPLICATIONS FOR THE UPPER CRUSTAL STRESS REGIME IN THE GARHWAL HIMALAYA

In the last two decades a number of studies have been carried out to determine the state of regional stresses from comprehensive inversion of nodal plane and slip orientation data for a group of fault plane solutions belonging to earthquakes in a limited region of the
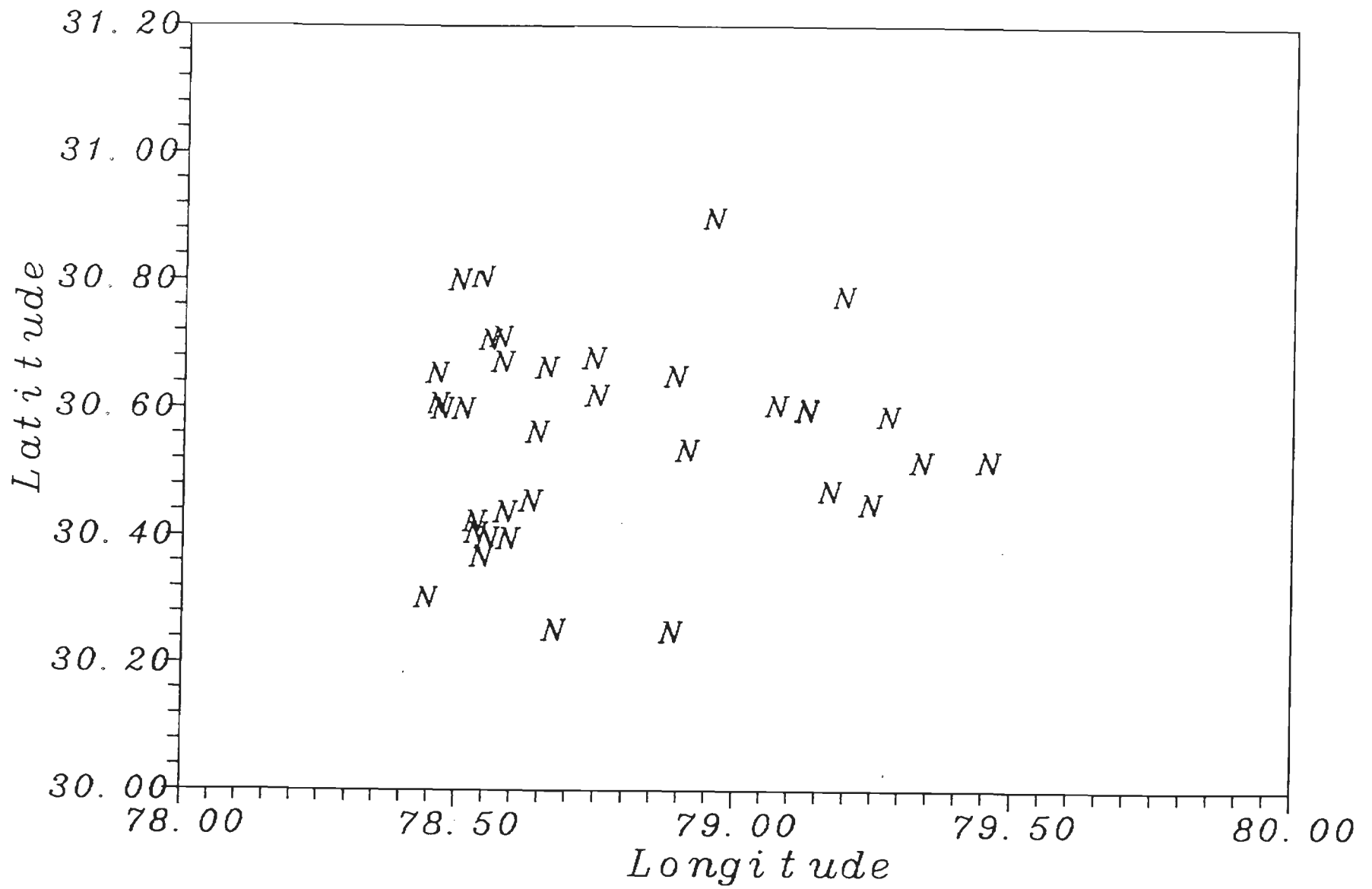
Figure 5·5   Epicentres of earthquakes contributing to normal fault solution of Fig. 5·6
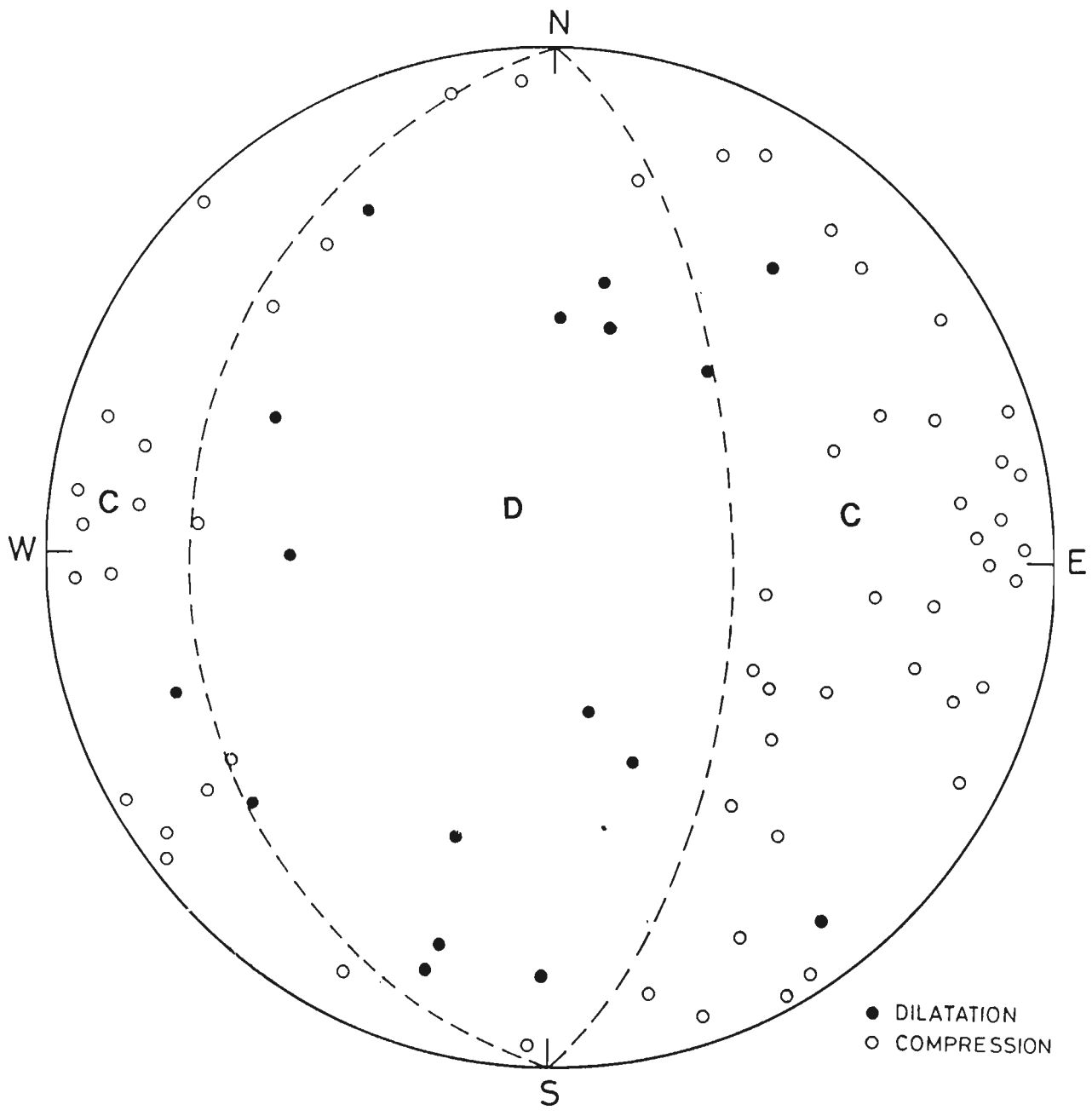
Figure 5·6   Composite fault plane solution for earthquakes of Fig. 5·5.
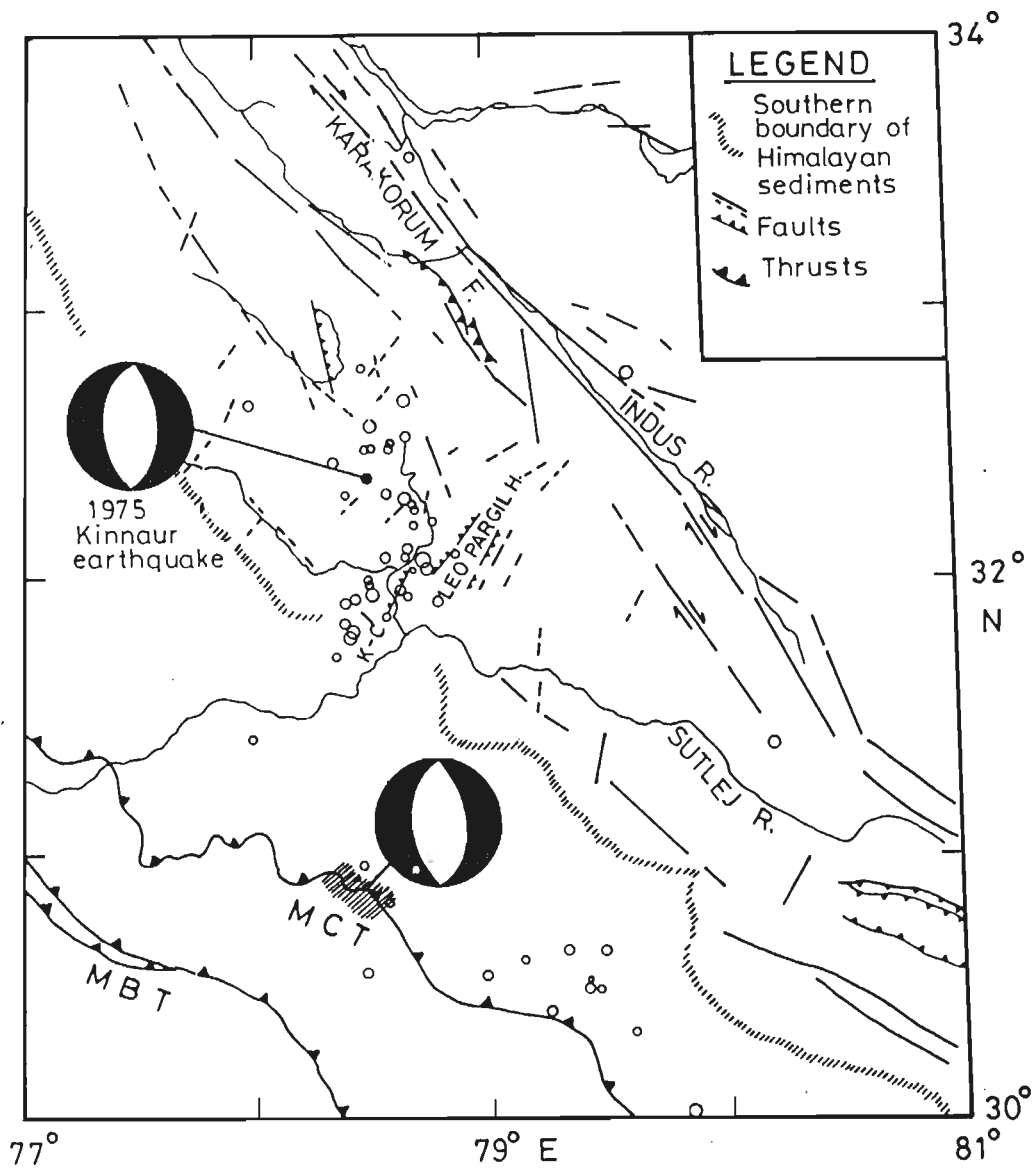
Figure 5·7   Comparison of normal fault solution of Kinnaur
earthquake and the solution of Fig. 5·6

crust. A key feature of such studies is the assumption that the inferred direction of slip is the direction of shear stress in the fault plane. The area in which the present 152 earthquakes have occurred is reasonably compact and it seems desirable to determine if a common stress field would cause all these earthquakes. Figs. 5.8, 5.9 and 5.10 are depth sections along east-west direction showing hypocentral positions of strike-slip, reverse/ thrust and normal fault type composite solutions. Examination of Figs. 5.1, 5.3, 5.5, 5.8, 5.9 and 5.10 suggests that hypocentres of earthquakes contributing to the three types of fault plane solutions are spatially inseparable. Thus at a cursory level it would have to be inferred that a fairly heterogeneous stress state prevails in the upper crust in the region of interest. However the following arguments tends to lessen the severity of this remark. Let us assume firstly that all these earthquakes occur by reactivation of pre-existing faults. Secondly let us recall that Mount and Suppe (1987) indicated from an analyses of well-bore breakout data from central California that the San Andreas fault is slipping under the action of maximum and intermediate principal stresses. We shall assume that this could happen in the case of strike slip faults involved in the occurrence of the concerned earthquakes of the Garhwal Himalaya also. Then a thrust fault type stress regime for which maximum principal stress is horizontal along N42°E and minimum principal stress is vertical could cause slip on strike slip and reverse/ thrust fault planes of the above orientations. The difficulty with this proposal is that we have to postulate suitably low angles of friction on these faults. Alternatively if angle of friction in the range of 35° (coefficient of friction of the order of 0.60 or 0.65) are postulated then suitably high pore pressures in the upper crust would be required. This is especially true for the reverse/thrust solution. We may recall again that the Miramachi earthquake sequence in eastern Canada involved motion on high angle reverse faults under a thrust fault type stress regime and that Sibson (1989) has postulated supralithostatic pore pressures to be involved. Davis et al (1983) have estimated pore pressures in the Himalaya at 0.76 lithostatic assuming a critically tapered wedge to exist in the Himalaya. Our
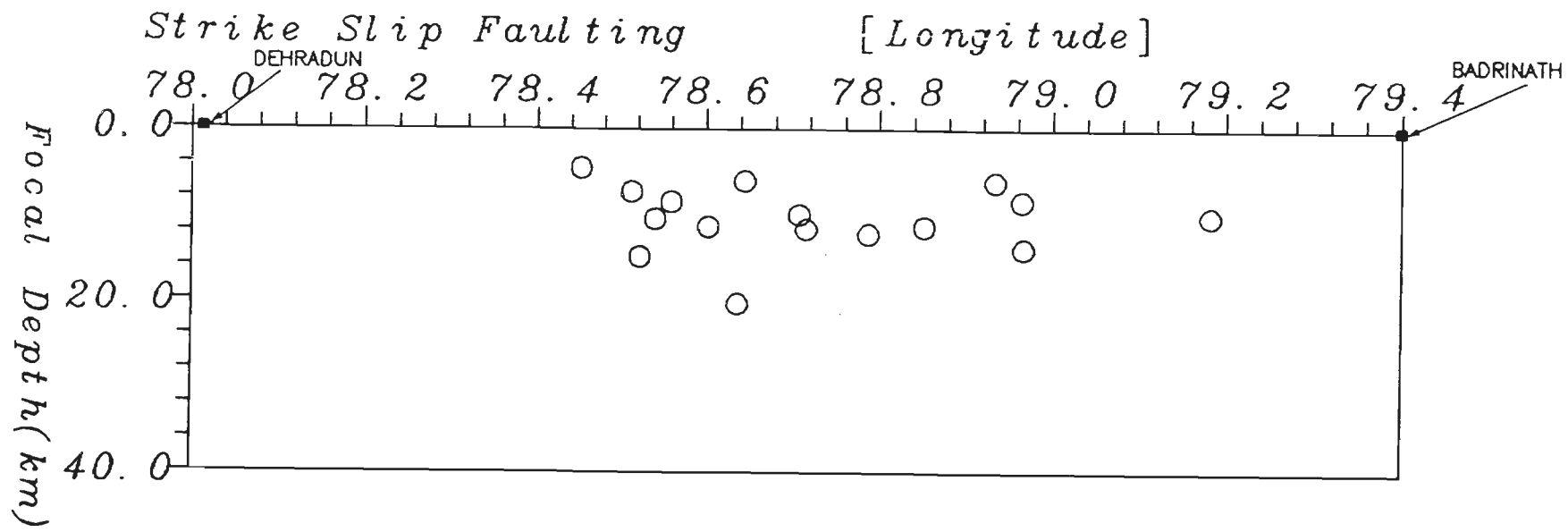
Figure 5·8   Depth section for earthquakes of Fig. 5·1 .
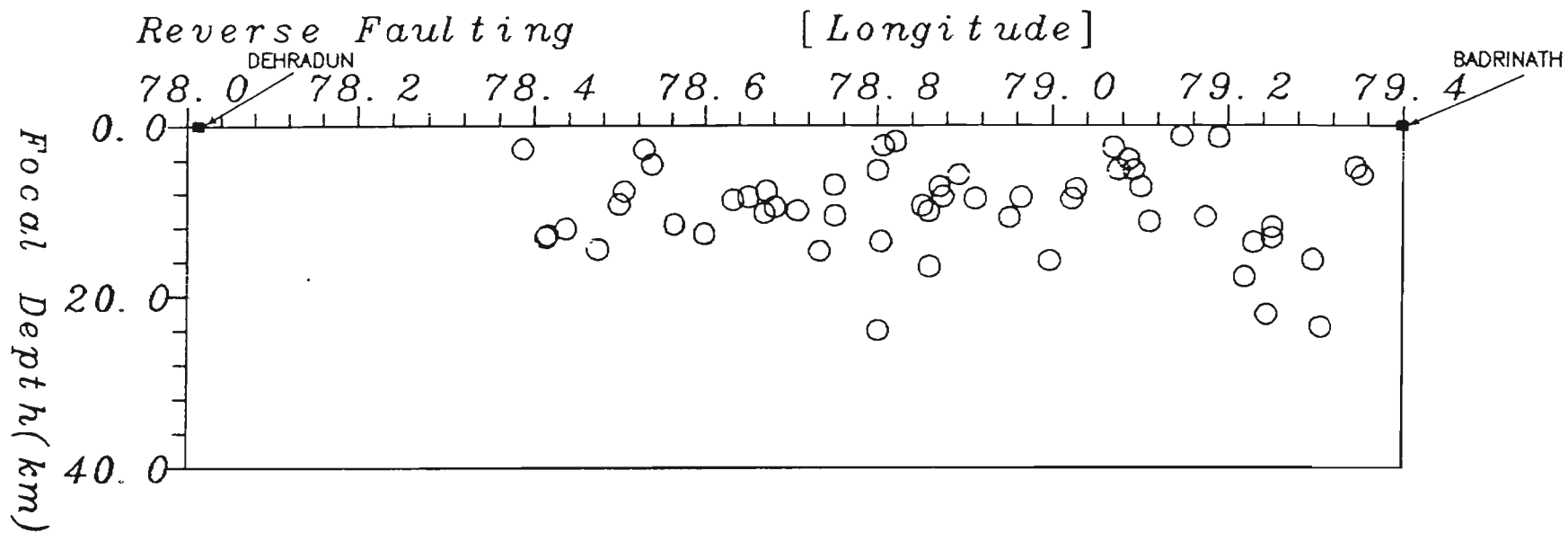
Figure 5·9   Depth section for earthquakes of Fig. 5·3.
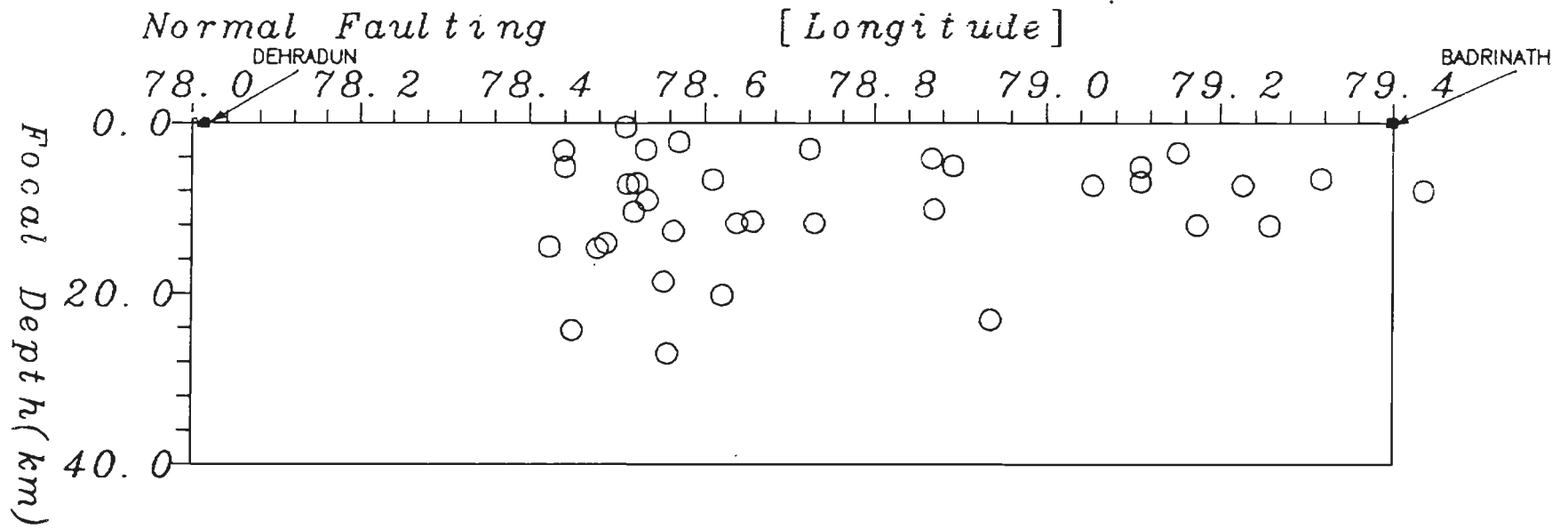
Figure 5·10 Depth section for earthquakes of Fig. 5·5.

preference would be to consider high but sublithostatic pore pressures and equivalently lower friction angles for the faults.

Unfortunately, in the present study, the normal fault type earthquakes are relatively more numerous then the strike slip type earthquakes. The reactivation of the former cannot be envisaged in a thrust type stress regime. Even the orientation of horizontal principal stresses has to be different for normal fault type earthquakes as compared to that postulated above for reverse/thrust and strike slip type earthquakes. Thus some spatial heterogeneity in the orientation of principal stresses has to be postulated.

5.5   SUMMARY

Keeping in mind that short period instruments and high frequency P waves had to be considered, the first P motion data for the earthquake investigated have yielded composite fault plane solutions with remarkably few inconsistencies. However the fault plane solutions are so different from each other that these are difficulties in formulating a homogeneous stress state for the region.

81

6

SYNTHESIS OF RESULTS FOR SMALL AND MICRO-EARTHQUAKES OF GARHWAL HIMALAYA

6.1   GENERAL

There were two distinct phases between 1979 and 1986 when substantial amounts of field recorded data for small and micro-earthquakes were obtained from the Garhwal Himalaya. The results obtained during 1984-86 have been presented in the previous two chapters. We synthesize here those results with results obtained during 1979-80.

6.2   RECORDING STATION ARRAYS

Figs. 2.10 and 3.1 display the recording stations used during 1979-80 and 1984-86. The 1979-80 data were obtained with stations set up in the Yamuna and Bhagirathi valleys. The 1984-86 results were obtained with stations setup in different accessible valleys between Bhagirathi and Alaknanda rivers. Only for a brief period one of the stations in 1984-85 was operated on the banks of the Bhagirathi river. However, since there were other nearby stations operating also, there is no loss in quality of the results from the stand point of station coverage in the region immediately southeast of the Bhagirathi valley. The only problem with the entire field work was that because of the hostile terrain sufficient number of stations could not be setup north of the MCT.

6.3 SYNTHESIS OF EPICENTRAL DATA

Fig. 6.1 is a combined display of 193 epicentres from the 1979-80 recordings and 152 epicentres from the 1984-86 recording which have been shown separately in Figs. 2.11 and 4.1 respectively. Seismicity over a distance of about 110 km in the Garhwal Himalaya is thus examined with relatively more reliable epicentral locations, falling within or close to the respective recording arrays. Information is obtained over an additional distance of about 50 km using data for earthquakes which occurred some distance outside the arrays. The maximum width of the roughly NW-SE oriented main belt is 50 km. However, a view could be entertained that the width of the belt is about 30 km generally, though a cluster of epicentres lies outside this belt at about 78.5° E and 30.4° N.

6.4 FOCAL DEPTHS

Fig. 6.2 and Table 6.1 provide frequency depth information about the combined 345 small and micro-earthquakes examined from the two periods of recording. The overwhelming conclusion remains that much of this seismicity occurs in the upper crustal layer with a relatively small percentage of earthquakes occurring at greater depths up to 30 km. A depth section along N128° is displayed in Fig. 6.3 and it reinforces this conclusion.

6.5 COMPOSITE FAULT PLANE SOLUTION

A composite fault plane solution (Fig. 2.12) has been reported by Sarkar (1983) and Gaur et al (1985) based on first P motion data from earthquakes occurring in 1979-80, west of Bhagirathi valley. As pointed out in the previous chapter. 19 earthquakes occurring southeast of Bhagirathi valley during 1984-86 have yielded first motion data consistent with this solution (Fig. 5.2). But the majority of the newer first P motion data indicate two additional types of earthquake source mechanisms operating in the region southeast of the Bhagirathi valley.
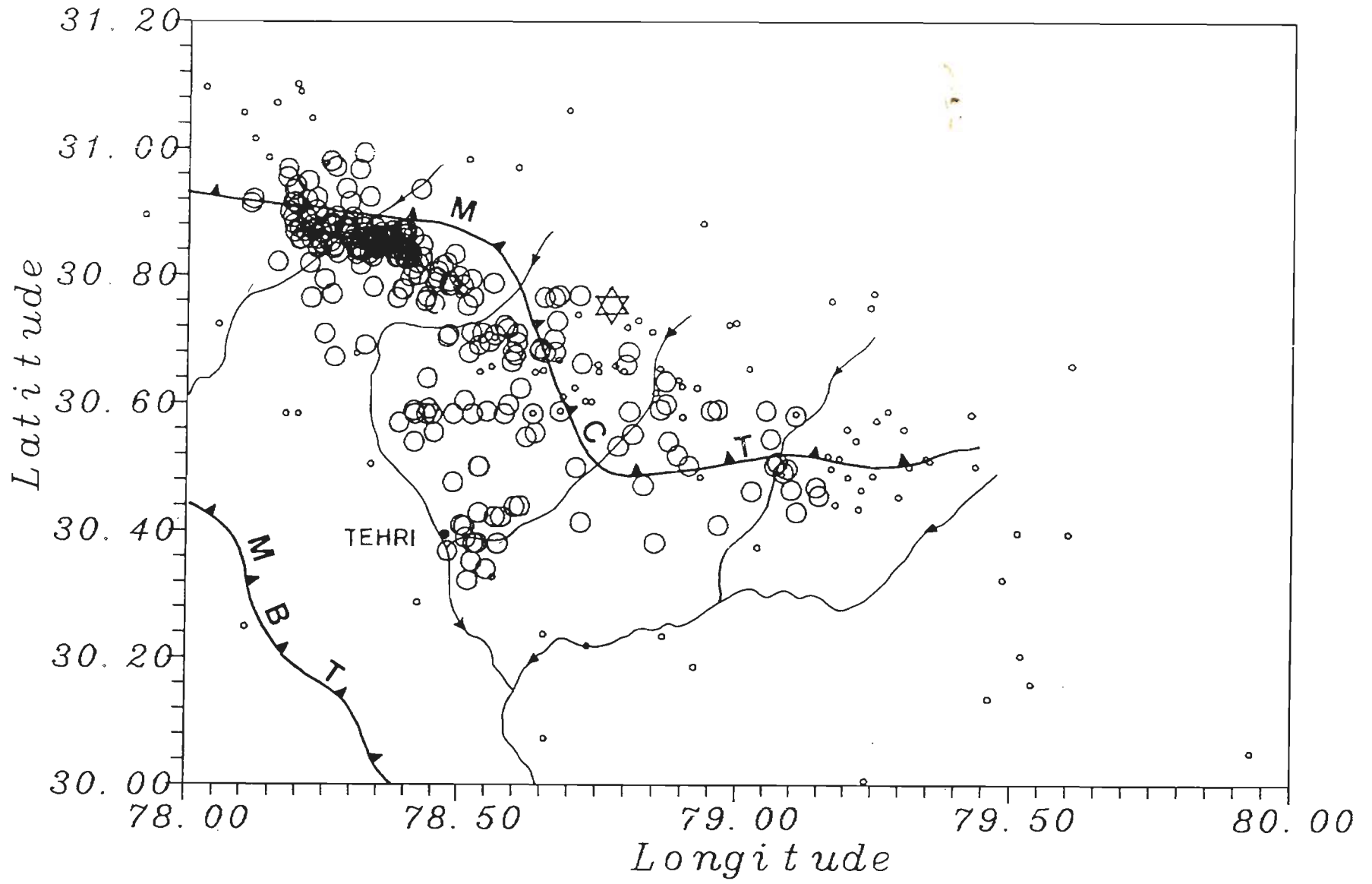
Figure 6·1 Combined epicentral plot of Figs. 2·11 and 4·1. Small circles for earthquakes occurring outside the array.
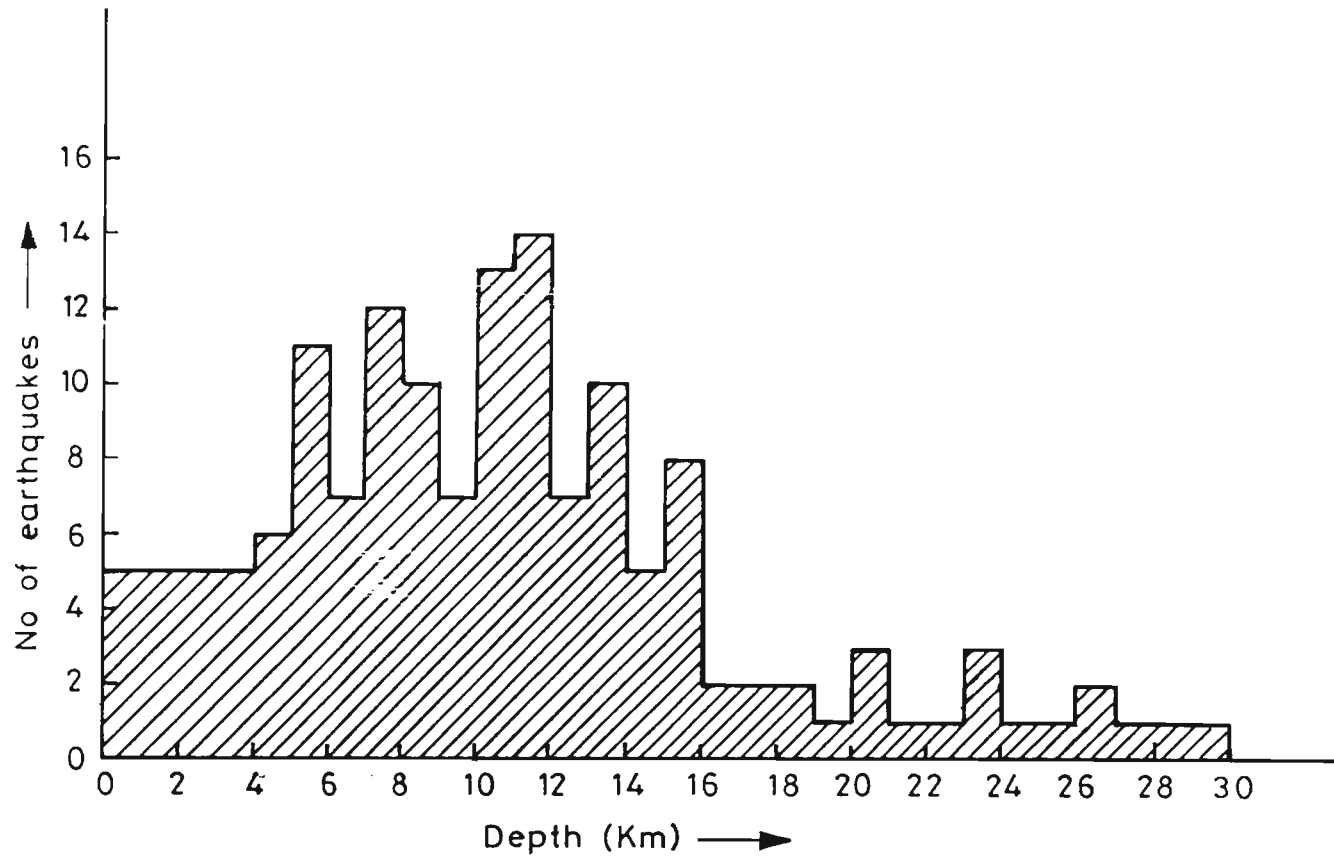
Figure 6·2   Histogram showing the number of earthquakes
versus depth of focus for an estimated 152
earthquakes recorded during 1984–86.

TABLE 6.1   DISTRIBUTION OF ESTIMATED FOCAL

DEPTHS IN 1 KM INTERVALS

Depth interval (km)	Number of earthquakes in the interval	Cumulative Number
0 -	21	21
1 - 2	25	46
2 - 3	30	76
3 - 4	26	102
4 - 5	20	122
5 - 6	28	150
6 - 7	24	174
7 - 8	17	191
8 - 9	21	212
9 - 10	13	225
10 - 11	19	244
11 - 12	21	265
12 - 13	13	278
13 - 14	12	290
14 - 15	09	299
15 - 16	10	309
16 - 17	03	312
17 - 18	03	315
18 - 19	06	321
19 - 20	04	325
20 - 21	04	329
21 - 22	01	330
22 - 23	04	334
23 - 24	04	338
24 - 25	01	339
25 - 26	01	340
26 - 27	02	342
27 - 28	01	343
28 - 29	01	344
29 - 30	01	345
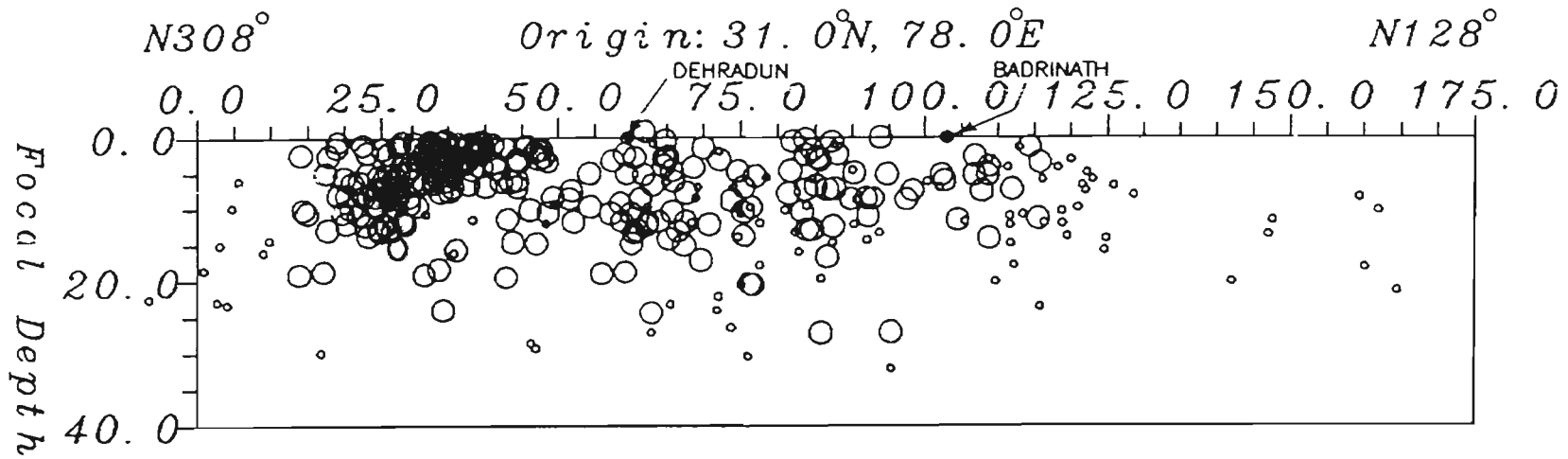
Figure 6·3 Combined depth section for earthquakes of Fig. 6·1.

6.6   SUMMARY

The hypocentral information for small and micro-earthquakes of the Garhwal Himalaya obtained from two periods of recording over different but adjacent parts of the region is of a piece. The seismic belt defined lies astride the MCT. The earthquakes occurred in the upper crust but show fault plane solution of all three main types namely, strike slip, reverse/thrust and normal fault type. South east of the Bhagirathi valley the three types of source mechanisms appear to be operative simultaneously on a regional scale.

7

DISCUSSION

7.1 GENERAL

We raise in this chapter several points which emerge when the data obtained from local recording of small and micro-earthquakes in the Garhwal Himalaya are combined with information for moderate and great earthquakes of the region.

7.2 CORRELATION BETWEEN HYPOCENTRES OF LOCALLY AND TELESEISMICALLY LOCATED EARTHQUAKES OF THE GARHWAL HIMALAYA

7.2.1 Epicentral locations

Fig. 2.7 is a display of teleseismically located earthquakes of the Garhwal Himalaya up to 1992. The rupture zone of the 1905 Kangra earthquake according to Gahalaut and Chander (1992) is also shown in the Fig. 2.7.

Figs. 7.1 and 7.2 show combined epicentral plots of the teleseismically located earthquakes (Fig. 2.7) and the 345 locally located earthquakes (Fig. 6.1). Both the Figs. 7.1 and 7.2 have identical data. However, the teleseismically located earthquakes are shown by the larger symbols in Fig. 7.1 and by smaller symbols in Fig. 7.2. This has been done to emphasise the relative importance of the two sets of the data from two different view points.
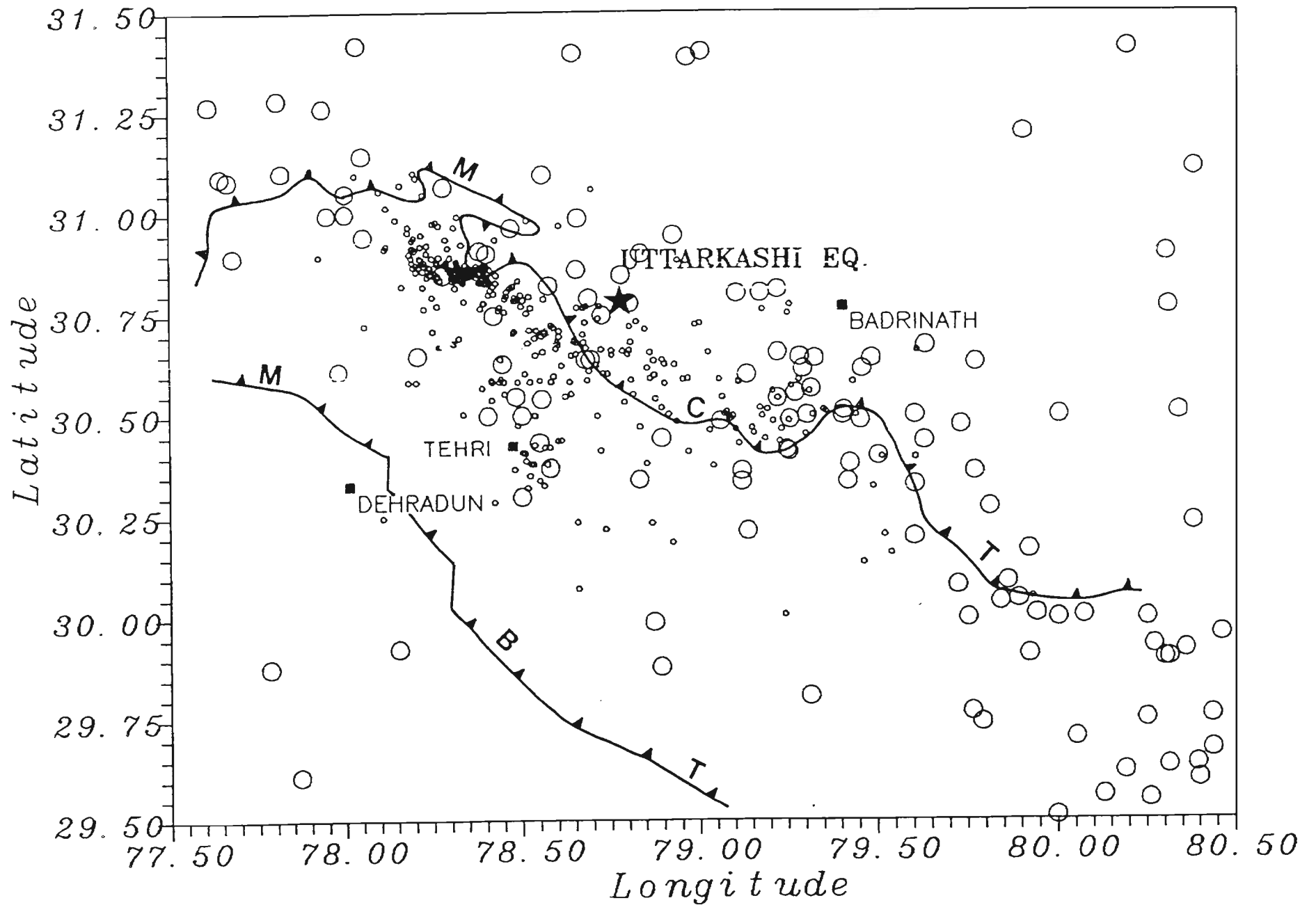
Figure 7.1 Seismicity of garhwal himalaya. Small circles for locally recorded earthquakes. Large circles for teleseismic epicentres.
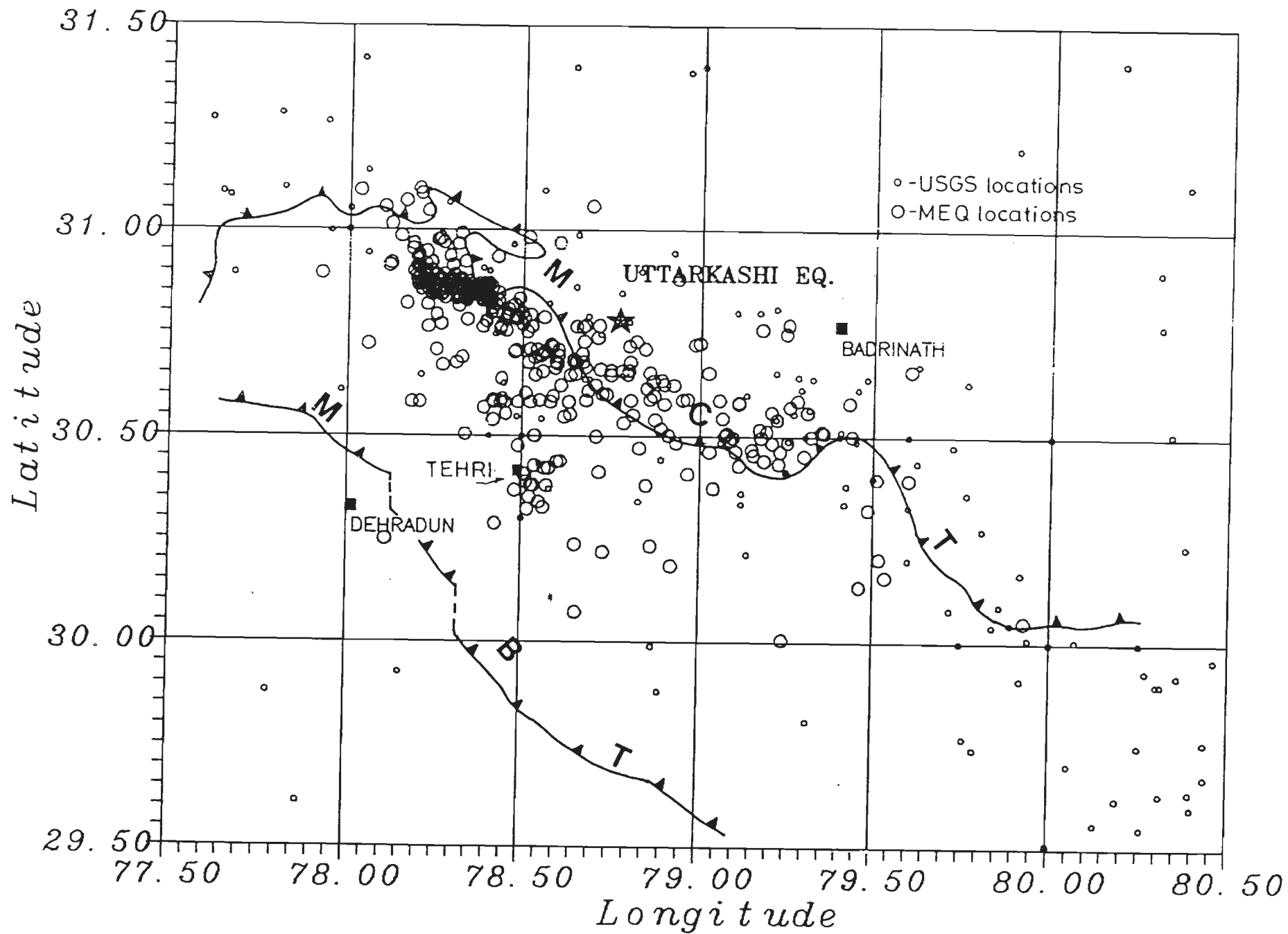
Figure 7·2 Same as fig. 7·1 sizes of symbols reversed.

The most important conclusion of Figs. 7.1 and 7.2 is that the epicentral belts of the moderate earthquakes on the one hand and small and micro-earthquakes on the other hand are spatially coincident. The teleseismically located epicenters are more dispersed. This probably reflects the point raised in Section 2.3.3.1. It was pointed out there that estimates of the epicentral location of a moderate earthquake of the Bhagirathi valley from the 1979-80 based on teleseismically and locally recorded data differed by about 23 km. The location based on local data is relatively more reliable in our opinion. Moreover, the scatter in teleseismically located epicentres may also be due in part to the fact that they cover a period of many decades over which the quality of locations has improved gradually.

7.2.2 Comparison of focal depths of locally and teleseismically located hypocentres

We mentioned in chapter-2 that the hypocentral depths of teleseismically located earthquakes so far have been unreliable in the vast majority of the cases. Focal depths of four such earthquakes are however known more reliably on the basis of depth phases in three cases and waveform synthesis in one case. These depths range between 10 and 13 km in three cases. The depth was 18 km. in the last case. When these data are combined with the fact that a vast majority of locally recorded earthquakes occur in the upper crustal layer, it appears that there may be reasonable overlap in the focal depths of the moderate, small and micro-earthquakes also.

7.2.3 Closure

Thus the hypocentres of the teleseismically and locally recorded earthquakes of the Garhwal Himalaya appear to occur in roughly the same region of the upper crust though at a slightly more refined level it may be suggested that the moderate earthquakes occur towards the basal part of the upper crustal region on which small and micro-earthquakes have been located.

7.3 FAULT PLANE SOLUTIONS OF MODERATE AND SMALL EARTHQUAKES

First P motion data from 60 small and micro-earthquakes of 1984-86 recording yielded a reverse/thrust type fault plane solution (Fig. 5.4). The northeast dipping plane had a high dip of 60°. Motion was reverse type on this as well as the other nodal plane. In comparison individual fault plane solutions of two moderate earthquakes of the region, namely, the earthquake of July 16, 1986, and the 1991 Uttarkashi earthquake, are available. The strikes of the nodal planes in these solutions differ to some extent but the similarity between the two is that in each case one nodal plane has a gentle dip in the NNE-NE range of directions and thrust type slip. In addition strike slip and normal fault type composite solutions for locally recorded earthquakes have been reported above.

It thus appears that although the small and micro-earthquakes and the moderate earthquakes occur in spatially coincident belts yet their fault plane solutions shows considerable variation. It is to be noted also that the general character of the fault plane solutions of moderate earthquakes from Garhwal Himalaya are similar to those from other parts of the Himalaya.

7.4 ABOUT CASES OF ACTIVE STRESSES

A discussion of stresses responsible for the observed small and micro-earthquakes of the Garhwal Himalaya has been given in section 5.4. A completely homogeneous stress field appears difficult to conceive. But the data are too few to proceed with inversion of fault plane solution for the causative stresses.

7.5 ON THE CAUSE OF GARHWAL HIMALAYAN EARTHQUAKES

It was pointed out in Chapter 2 that there is a consensus among several investigators, for example, Seeber and Armbruster (1981), Baranowski et al (1984), Ni and Barazangi (1984), Chander (1988), Molnar and Lyon Caen (1989), Yeats and Lillie (1991) that the great and moderate earthquakes of the Himalaya occur along the

detachment in direct response to the underthrusting of the Himalayan rocks by the Indian Shield rocks beneath. We discuss in the following subsections how reverse-thrust type small earthquakes of the region between the Bhagirathi and Alaknanda valleys could be due to the same underthrusting processes ultimately.

7.5.1 Possible cause of reverse/thrust type small and micro-earthquakes

Fig. 7.3 is a projected display of hypocentres of those earthquakes whose first motion data contributed to the reverse thrust type composite fault plane solution (Fig. 5.4). The section in Fig. 7.3 is along the N38° line. The small solid lines drawn through the hypocentres indicate possible faults corresponding to the nodal plane dipping at 60° to N38°. A possible comprehensive interpretation of this figure is that by recording these earthquakes we have identified a fault zone dipping in the northeasterly direction generally. The zone is composed of numerous parallel closely spaced high angle reverse faults. Reverse/thrust type earthquakes on these faults lead to upward slips of hanging wall rocks relative to footwall rocks. A cumulative result of numerous such earthquakes would be to cause a quantum of uplift of the Higher Himalaya relative to the Lesser Himalaya. This is not surprising because even according to Seeber and Armbruster (1981) a ramp may exist in the detachment in this same boundary region between Higher and Lesser Himalaya. Higher Himalayan rocks above the ramp should be moving up relative to the rocks below the ramp in response to the underthrusting by the Indian Shield. In another words, these reverse/thrust type earthquakes may be seen also to be the result of plate tectonic based underthrusting of Himalayan rocks by Indian Shield rocks.

7.5.1.1 Geomorphic evidence

Seeber and Gornitz (1983) examined the river bed gradients for 16 trans-Himalayan rivers which rise north of the Higher Himalaya but eventually flow on the plains of India. These authors showed that the rivers have higher bed gradients in their course
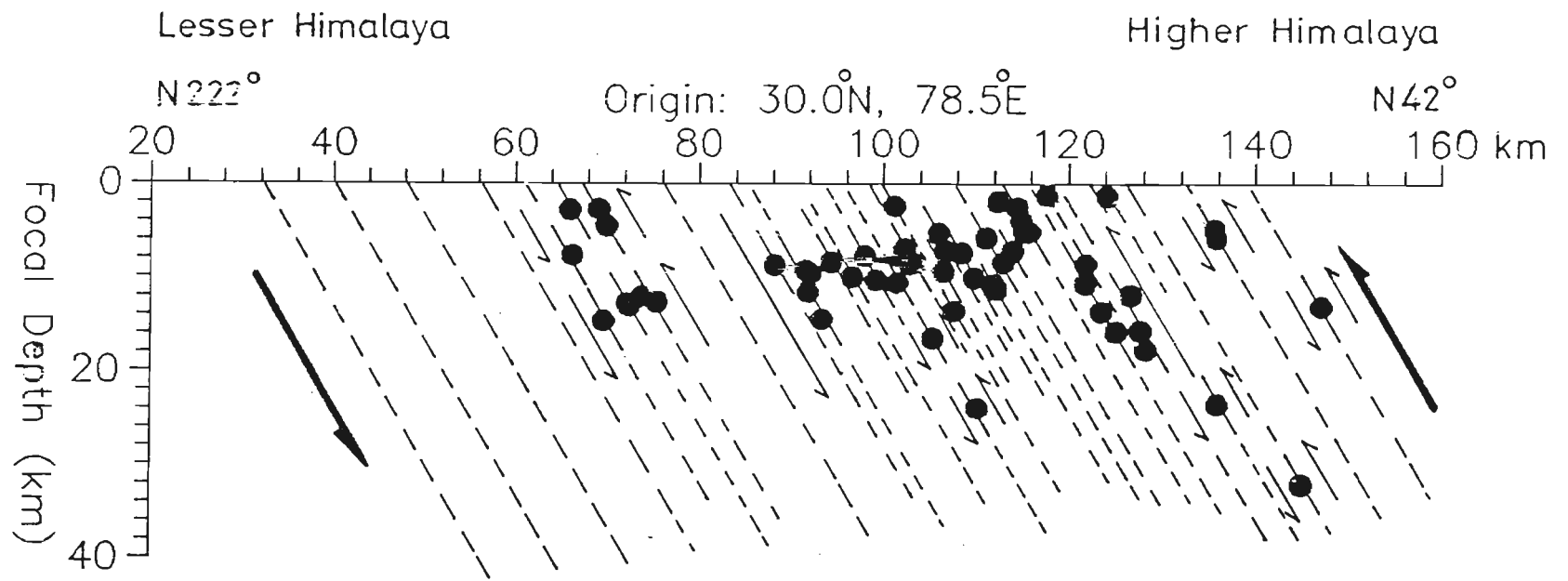
Figure 7·3   Inferred fault zone in the Garhwal Himalaya. Dots indicate hypocentres of earthquakes of Fig. 5·3. The dashed lines are inferred faults corresponding to steeper nodal plane of Fig. 5·4.

through the Higher Himalaya as compared to the gradients upstream and downstream. They put forward elaborate arguments to suggest that this strong evidence for their tectonic model of the Himalaya (section 2.3.1 and Fig. 2.3). Gupta (1983) carried out a similar exercise for six major rivers of the Garhwal Himalaya and found that they had steeper gradients upstream of MCT than downstream. We regard this evidence from geomorphology and fault plane solutions as mutually complementary support for the view that the Higher Himalaya are rising relative to the Lesser Himalaya currently.

7.5.2 About strike slip fault earthquakes

The occurrence of strike slip earthquakes in the same belt may indicate that, in response to the horizontal convergence of the Indian and Tibetan rocks, different transverse slices of the northwest Himalaya may be undergoing dextral relative slip to maintain or enhance the overall arcuate, southward convex shape of the Himalaya (Fig. 7.4). But for this view to hold we have to select the north-south nodal plane as the fault plane in Figs. 2.12 and 5.2.

7.5.3 About Normal fault earthquakes

The normal fault type earthquakes pose a new angle on this matter. The affinity of their fault plane solution (Fig. 5.6) to that for the 1975 Kinnaur earthquake (Fig. 5.7 and section 5.3.3) suggests a complication in this convergence process perhaps in response to some topographic features along the top of the underthrusting Indian Shield. For example, it has been suggested that north easterly trending, ancient Aravalli mountains of Peninsular India may extend under the Outer, Lesser and even the Higher Himalaya (Fig. 1.3). Such a topographic feature on the surface of the underthrusting plate could disturb the stress there in the overlying Himalayan rock cover (Fig. 7.5) to promote flexure and attendant tensile stresses.

96
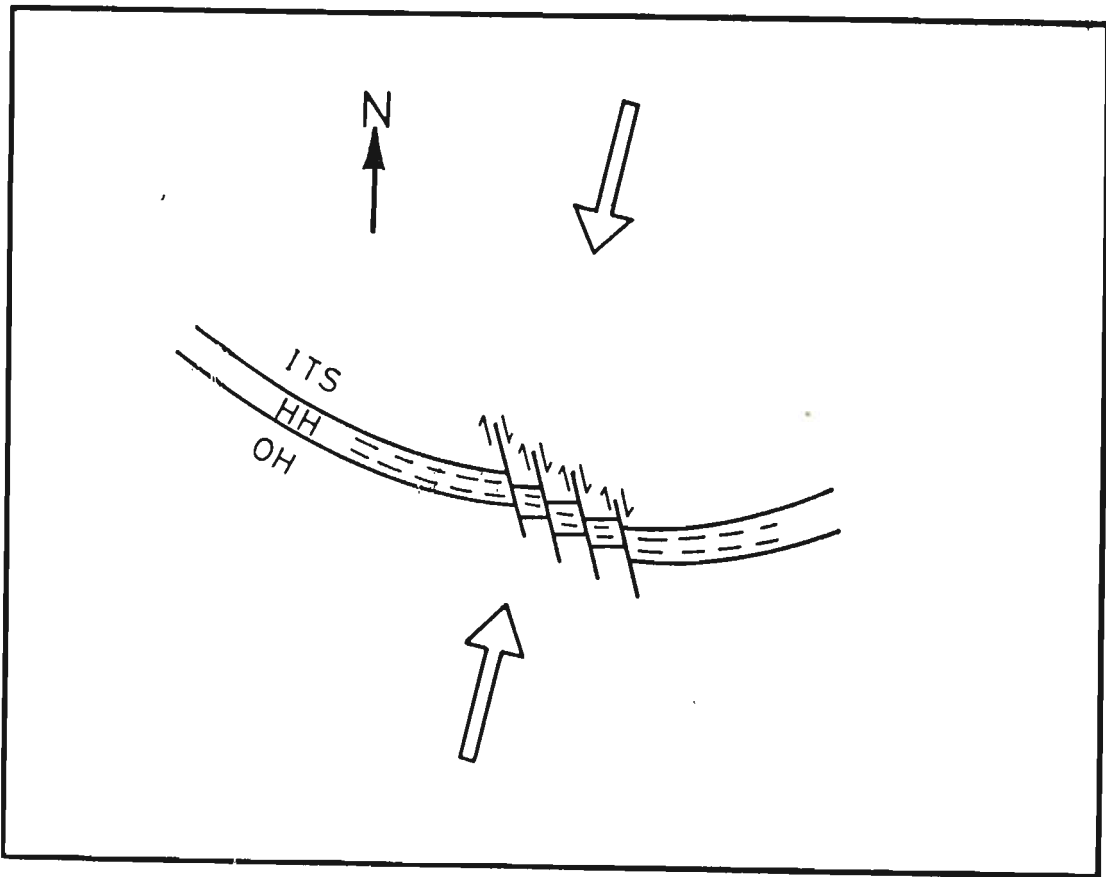
Figure 7·4   A schematic figure to show horizontal relative move-
ments of blocks in the Himalaya corresponding to fault
plane solution of Fig. 5·2.
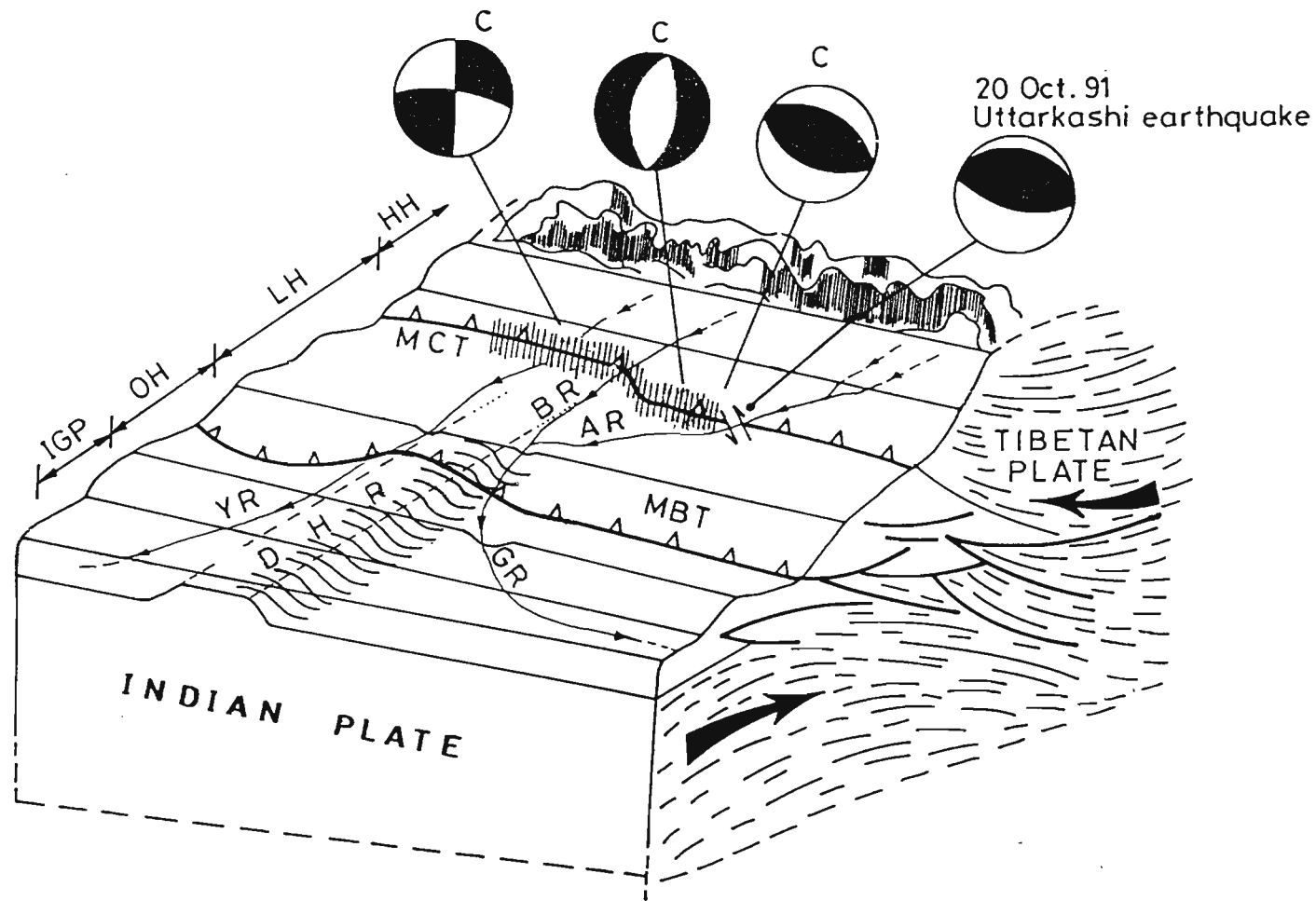
Figure 7·5   A cartoon to show the origin of flexure in the overriding plate due to topographic relief in the subducting plate. IGP: Indo-Gangetic Plains, OH: Outer Himalaya, LH: Lesser Himalaya, HH: Higher Himalaya, MBT: Main Boundary Thrust, MCT: Main Central Thrust, YR: Yamuna River, BR: Bhagirathi River, GR: Ganga River, AR: Alaknanda River, C: Composite focal mechanism and focal mechanism of 20th oct.,1991 Uttarkashi earthquake. DHR is the Dehli-Hardwar Ridge, a postulated buried northeast ward salient of the Pre-Cambrian Aravalli ranges of Rajasthan under the Indo-Gangetic Plains.

7.6   1991 UTTARKASHI EARTHQUAKE

This magnitude 7.0 earthquake has caused considerable damage and has been responsible for apprehension of an even greater earthquake in the minds of the local people. It is seen from Fig. 7 1 that the epicentre of this earthquake lies within the seismicity belt defined by local and teleseismic observations. Fig. 2.13 shows the aftershocks of this earthquake as reported by Indian Meteorological Department (Anonymous 1992). Comparing Figs. 7.1 and 2.7, it is evident that both the main shock and the aftershocks of this earthquake are a part of the normal seismicity of the Garhwal Himalaya.

7.7   ARE THE LOCALLY RECORDED SMALL AND MICRO-EARTHQUAKES AFTERSHOCKS ALSO

Since the Uttarkashi earthquake had a large number of aftershocks a question arises as to whether the small and micro-earthquakes recorded in 1979-80 and 1984-86 were also aftershocks of some earlier earthquakes.

The first point to note is that these earthquakes of 1984-86 occurred several years before the 1991 Uttarkashi earthquake. Also the spatial extent of those earthquakes hypocentres is much larger than the extent of mainshock and aftershocks of the 1991 Uttarkashi sequence. Thus the earthquakes investigated here do not appear to be related to the 1991 Uttarkashi earthquake. The 1905 Kangra earthquake had a magnitude of 8.6. Middlemiss (1910) compiled reports of numerous aftershocks of that earthquake but it would appear they ceased within an year or two of the earthquake. Also the rupture zone of the earthquake overlaps only a part of the area in which the 1979-80 and 1984-86 earthquakes were recorded locally. Hence it would be surprising that the seismicity under analysis is related to the Kangra earthquake. In other words the earthquakes investigated by us also belong to normal seismicity of the region during periods between great earthquakes.

7.8   ON THE POSSIBILITY OF RESERVOIR INDUCED SEISMICITY IN THE GARHWAL HIMALAYA

Ever since the occurrence of the Koyana earthquake of 1967 (Fig. 7.6) (Gupta and Rastogi 1972) the occurrence of reservoir induced earthquakes has been considered a distinct possibility in India. Thus case studies have been put forward documenting reservoir induced seismicity (RIS) at many reservoirs in the Shield region of India (e.g. Gupta 1983) (Fig. 7.6). However some doubts have begun to arise since the occurrence of the Maharashtra earthquake of 29 September, 1993, (date according to GMT) (Fig. 7.6) which had comparable magnitude and occurred at some distance from any major reservoir. However, as for the Himalaya, there has been for years a consistent attempt in some influential circles in India to deny the possibility of RIS. The arguments and our comments on them are as follows.

Firstly it is claimed that RIS has not been observed around the six larger reservoirs that have been completed so far in the Himalaya (Fig. 7.7). This argument is weak partly because proper seismological observations have not been carried out in at least five out of the six cases (Gupta and Rajendran 1986). In the sixth case, that of the Tarbela dam in the Pakistan Himalaya, a high quality telemetered network was installed about a year before the first filling of the reservoir. It was suggested from the preliminary data (Jacob et al 1979) again that there was an apparent lack of RIS. However a recent study by Ibenbrahim et al (1989) based on statistical analysis of data for seven years from the Tarbela network suggest that some micro-earthquakes may occur during periods of low level in the reservoir.

Secondly it is argued that a thrust fault environment prevails in the Himalaya and, in the now relatively older argument put forward by Snow (1972), RIS should be inhibited by the reservoir load in such environment. A part of the problem in this argument is that Snow assumed an infinite reservoir. More recent analyses by Bell and Nur (1978) and Roeloffs (1988) using finite reservoir loads suggest that pre-existing faults may
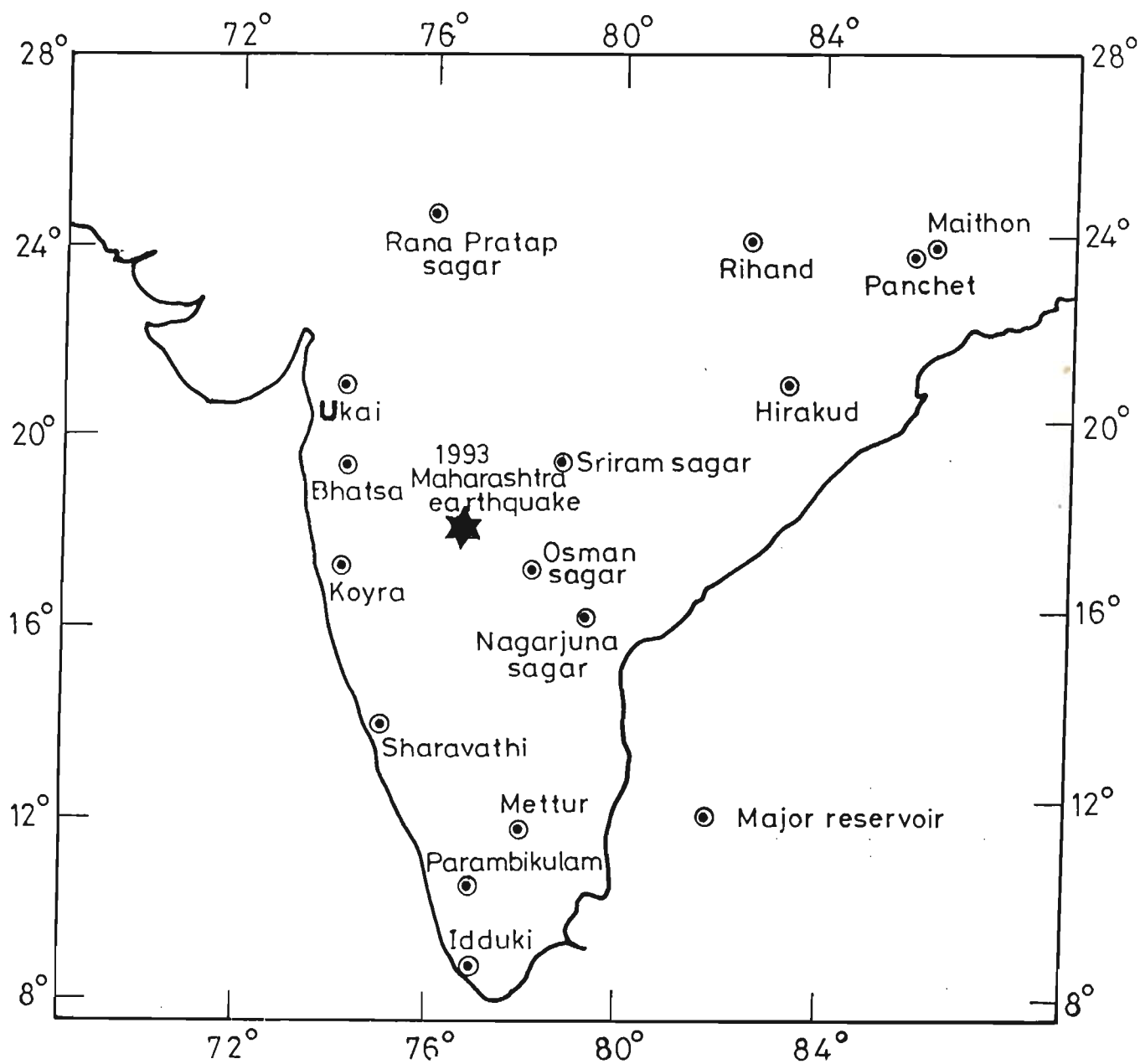
Figure 7·6   Water reservoirs in Peninsular India. The underlined reservoirs are seismically active. Epicentre of Maharashtra earthquake of 1993 is included.
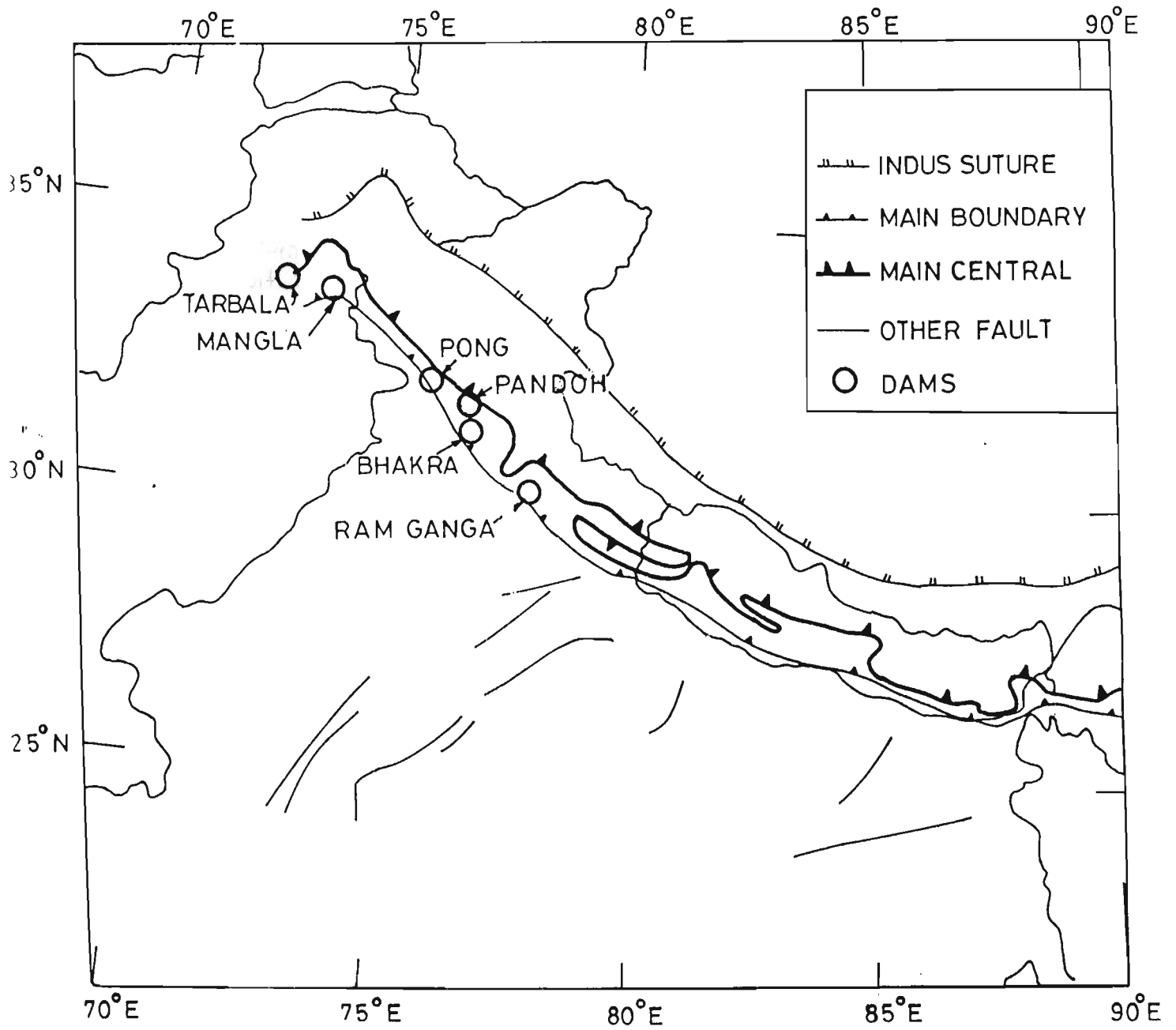
Figure 7·7 Locations of six major reservoirs in the northwestern Himalaya and Pakistan Himalaya.

be reactivated even in a thrust type stress environment if they are properly (unfavourably in the sense of seismic risk) located relative to the reservoir. Another fallacy in Snow (1972)'s argument is that during normal use reservoirs are loaded during the flood season and emptied in the dry season. Thus if loading of a reservoir inhibits RIS, then its draining should facilitate occurrence of earthquakes. This appears to be case at Tarbela reservoir.

Thirdly it has been argued (e.g. Gupta and Rajendran 1986) that rocks in the Outer Himalaya, where some of the high dams have been located so far, are relatively soft and cannot store strain to be released seismically. The occurrence of considerable damage in the Kangra and Dehra Dun region during the 1905 Kangra earthquake (Fig. 2.2) indicates that the strain can be stored in the Outer Himalayan rocks for earthquakes of magnitude 8 or greater.

7.8.1 Evidence from the present study

The possibility of RIS is a significant question for the Garhwal Himalaya because a 260 m high dam is envisaged at Tehri and several other high dams to be sited in the region are under active consideration (Fig. 1.2). In addition to the above arguments and counterarguments, the present study throws up another consideration. Composite fault plane solutions show that reverse/thrust, strike slip and normal faults may be under reactivation in the upper crust in the Garhwal Himalaya in response to the ongoing geodynamic processes related to plate tectonics. Even in the model of Snow (1972) such faults can be reactivated by reservoir loads. Though in fairness, the analysis of Roeloffs (1988) indicates that finite reservoir loads may stabilize suitably located strike-slip and normal faults.

7.9   IMPLICATIONS OF THE STUDY REGARDING TEHRI DAM

A part of the motivation for undertaking careful recording of small and micro-earthquakes in the Garhwal Himalaya using portable arrays was to carefully define the

precise regions of seismicity vis-a-vis the Tehri dam site. Results displayed in Figs. 6.1 and 7.1 indicate that the Tehri site is a few tens of kilometers from the main seismic belt delineated by the local recording. However a definite cluster of earthquake epicentres has been located within 10 km of the site. These are of course epicentres of small and micro-earthquakes.

We have provided evidence above to be slightly skeptical about teleseismic locations of moderate earthquakes of the Garhwal Himalaya. But if the scatter in these earthquakes epicentres seen in Fig. 7.1 is genuine than such earthquakes may also occur very close to the dam site.

Further, the dam site was about 30-40km from the mezoseismal region of the moderate (M_s =7.0) 1991 Uttarkashi earthquake. If the moderate and great earthquakes such as the Kangra earthquake, which caused some damage in the Tehri town (Middlemiss 1910) occur on the detachment then the nearest active fault for the Tehri dam is only as far as the depth of the detachment under the site. This is under the provision (Brune 1993) that a fault of the nature of a splay does not get reactivated at shallower depth, nearer to the site.

The data examined here shed no light on the anticipated acceleration during future earthquakes around the site although it is a question of considerable engineering importance.

8
CONCLUSIONS

1) Hypocentral locations and composite fault plane solutions of 152 small and micro-earthquakes occurring SE of Bhagirathi valley have been determined and compared with similar information obtained previously for 193 small and micro-earthquakes occurring mostly NW of the Bhagirathi valley. Many similarities and a few major differences have emerged.

2) Cumulatively, seismicity information is now available over a 100 km long section of the Garhwal Himalaya through analyses of data for earthquakes occurring within and close to the recording arrays. But the length of this strip may be extended by about 50 km by considering earthquakes located slightly further away from the recording arrays. The epicentral belt located from locally recorded earthquakes coincides with the belt of teleseismically located mostly moderate and a few small earthquakes. The locally determined seismicity belt appears to be relatively more compact reflecting difficulties in locating teleseismically recorded earthquakes of lower magnitudes picked up at a small number of stations.

3) The focal depth range for earthquakes was 0 to 30 km in this study and 0 to 23 km in the earlier study. But a very large percentage of earthquakes of both studies occurred in the upper crustal layer at depths less than 16 km. Carefully determined

focal depths of four moderate earthquakes of the region are in the range of 10 to 18 km. In the literature these earthquakes have been associated with the detachment. The great Himalayan earthquakes including the Kangra earthquake occur by extended ruptures in the detachment. Thus much of the seismicity of the Garhwal Himalaya occurs either along the detachment or in the overlying overthrusted Himalayan rocks. Only a few earthquakes occur in the underthrusting Indian Shield rocks.

4) First P motion data collected in this study have yielded three distinct composite fault plane solutions of strike-slip, reverse/thrust and normal fault types. The nodal planes are well constrained in all cases. The strike-slip solution is identical to the solution obtained in the earlier study.

i) The reverse/thrust solution with the nodal plane dipping at 60° along N 42° as the fault plane is based on data from 60 earthquakes. It implies the existence of a reverse fault type fault zone parallel to the trend of the Himalaya that facilitates the uplift of Higher Himalaya relative to the Lesser Himalaya.

ii) The strike-slip solution implies concurrent horizontally directed relative adjustments between different lengthwise segment of the Himalaya.

iii) The normal fault solution has close affinity with the solution for the 1975 Kinnaur earthquake and represents concurrent east-wast directed extensional tectonics.

5) The spatial contiguity of earthquakes contributing to the three types of solutions poses serious problems for drawing inferences about the state of stress in the region. The strike-slip solution is amenable to the interpretation that such faults are reactivated under the action of maximum and intermediate principal stresses of the thrust fault type stress regime in the region. The reverse/thrust solution demands high pore pressures if the northeasterly dipping nodal plane represents the reactivated faults under the same thrust type stresses. The normal fault solution forces us to invoke heterogeneity in crustal stresses in the region.

6) The present work reinforces the thought that the available observations about the seismicity of the Garhwal Himalaya may be regarded as consistent with the operation of plate tectonics in the region.

PART-2

TRAVEL TIME STUDY

9

TRAVEL TIME STUDY

9.1   INTRODUCTION

Among the various geophysical techniques, so far seismology has provided the most detailed information about the internal structure of the earth. Initially, chronometric information about the travel times of seismic body waves, dispersion of surface waves and periods of peaks in Fourier spectra of free oscillations of the earths were analyzed for the purpose. But, more recently, information about amplitudes of recorded seismic waves have been utilized also. Analyses of body wave travel times yield information about spatial distribution of compressional (V_p) and shear (V_s) wave speeds within the earth. Density distribution within the earth may be inferred from the V_p and V_s data. In this study we have analysed the travel times of seismic P waves from Hindu Kush earthquakes recorded at temporary seismograph stations in the Garhwal Himalaya (Fig. 9.1).

Construction of first reliable P and S travel time tables and their analysis for V_p and V_s structure of the earth is a remarkable chapter in the history of seismology. The problem in the era before the nuclear explosions was that one had to locate hypocentres of earthquakes and determine their origin times to construct travel time tables. But these tasks could not be accomplished unless reliable P travel time tables were available. Finally, this circular problem was solved iteratively by Jeffreys and Bullen on the one hand
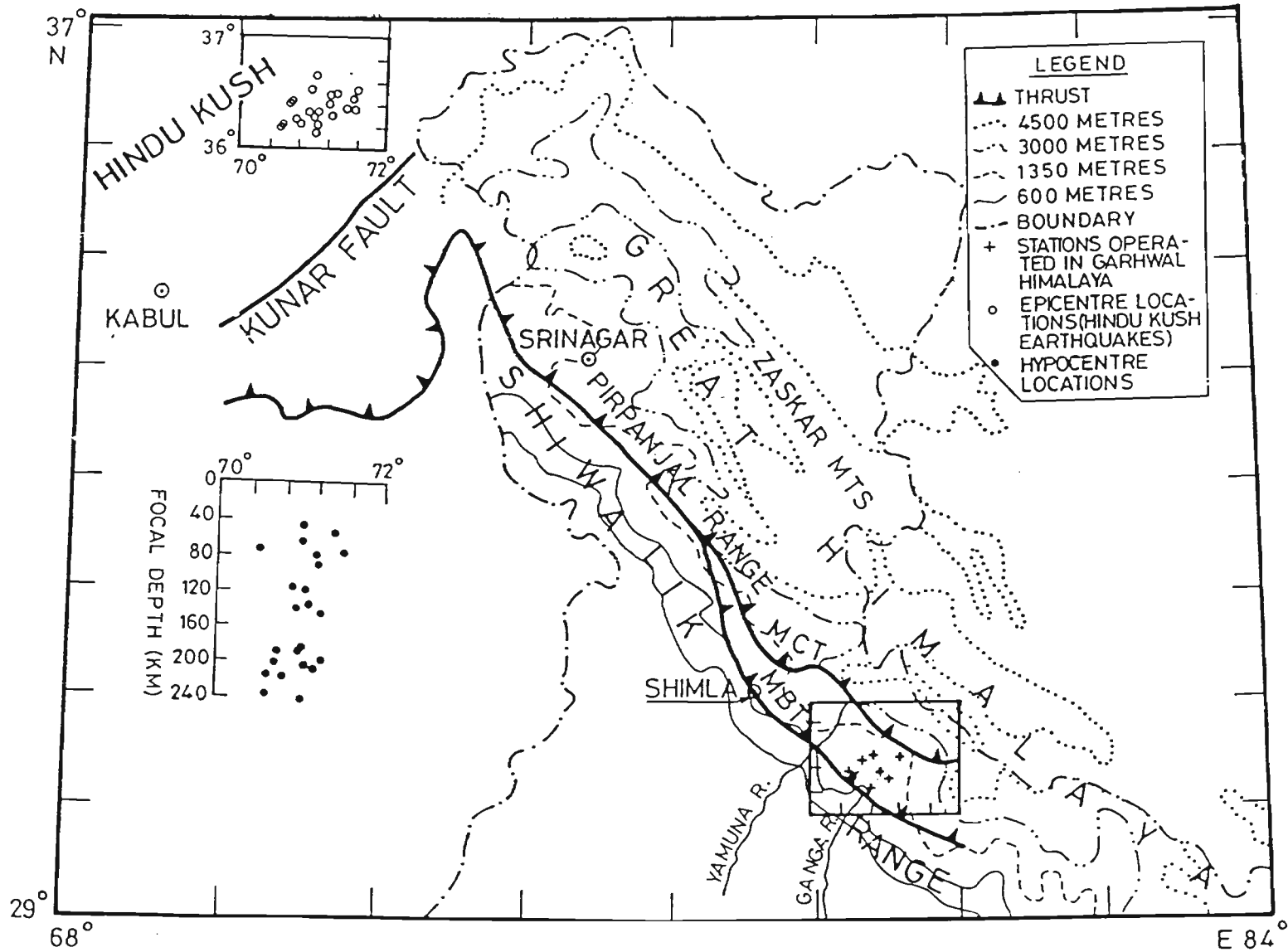
Figure 9·1   North – Western Himalaya with epicentres of Hindu Kush earthquakes and stations of recording array in Garhwal Himalaya.

and Gutenberg and Richter on the other. In the present study, we adopt the hypocentral locations and origin times of the concerned earthquakes as reported by the US Geological survey to obtain the necessary travel times.

Assuming a radially symmetric earth, Jeffreys and Bullen and Gutenberg and Richter interpreted the respective travel time tables for variation of V_p with r, [i.e., V_p (r)], using the Herglotz-Weichert-Bateman inversion (Bullen and Bolt, 1985, chapter 7). In this approach, under suitable restrictions on the nature of V_p (r), the integral representing the angular epicentral distance of a ray is transformed to yield the radial distance r_1 of the point of maximum penetration of the ray emerging at an epicentral angle Δ_1 from a straight-forward integration using information about the observed slopes of the travel time tables at different epicentral angles upto Δ_1. The magnitude of V_p at r_1 is estimated from the observed value of the ray parameter at Δ_1. An alternative ray tracing approach is used for inversion of travel times in the present case.

In the past few decades the inversion of travel time data for wave speed distribution in the earth using the ray tracing approach has been formulated as a programming problem and many ingenious but rigorous techniques have been employed (e.g. Aki and Richards, 1981). However the quality and quantity of the data at our disposal constrain us to evolve a simpler strategy for a limited goal. Thus we still solve a programming problem but estimate only two parameters at a time, namely, the magnitude of V_p in the deepest layer of a multilayered earth and the depth of the top boundary of this layer, (Fig. 9.2).

A special feature of the following investigation is that epicentres of the Hindu Kush earthquakes whose data are analyzed were clustered in a 100 km by 50 km area. The focal depths of these earthquakes as estimated by the USGS ranged between 50 and 245 km approximately. The aperture of the seismograph array in Garhwal was about 40 km. Thus for a very short range of epicentral distances we had travel time information about rays traversing the upper mantle at several depths in the 50 to 245 km range.
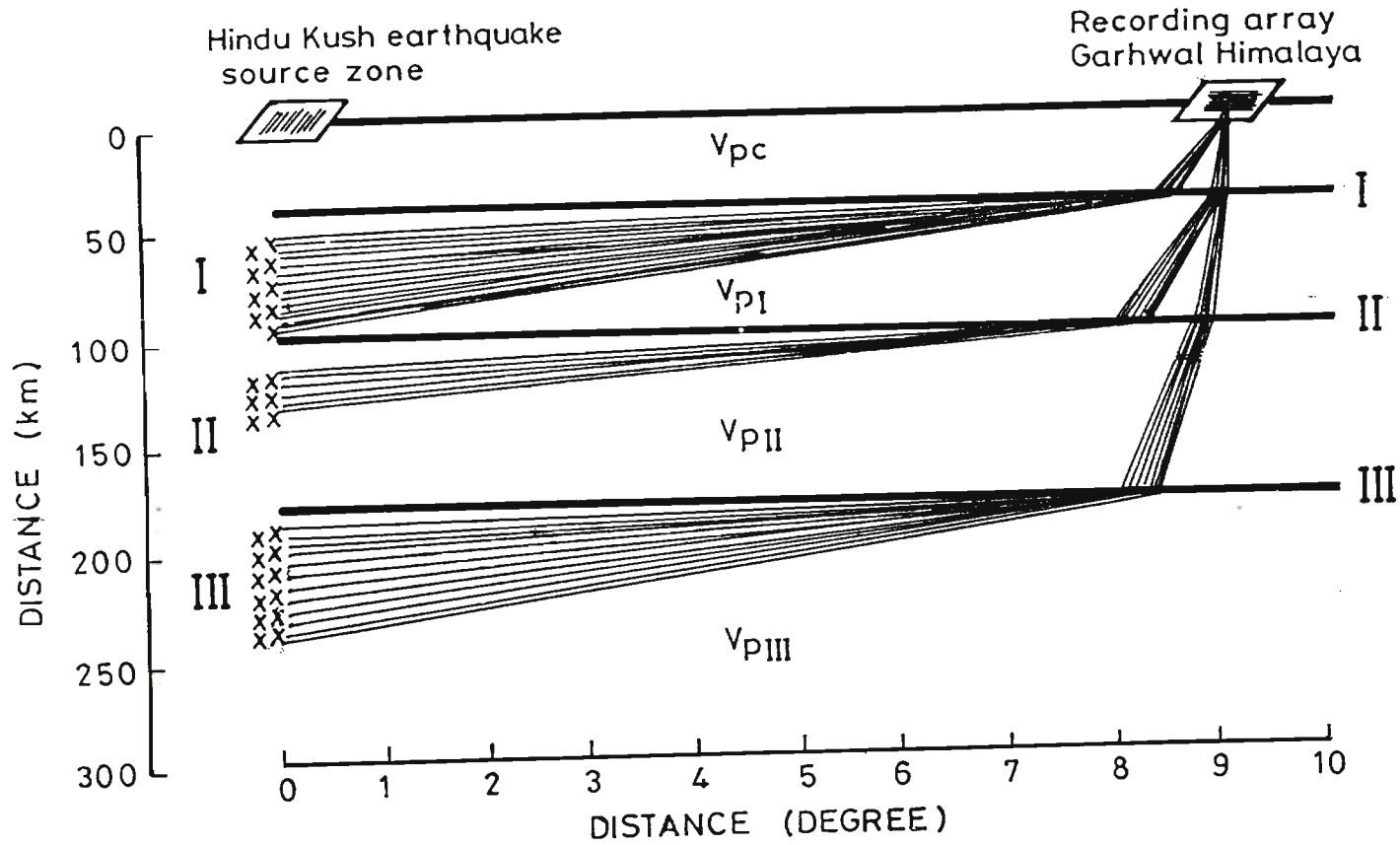
Figure 9.2   Cartoon of the layered model deduced from Hindu Kush earthquakes. I, II and III at left for different earthquake clusters. I, II and III at right for interfaces whose depths determined from the three respective earthquake clusters. Rays are drawn schematically (See text).

It was observed through ray tracing that these rays pass through the crust only once near the recording station. Moreover their travel time through the crust is a relatively small fraction of the total travel time. Hence distribution of V_p in the crust was not investigated. But an average crustal model was assumed to obtain estimates of V_p in the upper mantle.

Roecker (1982) determined a detailed V_p structure under the Hindu Kush mountains upto a depth of about 200 km. This was an elaborate exercise using locally recorded P wave data. We take account of Roecker's (1982) results in our estimations of upper mantle V_p values. In this way we feel justified in claiming that we have examined V_p distribution in the upper mantle under the NW Himalaya (Fig. 9.1). ·

Regional variations in travel times to distances of less than 20^0 make it impractical and unproductive to estimate world average times for shorter distances. As an alternative, for shorter distances, there is need to have regional travel times and wave speed models for crust and upper mantle. The Hindu Kush is a remarkably active region seismically. Many of these earthquakes cause damage in Afghanistan and northern Pakistan. The present analysis may contribute to improvements in hypocentral locations of Hindu Kush earthquakes and thus indirectly help in earthquake hazard estimation in those regions because readings from increased number of in NW Himalayan stations should be available in the coming decade.

9.2 REVIEW OF WAVE SPEED DETERMINATIONS BASED ON DATA FOR HINDU KUSH EARTHQUAKES

Earthquakes of the Hindu Kush region have attracted attention of seismologists for many years. A number of wave speed determinations have been made using recorded phases from these earthquakes (Tandon 1967, Matveyeva and Lukk 1968, Kaila et al 1969, Ram and Mereu 1977, Roecker 1982). These studies fall into two distinct categories. The work of Roecker (1982) is different from those of others in that seismographs were

installed at very short epicentral distances within the Hindu Kush region of Afghanistan. Thus the wave speed determination applies to the Hindu Kush region strictly. Table 9.1 and Fig. 9.3 are displays representing their initial, laterally homogeneous model determined for the region. Subsequently they estimated lateral variations of upto few percent of the average V_p at a given level in the region.

All the other studies have the common feature that earthquakes occurred in the Hindu Kush but they were recorded at stations outside the region. Thus the results do not strictly apply to a specific region. Still a comparison of the results is given in Table 9.2 and Fig. 9.4. This is because while our study also belongs to the latter category, still it has the distinction that essentially one path is investigated.

9.3   OBSERVATIONS

9.3.1 General

As mentioned in Chapter 1, many earthquakes occurring in the Hindu Kush region were also picked up by the portable recording stations installed in the Garhwal Himalaya for local seismicity studies. We analyse here the P wave readings obtained from seismograms of the seven stations operated in 1985-86. Records of 22 Hindu Kush earthquakes were found to have readable P phases on these seismograms. The hypocentral information about these earthquakes as determined by the US Geological survey is given in Table 9.3. As seen from this table, the distribution of the focal depths of the 22 earthquakes in not uniform. There is notable lack of earthquakes from the depths ranges of 94 to 117 km and 142 to 188 km.

9.3.2 Travel time graphs

Table 9.4 is a display of the arrival times of P phases at different stations of the array for these earthquakes. Using the reported epicentral coordinates of the earthquakes, 154 (22 earthquakes x 7 stations) epicentral distances were computed using the standard
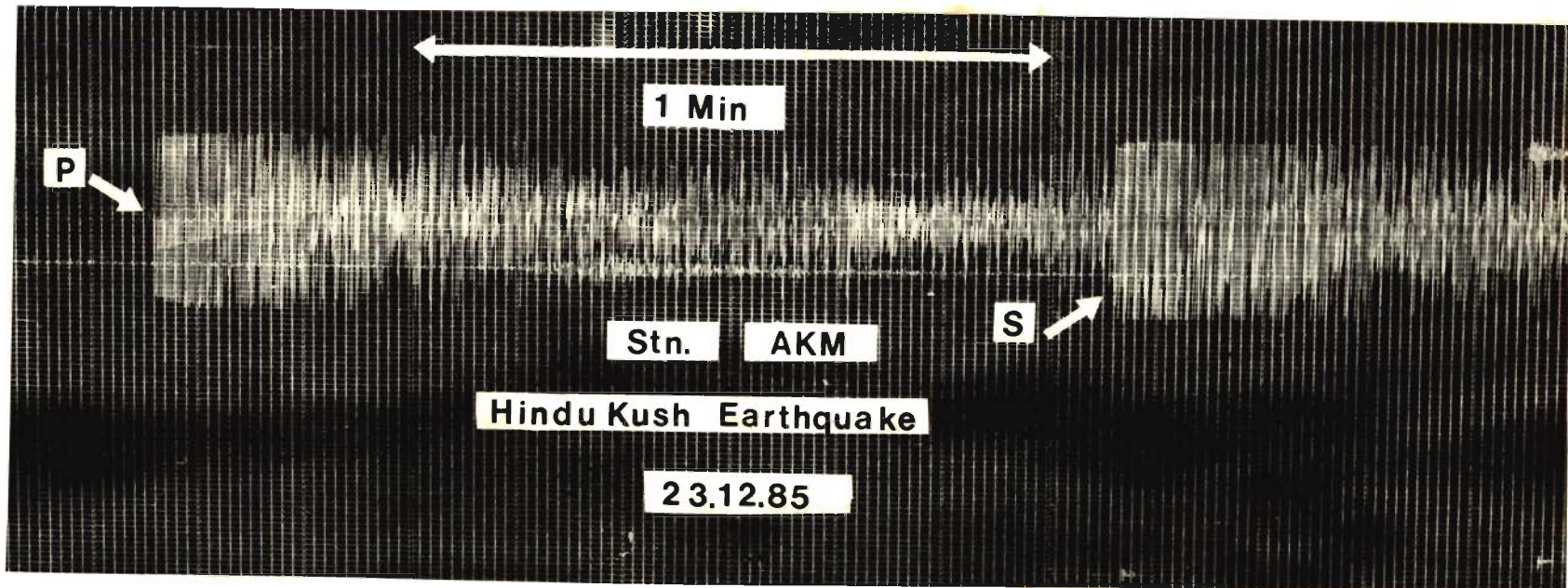
Plate 9.1. Part of the vertical component seismogram from station Akmundsam (AKM) showing clear P (Pn) and S (Sn) phases from a Hindu Kush earthquake of December 23, 1985 (m_b=4.8, focal depth=120 km).

TABLE 9.1 ROECKER'S MODEL OF P-WAVE SPEED

ROECKER (1982)	
Depth (km)	P-Wave Speed (km/sec)
00 - 40	5.80
40 - 70	6.40
70 - 110	8.05
110 - 160	8.50
160 - 185	8.30
185 - 230	9.10

TABLE 9.2   COMPARISON OF P-WAVE SPEED MODELS DEDUCED BY VARIOUS INVESTIGATORS USING HINDU KUSH DATA

KAILA et al (1969)		MATVEYEVA AND LUKK (1968)		TANDON (1967)		RAM AND MEREU (1977)	
Depth (km)	P-Wave Speed (km/sec)	Depth (km)	P-Wave Speed (km/sec)	Depth (km)	P-Wave Speed (km/sec)	Depth (km)	P-Wave Speed (km/sec)
45	8.14	00	5.90	31.85	8.01	15	5.50
70	8.32	50	6.10 - 7.90	63.71	8.03	33	6.50
85	8.29	80	8.00 - 8.35	95.56	8.02	113	7.90
100	8.30	110	8.05 - 8.36	127.40	8.07	362	8.13
120	8.37	150	8.20 - 8.35	159.27	8.40	545	9.67
150	8.39	200	8.37 - 8.54	191.13	8.45		
190	8.53	390	8.54 - 8.71				
210	8.35						
230	8.57						

TABLE 9.3 :   EARTHQUAKE EPICENTRAL DATA DETERMIND BY US GEOLOGICAL SURVEY

S. No.	Date M	D	Y	Origin Time H	M	S	M$_b$	Epicenter Lat °N (Dég.)	Long °E (Deg.)	Focal Depth km
1.	Dec.	22,	1985	07	32	17.82	4.8	36.331	70.992	49.7
2.	Nov.	29,	1985	10	10	03.64	5.0	36.404	71.409	57.4
3.	Dec.	26,	1985	13	46	22.00	4.2	36.301	71.001	65.6
4.	Feb.	24,	1986	05	57	29.37	5.0	36.086	70.479	77.1
5.	Jan	30,	1986	09	44	43.00	4.6	36.387	71.512	78.7
6.	Nov.	26,	1985	10	31	08.68	4.7	36.437	71.196	92.2
7.	Feb.	23,	1986	06	50	02.84	4.5	36.336	71.234	93.7
8.	May.	29,	1986	01	30	31.89	4.9	36.288	70.860	116.9
9.	Feb.	11,	1986	12	44	24.26	4.9	36.372	70.910	118.8
10.	Dec.	15,	1985	00	15	29.18	4.5	36.188	71.039	119.2
11.	Dec.	23,	1985	23	26	34.97	4.8	36.241	71.064	120.6
12.	May	24,	1986	02	01	57.73	4.6	36.367	70.957	141.8
13.	Dec.	14,	1985	07	55	49.99	4.2	36.683	71.014	184.6
14.	Dec.	06,	1985	12	34	41.44	4.7	36.564	70.981	188.2
15.	May,	25,	1986	17	08	56.85	4.4	36.465	70.720	189.2
16.	Mar.	10,	1986	07	41	29.95	4.2	36.532	71.265	199.7
17.	Feb.	05,	1986	01	13	56.69	4.8	36.426	70.696	202.7
18.	Jan.	11,	1986	02	43	03.37	4.3	36.370	71.067	204.2
19.	Mar.	11,	1986	20	39	19.48	4.7	36.512	71.187	207.8
20.	Mar.	07,	1986	02	45	28.51	4.4	36.314	70.789	218.0
21.	Nov.	22,	1985	13	14	55.04	3.8	36.236	70.576	238.1
22.	Jan.	14,	1986	08	33	37.46	5.2	36.341	71.024	245.1

TABLE 9.4 :   ARRIVAL TIME OF P PHASE AT DIFFERENT STATIONS OF THE ARRAY OF THE EARTHQUAKE OF TABLE 9.3

Event	Date			Nearest Arrival Time		AKM	CHA	BNA	ODA	DAG	TIL	UKH
	M	D	Y	H	M	Sec.	Sec.	Sec.	Sec.	Sec.	Sec.	Sec.
1.	Dec.	22,	1985	07	34	25.00	24.00	25.90	28.50	28.40	29.20	30.00
2.	Nov.	29,	1985	10	12	07.10	07.00	08.00	10.30	11.30	11.60	—
3.	Dec.	26,	1985	13	48	27.00	26.10	28.00	30.30	30.40	31.70	—
4	Feb.	24,	1986	05	59	35.90	35.80	37.20	39.00	39.00	40.15	40 30
5.	Jan.	30,	1986	09	46	44.20	44.20	45.60	47.40	47.60	47.40	48.80
6.	Nov.	26,	1985	10	33	13.00	14.00	14.30	16.20	17.00	16.90	17.90
7.	Feb.	23,	1986	06	52	07.00	06.40	07.80	09.50	10.00	10.75	11.00
8.	May.	29,	1986	01	32	36.00	—	37.60	39.40	40.00	40.80	41.30
9.	Feb.	11,	1986	12	46	28.30	—	29.20	31.30	31.70	32.40	32.60
10.	Dec.	15,	1985	00	17	29.80	30.50	32.00	33.90	34.50	35.00	35.40
11.	Dec.	23,	1985	23	28	36.00	36.00	—	38.90	39.00	35.00	37.00
12.	May	24,	1986	02	04	—	—	05.00	06.40	07.00	07.90	08.60
13.	Dec.	14,	1985	07	57	57.00	57.05	07.80	60.20	60.00	60.90	61.32
14.	Dec.	06,	1985	12	36	45.00	45.60	46.00	48.00	49.54	08.90	49.80
15.	May,	25,	1986	17	11	—	—	—	—	04.50	05.50	06.40
16.	Mar.	10,	1986	07	43	—	31.20	32.50	34.00	33.30	34.60	35.30
17.	Feb.	05,	1986	01	16	01.30	01.20	02.50	04.40	04.00	05.30	05.40
18.	Jan.	11,	1986	02	45	05.20	05.10	06.40	08.00	08.60	09.10	09.10
19.	Mar.	11,	1986	20	41	20.90	20.20	21.50	24.40	24.70	24.10	24.85
20.	Mar.	07,	1986	02	47	32.00	31.20	32.40	—	34.00	35.50	35.60
21.	Nov.	22,	1985	13	16	58.80	59.0	60.40	—	63.00	62.50	63.70
22.	Jan.	14,	1986	08	35	38.20	38.50	39.40	41.70	42.00	42.00	42.70
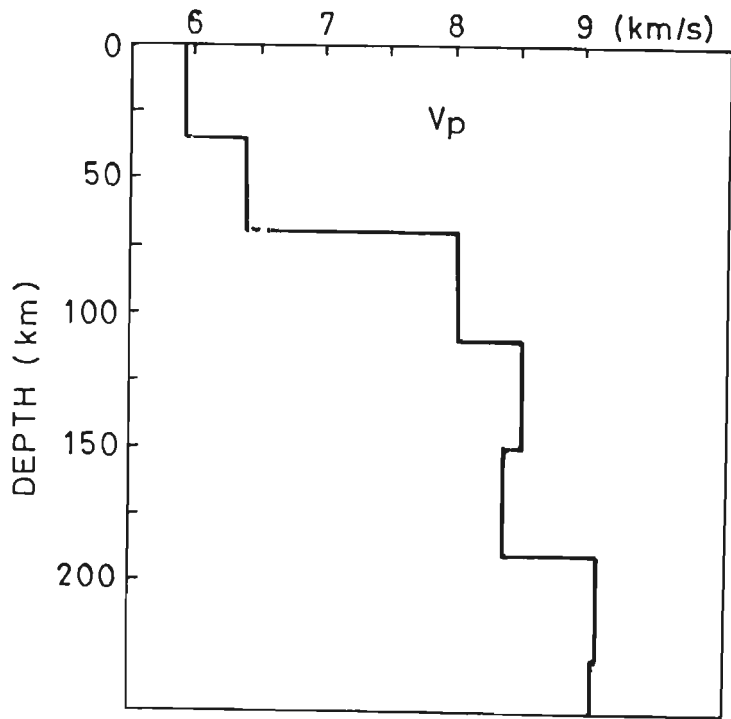
Figure 9·3 Wave speed model for Hindu Kush
according to Roecker (1982).
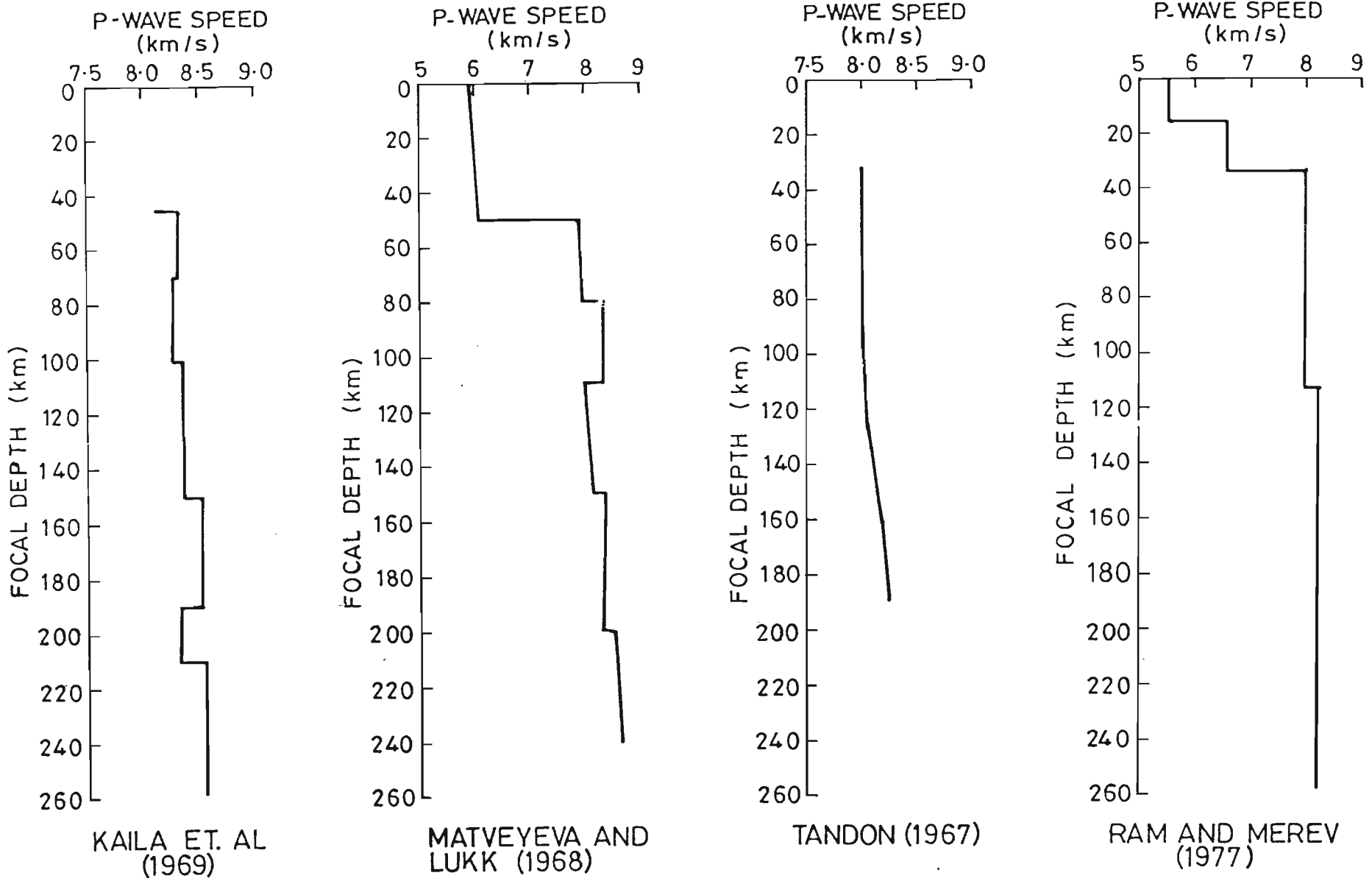
Figure 9·4 Comparison of wave speed models deduced by various investigators using Hindu Kush earthquake data.

formula (Bullen and Bolt, 1985). Corresponding travel times were obtained using the USGS determined origin times for these 22 earthquakes and the respective P wave arrival times. The estimated travel times are plotted for all the earthquakes together in Fig. 9.5. They are then displayed in Figs. 9.6 to 9.8 arranged according to the clusterings of depths ranges of the concerned earthquakes. There is a definite gradation in the travel times according to the depths of the earthquakes. Deeper earthquakes yield lesser travel times on the whole.

Fig. 9.1 is a combined display of epicentral locations and the recording array against the backdrop of a geological map of the Himalaya. It is seen that the great circles between epicentres and recording stations lie mostly in the NW Outer and Lesser Himalaya.

9.3.3 Sources of error in the travel time graphs

There are a number of sources of errors in the travel time data displayed in Figs.9.5 to 9.8. They are discussed conveniently under the headings of errors in travel times, errors in epicentral distances and errors in focal depths.

Errors in travel times : Two main sources of these errors can be considered here. Firstly the origin time estimates for earthquakes reported by the USGS are acknowledged to be in error The causes of these errors are again numerous. They are similar to those discussed here in many respects. But we shall not go into them here. We anticipate both systematic and random errors to be involved. Secondly the arrival times of P phases are in error for the same reasons as discussed in Part I. The errors in travel times are the sum of these two types of errors. We estimate that errors in individual travel times could be in the range of ±1s to ±2s. Here we have tried to err in the direction of overestimating the possible errors.
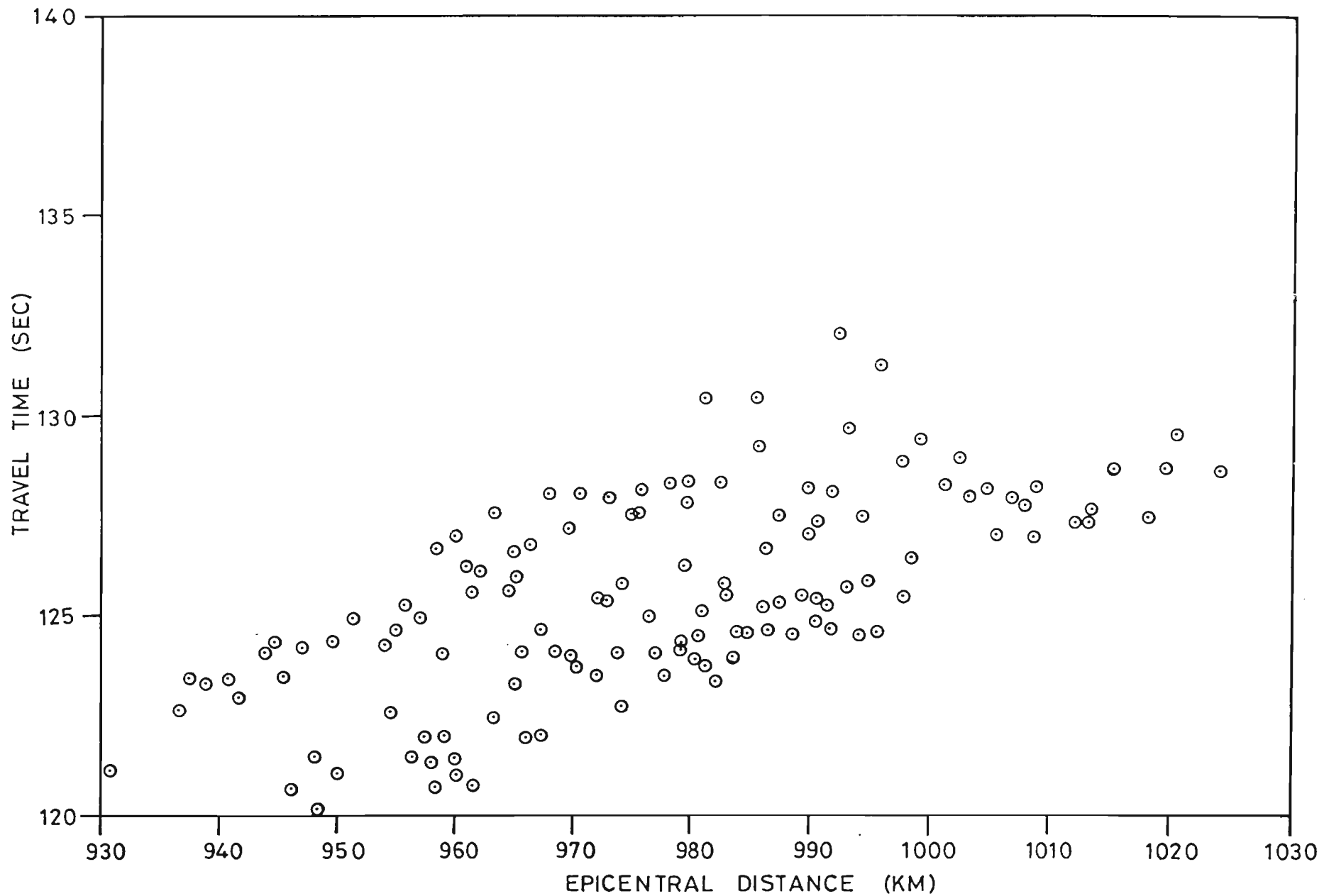
Figure 9·5   154 travel times observations examined here for 22 Hindu Kush earthquakes.
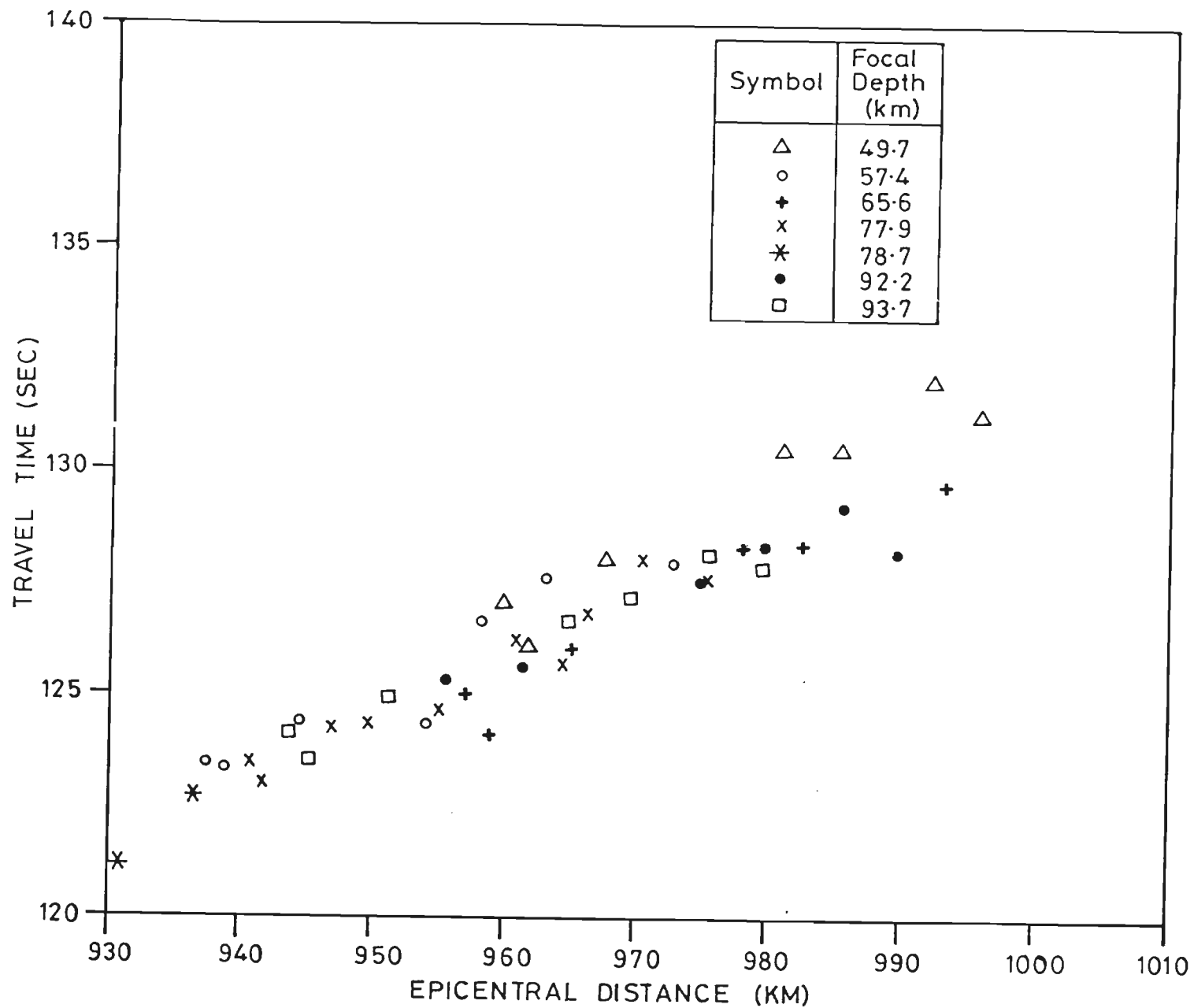
Figure 9·6   Travel time data for 1 earthquake cluster.
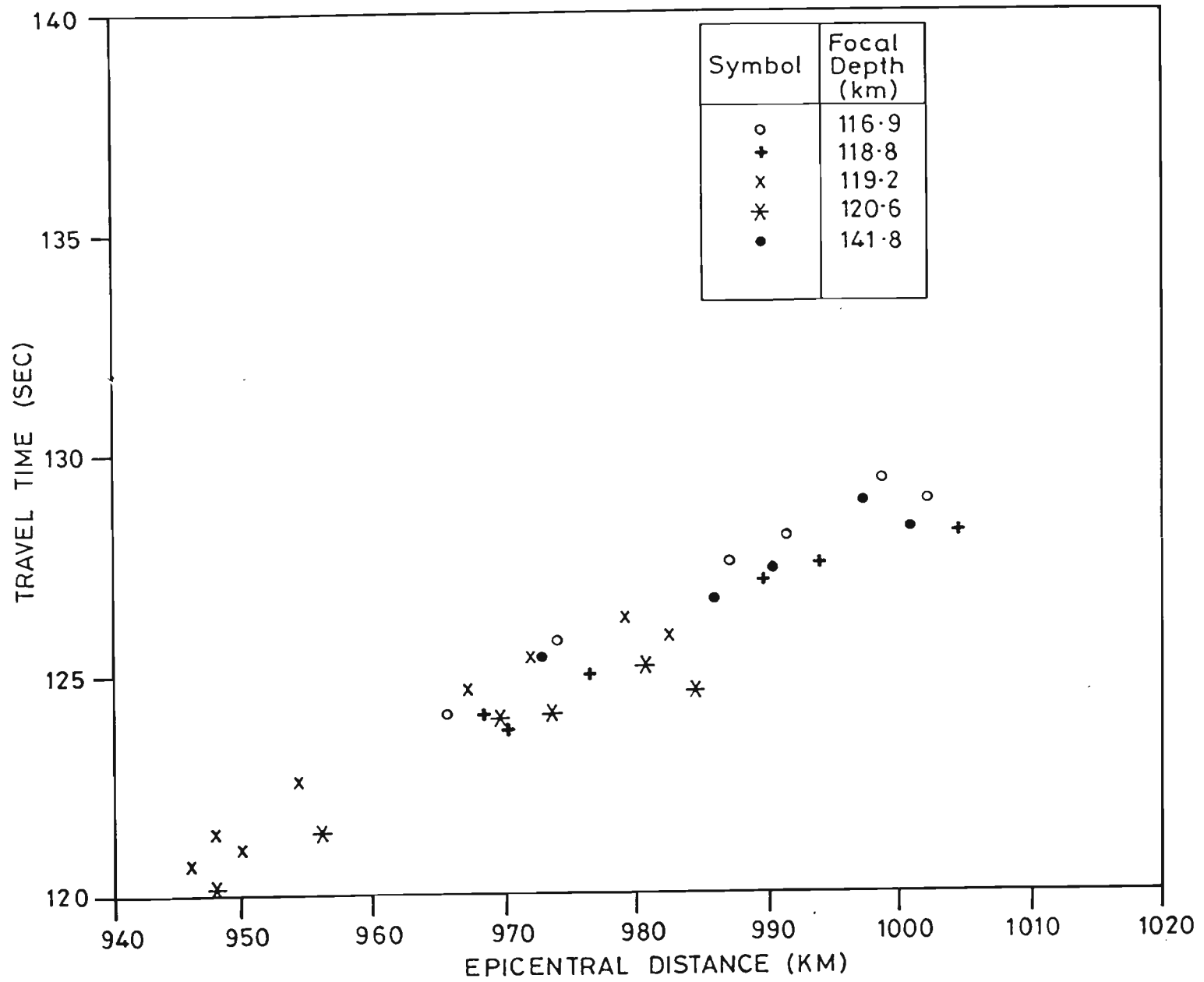
Figure 9·7 Travel time data for II earthquake cluster.
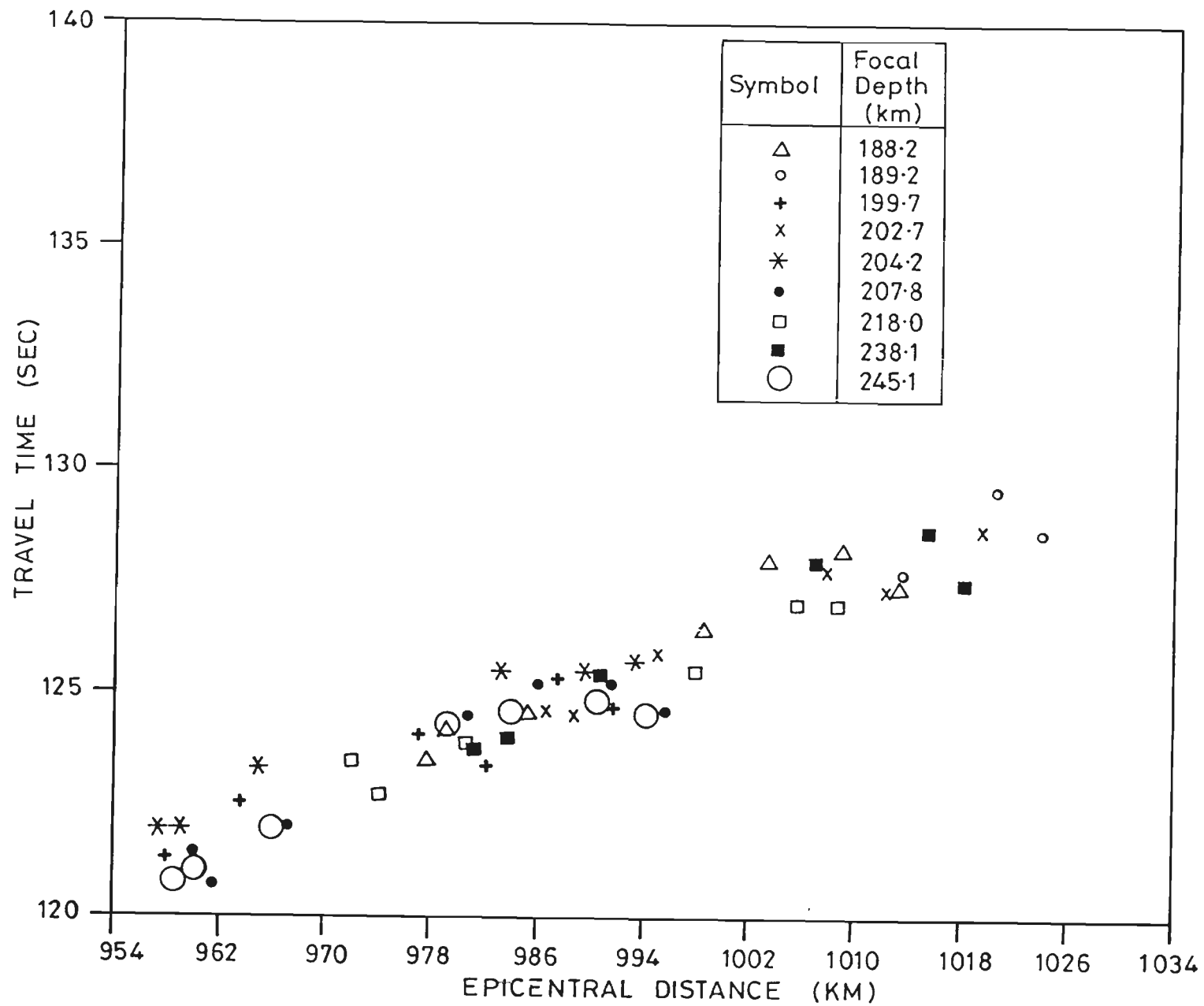
Figure 9-8   Travel time data for III earthquake cluster.

Errors in epicentral distances : Again two main groups of causes of errors can be identified. Firstly, the epicentral coordinates estimated are in error. Secondly, the station locations are in error as discussed in Part I. Cumulative error in an individual estimate of epicentral distance could be in the present case upto ± 5 km under the cautious approach mentioned in the the preceding paragraph.

Errors in focal depths : A third class of error affecting the interpretation of the travel time curves is that the reported focal depths of the earthquakes are in error. These errors bias the P wave speed determination because we may be using wrong focal depths while calculating theoretical travel times (see below).

9.4 METHOD OF INTERPRETATION OF TRAVEL TIMES

The method of interpretation adopted by us for the above data is the result of a conscious decision in view of a number of factors. Firstly, the number of observation is small. This has been governed by the number of readable seismograms obtained during the limited period of array operation. Also the number of stations operating was only seven. Secondly because of concentration of epicentres in a narrow geographic region and the small aperture of the array, the range of epicentral distances covered is too narrow. Thirdly the observations are subject to considerable errors which are difficult to quantify.

On a different note, a ray tracing exercise revealed that the travel times of the rays through the crust would be a small fraction of the total travel time. Therefore we decided to include an average crust with a single layer of average P wave speed in the models.

Finally, clusterings in focal depths among the concerned earthquakes suggested that inversion for upper mantle P wave speed could be carried out sequentially, starting with the group of earthquakes with the shallowest hypocentres to determine P wave speed in the upper most mantle layer. Then the next group of earthquakes could be used to investigate the next depths range in the upper mantle. Thus at the most two parameters

could be estimated using a comparatively large number of travel time observations at every step of the sequence. These parameters would be in each case layer P wave speed (V_p) and the depth of the top interface of the layer.

9.4.1 The travel time inversion algorithm

9.4.1.1 Estimation of wave speed in the last layer of a layered model

Let there be a stack of ℓ homogeneous layers with parallel interfaces. Let P wave speed in the top ℓ-1 layers be specified along with their thicknesses. Let m earthquakes with known hypocentral coordinates occur in the ℓth layer. Also let the arrival times of P waves at n seismograph stations be known along with their coordinates. Then the estimation of $V_{p\ell}$ (the V_p in the ℓth layer) can be set up as a least squares inversion problem. Let T_{oi} and T_{ci} stand for observed and theoretically computed travel times for the ith ray among the totality of mn rays between m earthquakes and n stations. The error function $E(V_{p\ell})$ is given by

$$E(V_{p\ell}) = \sum_{i=1}^{mn} \left(T_{oi} - T_{ci}(V_{p\ell}) \right)^2 \qquad ...(1)$$

If j is the running index for layer numbers then,

$$T_{ci}(V_{p\ell}) = \sum_{j=1}^{\ell} \frac{L_{ij}}{L_{pj}} \qquad ...(2)$$

where L_{ij} and $V_{p,}$ are the segment length of ith ray and P wave speed in the jth layer respectively.

We seek a value of $V_{p\ell}$ to minimize $E(V_{p\ell})$. In other words,

$$\frac{dE(V_{p\ell})}{dV_{p\ell}} = 0 \qquad ...(3)$$

Equation (3) is non-linear in $V_{p\ell}$. We used the Newton-Raphson procedure to solve this equation iteratively for $V_{p\ell}$ Thus, let us define

$$F(V_{p\ell}) = \frac{dE}{dV_{p\ell}}$$

for brevity. Let $V_{p\ell\, i}$ be an initial guess of $V_{p\ell}$. Let h be an increment in $V_{p\ell\, i}$ such that

$$F(V_{p\ell\, i} + h) = 0$$

Expanding F in a Taylor series and retaining only the first two terms, we may write that

$$h \approx -F(V_{p\ell}) \left/ \frac{\partial F}{\partial V_{p\ell}} \right|_{V_{p\ell\, i}}$$

Or, in terms of the original error function,

$$h \approx -\frac{\left(\dfrac{dE}{dV_{p\ell}} \right)}{\left(\dfrac{d^2 E}{dV^2_{p\ell}} \right)\Big|_{V_{p\ell\, i}}} \qquad \ldots (4)$$

Hence a better guess of $V_{p\ell}$ is obtained as $V_{p\ell\, i} + h$. The procedure can then be repeated until h becomes negligibly small. The last value of $V_{p\ell\, i} + h$ can be taken as an estimate of $V_{p\ell}$.

9.4.1.2 Three dimensional Ray tracing

The above iterative scheme to determine $V_{p\ell}$ cannot be implemented without an accompanying algorithm to trace a ray between specified positions of the hypocentres and the recording stations. The need for three dimensional ray tracing was visualized for the following reason We were prepared to simulate the structure under the NW Himalaya through models with parallel uniform layers because of the absence of sufficient other information to constrain a three dimensional visualisation of the distribution of V_p in the region of interest. Still, Roecker (1982) had published a three dimensional model of V_p distribution in the Hindu Kush mountains. The model is quite different from world average models of $V_{p\ell}$ in the upper mantle such as PREM (e.g., Bullen and Bolt ,1985). If Roecker's model were to be meshed with the parallel layer

model for the rest of the path, then this would have to be through three dimensional ray tracing.

A shooting strategy was adopted to trace the desired rays iteratively in specified models of V_p. A number of ray tracing formulation are available in the literature, i.e., Shah (1973), Sorrels et al (1971), Chander (1977). We adopted the formulation of Sorrels et al (1971) because of its generality. Details of the formulas are omitted because they are available in an international journal. A computer program was written for the purpose and thoroughly tested.

9.4.1.3 Computer Program

An original program to solve Equation (3) using Equation (4) was written in FORTRAN. The above ray tracing program was incorporated as a subroutine in this program. The FORTRAN code is reproduced here as Appendix IV.

The program was tested thoroughly on synthetic data and then put into use to interpret the travel time observations.

9.4.2 Grid search for estimation of the depth to top interface of ℓ th layer

A grid search strategy was adopted for this purpose. The above mentioned computer program was used to estimate $V_{p\ell}$ for a number of assumed values of depth of the top interface of the ℓ th layer. In each case the total squared error $E(V_{p\ell})$ of equation (1) was also computed. That value of depth was adopted for which the value of $E(V_{p\ell})$ was the least. The corresponding estimate of $V_{p\ell}$ became the accepted value of V_p in the ℓ th layer.

9.5 RESULTS

We now present the results of the exercise to interprete the observed travel times using the computer program and grid search algorithm just described.

9.5.1 Earthquake clusters

The clustering in focal depth of 22 earthquakes has been remarked already. We now formally call the 7 earthquakes in the focal depth range of 49 the 94 km as the I cluster. Similarly 5 earthquakes in the focal depth range of 117 to 142 km will be called the II earthquakes cluster. Finally the 10 earthquakes in the focal depth range of 188 to 245 km will be referred to as the III earthquakes cluster.

9.5.2 Average $V_{p\ell}$ in the crustal layer

The reason for assuming an average crustal layer have been given above. Here we justify the value of V_p adopted for it. According to Hirn et al (1984) average of value of V_p in the crustal layer in the Himalaya is of the order of 6.3 km/s. However, for the Garhwal Himalaya, Chander et al (1986) observed from analysis of local data that the V_p in the upper crustal layer has the relatively low value of 5.2 km/s. Hence we adopt a average V_p of 6.2 km/s for the crustal layer in order to carry out the following modelling exercise.

9.5.3 Results on the assumption of a laterally uniform layering in the upper mantle between Hindu Kush and Garhwal Himalaya

Results of analyzing data for I earthquake cluster: Fig. 9.9 is a display of $E(V_{p\ell})$ for different assumed thicknesses of the crustal layer while using the travel time data for the I earthquake cluster. It is seen that the minimum of $E(V_{p\ell})$ is a weak and broad one. But having setup the rule described above we have to conclude that a crustal thickness of 39 km and upper mantle $V_{p\ell}$ of 8.05 km/s do yield the least total squared error.

Results of analysing data for II earthquake cluster: Fig. 9.10 is analogous to the preceeding figure. But the minimum in $E(V_{p\ell})$ is quite sharp and pronounced for a depth of 99 to 100 km for the top interface of the last layer in this case. It corresponds to a V_p of
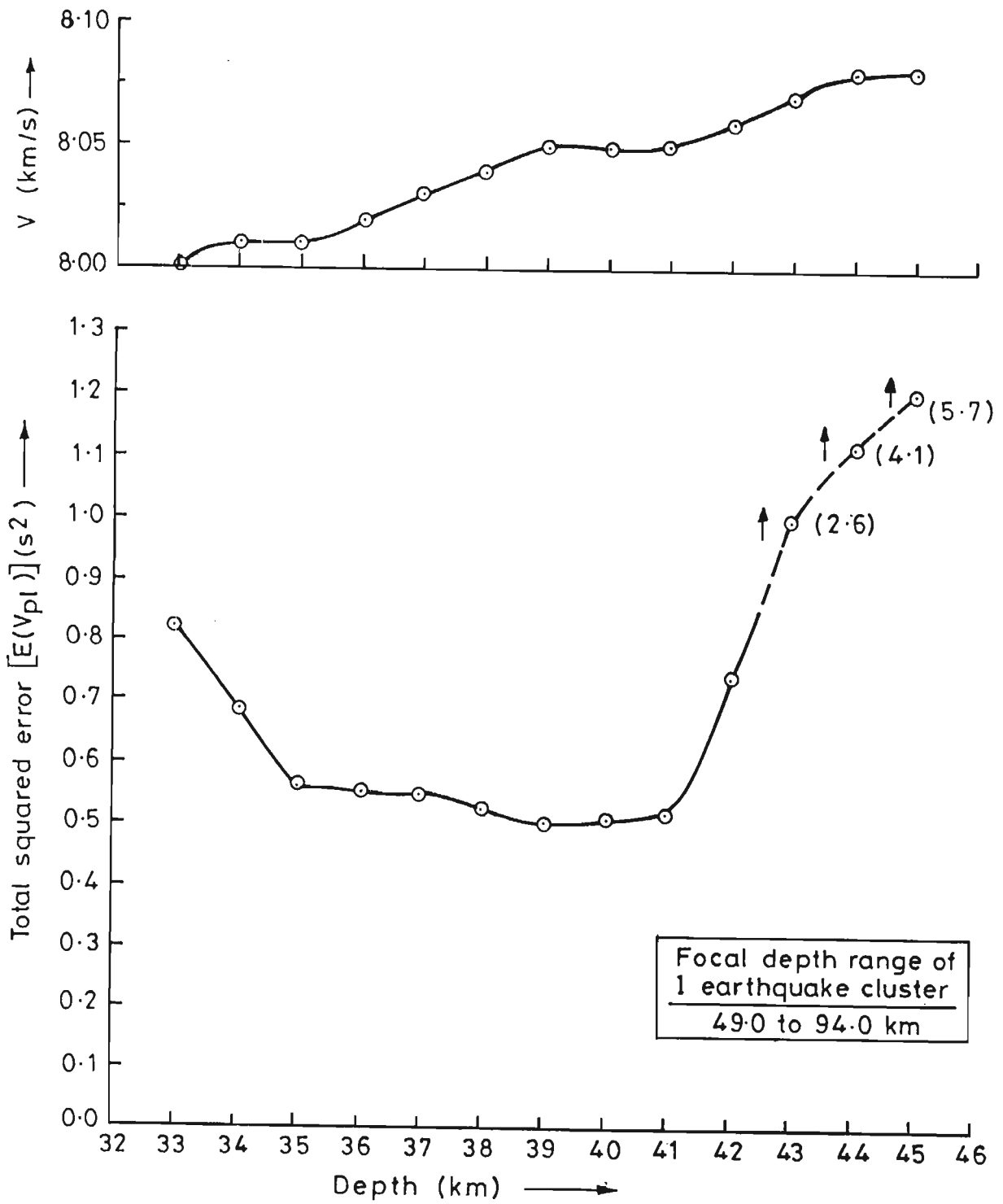
Figure 9.9   E(V_{pl}) and V_p for grid search using 1 earthquake cluster data. Depth on vertical axis for assumed depth of 1 interface.
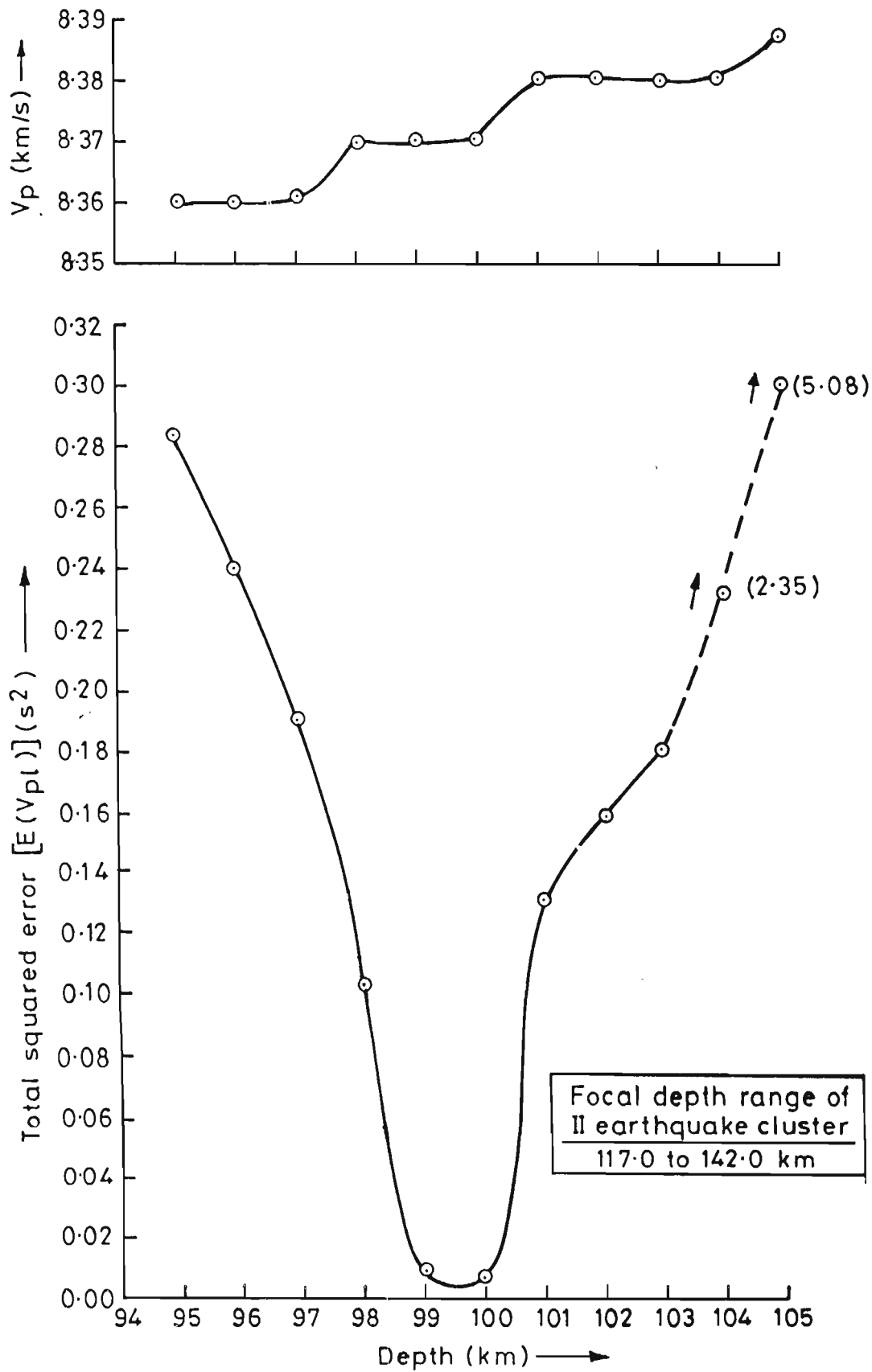
Figure 9.10   E(V_{pl}) and V_p for grid search using II earthquake cluster data. Depth on vertical axis for assumed depth of II interface.

8.37 km/s.

Results of analysing data for III earthquake cluster: Fig. 9.11 is the display of E ($V_{p\ell}$) using the data for the III earthquake cluster. It is observed that the minimum in E is again weak and there are three values namely 154 km, 164 km and 176 km for the depth to the top of the last layer in this case. The V_p in the layer however is not significantly different from these three possible depths.

In short the wave speed model obtained form this analyses may be summarized as in Table 9.5.

Table 9.5

Depth of boundaries from the surface (km)	p - wave speed obtained (km/s)
000	6.2 (Assumed)
039	8.1
100	8.4
154	8.7
OR 164	OR 8.8
OR 176	OR 8.8

9.5.4 Taking account of local velocity structure in the Hindu Kush region

As mentioned above, Roceker's estimate of $V_{p\ell}$ structure in the Hindu Kush region is also a multilayered one, though in subsequent refinements he has estimated lateral variation of V_p to occur in different layers. When we take account of this multilayered earth model, we are constrained to mesh it with the rest of the flat layered earth model by putting a vertical boundary between them. Estimating the extent to which Roecker's
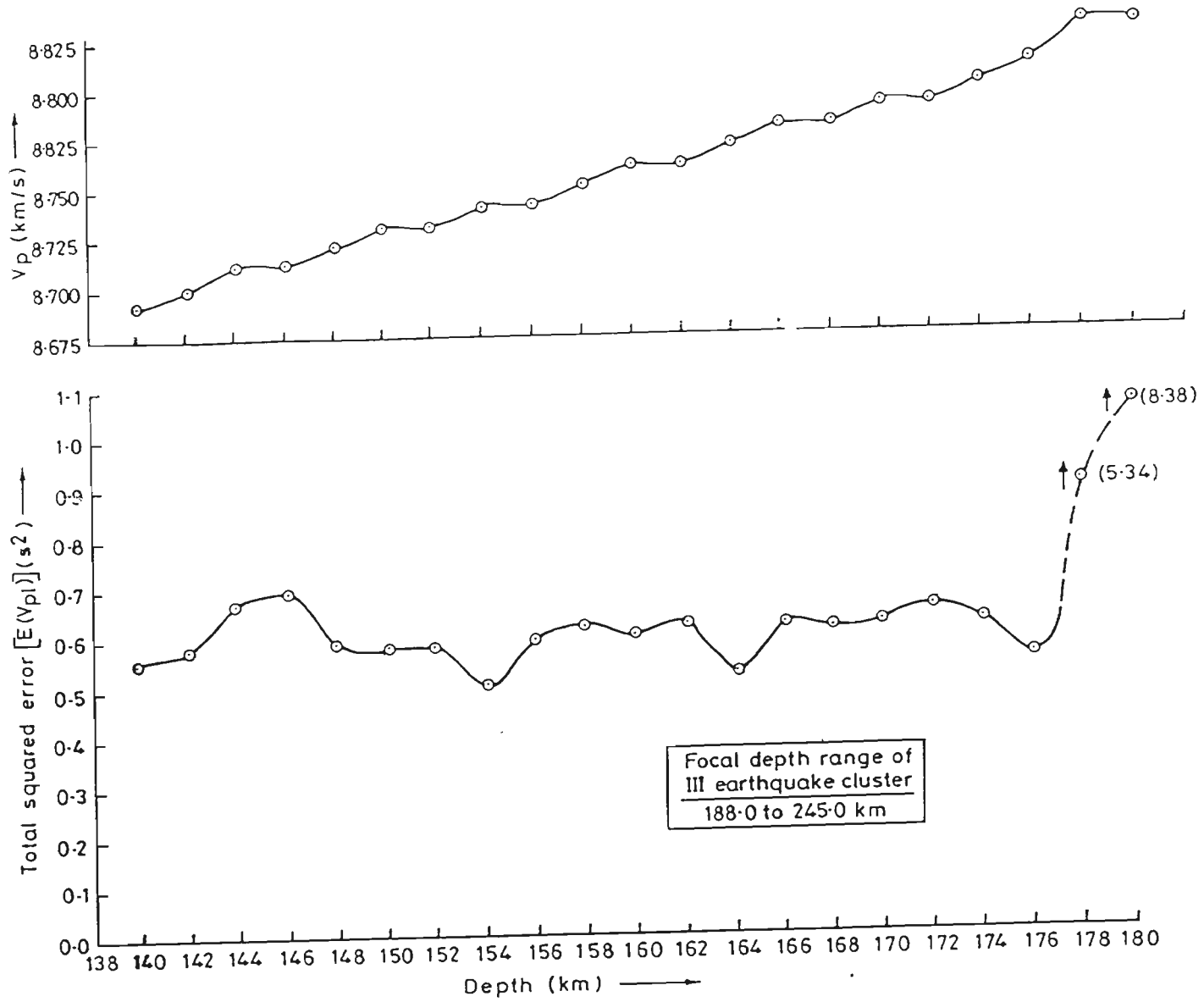
Figure 9.11 E(V_{pl}) and V_p for grid search using III earthquake cluster data. Depth on vertical axis for assumed depth of III interface.

model could exist along the ray path requires a some what arbitrary decision. Looking at the various maps and figures given by Roecker we estimate that the boundary may be placed along the northeast-southwest striking Kunar fault in the Hindu Kush region (Fig. 9.1).

Results: Figs. 9.12, 9.13 and 9.14 correspond to Figs. 9.9, 9.10 and 9.11 of the previous section. We conclude from Fig. 9.10 that the crustal thickness should still be 39 km and V_p at the top of the upper mantle should be 8.16 km/s. The error function in Fig. 9.14 shows that the layer boundary could be at 144, 158 and 174 km depth. The summary of the V_p structure is shown in Table 9.6.

<div align="center">

Table 9.6

</div>

Depth of boundaries from the surface (km)	p - wave speed obtained (km/s)
000	6.2 (Assumed)
039	8.2
100	8.4
154	8.7
OR 164	OR 8.7
OR 176	OR 8.8

A comparison of the information of Tables 9.5 and 9.6 is given in Table 9.7 We may conclude that the data from the I and II earthquake clusters give comparable results which can be considered as useful contributions of this exercise. The results for the III cluster loose in importance slightly because a clearcut depth to the top of the relevant layer can not be provided.

It is seen from Table 9.7 that taking account of the local structure in the Hindu Kush
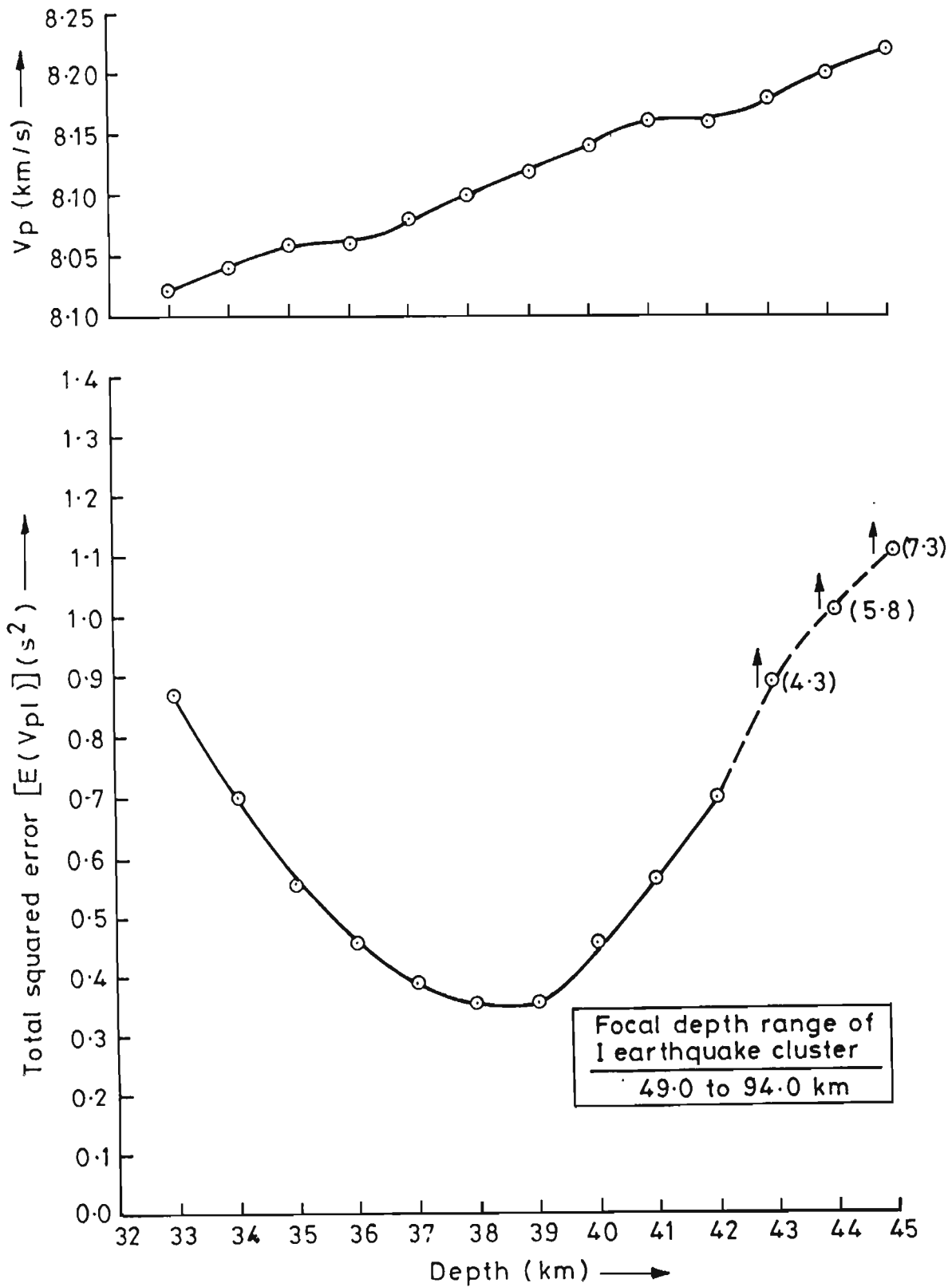
Figure 9·12   Same as fig. 9·9 but incorporating Roecker's model also for ray tracing.
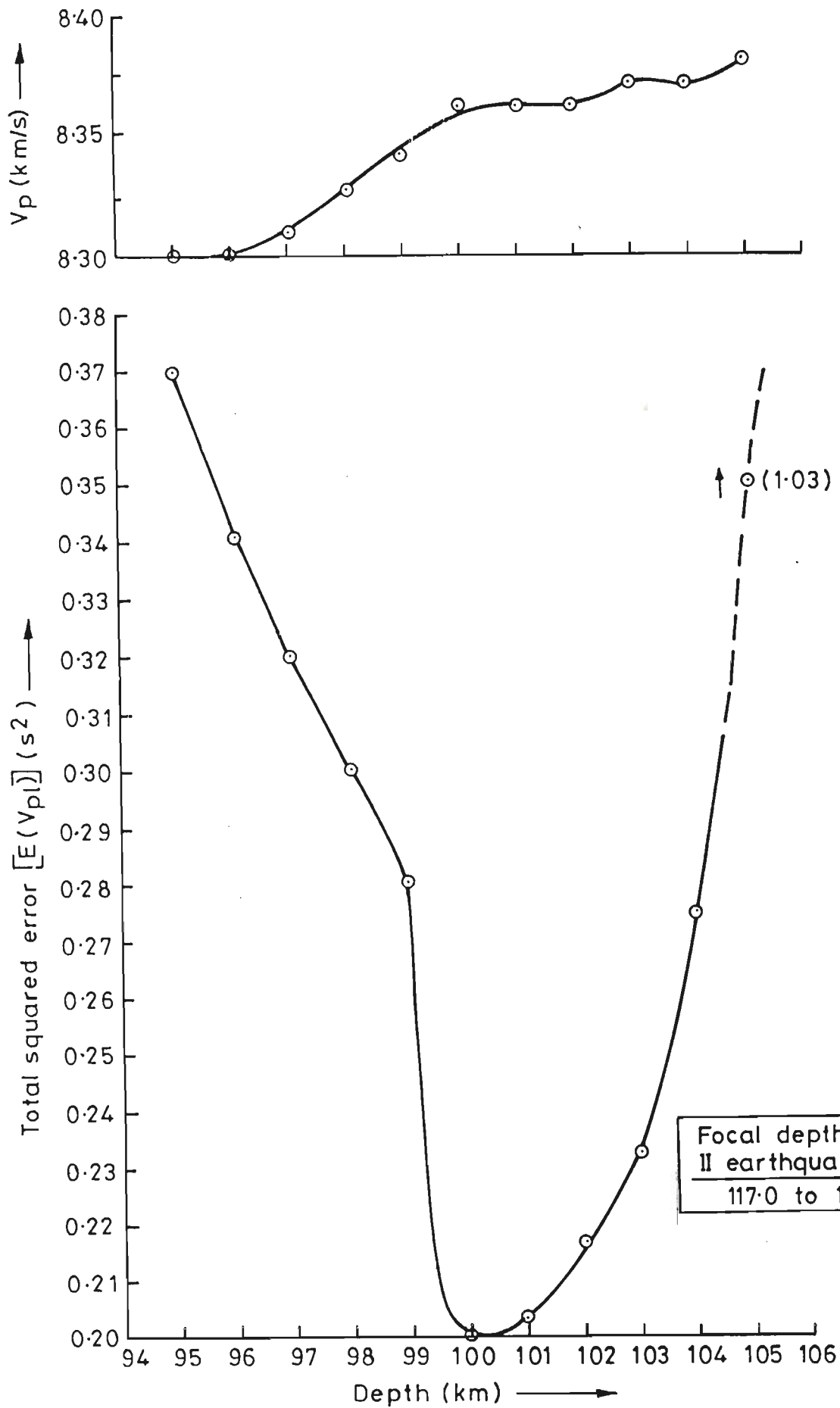
Figure 9·13 Same as 9·10 but incorporating Roecker's model also for ray tracing.
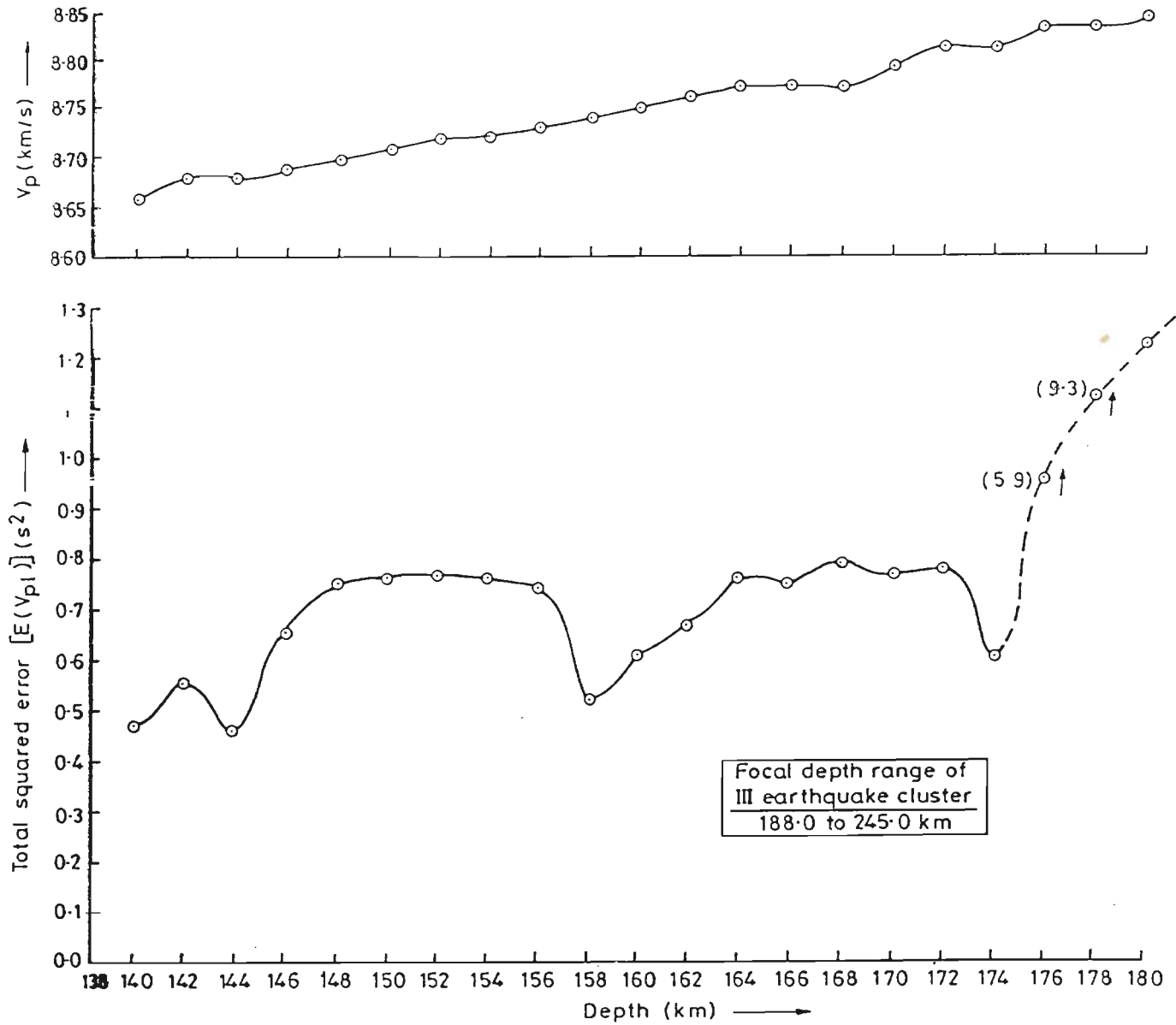
Figure 9.14 Same as fig. 9.11 but incorporating Roecker's model also for ray tracing.

region has not altered the results significantly. This must be ascribed to the fact that the total lengths of the ray paths in the Hindu Kush structure are comparatively short. Still we have the satisfaction of having made the effort to take local structure in account.

Table 9.7

Sr. No.	Focal depth range of different cluster (km)	Depth of boundaries from the surface(km)		p wave speed obtained	
				without local velocity structure (km/s)	with local velocity structure (km/s)
			000	6.2	6.2
			039	8.1	8.2
1.	049 - 034				
			100	8.4	8.4
2.	117 - 142				
			154	8.7	8.7
		OR	164	OR 8.8	OR 8.7
		OR	174	OR 8.8	OR 8.8
3.	188 - 245				

9.5.5 Summary of the results

We may conclude from the above exercise for estimating V_p structure along the NW Himalaya that the V_p at the top of upper mantle is about 8.1 km/s. At a depth of 100 km from the surface, or 60 km from the Moho, an increase in V_p occurs to a value of 8.35 km/s approximately. Below that level there is a further increase in V_p value indicated from the data of the III earthquake cluster. But the depth at which it could occur is uncertain

over a depth range of 20 km. The level of V_p below that boundary would be about 8.7 km/s.

9.6 DISCUSSION

Having obtained a V_p structure, it is natural to compare it with other determinations as far as possible. Of course comparison with the results given in Table 9.2 is there. But in our opinion a more useful comparison comes from the following remarks.

Ni and Barazangi (1983) studied body wave propagation in the India, Tibet and Afghanistan using high quality WWSSN data. They estimated a value of 8.45 ± 0.08 km/s for P_n wave speed in the Himalaya. This may be compared with our value of 8.1 km/s. The discrepancy between the two results is large and some explanation is required. All we can say is that when computing their values Ni and Barazangi had to use data in which the ray paths between earthquakes and recording stations were not strictly in the Himalaya. Whereas in our case, as seen from Fig. 9.1, the great circles between the epicentres in the Hindu Kush and the recording stations in the Garhwal Himalaya do lie along the NW Himalaya over a very large fraction of their lengths. Hence our determination is strictly for the Himalayan region.

Some DSS results for the Kashmir region are available in the literature. Fig. 9.15 is a comparison of the geographic location of DSS profiles and our great circle. The most significant point in this connection is that an upper mantle V_p of 8.1 km/s is obtained again and this supports our determination considerably. Along the DSS profile the Moho has wide depth variations. Towards the great circle of interest, the Moho appears to rise towards our estimated depth of 39 km (Fig. 9.16). In our opinion the data available to us do not bear a more extended discussion. Hence we refrain from it.

9.7 CONCLUSION

In this section a relatively straight forward analysis of data which were available
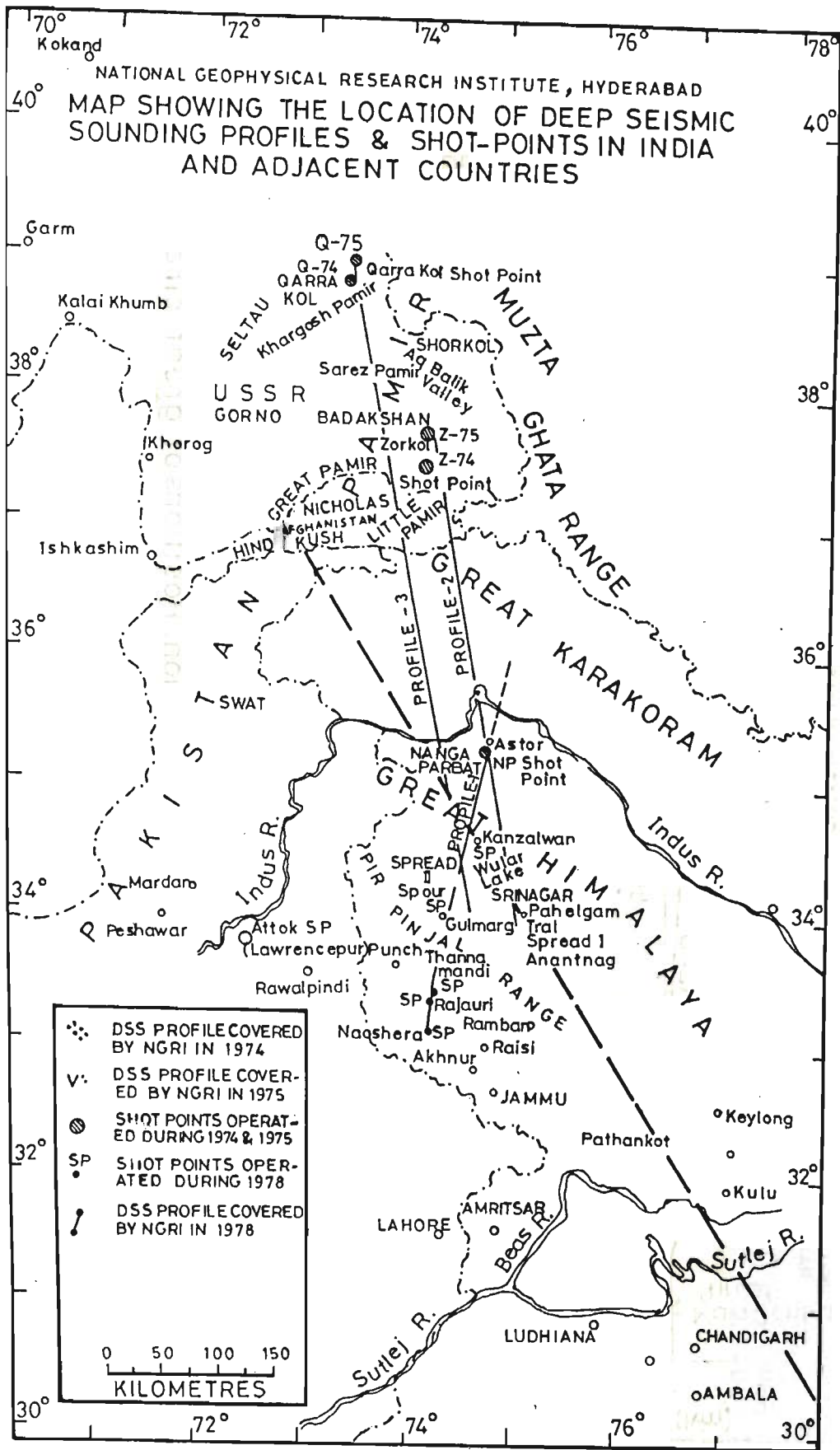
Figure 9·15 Relationship between DSS profiles (Kaila et al 1972) and the great circles between Hindu Kush epicentres and Garhwal stations. One great circle shown as representative of all the great circles.
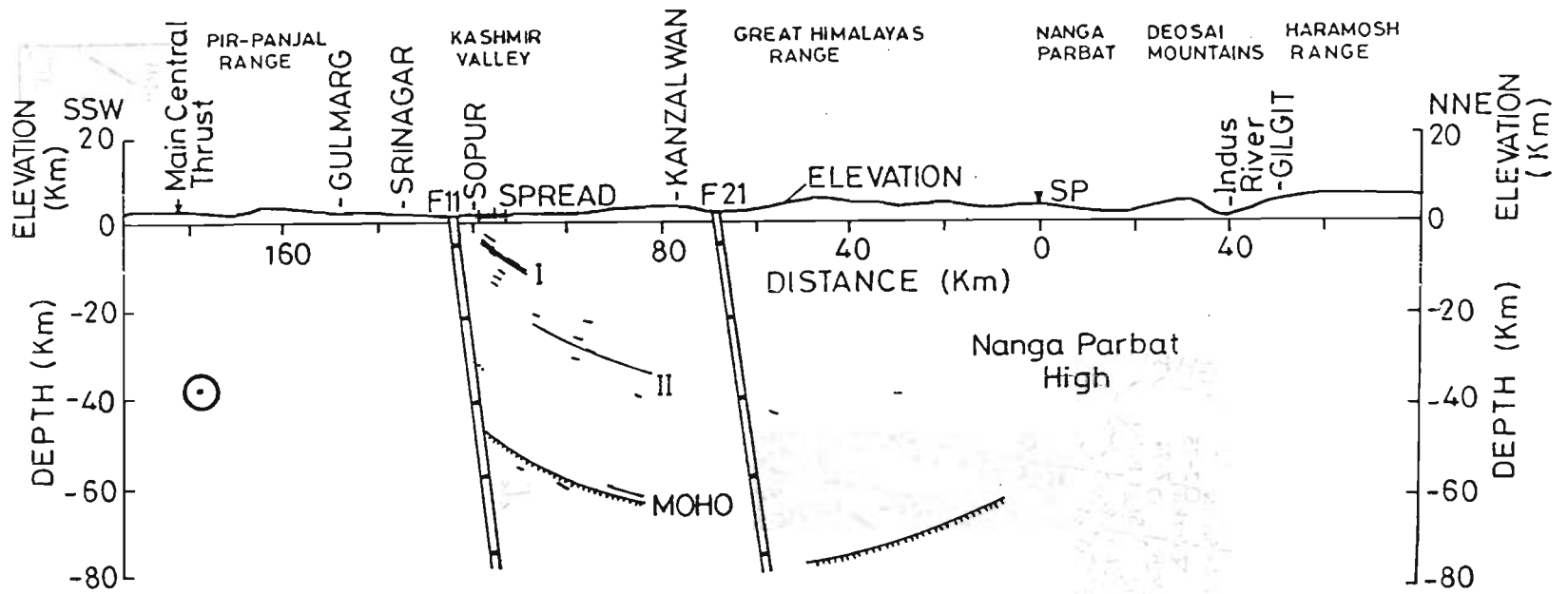
Figure 9·16   DSS results shown in depth section. Positions of great circles is also indicated.

to us freely, though in limited quantity, has been provided. We have obtained the V_p structure in the upper mantle under the northwest Himalaya. Ordinarily this determination would require considerable effort and resources. But for us it is a bonus.

REFERENCES

Aki, K. and P. Richards (1981). "Methods of Quantitative Seismology".Freeman,San Francisco, California.

Anonymous (1992), Uttarkashi Earthquake of October 20, 1991, Journal of Geological Society of India, Vol. 39, No. 1, pp. 83-88.

Baranowski, J., J. Armbruster, L. Seeber and P. Molnar (1984), Focal depths and fault plane solutions of earthquakes and active tectonics of the Himalaya, Jour. Geophys. Res., 89, 6918-6928.

Bell, M.L. and A. Nur (1978), Strength changes due to reservoir induced pore-pressure and application to Lake Oroville, Journal of Geophysical Research, Vol. 83, pp. 4469-4483.

Brune, J.N. (1993), The seismic hazard at Tehri Dam, Tectonophysics, Vol. 218, pp. 281-286.

Bullen, K.E. and B.A. Bolt (1985), Theory of seismology, Cambridge University press, Cambridge, pp.499.

Chander, R. (1988), Interpretation of observed ground level changes due to the 1905 Kangra earthquake, northwest Himalaya, Tectonophysics, Vol. 149, p. 289-298.

Chander, R., I. Sarkar, K.N. Khattri, and V.K. Gaur (1986), Upper crustal compressional wave velocity in the Garhwal Himalaya, Tectonophysics, 124, 133-140.

Chander, R. (1977), On tracing seismic rays with specified end points in layers of constant velocity and plane interfaces, Geophys. Prospect., 35, 120-124.

Davis, D., J. Suppe, and A.F. Dahlen (1983), Mechanics of fold and thrust belts and accretionary wedges, Jour. Geophys. Ref. 88, 1153-72.

Dunn, J.A., J.B. Auden, A.M.N. Ghosh and D.N. Wadia (1939), The Bihar Nepal earthquake of 1934, Geol. Surv. India Mem., 73.

Fitch, T.J. (1970), Earthquake mechanisms in the Himalayan, Burmese and Andaman regions and continental tectonics in central Asia ; J. Geophys. Res., 75, 2699-2709.

Gahalaut, V.K. and R. Chander (1992), On the active tectonics of Dehra Dun region from observations of ground elevation changes: Journal Geological Society of India, Vol. 38.

Gansser, A. (1964), The Geology of the Himalaya (London, New York, Sydney: Interscience Publishers), p. 289.

Gaur, V.K., R. Chander, I. Sarkar, K.N. Khattri and H. Sinvhal (1985), Seismicity and state of stress from investigations of local earthquakes in Kumaon Himalaya, Tectonophysics, 118, 243-251.

Gupta, H.K. (1983), Induced seismicity hazard mitigation through water level manipulation: a suggestion. Bull. Seismol. Soc. Am., 73: 679-682.

Gupta, H.K. and B.K. Rastogi (1972), Dams and earthquakes, Elsevier Sci. Pub. Comp., New York, pp. 229.

Gupta, D.P. (1978), Determination of hypocentral coordinates of local events in Kumaon Garhwal Himalaya (Unpublished M. Tech. dissertation, University of Roorkee, Roorkee, India).

Gupta, H.K. and K. Rajendran (1986), Large artificial water reservoirs in the vicinity of the Himalayan Foothills and reservoir-induced seismicity, Bull. Seismol. Soc. Am., 76 (1), pp. 205-215.

Gutenberg, B. and C.F. Richter (1954), Seismicity of the Earth, Princeton Univ. Press, pp. 310.

Hirn, A., J.C. Lapine, G. Jabert, M. Sapin, G. Wittlinger, X.Z. Xin, G.E. Yuan, W.X. Jing, T.J. Wen, X.S. Bai, M.R. Pandey and J. Tater (1984), Crustal structure and variability of the Himalayan border of Tibet, Nature, 307, 231 - 125.

Ibenbrahim, A., J. Ni, S. Salyards, and I.M. Ali (1989), Induced seismicity of the Tarbela Reservoir, Pakistan, Seismological Research Bulletin, Vol. 60, pp. 185-197.

Jacob, K.H., W.D. Pennigton, J. Armbruster, L. Seeber and S. Farhatulla (1979), Tarbela reservoir, Pakistan : A region of compressive tectonics with reduced seismicity upon initial reservoir filling, Bulletin of the Seismological Society of America, Vol. 69, pp. 1175-1192.

Jain, A.K. (1987), Kinematics of Transverse Regional Tectonics and Holocene stress field in the Garhwal Himalayas, Jour. Geol. Soc., Vol. 30, No. 3, pp. 160-186.

Kaila, K.L., V.G. Krishna and H. Narain (1969), Upper mantle elocity structure in the Hindu Kush region from travel time studies of deep earthquakes using a new analytical method, Bull. Seismol. Soc. Am., 59, 1949-1967.

Kumar, S., R. Chander and K.N. Khattri (1987), Compressional wave speed in the second crustal layer in Garhwal Himalaya, J. Assoc. Expl. Geophys., 8, 219-225.

Lee, W.H.K., R.E. Bennett and K.L. Meagher (1972), A method of estimating magnitude of local earthquakes from signal duration, Geol. Surv. Open - File Rep. (U.S.) 28.

Matveyeva, M.M. and A.A. Lukk (1968), Estimates of the accuracy in constructing travel time curves for the pamir-Hindu Kush zone and in the computer determination of the velocity profile in the upper mantle. Izv. Acad. Sci. U.S.S.R., Phys. Solid Earth, Engg. Transl. No. 8, A66-473.

Middlemiss, C.S. (1910), The kangra Earthquake of 4th April, 1905. Mem. Geol. Surv. India, 38, 1-409.

Molnar, P. and H. Lyon - Caen (1989), Fault plane solutions of earthquakes and active tectonics of the Tibetan plateau and its margins, Geophys. Jour. Int, 99, 123-153.

Molnar, P. (1987), The distribution of intensity associated with the 1905 Kangra earthquake and bound on extent of rupture zone; J. Geol. Soc. India, 29, 221-229.

Molnar, P. (1990), A Review of the Seismicity and Rates of Active Under thrusting, Journal of Himalayan Geology, Vol. 1, No. 2, pp. 131-154.

Mount, V. and J. Suppe (1987), State of stress near the San-Andreas fault : Implication for wrench tectonics Geology, Vol. 15, pp. 1143-1146.

Ni, J. and M. Barazangi (1984), Seismotectonics of the Himalayan collision zone: Geometry of the Underthrusting Indian Plate beneath the Himalaya, Jour. Geophys. Res., Vol. 89, p. 1147-1163.

Ni, J. and M. Barazangi (1983), High-frequency seismic wave propagation beneath the Indian Shield, Himalayan Arc, Tibetan Plateau and surrounding regions: high uppermost mantle velocities and efficient S propagation beneath Tibet, Geophy. J. R. Astr. Soc., 72, 665-689.

Rajal, B.S., N.S. Virdi and N.L. Hasija (1986), Recent crustal uplift in the doon valley : International Symposium of Neotectonics in south Asia, Dehra Dun, India, p. 146-159.

Ram, A. and R.F. Mereu (1977), Lateral variations in upper-mantle structure around India as obtained from Guaribidanur seismic array data, Geophys. J.R. astr. Soc., 49, 87-114.

Real, C.R. and T.L. Teng (1973), Local Richter magnitude and total signal duration in southern california, Bull. seismol. Soc. Am. 63, 1809-1827.

Richter, C.F. (1958), Elementary Seismology, W.H. Freeman and CO., San Fran cisco, pp.768.

Roecker, S.W. (1982), Velocity structure of the pamir - Hindu Kush region : Possible evidence of subducted crust, J. Geo. Res., 87, B2, 945-959.

Roeloffs, E.A. (1988), Fault stability changes induced beneath a reservoir with cyclic changes in water level, Journal of Geophysical Research, Vol. 93, 2107-2124.

Sarkar, *I (1983),* On seismological investigation of the Kumaon Himalaya using local earthquake data, Ph.D. thesis, Department of Earth Sciences, University of Roorkee, Roorkee, India.

Sarkar, I., R. Chander, K. N. Khattri and V. K. Gaur (1987), Estimation of hypocentral Parameters of local earthquakes when crustal layers have constant P-Velocities and dipping interfaces, Proc. Indian Acad. Sci. (Earth Planet, Sci.), Vol. 96, No. 3, pp. 229-238.

Seeber, L. and V. Gornitz (1983), River Profiles along the Himalayan arc as indicators of active tectonics : Tectonophysics, Vol. 92, p. 335-367.

Seeber, L. and J.G. Armbruster (1981), Great detachment earthquakes along the Himalayan arc and long term forcasting in earthquake prediction, An Interna tional Review, Maurice Ewing Series 4, Am. Geophys. Union, 259-277.

Shah, P.M. (1973), Ray tracing in three dimensions, Geophysics, Vol. 38, No.3, p. 600-604.

Sibson, R. (1989), High angle reverse Faulting in northern New Brunswkick, Canada, and its implication for fluid pressure levels, J. Struct. Geol., Vol. 11, pp. 873-877.

Singh, S., T. Singh and P. N. Agarwal (1976), Determination of Earthquake Magnitude from total signal duration for Tehri- Garhwal and Koyna regions, India, Bull. ISET, Vol. 13, pp.29-34.

Snow, D.T. (1972), Geodynamics of seismic reservoirs, Proceedings of Symposium on Flow through fractured rocks, Deutsche Ges. Erd-und Grundbau, Stuttgart, T2-j, pp. 1-19.

Sorrells, G.G., J. B. Crowley and K.F. Veith (1971). Methods for computing ray paths in complex geological structures, Bull. Seism. Soc. Am., Vol. 61, No.1, pp. 27-53

Srivastava, H.N. (1986), Status of seismicity and observational networks. In Proceedings of the national Meet of Earthquake Mechanism and Mitigation, Department of Science and Technology, Government of India, New Delhi, pp.51-58.

Tandon, A.N. (1967), Upper mantle seismic wave velocities in the Hindu Kush region, Indian J. Met. Geophys., 18, 385-390.

Valdiya, K.S. (1976), Himalayan transverse faults and folds and their parallelism with sub-surface structures of north Indian plains, Tectonophysics, 23, 353-386.

Valdiya, K.S. (1980), Geology of the Kumaun Himalaya (Dehra Dun : Wadia Institute of Himalayan Geology), p. 289.

Yeats, R.S. and R.J. Lillie (1991), Contemporary tectonics of the Himalayan Frontal Fault System : Folds, blind thrusts, and the 1905 Kangra earthquake : Journal of structural Geology, vol. 13, p. 215-225.

APPENDIX - I

```fortran
C———EARTHQUAKE LOCATION PROGRAM
      DIMENSION A1(12,20),B1(12,20),C1(12,20),D1(12,20)
      DIMENSION STE(4,4),PC(4),EF(4,20)
      DIMENSION X1(25,20),Y1(25,20),Z1(25,20),PCP(4),CORG(3,1)
      COMMON/A1/ CORD(4,20),RCORD(4,20),ER(20),RAT(20),FN(4,4),AM(4,4)
      COMMON/A2/ N,NS,NCORD,NCORT,L,M,NTS,N1,N2,W(4,20),CAT(20)
      COMMON/A3/ EPSM,CQ,EPS,LL,TSQ,DDF(3,6,6),E(6,6),SQE(6,6)
      COMMON/A4/ DF(4,20),SQER(20),V9(12,20),L9(25),NT
      COMMON/A5/ IRP,IPR,NSBI,NSPI,NIT
      COMMON/A6/ NST,TAU(20)
      OPEN(1,FILE='C4.DAT',STATUS='OLD')
      OPEN(2,FILE='C4.RES')
      PI=3.141592/180.
      LH=0.0
      NEE=1
5095  CONTINUE
      READ(1,*)NE
C     PRINT*,'1'
```

```
5090  CONTINUE

      LHT=1

      NCQ=1

      READ(1,*)NE

C     PRINT*,'1'

      PRINT*,'TYPE CTRI+C TO STOP ANY OTHER KEY TO CONTINUE'

      READ(*,*)

      READ(1,*) NDAY,NMTH,NYEAR

C     PRINT*,'2'

      READ(1,*) NHR,NMIN,NSEC

C     PRINT*,'3'

      WRITE(2,5096)

5096  FORMAT(1H1,1X,3HDAY,1X,3HMTH,1X,4HYEAR)

      WRITE(2,1) NDAY,NMTH,NYEAR

      WRITE(2,5906)

5906  FORMAT(1X,3HNHR,1X,3HNMN,1X,4HNSEC)

      WRITE(2,1) NHR,NMIN,NSEC

      READ(1,*) NS,NCORD,NST

C     PRINT*,'4'

      READ(1,*) NSPI

C     PRINT*,'5'

      READ(1,*) NSBI

C     PRINT*,'6'

      READ(1,*) IRP,IPR

C     PRINT*,'7'

      NCORT=NCORD+1

      NTS=NS+1
```

```
        NST=NST+1

        NIT=1

        LN=NS+2

        L=LN

*———I DEFINES CORD AXES NO. AND J DEFINES INTER FACE NO.

        READ(1,*) (CORG(I,1),I=1,NCORT)

C       PRINT*,'8'

        READ(1,*) (CORD(I,1),I=1,NCORT)

C       PRINT*,'9'

        CORD(1,1)=(CORD(1,1)-CORG(1,1))*60.*1.848218

        CORD(2,1)=(CORD(2,1)-CORG(2,1))*60.*1.601680

        CORD(3,1)=(CORG(3,1)-CORD(3,1))

        WRITE(2,10) (CORD(I,1),I=1,NCORT)

        DO 110 J=1,LN

        READ(1,*) (RCORD(I,J),I=1,NCORT)

C       PRINT*,'10'

        RCORD(1,J)=(RCORD(1,J)-CORG(1,1))*60.*1.848218

        RCORD(2,J)=(RCORD(2,J)-CORG(2,1))*60.*1.601680

        RCORD(3,J)=(CORG(3,1)-RCORD(3,J))

        WRITE(2,10) (RCORD(I,J),I=1,NCORT)

110     CONTINUE

        X0=CORD(1,1)*60.*1.848218

        Y0=CORD(2,1)*60.*1.60168

        Z0=-CORD(3,1)

        DELX=(RCORD(1,2)-CORD(1,1))*60.*1.848218

        DELY=(RCORD(2,2)-CORD(2,1))*60.*1.60168

        PHI=ATAN2(DELY,DELX)/PI
```

```
        AZR=PHI

        DACTUAL=SQRT(DELX**2+DELY**2)

        THETA=ATAN(DACTUAL/Z0)/PI

        DIP=180.-THETA

        S9=1.0

        H9=60*60*S9

        CM9=60*S9

        READ(1,*) XHC,XMC,XSC,XSC1,XSC2

C       PRINT*,'11' 100

        FORMAT(8F10.4)

        SS9=(XHC*H9)+(XMC*CM9)

        CORD(4,1)=SS9+XSC

        RCORD(4,1)=SS9+XSC1

        RCORD(4,LN)=SS9+XSC2

        DO 5099

        II=2,NTS

        READ(1,*) XHR,XMR,XSR

C       PRINT*,'12'

        RAT(II)=(XHR*H9)+(XMR*CM9)+XSR

        WRITE(2,10) RAT(II)

5099    CONTINUE

        READ(1,*) EPSM,CQ,EPS

C       PRINT*,'13'

        DO 1234 I=1,NCORT

        READ(1,*) W(I,1),W(I,L)

C       PRINT*,'14'

1234    CONTINUE
```

```
        READ(1,*) CFIS
C       PRINT*,'15'
        DO 119 I=1,NCORT
119     PC(I)=CORD(I,1)
        DO 101 IJ=2,NTS
        READ(1,*) L9(IJ)
C       PRINT*,'16'
        WRITE(2,1) L9(IJ)
        L8=L9(IJ)
        L81=L8+1
        DO 102 IK=2,L81
102     READ(1,*) V9(IJ,IK)
C       PRINT*,'17'
C       PRINT*,'   L8',L8
        IF(L8.EQ.1) GO TO 101
        DO 103 IK=2,L8
        READ(1,*) A1(IJ,IK),B1(IJ,IK),C1(IJ,IK),D1(IJ,IK)
C       PRINT*,'18'
        ZP=-D1(IJ,IK)
        CALL STRIKE(X0,Y0,Z0,DIP,AZR,ZP,XX1,YY1,PI)
        X1(IJ,IK)=XX1/(60.*1.848218)
        Y1(IJ,IK)=YY1/(60.*1.60168)
C       READ(1,*) X1(IJ,IK),Y1(IJ,IK)
C       PRINT*,'19'
C       IF(L8.EQ.1) GO TO 2804
        A1(IJ,IK)=A1(IJ,IK)/C1(IJ,IK)
        B1(IJ,IK)=B1(IJ,IK)/C1(IJ,IK)
```

```
         D1(IJ,IK)=D1(IJ,IK)/C1(IJ,IK)

         C1(IJ,IK)=1.0

         Z1(IJ,IK)=-A1(IJ,IK)*X1(IJ,IK)-B1(IJ,IK)*Y1(IJ,IK)-D1(IJ,IK)

         IF(L8.GT.1) GO TO 2805

2804     WRITE(2,2806)

2806     FORMAT(5X,4HSKIP)

2805     CONTINUE

103      CONTINUE

101      CONTINUE

         READ(1,*) (TAU(II),II=2,NST)

C        PRINT*,'20'

         NT=0.0

1001     CONTINUE

         IF(NT.EQ.8) GO TO 6520

         NTT=0.0

         NT=NT+1

         WRITE(2,1479) NT

1479     FORMAT(5X,3HNT=,I2)

1000     CONTINUE

         IF(NTT.EQ.15) GO TO 6520

         NTT=NTT+1

         WRITE(2,*)'NTT=', NTT

         WRITE(2,1497) NTT

1497     FORMAT(5X,4HNTT=,I50)

         CALL VAR(A1,B1,C1,D1,X1,Y1,Z1)

         IF(LL.EQ.1) LH=LH+1

         IF(LL.EQ.1) GO TO 5095
```

```
       IF(NCQ.EQ.2) GO TO 4249

C———OPTIMISATION OF ERROR FUNCTION

C———CALCULATING OF AUXILIARY FUNCTION AND MATRIX FUNCTION

       IF(IPR) 6611,6612,6611

6612   CALL MTFN1

       GO TO 6613

6611   CALL MTFN(DF)

C———CALCULATING STEP FUNCTION

6613   CALL MTINV(BM)

       IF(UL.EQ.1) LH=LU+1

       IF(LL.EQ.1) GO TO 5095

       IC=NCORT

       JC=NCORT

       KC=1

       CALL MTML(AM,FN,STE,IC,JC,KC)

       DO 2001 I=1,NCORT

2001   CORD(I,1)=CORD(I,1)-STE(I,1)

       WRITE(2,92)(CORD(I,1),I=1,NCORT)

       IF(LHT.EQ.2) NCQ=NCQ+1

       IF(NCQ.EQ.2) GO TO 1000

       LCT=1

       DO 4246 I=1,NCORT

       IF(CORD(I,1).GE.RCORD(I,1)) GO TO 4247

       LCT=2

       W(I,1)=10*W(I,1)

       CORD(I,1)=RCORD(I,1)+0.1*(RCORD(I,L)-RCORD(I,1))

       WRITE(2,4252)
```

```
        WRITE(2,807) I,W(I,1),CORD(I,1)

        GO TO 4246

C       WRITE(2,10) RCORD(4,LN)

4247    IF(CORD(I,1).LE.RCORD(I,LN)) GO TO 4250

        LCT=2

        W(I,L)=10*W(I,L)

        WRITE(2,10) RCORD(4,L)

        CORD(I,1)=RCORD(I,L)-0.1*(RCORD(I,L)-RCORD(I,1))

        WRITE(2,4252)

        WRITE(2,807) I,W(I,L),CORD(I,1)

        IF(LCT.EQ.2) GO TO 4246

4250    WRITE(2,4251)

4251    FORMAT(10X,4HFINE)

4252    FORMAT(10X,11HCHANGE MADE)

4246    CONTINUE

        IF(LCT.EQ.2) GO TO 1000

        IF(LCT.EQ.1) GO TO 4249

4249    CONTINUE

        IF(LHT.EQ.2) GO TO 41

C-------TESTING THE STEP FUNCTION

        AST=0.0

        DO 20 I=1,NCORT

20      AST=AST+(CORD(I,1)-PC(I))**2

        AST=SQRT(AST)

        EPSA=0.5

        IF(AST.LE.EPSA) GO TO 174

        DO 30 I=1,NCORT
```

```
30      PC(I)=CORD(I,1)

        IF(AST.LE.EPSA) GO TO 174

        GO TO 1000

174     DO 163 I=1,NCORT

163     PCP(I)=CORD(I,1)

        IF(NT.EQ.1) GO TO 1755

        AST=0.0

        DO 173 I=1,4

173     AST=AST+(CORD(I,1)-PCP(I))**2

        AST=SQRT(AST)

        IF(AST.LE.EPSA) GO TO 41

1755    CQ=CQ/10.

        WRITE(2,10) CQ

        GO TO 1001

41      WRITE(2,806)

806     FORMAT(1X,9HEVENT NO.,4X,5HXCORD,4X,5HYCORD,4X,

     1  5HZCORD,5X,5HTCORD)

        WRITE(2,807) LH,(CORD(I,1),I=1,NCORT)

807     FORMAT(7X,I3,4E14.6)

        IF(IPR) 6617,6614,6617

6617    TCORD=(CORD(4,1))/(60*60)

        IHR=TCORD

        AIHR=IHR

        CMIN=(TCORD-AIHR)*60

        MIN=CMIN

        AMIN=MIN

        SEC=(CMIN-AMIN)*60
```

```
6614    HLAT=(CORD(1,1)/(60*1.848218))+CORG(1,1)

        HLONG=(CORD(2,1)/(60*1.601680))+CORG(2,1)

        DPTH=CORD(3,1)-CORG(3,1)

        WRITE(2,5506)

5506    FORMAT ('~~~~~~~~~~~~~~~~~~~~~~~~~~~~~~~~~~~')

        WRITE(2,5507) HLAT,HLONG,DPTH

5507    FORMAT(5X,'LAT=',E14.6,'LONG=',E14.6,'DPTH=',E14.6)

        WRITE(2,*) HLAT,HLONG,DPTH

        PRINT *, HLAT,HLONG,DPTH

        IF(IPR) 6615,6616,6615

6615    WRITE(2,5906)

        WRITE(2,5) IHR,MIN,SEC

        CALL MAGNTD

6616    WRITE(2,5506)

        IF(LHT.EQ.2) GO TO 6520

        CALL CONF(CFIS)

        IF(LHT.EQ.1) GO TO 6519

6519    LHT=LHT+1

        CQ=0.0

        GO TO 1001

6520    WRITE(2,5091)

        PRINT*,'    *****LH= ',LH

        IF(NEE.EQ.NE)GO TO 99

        NEE=NEE+1

        GO TO 5090

5091    FORMAT(1X,'MODEL TEST COMPLETED')

1       FORMAT(8I5)
```

```
92      FORMAT(1X,4E14.6)

10      FORMAT(8F10.3)

5       FORMAT(1X,2I5,2X,3E14.6)

315     FORMAT(8F10.8)

11      FORMAT(1X,I5,2X,E14.6)

99      STOP

        END
```

```
        SUBROUTINE MTML(AMM,BMM,CMM,IC,JC,KC)

        DIMENSION AMM(4,4),BMM(4,4),CMM(4,4)

        COMMON/A1/ CORD(4,20),RCORD(4,20),ER(20),RAT(20),FN(4,4),AM(4,4)

        COMMON/A2/ N,NS,NCORD,NCORT,L,M,NTS,N1,N2,W(4,20),CAT(20)

        COMMON/A3/ EPSM,CQ,EPS,LL,TSQ,DDF(3,6,6),E(6,6),SQE(6,6)

        DO 15 I=1,IC

        DO 13 K=1,KC

        CMM(I,K)=0.0

        DO 11 J=1,JC

11      CMM(I,K)=CMM(I,K)+AMM(I,J)*BMM(J,K)

13      CONTINUE

15      CONTINUE

        RETURN

        END
```

```
        SUBROUTINE MTFN(DF)

        DIMENSION DF(4,20)

        COMMON/A1/ CORD(4,20),RCORD(4,20),ER(20),RAT(20),FN(4,4),AM(4,4)

        COMMON/A2/ N,NS,NCORD,NCORT,L,M,NTS,N1,N2,W(4,20),CAT(20)
```

```
        COMMON/A3/ EPSM,CQ,EPS,LL,TSQ,DDF(3,6,6),E(6,6),SQE(6,6)

        PRINT*,'     MTFN'

        DO 44 I=1,NCORT

        DO 54 K=1,NCORT

        AM(I,K)=0.0

        DO 64 J=2,NTS

64      AM(I,K)=AM(I,K)+DF(I,J)*DF(K,J)

54      CONTINUE

        FN(I,1)=0.0

        DO 55 J=2,NTS

        FN(I,1)=FN(I,1)+ER(J)*DF(I,J)

55      CONTINUE

44      CONTINUE

        DO 56 I=1,NCORT

        A1=2.*CQ*(W(I,L)/(RCORD(I,L)-CORD(I,1))**3

1       +W(I,1)/(CORD(I,1)-RCORD(I,1))**3)

        AM(I,1)=AM(I,I)+A1

        FN(I,1)=FN(I,1)+CQ*(W(I,L)/(RCORD(I,L)-CORD(I,1))**2

1       -W(I,1)/(CORD(I,1)-RCORD(I,1))**2)

56      CONTINUE

79      FORMAT(4X,4E14.6)

        RETURN

        END
```

```
        SUBROUTINE MTINV(BM)

        DIMENSION BM(4,4),DM(4,4),AMM(4,4)

        COMMON/A1/ CORD(4,20),RCORD(4,20),ER(20),RAT(20),FN(4,4),AM(4,4)
```

```
        COMMON/A2/ N,NS,NCORD,NCORT,L,M,NTS,N1,N2,W(4,20),CAT(20)
        COMMON/A3/ EPSM,CQ,EPS,LL,TSQ,DDF(3,6,6),E(6,6),SQE(6,6)
        PRINT*,' MTINV'
        LL=2
        DO 50 I=1,NCORT
        DO 50 J=1,NCORT
50      AMM(I,J)=AM(I,J)
C———CONSTRUCT IDENTITY MATRIX BM(I,J)=I
        DO 6 I=1,NCORT
        DO 5 J=1,NCORT
        IF(I-J) 4,3,4
3       BM(I,J)=1.0
        GO TO 5
4       BM(I,J)=0.0
5       CONTINUE
6       CONTINUE
C———LOCAL MAXIMUM MAGNITUDE AM(I,K) ON OR BELOW MAIN DIAGONAL
        DEL=1.0
        DO 45 K=1,NCORT
        IF(K-NCORT) 12,30,30
12      IMAX=K
        AMAX=ABS(AM(K,K))
        KP1=K+1
        DO 20 I=KP1,NCORT
        IF(AMAX-ABS(AM(I,K))) 15,20,20
15      IMAX=I
        AMAX=ABS(AM(I,K))
```

```
20     CONTINUE
C———INTERCHANGE ROWS IMAX AND K IF IMAX NOT EQUAL TO K
       IF(IMAX-K) 25,30,25
25     DO 29 J=1,NCORT
       ATMP=AM(IMAX,J)
       AM(IMAX,J)=AM(K,J)
       AM(K,J)=ATMP
       BTMP=BM(IMAX,J)
       BM(IMAX,J)=BM(K,J)
29     BM(K,J)=BTMP
       DEL=-DEL
30     CONTINUE
C———TEST FOR SINGULAR MATRIX
       IF(ABS(AM(K,K))-EPSM) 93,93,35
93     WRITE(2,101) K
       LL=1
C99    RETURN 35  DEL=AM(K,K)*DEL
C———DIVIDE PIVOT ROW BY ITS MAIN DIAGONAL ELEMENT
       DIV=AM(K,K)
       DO 38 J=1,NCORT
       AM(K,J)=AM(K,J)/DIV
38     BM(K,J)=BM(K,J)/DIV
C———REPLACE EACH ROW BY LINEAR COMBINATION WITH PIVOT ROW
       DO 43 I=1,NCORT
       AMULT=AM(I,K)
       IF(I-K) 39,43,39
39     DO 42 J=1,NCORT
```

```
         AM(I,J)=AM(I,J)-AMULT*AM(K,J)
42       BM(I,J)=BM(I,J)-AMULT*BM(K,J)
43       CONTINUE
45       CONTINUE
         DO 55 I=1,NCORT
         DO 55 J=1,NCORT
55       DM(I,J)=BM(I,J)
         CALL ERR(AMM,DM)
         IF(LL.EQ.1) GO TO 666
101      FORMAT(1X,'PROGRAM STOPPED IN INVERSE IN COLUMN NO.',I3)
666      RETURN
         END
```

```
         SUBROUTINE ERR(AMM,DM)
         DIMENSION DM(4,4),CM(4,4),EE(4,4),U(4,4),PM(4,4),
1        SE(4),AMM(4,4)
         COMMON/A1/ CORD(4,20),RCORD(4,20),ER(20),RAT(20),FN(4,4),AM(4,4)
         COMMON/A2/ N,NS,NCORD,NCORT,L,M,NTS,N1,N2,W(4,20),CAT(20)
         COMMON/A3/ EPSM,CQ,EPS,LL,TSQ,DDF(3,6,6),E(6,6),SQE(6,6)
         PRINT*,'     ERR'
         KI=4
         IC=NCORT
         JC=NCORT
         KC=NCORT
         K=1
C———CONSTRUCT UNIT MATRIX U(I,J)
```

```
        DO 60 I=1,NCORT

        DO 61 J=1,NCORT

        IF(I-J) 62,63,62

63      U(I,J)=1.0

        GO TO 61

62      U(I,J)=0.0 61 CONTINUE

60      CONTINUE

100     CONTINUE

        IC=NCORT

        JC=NCORT

        KC=NCORT

        CALL MTML(AMM,DM,CM,IC,JC,KC)

C------CONSTRUCT ERROR MATRIX E(I,J)

        DO 64 I=1,NCORT

        DO 64 J=1,NCORT

        EE(I,J)=U(I,J)-CM(I,J)

64      CONTINUE

        IF(K.GT.KI) GO TO 180

C------TESTING NORM OF ERROR FUNCTION

        DO 101 I=1,NCORT

        SE(I)=0.0

        DO 102 J=1,NCORT

102     SE(I)=SE(I)+ABS(EE(I,J))

101     CONTINUE

        AMAX=SE(1)

        DO 103 I=2,NCORT

        IF(SE(I).GT.AMAX) AMAX=SE(I)
```

```
103    CONTINUE
       IF(K.NE.1) GO TO 106
       IF(AMAX.GE.1) GO TO 200
106    CONTINUE
       IF(AMAX.LE.EPS) GO TO 190
       K=K+1
       DO 104 I=1,NCORT
       DO 104 J=1,NCORT
104    EE(I,J)=EE(I,J)+U(I,J)
       CALL MTML(DM,EE,PM,IC,JC,KC)
       DO 205      I=1,NCORT
       DO 205      J=1,NCORT
205    DM(I.J)=PM(I,J)
       GO TO 100
180    WRITE(2,20) AMAX
190    CONTINUE
       DO 185 I=1,NCORT
       DO 185 J=1,NCORT
185    AM(I,J)=DM(I,J)
       RETURN
200    WRITE(2,202) 202  FORMAT(1X,'STOPPED IN ERR')
       LL=1
       RETURN
20     FORMAT(1X,8F10.3)
       END
```

```
       SUBROUTINE VAR(A1,B1,C1,D1,X1,Y1,Z1)
```

```
      DIMENSION X1(25,20),Y1(25,20),Z1(25,20),CORG(3,1)

      DIMENSION A1(12,20),B1(12,20),C1(12,20),D1(12,20)

      DIMENSION X(20),Y(20),Z(20),A(20),B(20),C(20),D(20)

      DIMENSION V(20),A5(25),B5(25),A6(25),B6(25),V2(25)

      DIMENSION BA1(25),AB1(25),AB2(25),AB3(25),BA3(25),BA(25)

      DIMENSION FNX(25),FNY(25),DGX(25),DGY(25),SBX(25),SBY(25),SPX(25)

      DIMENSION SPY(25),G1X(25),G1Y(25),G2X(25),G2Y(25),G3X(25)

      DIMENSION G3Y(25),CH(25),CI(25),SB(25),SP(25),DG(25),BB(25)

      COMMON/A1/ CORD(4,20),RCORD(4,20),ER(20),RAT(20),FN(4,4),AM(4,4)

      COMMON/A2/ N,NS,NCORD,NCORT,L,M,NTS,N1,N2,W(4,20),CAT(20)

      COMMON/A3/ EPSM,CQ,EPS,LL,TSQ,DDF(3,6,6),E(6,6),SQE(6,6)

      COMMON/A4/ DF(4,20),SQER(20),V9(12,20),L9(25),NT

      COMMON/A5/ IRP,IPR,NSBI,NSPI,NIT

      PRINT*,'      VAR'

      LL=2

      X(1)=CORD(1,1)

      Y(1)=CORD(2,1)

      Z(1)=CORD(3,1)

C———GRAND LOOP START

      DO 111 II=2,NTS

      N=L9(II)

      N1=N+1

      N2=N-1

      V(N1)=V9(II,N1)

      X(N1)=RCORD(1,II)

      Y(N1)=RCORD(2,II)

      Z(N1)=RCORD(3,II)
```

```
        IF(N-1) 5092,5093,5092
5092    CONTINUE
        DO 105 IK=2,N
        V(IK)=V9(II,IK)
        A(IK)=A1(II,IK)
        B(IK)=B1(II,IK)
        C(IK)=C1(II,IK)
        D(IK)=D1(II,IK)
        X(IK)=X1(II,IK)
        Y(IK)=Y1(II,IK)
        Z(IK)=Z1(II,IK)
105     CONTINUE
C———VARIATIONAL ALGORITHM
        DO 23 I=2,N
        V2(I)=(V(I)/V(I+1))**2
        A5(I)=1.+A(I)*A(I)
        B5(I)=1.+B(I)*B(I)
        AB2(I)=A(I)*B(I)
        CH(I)=0.0
        CI(I)=0.0
23      CONTINUE
        DO 24 I=3,N
        A6(I)=1.+A(I)*A(I-1)
        B6(I)=1.+B(I)*B(I-1)
        AB1(I)=A(I)*B(I-1)
        BA1(I)=B(I)*A(I-1)
24      CONTINUE
```

```
         DO 50 I=2,N2

         AB3(I)=A(I)*B(I+1)

         BA3(I)=B(I)*A(I+1)

50       CONTINUE

         DO 60 J=1,NIT

         DO 62 M=1,NSPI

         DO 26 I=2,N

         I1=I-1

         I2=I+1

         DX1=X(I)-X(I1)

         DX2=X(I)-X(I2)

         DY1=Y(I)-Y(I1)

         DY2=Y(I)-Y(I2)

         DZ1=Z(I)-Z(I1)

         DZ2=Z(I)-Z(I2)

         AL12=DX1*DX1+DY1*DY1+DZ1*DZ1

         AL22=DX2*DX2+DY2*DY2+DZ2*DZ2

         F1X=DX1-A(I)*DZ1

         F2X=DX2-A(I)*DZ2

         F1Y=DY1-B(I)*DZ1

         F2Y=DY2-B(I)*DZ2

         F12X=F1X*F1X

         F22X=F2X*F2X

         F12Y=F1Y*F1Y

         F22Y=F2Y*F2Y

         V3=V2(I)*AL12

         V4=AL22*F1X
```

V5=AL22*F1Y

V6=AL12*F2X

V7=AL12*F2Y

FNX(I)=-(AL22*F12X-V3*F22X)*0.5

FNY(I)=-(AL22*F12Y-V3*F22Y)*0.5

DGX(I)=F12X*F2X+V4*A5(I)-V2(I)*(F22X*F1X+V6*A5(I))

DGY(I)=F12Y*F2Y+V5*B5(I)-V2(I)*(F22Y*F1Y+V7*B5(I))

G2X(I)=F12X*F2Y+V4*AB2(I)-V2(I)*(F22X*F1Y+V6*AB2(I))

G2Y(I)=F12Y*F2X+V5*AB2(I)-V2(I)*(F22Y*F1X+V7*AB2(I))

IF(I-N) 120,221,221

120   CONTINUE

F3X=DX2-A(I2)*DZ2

F3Y=DY2-B(I2)*DZ2

H1X=V3*F2X

SPX(I)=H1X*A6(I2)-F12X*F3X

G3X(I)=H1X*AB3(I)-F12X*F3Y

H1Y=V3*F2Y

SPY(I)=H1Y*B6(I2)-F12Y*F3Y

G3Y(I)=H1Y*BA3(I)-F12Y*F3X

IF(I-2) 26,26,221

221   CONTINUE

F3X=DX1-A(I1)*DZ1

F3Y=DY1-B(I1)*DZ1

H2X=V2(I)*F22X

SBX(I)=-V4*A6(I)+H2X*F3X

G1X(I)=-V4*AB1(I)+H2X*F3Y

H2Y=V2(I)*F22Y

```
        SBY(I)=-V5*B6(I)+H2Y*F3Y

        G1Y(I)=-V5*BA1(I)+H2Y*F3X

26      CONTINUE

        IF(IRP) 73,74,73

73      CONTINUE

74      CONTINUE

        DO 200 IJ=1,NSBI

        BB(2)=FNX(2)-G2X(2)*CI(2)-G3X(2)*CI(3)

        BB(N)=FNX(N)-G2X(N)*CI(N)-G1X(N)*CI(N2)

        SB(N)=SBX(N)

        SP(2)=SPX(2)

        DG(2)=DGX(2)

        DG(N)=DGX(N)

        DO 201 I=3,N2

        BB(I)=FNX(I)-G1X(I)*CI(I-1)-G2X(I)*CI(I)-G3X(I)*CI(I+1)

        SP(I)=SPX(I)

        SB(I)=SBX(I)

        DG(I)=DGX(I)

201     CONTINUE

        IP=1

        GO TO 250

202     CONTINUE

        DO 203 I=2,N

        CH(I)=BB(I)

203     CONTINUE

        BB(2)=FNY(2)-G2Y(2)*CH(2)-G3Y(2)*CH(3)

        BB(N)=FNY(N)-G2Y(N)*CH(N)-G1Y(N)*CH(N2)
```

```
        SB(N)=SBY(N)

        SP(2)=SPY(2)

        DG(2)=DGY(2)

        DG(N)=DGY(N)

        DO 204 I=3,N2

        BB(I)=FNY(I)-G1Y(I)*CH(I-1)-G2Y(I)*CH(I)-G3Y(I)*CH(I+1)

        SP(I)=SPY(I)

        SB(I)=SBY(I)

        DG(I)=DGY(I)

204     CONTINUE

        IP=2

250     CONTINUE

        SP(2)=SP(2)/DG(2)

        BB(2)=BB(2)/DG(2)

        DO 32 I=3,N

        IR=I-1

        DG(I)=DG(I)-SP(IR)*SB(I)

        IF(I-N) 33,32,32

33      SP(I)=SP(I)/DG(I)

32      BB(I)=(BB(I)-SB(I)*BB(IR))/DG(I)

        DO 34 K=2,N2

        I=N1-K

34      BB(I)=BB(I)-SP(I)*BB(I+1)

        GO TO (202,211), IP

211     DO 212 I=2,N

        CI(I)=BB(I)

212     CONTINUE
```

```
        IF(IJ-1) 71,71,72

72      IF(IJ-NSBI) 200,71,71

71      CONTINUE

        IF(IRP) 75,200,75

75      CONTINUE

200     CONTINUE

        DO 137 I=2,N

        X(I)=X(I)+CH(I)

        Y(I)=Y(I)+CI(I)

        Z(I)=-A(I)*X(I)-B(I)*Y(I)-D(I)

        CI(I)=0.0

137     CONTINUE

        DO 36 I=2,N

36      PRINT *,L,I,X(I),Y(I),Z(I)

        WRITE(2,*) L,I,X(I),Y(I),Z(I)

62      CONTINUE

60      CONTINUE

5093    CONTINUE

        DO 106 IK=2,N1

        CORD(1,IK)=X(IK)

        CORD(2,IK)=Y(IK)

        CORD(3,IK)=Z(IK)

        Z1(II,IK)=Z(IK)

        X1(II,IK)=X(IK)

        Y1(II,IK)=Y(IK)

106     CONTINUE

        CAT(II)=CORD(4,1)
```

```
        DO 107 IK=2,N1
        AL21=SQRT((CORD(1,IK-1)-CORD(1,IK))**2+(CORD(2,IK-1)-
     1  CORD(2,IK))**2+(CORD(3,IK-1)-CORD(3,IK))**2)
        CAT(II)=CAT(II)+AL21/V(IK)
        PRINT *, II,CAT(II)
        WRITE(2,*) II,CAT(II)
107     CONTINUE
        ER(II)=CAT(II)-RAT(II)
        SQER(II)=ER(II)**2
        IF(IPR) 6621,6622,6621
6621    PRINT *, SQER(II),ER(II)
        WRITE(2,*) SQER(II),ER(II)
6622    AL97=(CORD(1,2)-CORD(1,1))**2+(CORD(2,2)-CORD(2,1))**2+
     1  (CORD(3,2)-CORD(3,1))**2
        AL97=SQRT(AL97)
        DO 91 IK=1,NCORT
        IF(IK.EQ.4) GO TO 91
        DF(IK,II)=-(CORD(IK,2)-CORD(IK,1))/(V(2)*AL97)
91      CONTINUE
        DF(4,II)=1.0
111     CONTINUE
        TSQ=0.0
        IF(IPR) 6607,6608,6607
6607    DO 9823 II=2,NTS
9823    TSQ=TSQ+SQER(II)
        GO TO 6609
6608    DO 6610 II=2,NS
```

```
        MM=II+1

        DO 6610 JJ=MM,NTS

        E(II,JJ)=ER(JJ)-ER(II)

        SQE(II,JJ)=E(II,JJ)**2

        PRINT *,II,JJ,ER(II),ER(JJ)

        WRITE(2,*) II,JJ,ER(II),ER(JJ)

        PRINT *,II,JJ,E(II,JJ),SQE(II,JJ)

        WRITE(2,*) II,JJ,E(II,JJ),SQE(II,JJ)

        DO 6602 IK=1,3

6602    DDF(IK,II,JJ)=DF(IK,JJ)-DF(IK,II)

6610    CONTINUE

        DO 6620 II=2,NS

        MM=II+1

        DO 6620 JJ=MM,NTS

6620    TSQ=TSQ+SQE(II,JJ)

6609    PRINT *,'TOTAL SQUARE ERROR'

        WRITE(2,*) 'TOTAL SQUARE ERROR'

        PRINT *,TSQ

        WRITE(2,*) TSQ

        IF(TSQ.LT.100) GO TO 777

        IF(TSQ.GT.100) GO TO 776

776     LL=1

        PRINT *,'ERROR TOTAL SUM OF SQUARE EXCEED 100'

777     RETURN

        END
```

```
        SUBROUTINE CONF(CFIS)
```

```
       DIMENSION T(4,4),SER(4),CEFF(4),CFF(4,4),CONS(4,4),CT(4),ST(4)
       COMMON/A1/ CORD(4,20),RCORD(4,20),ER(20),RAT(20),FN(4,4),AM(4,4)
       COMMON/A2/ N,NS,NCORD,NCORT,L,M,NTS,N1,N2,W(4,20),CAT(20)
       COMMON/A3/ EPSM,CQ,EPS,LL,TSQ,DDF(3,6,6),E(6,6),SQE(6,6)
       EVAR=TSQ/(NS-NCORT)
       PRINT*,'     CONF'
       PRINT *,'EVAR=',EVAR
       WRITE(2,*) 'EVAR=',EVAR
       DO 2601    I=1,NCORT
       DO 2602    J=1,NCORT
 2602  AM(I,J)=EVAR*AM(I,J)
       SER(I)=SQRT(AM(I,I))
       PRINT *, I,'EST OF STD ERROR=',SER(I)
       WRITE(2,*) I,'EST OF STD ERROR=',SER(I)
 2601  CONTINUE
       CALL MTINV(BM)
       DO 2604 I=1,NCORT
       CEFF(I)=AM(I,I)
       PRINT *, I,'CEFF=',CEFF(I)
       WRITE(2,*) I,'CEFF=',CEFF(I)
 2604  CONTINUE
       DO 2606 I=1,NCORT
       DO 2607 J=1,NCORT
       CFF(I,J)=AM(I,J)+AM(J,I)
       T(I,J)=CFF(I,J)*CORD(J,I)
       CONS(I,J)=T(I,J)*CORD(I,1)
 2607  CONTINUE
```

```
2606  CONTINUE

      DO 2670 I=1,NCORT

      ST(I)=0.0

      DO 2680 J=1,NCORT

      ST(I)=ST(I)+T(I,J)

2680  CONTINUE

      ST(I)=-ST(I)

2670  CONTINUE

      DO 2613 I=1,NCORT

      CT(I)=0.0

      DO 2609 J=1,NCORT

2609  CT(I)=CT(I)+CONS(I,J)

2613  CONTINUE

      CTM=(CT(1)+CT(2)+CT(3)+CT(4))*0.5

      CKSQ=(NCORT*TSQ*CFIS)/(NS-NCORT)

      CTM1=CTM-CKSQ

C———CALCULATING FOR EPICENRTES PUTTING Z T ZERO

      PRINT *,'FOR THE CASE OF X AND Y ONLY'

      WRITE(2,*) 'FOR THE CASE OF X AND Y ONLY'

      CKS=(2*TSQ*CFIS)/(NS-2)

      ST(1)=-(CFF(1,1)*CORD(1,1))-(CFF(1,2)*CORD(2,1))

      ST(2)=-(CFF(2,2)*CORD(2,1))-(CFF(1,2)*CORD(1,1))

      CTM=(CEFF(1)*CORD(1,1)*CORD(1,1))+

    1 (CFF(1,2)*CORD(1,1)*CORD(2,1))+

    1 (CEFF(2)*CORD(2,1)*CORD(2,1))

      CTM2=CTM-CKS

      WRITE(2,*) 'XSQ=',CEFF(1),'YSQ=',CEFF(2),'XY=',CFF(1,2),
```

```
   1  'X=',ST(1),'Y=',ST(2),'CTERM=',CTM2

      HSQ=CFF(1,2)*CFF(1,2)*0.25

      AB=CEFF(1)*CEFF(2)

      COND=HSQ-AB

      IF(COND.LT.0.0) GO TO 2616

      IF(COND.GE.0.0) GO TO 2617

2617  PRINT *,'NO CONFIDENCE ELLIPSE'

      WRITE(2,*) 'NO CONFIDENCE ELLIPSE'

      STOP

2616  PRINT *,'THIS IS AN ELLIPSE'

      WRITE(2,*) 'THIS IS AN ELLIPSE'

      NUM1=(ST(2)*CFF(1,2)*0.25)-(CEFF(2)*ST(1)*0.5)

      NUM2=(ST(1)*CFF(1,2)*0.25)-(CEFF(1)*ST(2)*0.5)

      X=-NUM1/COND

      Y=-NUM2/COND

      PRINT *, 'XCORD=',X,'YCORD=',Y

      WRITE(2,*) 'XCORD=',X,'YCORD=',Y

      CTERM=(ST(1)*X*0.5)+(ST(2)*Y*0.5)+CTM2

      THETA=CFF(1,2)/(CEFF(1)-CEFF(2))

      THETA1=ATAN(THETA)*0.5

      THETA2=90.+THETA1

      S1=SIN(THETA1)

      S2=SIN(THETA2)

      C1=COS(THETA1)

      C2=COS(THETA2)

      T1=(CEFF(1)*S1*S1)+(CFF(1,2)*S1*C1)+(CEFF(2)*C1*C1)

      T2=(CEFF(2)*S2*S2)+(CFF(1,2)*S2*C2)+(CEFF(2)*C2*C2)
```

```
R1=-CTERM/T1

R2=-CTERM/T2

PRINT *,'ANG1=',THETA1,'ANG2=',THETA2,'RAD1=',R1,'RAD2=',R2

WRITE(2,*) 'ANG1=',THETA1,'ANG2=',THETA2,'RAD1=',R1,'RAD2=',R2

R1=ABS(R1)

R2=ABS(R2)

R1=SQRT(R1)

R2=SQRT(R2)

AREA=3.142*R1*R2

PRINT *,'RAD1=',R1,'RAD2=',R2,'AREA=',AREA

WRITE(2,*) 'RAD1=',R1,'RAD2=',R2,'AREA=',AREA

PRINT *,'CONFIDENCE REGION FOUND'

WRITE(2,*) 'CONFIDENCE REGION FOUND'

RETURN

END
```

```
SUBROUTINE MTFN1

COMMON/A1/ CORD(4,20),RCORD(4,20),ER(20),RAT(20),FN(4,4),AM(4,4)

COMMON/A2/ N,NS,NCORD,NCORT,L,M,NTS,N1,N2,W(4,20),CAT(20)

COMMON/A3/ EPSM,CQ,EPS,LL,TSQ,DDF(3,6,6),E(6,6),SQE(6,6)

COMMON/A4/ DF(4,20),SQER(20),V9(12,20),L9(25),NT

PRINT*,'    MTFN1'

DO 74 I=1,3

DO 75 K=1,3

AM(I,K)=0.0

IF(K.GT.1) GO TO 76

FN(I,1)=0.0
```

```
76      DO 77 II=2,NS

        MM=II+1

        DO 78 JJ=MM,NTS

        AM(I,K)=AM(I,K)+DDF(K,II,JJ)*DDF(I,II,JJ)   ,

        IF(K.GT.1) GO TO 78

        FN(I,1)=FN(I,1)+DDF(I,II,JJ)*E(II,JJ)

78      CONTINUE

77      CONTINUE

75      CONTINUE

74      CONTINUE

        DO 56 I=1,NCORT

        A1=2.0*CQ*(W(I,L)/(RCORD(I,L)-CORD(I,1))**3+

     1  W(I,1)/(CORD(I,1)-RCORD(I,1))**3)

        AM(I,I)=AM(I,I)+A1

        FN(I,1)=FN(I,1)+CQ*(W(I,L)/(RCORD(I,L)-CORD(I,1))**2-

     1  W(I,1)/(CORD(I,1)-RCORD(I,1))**2)

56      CONTINUE

        WRITE(2,*) ((AM(I,K),I=1,3),K=1,3)

        WRITE(2,*) (FN(I,1),I=1,3)

        RETURN

        END
```

```
        SUBROUTINE MAGNTD

        DIMENSION DELTA(20)

        COMMON/A1/ CORD(4,20),RCORD(4,20),ER(20),RAT(20),FN(4,4),AM(4,4)

        COMMON/A2/ N,NS,NCORD,NCORT,L,M,NTS,N1,N2,W(4,20),CAT(20)

        COMMON/A6/ NST,TAU(20)
```

```
        PRINT*,'    MAGNTD'
        DO 700 II=2,NST
        DELTA(II)=(RCORD(1,II)-CORD(1,1))**2+(RCORD(2,II)-CORD(2,1))**2
        DELTA(II)=SQRT(DELTA(II))
        PRINT *,DELTA(II),TAU(II)
        WRITE(2,*) DELTA(II),TAU(II)
700     CONTINUE
        AVDLT=0.0
        AVTAU=0.0
        DO 702      II=2,NST
        IF(TAU(II).EQ.0.0) DELTA(II)=0.0
        AVDLT=AVDLT+DELTA(II)
        AVTAU=AVTAU+TAU(II)
702     CONTINUE
        PRINT *,NST
        WRITE(2,*) NST
        AVDLT=AVDLT/NST
        AVTAU=AVTAU/NST
        PRINT *,AVDLT,AVTAU
        WRITE(2,*) AVDLT,AVTAU
        CMAG=(-0.87)+(2.0*ALOG10(AVTAU))+(0.0035*AVDLT)
        PRINT *,'MAGNITUDE=',CMAG
        WRITE(2,*) 'MAGNITUDE=',CMAG
        RETURN
        END
****************SUBROUTINE  STRIKE *************
        SUBROUTINE STRIKE(X0,Y0,Z0,DIPR,AZR,ZP,X1,Y1,PI)
```

```
XP=0.0

YP=0.0

DIPP=180.+90.

AZP=180.0

PR1=SIN(DIPR*PI)*COS(AZR*PI)

PR2=SIN(DIPR*PI)*SIN(AZR*PI)

PR3=COS(DIPR*PI)

PN1=SIN(DIPN*PI)*COS(AZN*PI)

PN2=SIN(DIPN*PI)*SIN(AZN*PI)

PN3=COS(DIPN*PI)

SNUM=(XP-X0)*PN1+(YP-Y0)*PN2+(ZP-Z0)*PN3

SDEN=PR1*PN1+PR2*PN2+PR3*PN3

S=SNUM/SDEN

X1=X0+S*PR1

Y1=Y0+S*PR2

Z1=Z0+S*PR3

RETURN

END
```

APPENDIX - II

TABLE II.1 RECORDED P AND S ARRIVAL TIMES FOR EARTHQUAKES WHOSE HYPOCENTRAL COORDINATES WERE DETERMINED.

ARRIVAL TIMES AT STATIONS

S. No.	DATE			NEAREST COMMON HOURS & MINUTES		AKMUNDSAM		CHAMIYALA		LAMBGAON / LATASERA		BEENAGAON		DHONTRI	
	Y	M	D	H	M	P PHASE SECS	S PHASE SECS	P PHASE SECS	S PHASE SECS	P PHASE SECS	S PHASE SECS	P PHASE SECS	S PHASE SECS	P PHASE SECS	S PHASE SECS
(1)	(2)	(3)	(4)	(5)	(6)	(7)	(8)	(9)	(10)	(11)	(12)	(13)	(14)	(15)	(16)
1)	1984	12	12	12	25	35.0	39.7	32.4	35.6	33.8	37.1	—	—	—	—
2)	1984	12	18	17	59	39.1	—	36.5	38.5	37.2	40.1	—	—	—	—
3)	1984	12	19	12	27	11.9	13.6	12.6	14.0	13.5	15.3	—	—	—	—
4)	1984	12	24	04	17	23.0	28.0	20.2	23.0	21.6	24.6	—	—	—	—
5)	1985	01	01	16	40	60.7	65.6	57.6	60.2	59.6	63.5	—	—	—	—
6)	1985	02	03	15	55	54.8	59.7	54.1	57.3	53.9	56.7	—	—	51.2	52.8
7)	1985	02	06	05	53	58.3	66.2	55.1	60.5	57.5	63.1	53.1	56.8	—	—
8)	1985	02	10	20	57	27.2	30.5	23.6	25.6	—	—	20.5	21.5	—	—
9)	1985	02	14	03	40	8.2	24.8	7.4	22.0	7.5	21.4	6.3	21.1	5.5	17.3
10)	1985	02	15	21	01	24.7	29.6	21.8	25.8	24.6	28.8	19.7	22.2	29.2	31.4
11)	1985	03	01	18	49	18.2	24.0	17.7	21.9	16.3	19.8	17.7	—	14.6	17.7
12)	1985	03	02	04	47	27.7	32.5	27.1	31.3	26.1	29.9	26.8	30.5	24.9	28.5
13)	1985	03	28	05	57	36.2	39.0	—	—	—	—	35.3	37.3	32.9	—

(1)	(2)	(3)	(4)	(5)	(6)	(7)	(8)	(9)	(10)	(11)	(12)	(13)	(14)	(15)	(16)
14)	1985	03	30	19	06	24.5	32.9	21.8	30.2	—	—	21.1	28.9	19.7	26.0
15)	1985	03	30	20	33	27.6	34.0	26.6	32.5	—	—	27.1	32.5	25.5	30.4
16)	1985	03	30	20	44	11.8	25.5	10.5	23.8	—	—	11.4	22.8	8.7	20.0
17)	1985	03	31	00	51	—	—	33.1	37.1	—	—	34.1	35.5	30.0	32.4
18)	1985	03	31	05	13	27.5	—	26.4	40.0	—	—	25.9	36.8	23.8	37.1
19)	1985	03	31	16	04	56.5	63.5	54.5	61.5	—	—	52.7	54.5	57.9	63.6
20)	1985	04	01	14	15	28.3	29.2	30.0	32.6	—	—	33.8	38.0	32.3	36.5
21)	1985	04	02	01	49	30.2	37.5	32.1	37.6	26.3	28.5	31.7	37.4	28.6	32.5
22)	1985	04	03	21	23	—	—	40.6	45.2	35.5	36.6	40.8	45.0	38.3	41.5
23)	1985	04	06	06	52	15.2	15.5	17.5	19.8	—	—	20.5	22.5	19.1	19.6
24)	1985	04	07	22	21	—	—	51.5	54.7	49.5	51.9	50.9	53.9	51.0	53.5
25)	1985	04	08	00	19	—	—	29.5	34.0	25.5	27.7	20.2	27.7	16.6	17.6
26)	1985	04	08	06	50	—	—	61.7	64.5	—	—	64.0	67.5	63.5	67.9
27)	1985	04	08	00	36	—	—	33.5	38.6	29.3	32.2	32.0	36.5	32.6	36.4
28)	1985	04	08	17	55	—	—	11.7	16.3	12.5	16.5	9.4	11.6	13.2	18.3
29)	1985	04	10	22	04	—	—	47.3	—	50.0	—	46.3	—	47.9	—
30)	1985	04	11	06	43	—	—	45.8	48.4	—	—	48.6	—	47.0	51.3
31)	1985	04	13	07	07	5.1	6.1	6.5	8.6	11.5	16.1	10.0	15.1	8.2	12.4
32)	1985	04	14	07	35	—	—	46.1	50.6	43.0	47.9	47.2	52.5	43.7	48.5
33)	1985	04	16	04	16	27.7	—	25.1	33.5	25.5	35.0	23.3	30.0	27.8	38.4
34)	1985	04	16	19	04	11.6	21.5	9.5	17.7	7.4	14.6	8.1	15.6	9.5	18.0
35)	1985	04	17	02	18	13.1	16.0	15.1	19.8	—	—	18.6	25.0	16.6	20.3
36)	1985	04	17	16	00	15.3	19.5	15.3	19.3	—	—	17.6	21.5	13.2	15.5
37)	1985	04	17	06	59	42.6	43.6	45.0	47.5	—	—	48.2	50.3	47.1	51.9

(1)	(2)	(3)	(4)	(5)	(6)	(7)	(8)	(9)	(10)	(11)	(12)	(13)	(14)	(15)	(16)
38)	1985	04	19	21	25	50.0	52.8	50.6	55.0	—	—	52.0	57.7	53.4	60.0
39)	1985	04	19	22	23	56.0	58.6	56.7	60.0	—	—	—	—	55.0	57.0
40)	1985	04	19	22	26	26.0	28.1	26.5	28.6	28.5	32.0	28.9	32.5	24.6	26.0
41)	1985	04	20	07	17	4.1	6.2	4.5	7.0	—	—	—	—	5.7	8.2
42)	1985	04	20	15	28	64.2	68.4	62.6	66.5	60.1	62.0	63.1	67.4	60.6	63.2
43)	1985	04	23	17	43	5.8	15.2	2.4	9.4	3.4	9.9	0.4	4.0	4.3	12.7
44)	1985	04	24	04	45	39.5	51.3	36.0	45.6	37.8	48.8	34.5	41.8	39.8	52.9
45)	1985	04	25	12	46	—	—	—	—	38.0	40.0	39.5	42.5	39.5	41.1
46)	1985	04	25	12	47	—	—	33.0	36.0	31.0	32.6	32.4	35.6	32.0	34.0
47)	1985	04	25	15	59	—	—	52.9	56.8	50.2	52.0	—	—	50.5	53.0
48)	1985	04	25	18	36	—	—	25.2	28.8	23.4	25.0	25.1	28.0	24.4	26.4
49)	1985	04	25	19	19	12.5	14.8	14.8	17.4	20.6	24.6	17.9	—	16.7	20.7
50)	1985	04	25	21	45	—	—	21.3	24.9	17.9	19.6	19.7	23.6	19.3	23.2
51)	1985	04	26	20	44	14.0	17.2	11.0	14.7	10.5	13.5	8.8	11.0	12.5	15.3
52)	1985	04	26	21	06	55.0	—	53.5	58.4	48.7	51.1	53.6	59.0	50.5	54.3

S. No.	DATE			NEAREST COMMON HOUSE & MINUTES		AKMUNDSAM		CHAMIYALA		BEENAGAON		DAGCHAURA		ODADHAR		TILWARA		UKHIMATH	
						P PHASE	S PHASE	P PHASE	S PHASE	P PHASE	S PHASE	P PHASE	S PHASE	P PHASE	S PHASE	P PHASE	S PHASE	P PHASE	S PHASE
	Y	M	D	H	M	SECS	SECS	SECS	SECS	SECS	SECS	SECS	SECS	SECS	SECS	SECS	SECS	SECS	SECS
1)	(2)	(3)	(4)	(5)	(6)	(7)	(8)	(9)	(10)	(11)	(12)	(13)	(14)	(15)	(16)	(17)	(18)	(19)	(20)
53)	1985	10	31	17	41	—	—	53.7	66.1	51.4	61.4	—	—	50.6	58.6	48.0	54.4	45.1	48.7
54)	1985	11	01	03	37	55.0	64.2	55.1	64.3	56.5	67.6	—	—	—	—	55.8	67.0	58.0	71.5
55)	1985	11	01	17	25	57.6	58.6	60.4	62.8	33.0	67.5	61.8	64.9	62.8	—	—	—	—	—
56)	1985	11	01	23	06	30.7	41.3	28.5	38.1	26.3	32.1	28.0	34.1	26.0	31.6	23.1	29.0	17.5	24.9
57)	1985	11	05	22	08	—	—	39.1	44.4	37.4	39.9	—	—	40.1	45.5	—	—	—	—
58)	1985	11	06	05	42	—	—	—	—	11.8	—	—	—	11.5	15.8	8.7	12.4	7.0	10.4
59)	1985	11	06	10	17	—	—	—	—	40.5	44.4	—	—	—	—	38.0	40.5	35.9	37.5
60)	1985	11	07	15	29	—	—	5.4	9.4	2.3	4.7	—	—	4.5	—	5.2	—	3.2	5.9
61)	1985	11	07	18	03	46.0	48.5	48.0	50.6	51.5	52.7	50.0	53.0	50.7	—	53.7	55.5	53.5	57.7
62)	1985	11	09	01	31	38.5	44.5	37.2	44.3	38.3	46.2	42.8	52.7	40.5	48.5	42.5	52.2	43.8	53.8
63)	1985	11	10	02	29	66.0	76.0	62.3	70.8	59.9	67.0	—	—	—	—	60.2	67.5	55.3	60.5
64)	1985	11	18	05	26	—	—	—	—	—	—	—	—	36.9	—	34.9	37.9	32.4	33.4
65)	1985	11	18	14	47	—	—	12.0	15.6	10.5	12.9	—	—	—	—	13.2	17.3	12.1	15.5
66)	1985	11	18	20	45	32.5	36.1	30.3	33.6	31.1	34.6	—	—	33.0	37.1	35.2	40.4	35.7	41.1
67)	1985	11	18	23	30	—	—	19.9	24.0	19.6	23.4	—	—	22.1	27.0	—	—	27.1	34.9
68)	1985	11	19	06	50	9.0	14.3	7.1	11.6	7.9	12.5	—	—	10.0	16.5	—	—	14.1	20.8
69)	1985	11	19	19	41	27.0	31.5	26.2	30.5	35.5	29.3	26.8	31.4	—	—	24.1	28.1	23.1	26.9

1)	(2)	(3)	(4)	(5)	(6)	(7)	(8)	(9)	(10)	(11)	(12)	(13)	(14)	(15)	(16)	(17)	(18)	(19)	(20)
70)	1985	11	19	21	21	41.7	44.2	40.7	43.2	40.0	42.4	—	—	—	—	38.9	40.9	37.9	39.9
71)	1985	11	24	15	52	31.9	34.2	34.3	36.8	37.5	39.8	35.8	39.0	36.4	39.6	—	—	—	—
72)	1985	11	25	05	49	—	—	31.4	—	28.6	—	29.8	—	27.8	—	25.0	—	24.1	30.4
73)	1985	11	28	02	32	—	—	23.6	27.3	22.8	24.3	—	—	25.9	—	27.2	—	—	—
74)	1985	11	29	17	24	8.0	10.5	10.4	13.0	—	—	12.8	15.8	—	—	—	—	—	—
75)	1985	12	02	00	24	—	—	27.4	31.0	26.8	29.4	—	—	—	—	—	—	29.6	—
76)	1985	12	04	17	13	37.0	39.2	39.0	41.5	42.0	44.3	41.9	45.0	—	—	—	—	—	—
77)	1985	12	06	17	33	47.0	—	44.0	—	41.8	—	—	—	40.1	—	38.2	—	36.3	38.8
78)	1985	12	08	04	40	21.0	28.8	18.3	27.6	18.0	25.4	19.1	27.0	17.3	—	14.8	20.0	7.5	13.0
79)	1985	12	12	01	41	55.0	60.0	53.4	55.9	54.8	58.6	—	—	57.2	62.9	—	—	—	—
80)	1985	12	12	12	18	43.8	49.5	40.0	47.4	38.8	58.6	—	—	40.8	44.0	39.0	46.2	30..8	35.2
81)	1985	12	12	18	24	16.2	—	12.8	17.2	11.8	16.1	—	—	12.0	—	8.8	—	5.9	—
82)	1985	12	13	06	12	52.0	—	49.2	52.5	50.2	53.9	—	—	—	—	52.5	56.5	—	—
83)	1985	12	15	00	08	23.0	41.3	—	—	19.5	35.0	21.0	38.0	—	—	—	—	14.6	25.3
84)	1985	12	18	11	09	29.4	38.0	24.1	30.5	23.2	29.0	—	—	—	—	18.2	21.5	17.0	19.9
85)	1985	12	18	14	20	27.2	—	22.8	—	21.9	26.6	25.6	32.0	—	—	16.8	19.9	15.5	17.3
86)	1985	12	22	04	15	—	—	—	—	62.8	—	—	—	62.2	—	60.0	—	57.2	60.2
87)	1985	12	22	13	25	33.6	36.5	31.7	36.5	31.9	36.9	36.5	44.0	34.5	40.5	32.2	40.2	33.5	39.0
88)	1985	12	22	23	58	—	—	66.5	—	63.9	—	—	—	62.8	—	60.5	—	58.7	59.6
89)	1985	12	23	00	52	0.8	3.0	0.0	1.8	2.5	5.8	2.8	6.5	2.6	5.5	0.2	5.4	—	—
90)	1985	12	23	13	36	—	—	—	—	—	—	—	—	28.8	—	27.1	30.2	25.1	26.5
91)	1985	12	24	19	51	—	—	37.2	—	33.9	—	—	—	35.6	—	—	—	33.7	37.0
92)	1985	12	26	05	51	—	—	58.1	—	55.8	—	57.4	—	55.0	—	52.7	55.6	—	—
93)	1985	12	29	02	38	—	—	12.7	—	9.2	—	—	—	9.0	—	6.6	—	3.9	7.3

1)	(2)	(3)	(4)	(5)	(6)	(7)	(8)	(9)	(10)	(11)	(12)	(13)	(14)	(15)	(16)	(17)	(18)	(19)	(20)
94)	1985	12	31	02	27	—	—	42.5	—	—	—	—	—	42.0	—	41.9	47.9	39.5	44.1
95)	1986	01	02	04	39	—	—	58.1	—	55.9	59.6	58.0	—	55.2	—	53.6	—	51.6	52.6
96)	1986	01	04	10	48	—	—	—	—	58.6	—	—	—	—	—	57.8	61.4	55.3	56.5
97)	1986	01	04	14	29	19.6	26.2	16.7	24.6	14.6	20.6	17.2	24.3	14.5	26.0	12.0	17.6	9.2	—
98)	1986	01	04	18	35	—	—	37.6	43.2	36.5	41.5	—	—	38.8	45.0	—	—	—	—
99)	1986	01	05	00	18	—	—	—	—	45.7	—	—	—	45.1	—	42.9	—	40.7	43.5
100)	1986	01	05	02	02	—	—	—	—	—	—	—	—	4.3	7.1	3.9	6.3	0.6	1.8
101)	1986	01	05	04	31	—	—	—	—	—	—	—	—	35.2	39.0	33.7	37.9	31.5	32.8
102)	1986	01	05	07	43	—	—	—	—	43.1	47.0	—	—	43.0	46.0	41.5	45.1	39.2	40.4
103)	1986	01	05	07	44	—	—	—	—	30.7	33.8	—	—	30.8	34.7	29.2	32.7	—	—
104)	1986	01	05	24	18	—	—	—	—	—	—	—	—	45.1	50.3	42.8	46.6	41.2	43.9
105)	1986	01	06	05	59	35.0	43.0	34.7	41.0	36.3	45.9	—	—	—	—	—	—	—	—
106)	1986	01	06	10	57	24.5	42.3	22.6	39.6	21.7	37.8	20.4	36.0	—	—	16.5	30.0	15.7	28.6
107)	1986	01	07	20	49	—	—	—	—	37.6	—	—	—	38.6	—	37.6	—	35.1	36.8
108)	1986	01	08	05	47	—	—	57.2	—	55.0	—	—	—	55.0	—	52.9	—	49.8	52.7
109)	1986	01	09	13	15	60.4	64.5	58.3	61.5	58.5	61.7	51.7	—	—	—	—	—	—	—
110)	1986	01	09	23	17	59.7	70.0	58.3	77.7	57.3	75.6	—	—	—	—	53.0	68.6	53.5	69.7
111)	1986	01	12	03	33	—	—	41.0	—	—	—	—	—	39.7	—	37.0	—	35.3	44.0
112)	1986	01	12	12	43	7.8	14.2	12.8	22.5	10.7	19.2	—	—	—	—	—	—	—	—
113)	1986	01	16	09	45	3.6	8.8	2.6	5.8	2.6	6.2	7.0	13.0	4.6	9.0	—	—	7.2	13.6
114)	1986	01	19	06	45	43.8	56.3	41.5	50.9	38.9	44.0	41.9	51.3	39.4	44.4	37.0	41.5	33.9	37.0
115)	1986	01	19	16	43	24.1	36.9	22.5	32.5	18.9	25.0	—	—	19.4	23.3	17.6	22.5	13.9	16.9
116)	1986	01	24	04	33	62.8	71.5	60.5	67.8	—	—	60.0	66.8	58.0	64.0	55.6	60.7	—	—
117)	1986	01	24	02	54	24.5	40.4	26.5	44.0	29.5	50.2	27.2	45.6	28.9	49.2	—	—	—	—

1)	(2)	(3)	(4)	(5)	(6)	(7)	(8)	(9)	(10)	(11)	(12)	(13)	(14)	(15)	(16)	(17)	(18)	(19)	(20)
118)	1986	01	25	15	40	63.0	79.0	60.0	74.8	57.0	70.0	62.0	78.0	58.8	74.6	57.5	70.5	53.4	74.8
119)	1986	01	26	07	58	67.0	—	58.2	62.2	57.5	60.2	—	—	63.0	64.8	—	—	—	—
120)	1986	01	27	05	55	18.1	24.4	15.4	19.0	13.0	—	17.5	22.2	14.3	—	10.0	—	—	—
121)	1986	01	27	16	11	34.0	39.5	31.1	34.5	29.0	30.9	35.0	42.0	31.4	35.2	32.4	36.4	31.7	35.0
122)	1986	01	28	12	51	38.5	50.5	35.5	44.5	32.7	39.3	35.6	43.6	32.6	39.2	32.2	34.9	28.2	31.9
123)	1986	02	05	01	39	51.9	54.8	49.8	51.5	50.5	52.6	51.2	54.6	50.0	51.6	52.6	55.6	54.2	59.3
124)	1986	02	06	15	59	—	—	33.2	36.4	—	—	38.5	44.5	35.0	39.7	36.6	42.0	37.1	42.6
125)	1986	02	06	17	58	56.6	66.7	53.8	62.6	51.0	56.0	—	—	51.2	57.0	49.3	53.2	46.6	48.5
126)	1986	02	06	20	50	—	—	47.6	59.4	46.6	56.0	—	—	42.2	49.0	39.3	43.8	—	—
127)	1986	02	07	00	07	50.3	60.4	47.7	59.0	44.7	53.0	—	—	44.0	53.0	41.4	46.9	39.4	43.0
128)	1986	02	07	06	00	46.9	56.9	44.2	52.0	41.2	52.0	—	—	41.1	46.8	39.4	43.3	36.6	39.0
129)	1986	02	07	21	00	42.3	47.5	41.3	45.2	42.0	46.5	—	—	44.2	51.7	46.5	57.4	46.0	56.2
130)	1986	02	07	21	11	46.9	56.9	44.2	52.0	41.2	46.0	—	—	—	—	39.4	43.3	36.6	39.0
131)	1986	02	08	16	27	12.0	22.2	11.1	20.3	8.0	15.1	—	—	9.0	17.2	6.5	12.6	3.8	7.3
132)	1986	02	09	05	47	—	—	7.8	12.2	5.0	6.5	—	—	—	—	6.8	10.3	4.9	6.2
133)	1986	02	09	07	41	—	—	33.0	37.7	30.0	33.0	—	—	32.2	36.5	—	—	—	—
134)	1986	02	09	13	19	20.8	25.5	17.8	21.6	15.4	16.4	20.0	23.5	17.0	18.8	16.8	18.5	14.6	18.4
135)	1986	02	15	02	09	52.0	59.5	52.6	59.0	52.6	61.8	—	—	—	—	—	—	—	—
136)	1986	02	15	02	46	2.2	11.8	2.0	11.2	2.3	13.3	—	—	5.0	17.5	8.0	24.1	—	—
137)	1986	02	15	09	57	46.0	48.5	48.0	50.6	51.0	54.5	50.0	52.5	—	—	53.5	57.7	55.4	60.1
138)	1986	02	20	07	16	8.8	15.7	7.5	11.0	8.1	13.4	—	—	—	—	—	—	—	—
139)	1986	02	21	05	11	9.7	14.5	10.2	15.3	11.0	16.6	—	—	—	—	—	—	—	—
140)	1986	02	23	09	11	42.0	46.0	39.4	41.6	40.6	43.5	—	—	—	—	—	—	—	—
141)	1986	02	24	20	20	23.0	32.0	20.6	28.6	17.9	24.0	20.0	27.8	18.7	25.3	16.5	21.8	—	—

1)	(2)	(3)	(4)	(5)	(6)	(7)	(8)	(9)	(10)	(11)	(12)	(13)	(14)	(15)	(16)	(17)	(18)	(19)	(20)
142)	1986	02	26	04	16	—	—	11.6	23.9	13.0	26.3	7.8	15.0	10.0	21.6	—	—	—	—
143)	1986	02	28	22	16	16.0	20.0	14.2	17.4	12.4	14.4	16.5	20.7	14.5	18.0	—	—	13.0	15.4
144)	1986	03	02	23	02	40.0	50.0	39.7	49.5	—	—	35.3	42.5	38.0	46.3	36.1	43.1	39.5	48.9
145)	1986	03	03	02	41	49.3	56.0	46.5	50.7	—	—	—	—	47.0	53.6	47.0	53.6	46.5	50.5
146)	1986	03	09	11	33	31.4	41.5	30.5	42.5	31.6	42.0	—	—	—	—	—	—	—	—
147)	1986	03	18	16	14	16.5	26.5	14.6	22.5	—	—	11.1	18.5	11.9	17.5	8.5	10.5	5.0	10.9
148)	1986	03	19	10	00	20.8	26.8	17.2	22.0	14.9	18.5	15.8	18.4	14.2	16.8	—	—	7.0	9.9
149)	1986	05	13	02	32	—	—	—	—	9.7	20.0	—	—	12.8	26.4	13.9	28.2	11.7	23.2
150)	1986	05	25	12	23	60.5	69.7	58.1	64.4	—	—	58.5	66.0	55.3	59.9	53.6	56.6	51.6	52.9
151)	1986	05	29	04	09	59.7	70.0	58.3	77.7	57.3	75.6	—	—	—	—	53.0	68.6	53.5	69.7
152)	1986	10	19	16	13	—	—	22.5	32.5	18.9	25.0	—	—	—	—	17.1	22.5	13.9	16.9

TABLE II.2 :   ESTIMATED HYPOCENTRAL COORDINATES FOR EARTHQUAKES WHOSE DATA ARE LISTED IN TABLE II.1

THE ENTRIES FOR EACH EVENT APPEAR IN TWO LINES. THE RESULTS CORRESPONDING TO COLUMN HEADINGS APPEAR IN THE FIRST LINE. ESTIMATES OF ERRORS IN RESPECTIVE RESULTS APPEAR COLUMN BY COLUMN IN THE SECOND LINE. STANDARD ERRORS FOR EPICENTRAL COORDINATES (LATITUDE AND LONGITUDE) AND FOCAL DEPTH ARE IN KILOMETERS AND ORIGIN TIME IN SECONDS.

S. No.	DATE			ORIGIN TIME			LOCATION		FOCAL DEPTH	TOTAL SQUARE RESIDUAL ERROR
	Y	M	D	H	M	S	LATITUDE °N	LONGITUDE °E	KM	S²
(1)	(2)	(3)	(4)	(5)	(6)	(7)	(8)	(9)	(10)	(11)
1.	1984	12	12	12	25	28.60	30.61	78.69	13.8	0.1
						0.3	0.7	1.6	2.4	
2.	1984	12	18	17	59	33.73	30.59	78.68	09.6	0.1
						0.3	2.1	1.7	1.6	
3.	1984	12	19	12	27	10.96	30.42	78.58	01.7	0.3
							0.2	1.0	2.4	1.1
4.	1984	12	24	04	17	16.06	30.60	78.73	11.8	0.1
						1.0	4.4	1.6	3.9	
5.	1985	01	01	16	40	54.42	30.60	78.74	05.5	0.6
						0.6	2.4	1.7	4.0	
6.	1985	02	03	15	55	47.90	30.69	78.54	09.1	0.8
						0.4	1.3	3.2	2.1	

(1)	(2)	(3)	(4)	(5)	(6)	(7)	(8)	(9)	(10)	(11)
7.	1985	02	06	05	53	50.14	30.60	78.87	07.2	0.3
						0.6	2.7	3.8	1.9	
8.	1985	02	10	20	57	20.14	30.55	78.81	00.6	0.5
						0.5	2.3	3.4	0.3	
9.	1985	02	14	03	39	46.40	30.71	78.52	18.8	0.6
						0.7	1.8	3.8	5.5	
10.	1985	02	15	21	01	17.74	30.59	78.81	02.4	0.9
						0.6	1.7	3.3	0.8	
11.	1985	03	01	18	49	10.44	30.75	78.51	07.4	0.3
						0.9	4.7	2.5	0.8	
12.	1985	03	02	04	47	20.32	30.70	78.55	18.6	0.4
						0.2	1.9	3.1	1.4	
13.	1985	03	28	05	57	30.87	30.60	78.59	01.4	0.3
						1.2	4.8	3.7	1.1	
14.	1985	03	30	19	06	10.69	30.97	78.60	11.4	0.4
						0.3	1.6	3.4	2.7	
15.	1985	03	30	20	33	18.36	30.78	78.48	14.7	0.6
						1.1	2.2	4.4	3.9	
16.	1985	03	30	20	43	53.18	30.79	78.56	08.5	0.4
						0.7	1.5	4.6	4.2	
17.	1985	03	31	00	51	28.45	30.50	78.54	10.3	1.0
						1.0	3.7	3.7	0.6	
18.	1985	03	31	05	13	14.73	30.98	78.51	10.6	0.2
						2.0	3.8	4.4	1.1	

(1)	(2)	(3)	(4)	(5)	(6)	(7)	(8)	(9)	(10)	(11)
19.	1985	03	31	16	04	48.51	30.48	78.93	06.1	0.5
						0.3	1.5	2.5	3.2	
20.	1985	04	01	14	15	27.03	30.38	78.53	03.2	0.3
						1.1	3.4	4.8	3.8	
21.	1985	04	02	01	49	24.67	30.58	78.42	12.8	1.1
						0.8	3.0	4.3	3.3	
22.	1985	04	03	21	23	33.95	30.58	78.44	12.1	1.0
						1.0	3.7	3.2	2.5	
23.	1985	04	06	06	52	14.24	30.41	78.51	00.5	0.9
						0.9	3.6	5.2	0.2	
24.	1985	04	07	22	21	46.62	30.68	78.67	07.7	0.9
						1.2	4.1	3.1	4.0	
25.	1985	04	08	00	19	13.50	30.77	78.72	11.7	1.0
						1.0	3.2	6.4	4.2	
26.	1985	04	08	00	36	26.22	30.63	78.87	10.2	1.1
						0.7	2.3	1.2	4.0	
27.	1985	04	08	06	50	58.07	30.44	78.60	12.7	0.2
						1.0	0.4	1.3	3.1	
28.	1985	04	08	17	55	6.19	30.68	78.80	13.6	0.6
						1.0	3.8	2.5	3.0	
29.	1985	04	10	22	04	43.35	30.66	78.72	03.1	0.5
						1.1	3.7	4.1	2.9	
30.	1985	04	11	06	43	41.31	30.37	78.48	00.2	0.2
						1.3	4.4	2.9	1.0	

(1)	(2)	(3)	(4)	(5)	(6)	(7)	(8)	(9)	(10)	(11)
31	1985	04	13	07	07	2.08	30.39	78.51	07.2	0.0
						0.9	3.0	1.5	2.6	
32.	1985	04	14	07	35	40.26	30.64	78.44	03.2	0.5
						0.4	1.5	1.1	2.4	
33.	1985	04	16	04	16	14.17	30.58	79.11	07.0	0.7
						0.3	1.4	1.8	3.0	
34.	1985	04	16	19	03	58.59	30.88	78.94	23.1	1.0
						0.5	1.8	2.3	2.2	
35.	1985	04	17	02	18	9.47	30.29	78.42	14.5	0.4
						0.4	1.3	0.4	2.4	
36.	1985	04	17	06	59	40.85	30.34	78.55	04.9	0.7
						0.6	2.7	1.7	1.6	
37.	1985	04	17	16	00	10.17	30.59	78.41	13.1	0.3
						1.0	0.3	1.9	1.1	
38.	1985	04	19	21	25	44.70	30.24	78.66	11.6	0.2
						0.6	0.4	1.2	2.3	
39.	1985	04	19	22	23	52.06	30.54	78.42	00.5	0.3
						0.5	0.9	0.8	0.3	
40.	1985	04	19	22	26	21.23	30.55	78.45	04.6	1.1
						0.5	1.2	1.5	2.2	
41.	1985	04	20	07	17	1.29	30.71	78.56	11.6	0.1
						0.1	0.5	1.4	2.0	
42.	1985	04	20	15	28	57.42	30.82	78.47	14.5	0.7
						0.2	0.6	2.8	4.1	

(1)	(2)	(3)	(4)	(5)	(6)	(7)	(8)	(9)	(10)	(11)
43.	1985	04	23	17	42	53.65	30.72	78.98	13.1	0.9
						1.1	1.8	0.7	2.7	
44.	1985	04	24	04	45	23.67	30.71	78.54	10.5	0.7
						0.3	0.6	1.0	3.4	
45.	1985	04	25	12	46	35.72	30.68	78.65	06.1	0.3
						0.3	0.5	0.8	3.0	
46	1985	04	25	12	47	28.14	30.35	78.52	07.1	0.9
						1.7	1.6	0.5	2.6	
47.	1985	04	25	15	59	47.32	30.57	78.39	02.8	0.2
						0.3	1.2	1.0	0.5	
48.	1985	04	25	18	36	19.90	30.58	78.52	14.9	0.7
						1.3	4.5	0.8	1.9	
49.	1985	04	25	19	19	10.36	30.32	78.52	08.5	1.0
						2.2	3.4	0.4	2.4	
50.	1985	04	25	21	45	15.30	30.70	78.67	10.3	1.1
						0.5	2.8	1.2	1.1	
51.	1985	04	26	20	44	5.90	30.66	78.80	05.3	0.9
						0.2	0.5	1.2	0.8	
52.	1985	04	26	21	06	46.10	30.79	78.52	10.4	1.2
						0.6	0.2	1.3	2.0	
53.	1985	10	31	17	41	40.62	30.51	79.35	04.9	0.0
						0.3	0.8	3.5	1.4	
54.	1985	11	01	03	37	40.67	31.05	78.22	16.0	0.7
						1.0	0.8	0.9	2.9	

(1)	(2)	(3)	(4)	(5)	(6)	(7)	(8)	(9)	(10)	(11)
55.	1985	11	01	17	25	56.61	30.38	78.53	02.8	0.5
						0.4	0.6	0.7	2.2	
56.	1985	11	01	23	06	15.48	30.76	79.17	12.0	1.1
						0.8	1.1	2.1	1.4	
57.	1985	11	05	22	08	33.76	30.65	78.86	10.1	0.5
						0.3	1.7	0.7	1.9	
58.	1985	11	06	05	42	02.06	30.45	79.30	15.7	0.8
						0.5	0.7	0.8	1.7	
59.	1985	11	06	10	17	34.18	30.46	79.10	07.2	0.2
						0.2	0.7	1.4	2.6	
60.	1985	11	07	15	28	59.06	30.62	78.93	01.0	0.1
						0.2	0.5	3.3	0.8	
61.	1985	11	07	18	03	44.37	30.42	78.57	12.7	1.1
						0.4	1.4	0.8	2.0	
62.	1985	11	09	01	31	27.42	30.59	78.44	05.2	0.6
						0.4	2.3	0.9	1.1	
63.	1985	11	10	02	29	49.53	30.77	79.25	13.1	0.4
						0.7	0.7	1.1	2.3	
64.	1985	11	18	05	26	31.17	30.64	78.89	05.8	0.3
						0.5	1.4	0.9	1.9	
65.	1985	11	18	14	47	6.48	30.59	78.86	16.5	0.6
						0.6	3.3	0.8	1.3	
66.	1985	11	18	20	45	26.60	30.55	78.64	20.4	0.2
						0.6	0.1	0.8	2.7	

(1)	(2)	(3)	(4)	(5)	(6)	(7)	(8)	(9)	(10)	(11)
67.	1985	11	18	23	30	16.89	30.65	78.64	11.8	0.5
						0.5	1.4	1.1	1.7	
68.	1985	11	19	06	50	3.69	30.55	78.62	20.2	0.6
						0.5	0.6	0.7	1.7	
69.	1985	11	19	21	21	33.80	30.50	78.91	08.6	1.1
						0.2	1.6	2.1	1.8	
70.	1935	11	24	15	52	30.99	30.38	78.57	02.3	0.2
						0.3	0.5	1.1	1.0	
71.	1985	11	25	05	49	14.90	30.32	79.49	13.4	0.2
						0.2	1.9	0.9	2.3	
72.	1985	11	26	22	22	25.41	30.66	78.56	27.0	0.3
						0.1	3.0	1.3	4.3	
73.	1985	11	28	02	32	19.20	30.66	78.75	07.0	0.3
						0.6	0.8	1.9	1.2	-
74.	1985	11	29	17	24	6.66	30.41	78.50	07.7	0.0
						0.3	2.2	2.9	2.5	
75.	1985	12	02	00	24	21.54	30.38	78.85	11.4	0.2
						0.3	3.4	1.3	3.5	
76.	1985	12	04	17	13	36.07	30.43	78.54	04.6	0.4
						0.2	1.4	0.4	2.5	
77.	1985	12	06	17	33	32.87	30.43	79.23	07.4	0.3
						0.8	2.5	1.3	2.7	
78.	1985	12	08	04	40	13.00	30.46	79.03	07.4	0.9
						0.4	3.4	1.7	0.7	

(1)	(2)	(3)	(4)	(5)	(6)	(7)	(8)	(9)	(10)	(11)
79.	1985	12	12	01	41	49.89	30.58	78.58	12.0	1.0
						0.4	1.5	1.2	2.3	
80.	1985	12	12	12	18	14.90	30.66	79.61	14.0	1.2
						0.3	2.8	1.5	0.2	
81.	1985	12	12	18	24	6.18	30.47	78.83	27.1	0.1
						0.3	1.3	0.9	1.2	
82.	1985	12	13	06	12	43.63	30.50	78.71	27.1	0.8
						0.2	1.9	1.1	2.7	
83.	1985	12	15	00	08	56.74	30.40	79.60	11.5	0.7
						0.1	0.7	1.7	1.6	
84.	1985	12	18	11	09	16.31	30.58	79.11	05.1	0.3
						0.1	0.8	0.8	2.3	
85.	1985	12	18	14	20	14.29	30.50	79.17	10.7	0.2
						0.3	7.1	0.6	2.1	
86.	1985	12	22	04	15	52.89	30.50	79.32	06.6	0.2
						0.4	1.3	1.1	0.8	
87.	1985	12	22	13	25	25.40	30.58	78.49	14.1	0.9
						0.2	0.5	1.1	1.4	
88.	1985	12	22	23	58	56.88	30.47	79.15	01.3	0.1
						0.2	1.1	1.7	2.2	
89.	1985	12	23	00	51	57.97	30.44	78.61	06.7	0.1
						0.1	1.1	1.7	2.4	
90.	1985	12	23	13	36	23.05	30.46	79.15	03.5	0.1
						0.4	2.1	1.6	2.6	

(1)	(2)	(3)	(4)	(5)	(6)	(7)	(8)	(9)	(10)	(11)
91.	1985	12	24	19	51	29.48	30.65	78.65	08.4	0.4
						0.2	0.7	1.2	2.1	
92.	1985	12	26	05	51	48.99	30.43	79.11	11.3	0.8
						0.2	2.2	3.0	2.3	
93.	1985	12	29	02	37	58.99	30.51	79.35	05.8	0.2
						0.1	1.3	1.6	1.3	
94	1985	12	31	02	27	33.32	30.73	79.00	15.8	0.8
						0.3	1.7	1.1	3.4	
95.	1986	01	02	04	39	49.25	30.44	79.18	10.2	0.2
						0.3	3.6	1.7	3.2	
96.	1986	01	04	10	48	53.21	30.54	79.06	06.0	0.4
						0.2	0.9	4.4	2.3	
97.	1986	01	04	14	29	2.43	30.58	79.43	09.7	0.3
						0.4	2.6	1.3	1.8	
98.	1986	01	04	18	35	30.16	30.72	78.80	24.0	1.2
						0.1	1.3	3.2	3.9	
99.	1986	01	05	00	18	36.74	30.49	79.25	11.9	0.8
						0.5	1.1	0.9	3.8	
100.	1986	01	05	02	01	59.25	30.50	79.07	02.6	0.2
						0.6	0.8	0.9	2.4	
101.	1986	01	05	04	31	29.90	30.51	79.08	05.2	0.1
						0.3	0.9	0.7	2.4	
102.	1986	01	05	07	43	39.70	30.49	79.09	04.0	0.0
						0.2	1.8	1.7	0.8	

(1)	(2)	(3)	(4)	(5)	(6)	(7)	(8)	(9)	(10)	(11)
103.	1986	01	05	07	44	25.26	30.50	79.09	05.2	0.1
						0.1	3.1	2.2	1.9	
104.	1986	01	05	24	18	23.92	30.58	78.20	12.0	1.3
						0.4	1.2	3.5	1.6	
105.	1986	01	06	05	59	23.83	30.68	78.31	28.5	0.6
						0.9	1.7	2.3	2.7	
106.	1986	01	06	10	57	59.02	30.05	79.93	16.0	0 5
						0.8	1.0	2.9	1.6	
107.	1986	01	07	20	49	32.38	30.59	79.05	07.3	0.5
						0.6	0.5	1.9	3.9	
108.	1986	01	08	05	47	45.65	30.57	79.26	12.1	0.6
						0.2	0.3	1.0	1.7	
109.	1986	01	09	13	15	50.41	30.23	78.87	04.2	0.3
						0.1	0.3	0.5	0.7	
110.	1986	01	09	23	17	31.47	30.89	77.92	09.8	0.1
						1.2	0.5	0.2	3.5	
111.	1986	01	12	03	33	28.29	30.75	79.24	22.1	1.3
						0.2	2.4	0.4	5.7	
112.	1986	01	12	13	43	0.21	30.58	78.18	29.2	1.0
						0.7	1.7	1.0	3.7	
113.	1986	01	16	09	44	58.17	30.62	78.71	10.0	0.5
						0.2	2.1	2.2	2.2	
114.	1986	01	19	06	45	29.33	30.59	79.28	10.9	0.9
						0.3	0.5	0.8	1.4	

(1)	(2)	(3)	(4)	(5)	(6)	(7)	(8)	(9)	(10)	(11)
115.	1986	01	19	16	43	1.95	30.20	79.52	08.3	1.1
						0.5	0.6	1.3	0.4	
116.	1986	01	24	04	33	49.54	30.01	79.24	18.0	0.8
						1.4	0.6	1.0	2.1	
117.	1986	01	25	02	54	1.87	29.84	78.37	16.0	0.7
						0.3	0.4	0.9	5.3	
118.	1986	01	25	15	40	39.61	31.07	79.61	16.6	0.4
						0.2	0.8	1.4	2.1	
119.	1986	01	26	07	58	49.12	30.66	78.78	20.3	1.8
						0.2	2.9	2.6	4.4	
120.	1986	01	27	16	11	26.05	30.62	78.85	09.4	0.4
						0.4	3.1	3.6	1.0	
121.	1986	01	27	05	55	10.1	30.54	78.88	08.4	0.2
						0.6	1.3	2.2	0.6	
122.	1986	01	28	12	51	16.44	30.16	79.54	21.3	1.1
						0.2	1.1	2.2	2.6	
123.	1986	02	05	01	39	38.78	30.19	78.93	06.7	0.1
						0.8	0.8	1.8	2.7	
124.	1986	02	06	15	59	29.67	30.65	78.75	10.6	0.6
						0.2	2.7	1.3	2.8	
125.	1986	02	06	17	58	42.82	30.46	79.23	13.7	0.7
						0.4	0.7	1.1	3.1	
126.	1986	02	06	20	50	33.39	30.14	79.46	10.1	0.7
						0.2	0.3	1.1	0.7	

(1)	(2)	(3)	(4)	(5)	(6)	(7)	(8)	(9)	(10)	(11)
127.	1986	02	07	00	07	32.31	30.50	79.44	08.0	1.0
						0.7	1.8	0.6	2.9	
128.	1986	02	07	06	00	26.71	30.40	79.51	20.0	0.5
						0.3	0.7	0.5	1.7	
129.	1986	02	07	21	00	33.39	30.77	78.50	09.3	0.7
						0.6	1.1	1.1	1.1	
130.	1986	02	07	21	11	33.53	30.48	79.21	11.8	0.4
						0.2	1.0	1.8	1.1	
131.	1986	02	08	16	27	57.90	30.56	79.31	23.5	0.6
						0.3	1.1	0.7	2.4	
132.	1986	02	09	05	47	1.40	30.59	78.95	10.8	0.5
						0.5	0.4	1.8	4.1	
133.	1986	02	09	07	41	26.23	30.59	78.96	08.4	0.1
						0.5	1.0	0.7	2.3	
134.	1986	02	09	13	19	12.88	30.52	78.89	05.1	0.9
						1.3	1.7	1.0	1.1	
135.	1986	02	15	02	09	41.56	30.58	78.45	24.2	1.1
						0.4	1.2	1.8	8.2	
136.	1986	02	15	02	45	48.39	30.98	78.25	29.8	0.3
						0.1	0.5	1.0	3.3	
137.	1986	02	15	09	57	50.50	30.65	79.02	08.6	0.4
						0.5	3.7	4.1	4.0	
138.	1986	02	20	07	16	2.16	30.58	78.63	26.4	0.9
						0.3	1.9	1.9	4.3	

(1)	(2)	(3)	(4)	(5)	(6)	(7)	(8)	(9)	(10)	(11)
139.	1986	02	21	05	11	3.00	30.22	78.73	14.7	0.1
						0.3	6.4	4.1	3.2	
140.	1986	02	23	09	11	36.68	30.58	˙78.63	08.7	0.2
						0.3	0.8	2.6	0.0	
141	1986	02	24	20	20	9.31	30.51	79.19	01.4	0.8
						0.5	2.7	1.1	0.7	
142.	1986	02	26	04	16	55.58	29.75	78.59	07.1	0.6
						0.6	1.9	1.0	1.8	
143.	1986	02	28	22	16	9.74	30.53	78.79	12.3	0.3
						0.3	1.2	1.1	1.4	
144.	1986	03	02	23	02	26.19	29.89	78.98	15.3	0.7
						0.9	0.7	0.9	0.2	
145.	1986	03	03	02	41	39.57	30.73	78.82	01.9	0.3
						0.8	1.5	0.9	1.5	-
146.	1986	03	09	11	33	15.92	30.59	78.55	04.2	0.0
						1.0	1.4	1.5	2.2	
147.	1986	03	18	16	14	2.01	30.56	79.20	20.0	0.8
						0.4	2.8	2.6	4.7	
148.	1986	03	19	10	00	9.78	30.41	78.97	14.0	0.1
						0.9	0.5	0.6	2.4	
149.	1986	05	13	02	32	55.02	31.06	78.69	16.0	0.7
						0.3	2.7	2.3	2.4	
150.	1986	05	25	12	23	21.29	30.94	79.52	06.2	0.1
						0.4	3.4	2.7	2.2	

(1)	(2)	(3)	(4)	(5)	(6)	(7)	(8)	(9)	(10)	(11)
151.	1986	05	29	04	09	10.77	31.02	79.81	16.0	0.3
						0.2	4.3	4.1	1.5	
152.	1986	10	19	16	13	10.01	30.54	79.22	17.7	0.1
						0.2	1.1	1.6	0.2	

TABLE II.3 CODA MAGNITUDES OF LOCAL EARTHQUAKES OCCURRED IN THE GARHWAL HIMALAYAS

S. NO.	DATE Y M D	CODA LENGTHS (T) AT THE STATIONS AKM SECS	CHA SECS	LAM / LAT SECS	BNA SECS	DHO SECS	MAGNITUDE M1 LEE	M2 SINGH
(1)	(2) (3) (4)	(5)	(6)	(7)	(8)	(9)	(10)	(11)
1.	1984 12 12	42	—	47	—	—	2.5	1.1
2.	1984 12 18	30	40	36	—	—	2.3	0.7
3.	1984 12 19	38	40	—	—	—	2.9	0.9
4.	1984 12 24	53	—	58	—	—	2.7	1.4
5.	1985 01 01	40	38	—	—	—	2.4	0.9
6.	1985 02 03	56	62	38	—	45	2.5	1.2
7.	1985 02 06	64	63	35	44	—	2.6	1.2
8.	1985 02 10	25	22	—	30	—	2.0	0.3
9.	1985 02 14	166	37	93	112	88	3.1	2.0
10.	1985 02 15	41	47	28	36	18	2.2	0.6
11.	1985 03 01	42	29	18	30	19	2.1	0.3
12.	1985 03 02	67	79	45	63	44	2.7	1.4
13.	1985 03 28	115	—	—	120	96	3.3	2.3
14.	1985 03 30	—	174	112	—	55	3.3	2.2
15.	1985 03 30	33	50	48	31	—	2.4	0.9
16.	1985 03 30	96	90	80	56	—	3.0	1.9
17.	1985 03 31	—	26	24	15	—	1.9	0.0
18.	1985 03 31	93	102	74	—	51	3.1	1.8
19.	1985 03 31	61	61	65	50	—	2.8	1.5
20	1985 04 01	40	49	40	30	—	2.4	0.9

(1)	(2)	(3)	(4)	(5)	(6)	(7)	(8)	(9)	(10)	(11)
21.	1985	04	02	56	67	36	53	36	2.6	1.2
22.	1985	04	03	—	48	22	37	30	2.2	0.6
23.	1985	04	06	—	34	—	25	26	2.1	0.4
24.	1985	04	07	—	68	46	60	50	2.7	1.4
25.	1985	04	08	—	31	—	37	19	2.1	0.4
26.	1985	04	08	—	37	—	28	26	2.1	0.5
27.	1985	04	08	—	39	16	33	20	2.0	0.3
28.	1985	04	08	—	54	75	80	—	2.9	1.7
29.	1985	04	10	—	—	152	—	234	3.7	3.1
30.	1985	04	11	—	62	—	23	16	2.1	0.4
31.	1985	04	13	16	44	20	41	31	2.1	0.4
32.	1985	04	14	—	109	69	79	90	3.1	2.0
33.	1985	04	16	—	94	25	57	48	2.7	1.2
34.	1985	04	16	72	—	19	49	28	2.4	0.8
35.	1985	04	17	62	73	—	50	38	2.7	1.3
36.	1985	04	17	19	13	—	—	12	1.5	-0.5
37.	1985	04	17	50	64	—	45	57	2.7	1.3
38.	1985	04	19	46	47	—	42	22	2.4	0.8
39.	1985	04	19	63	60	41	60	47	2.7	1.3
40.	1985	04	19	18	13	—	—	—	3.1	-0.5
41.	1985	04	20	—	123	—	—	—	3.4	2.5
42.	1985	04	20	—	46	34	40	—	2.4	0.9
43.	1985	04	23	88	—	57	90	82	3.1	1.9
44.	1985	04	24	101	167	109	141	121	3.4	2.5

(1)	(2)	(3)	(4)	(5)	(6)	(7)	(8)	(9)	(10)	(11)
45.	1985	04	25	–	–	–	10	22	1.5	-0.5
46.	1985	04	25	–	–	9	18	9	1.4	-0.9
47.	1985	04	25	–	–	10	–	23	1.6	-0.5
48.	1985	04	25	–	10	7	–	7	1.0	-1.4
49.	1985	04	25	26	–	–	24	18	1.9	0.1
50.	1985	04	25	–	–	8	12	–	1.2	-1.1
51.	1985	04	26	27	25	–	–	–	2.1	0.3
52.	1985	04	26	27	42	–	32	28	2.3	0.6

S. NO.		DATE		AKM	CHA	BNA	DAG	ODA	TIL	UKH	M1	M2
	Y	M	D	SECS	SECS	SECS	SECS	SECS	SECS	SECS	LEE	SINGH
(1)	(2)	(3)	(4)	(5)	(6)	(7)	(8)	(9)	(10)	(11)	(12)	(13)
53.	1985	10	31	—	27	30	—	31	26	41	2.3	0.5
54.	1985	11	01	230	240	260	—	300	220	—	4.2	3.5
55.	1985	11	01	49	41	39	—	—	—	—	2.5	1.0
56.	1985	11	01	144	170	172	123	114	163	194	3.7	2.8
57.	1985	11	05	—	11	17	—	32	—	—	1.7	-0.2
58.	1985	11	06	—	—	38	—	46	17	32	2.3	0.6
59.	1985	11	06	—	—	11	—	—	32	17	1.7	-0.2
60.	1985	11	07	—	18	17	—	—	08	24	1.6	-0.4
61.	1985	11	07	64	59	60	50	52	41	—	2.7	1.3
62.	1985	11	09	42	96	102	80	86	70	—	3.0	1.8
63.	1985	11	10	31	35	40	—	46	21	48	2.4	0.7
64.	1985	11	18	—	—	—	—	16	06	15	1.3	-0.9
65.	1985	11	18	—	28	—	—	—	29	36	2.2	0.5
66.	1985	11	18	23	31	39	—	37	36	41	2.3	0.7
67.	1985	11	18	—	22	30	—	26	—	15	1.9	0.3
68.	1985	11	19	31	34	42	—	40	—	28	2.3	0.7
69.	1985	11	19	43	54	—	—	—	40	45	2.5	1.1
70.	1985	11	19	30	35	35	—	—	—	—	2.2	0.6
71.	1985	11	24	—	52	56	40	63	40	57	2.8	1.2
72.	1985	11	25	50	60	70	—	55	50	50	2.7	1.4

(1)	(2)	(3)	(4)	(5)	(6)	(7)	(8)	(9)	(10)	(11)	(12)	(13)
73.	1985	11	28	—	—	17	—	29	11	—	1.7	-0.3
74.	1985	11	29	22	19	—	22	—	—	—	1.8	0.0
75.	1985	12	02	—	30	33	30	—	—	—	2.2	0.5
76.	1985	12	04	28	21	26	18	—	—	—	1.9	0.1
77.	1985	12	06	25	29	29	—	46	28	39	2.3	0.6
78.	1985	12	08	39	48	62	41	58	65	55	2.7	1.3
79.	1985	12	12	40	60	45	—	—	—	—	2.6	1.2
80.	1985	12	12	60	70	60	—	70	60	70	3.0	1.6
81.	1985	12	12	95	107	100	—	100	—	—	3.5	2.2
82.	1985	12	13	20	30	25	—	—	30	—	2.0	0.3
83.	1985	12	15	60	80	60	50	50	70	55	3.0	1.5
84.	1985	12	18	21	28	24	—	36	31	23	2.1	0.3
85.	1985	12	18	32	32	30	25	45	39	36	2.3	0.7
86.	1985	12	22	—	—	11	—	34	13	18	1.7	0.3
87.	1985	12	22	77	98	78	64	86	67	73	3.0	1.8
88.	1985	12	22	—	10	08	—	23	13	25	1.5	0.5
89.	1985	12	23	—	38	29	26	28	—	—	2.1	0.5
90.	1985	12	23	—	—	—	—	32	11	13	1.6	0.3
91.	1985	12	24	36	39	33	—	57	35	39	2.6	0.9
92.	1985	12	26	—	108	87	78	72	84	75	3.1	1.9
93.	1985	12	29	—	—	—	—	40	27	16	2.2	0.3
94.	1985	12	31	—	04	06	—	15	—	06	0.9	-1.6
95.	1986	01	02	—	21	15	10	36	22	—	1.8	-0.1
96.	1986	01	04	—	26	24	—	36	22	21	2.1	0.3

(1)	(2)	(3)	(4)	(5)	(6)	(7)	(8)	(9)	(10)	(11)	(12)	(13)
97.	1986	01	04	35	39	41	—	—	42	20	2.3	0.7
98.	1986	01	04	39	36	37	25	45	29	32	2.3	0.7
99.	1986	01	05	—	—	07	—	—	08	08	1.0	-1.4
100.	1986	01	05	85	89	84	72	—	86	80	3.2	1.9
101.	1986	01	05	—	18	14	—	27	—	—	1.8	-0.2
102.	1986	01	05	—	—	16	—	33	26	10	-1.8	-0.1
103.	1986	01	05	—	—	—	—	16	10	11	1.4	-0.8
104.	1986	01	05	—	20	13	—	25	17	14	1.7	-0.3
105.	1986	01	06	—	—	06	—	14	08	11	1.1	-1.2
106.	1986	01	06	—	14	15	—	24	13	14	1.6	-0.4
107.	1986	01	07	76	68	68	59	85	88	62	3.3	1.7
108.	1986	01	08	—	—	05	—	10	06	10	0.9	-1.5
109.	1986	01	09	—	12	13	—	24	16	20	1.7	-0.3
110.	1986	01	09	25	25	23	24	—	—	—	2.0	0.2
111.	1986	01	12	57	60	—	52	—	—	—	2.9	1.4
112.	1986	01	12	39	42	36	—	—	—	—	2.5	0.9
113.	1986	01	16	82	102	84	—	73	91	91	3.2	2.0
114.	1986	01	19	38	43	38	34	58	48	42	2.6	1.0
115.	1986	01	19	40	36	34	—	—	—	—	2.4	0.8
116.	1986	01	24	—	28	—	—	39	26	—	2.3	0.5
117.	1896	01	25	13	13	10	—	17	—	—	1.5	-0.7
118.	1986	01	25	56	54	50	90	65	—	—	3.0	1.5
119.	1986	01	26	78	80	73	48	41	86	62	3.1	1.6
120.	1986	01	27	48	60	56	—	55	55	48	3.3	1.3

(1)	(2)	(3)	(4)	(5)	(6)	(7)	(8)	(9)	(10)	(11)	(12)	(13)
121.	1986	01	27	112	115	117	103	116	140	94	3.4	2.4
122.	1986	01	28	51	40	42	—	57	47	—	2.8	1.1
123.	1986	02	05	32	30	30	28	36	31	—	2.2	0.6
124.	1986	02	06	95	77	70	60	87	74	53	3.0	1.7
125.	1986	02	06	23	21	22	—	34	39	22	2.1	0.3
126.	1986	02	06	32	28	29	—	—	44	29	2.4	0.6
127.	1986	02	07	88	98	80	63	66	76	64	3.2	1.8
128.	1986	02	07	63	85	—	—	57	90	62	3.0	1.7
129.	1986	02	07	40	40	32	—	72	54	30	2.6	1.0
130.	1986	02	07	—	33	25	—	33	34	16	2.1	0.4
131.	1986	02	08	—	27	20	—	28	18	—	1.9	0.1
132.	1986	02	09	80	92	75	49	63	64	51	2.9	1.6
133.	1986	02	09	40	42	33	—	—	—	—	2.4	0.8
134.	1986	02	09	44	38	34	—	59	—	30	2.5	0.9
135.	1986	02	15	26	26	17	—	—	—	—	1.9	0.1
136.	1986	02	15	24	29	23	—	36	33	23	2.2	0.4
137.	1986	02	15	31	37	33	—	40	36	33	2.5	0.7
138.	1986	02	20	58	61	48	—	57	40	—	2.8	1.3
139.	1986	02	21	31	31	20	—	—	—	—	2.1	0.3
140.	1986	02	23	39	30	25	—	—	—	—	2.2	0.5
141.	1986	02	24	75	80	82	60	72	88	55	3.0	1.7
142.	1986	02	26	58	59	65	37	55	46	53	2.8	1.3
143.	1986	02	28	39	56	60	24	48	41	34	2.5	1.0
144.	1986	03	02	55	80	—	45	60	57	43	2.8	1.4

(1)	(2)	(3)	(4)	(5)	(6)	(7)	(8)	(9)	(10)	(11)	(12)	(13)
145.	1986	03	03	70	70	60	—	—	—	—	2.8	1.6
146.	1986	03	09	49	62	45	—	65	—	53	2.7	1.3
147.	1986	03	18	—	—	50	—	67	37	39	2.7	1.1
148.	1986	03	19	—	—	42	—	—	50	45	2.7	1.2
149.	1986	05	13	105	—	110	95	—	91	100	3.5	2.2
150.	1986	05	25	52	—	58	—	63	—	—	2.8	1.4
151.	1986	05	29	14	21	—	—	25	16	13	1.7	-0.3
152.	1986	10	19	144	156	—	139	98	117	125	3.5	2.6

APPENDIX - III

TABLE III.1 : FIRST MOTION DATA, FOR EARTHQUAKES CONTRIBUTING STRIKE-SLIP TYPE COMPOSITE FAULT PLANE SOLUTIONS (U FOR COMPRESSION AND D FOR DILATATION)

S. NO.	DATE			ORIGIN TIME			EPICENTRE LOCATION			FIRST P MOTION AT THE STATIONS				
							LATITUDE	LONGITUDE	DEPTH					
	Y	M	D	H	M	S	°N	°E	KM	AKM	CHA	LAM / LAT	BNA	DHO
(1)	(2)	(3)	(4)	(5)	(6)	(7)	(8)	(9)	(10)	(11)	(12)	(13)	(14)	(15)
1.	1985	03	01	18	49	10.44	30.75	78.51	07.4	U	U	U	D	U
2.	1985	03	30	19	06	10.69	30.90	78.60	11.4	—	D	—	D	—
3.	1985	03	30	20	43	53.18	30.79	78.56	08.5	—	U	U	D	D
4.	1985	03	31	16	04	48.51	30.48	78.93	06.1	D	U	—	U	U
5.	1985	04	08	00	19	13.50	30.77	78.72	11.7	—	D	D	—	D
6.	1985	04	19	22	26	21.23	30.55	78.45	04.6	D	U	—	U	D
7.	1985	04	24	04	45	23.67	30.71	78.54	10.5	—	—	D	—	D
8.	1985	04	25	12	46	35.72	30.68	78.65	06.1	—	U	D	U	D
9.	1985	04	25	18	36	19.90	30.58	78.52	14.9	—	U	D	U	D

S. NO.	DATE			ORIGIN TIME			EPICENTRE LOCATION			FIRST P MOTION AT THE STATIONS						
	Y	M	D	H	M	S	LATITUDE °N	LONGITUDE °E	DEPTH KM	AKM	CHA	BNA	DAG	ODA	TIL	UKH
(1)	(2)	(3)	(4)	(5)	(6)	(7)	(8)	(9)	(10)	(11)	(12)	(13)	(14)	(15)	(16)	(17)
10.	1985	11	18	20	45	26.60	30.55	78.64	20.4	D	—	—	—	—	U	U
11.	1985	11	25	05	49	14.90	30.32	79.49	13.4	—	—	U	U	—	D	—
12.	1985	12	02	00	24	21.54	30.38	78.85	11.4	—	U	U	—	—	—	D
13.	1985	12	12	12	18	14.90	30.66	79.61	14.0	U	—	—	—	U	—	U
14.	1986	01	02	04	39	49.25	30.44	79.18	10.2	—	—	U	—	D	D	D
15.	1986	01	16	09	44	58.17	30.62	78.71	10.0	D	D	U	—	U	U	U
16.	1986	01	26	07	58	49.12	30.66	78.78	20.3	D	D	U	—	—	—	—
17.	1986	02	09	07	41	26.23	30.59	78.96	08.4	—	D	D	—	—	U	—
18.	1986	02	28	22	16	09.74	30.53	78.79	12.3	U	D	D	U	—	U	U
19.	1986	03	19	10	00	09.78	30.41	78.97	14.0	U	U	U	—	U	—	U

TABLE III.2 : FIRST MOTION DATA, FOR EARTHQUAKES CONTRIBUTING REVERSE/THRUST TYPE COMPOSITE FAULT PLANE SOLUTIONS

(U FOR COMPRESSION AND D FOR DILATATION)

| S. NO. | DATE | | | ORIGIN TIME | | | EPICENTRE LOCATION | | | FIRST P MOTION AT THE STATIONS | | | | |
| | | | | | | | LATITUDE | LONGITUDE | DEPTH | | | | | |
	Y	M	D	H	M	S	°N	°E	KM	AKM	CHA	LAM/ LAT	BNA	DHO
1.	1984	12	18	17	59	33.73	30.59	78.68	09.6	D	-	D	-	-
2.	1985	02	06	05	53	50.14	30.57	78.87	07.2	D	-	D	-	-
3.	1985	02	15	21	01	17.74	30.59	78.81	02.4	D	D	-	U	-
4.	1985	04	02	01	49	24.67	30.58	78.42	12.8	D	D	U	D	D
5.	1985	04	03	21	23	33.95	30.58	78.44	12.1	-	U	U	D	D
6.	1985	04	07	22	21	46.62	30.68	78.67	07.7	-	D	D	U	U
7.	1985	04	08	06	50	58.07	30.44	78.60	12.7	-	U	-	U	U
8.	1985	04	08	17	55	06.19	30.68	78.80	13.6	-	U	D	U	U
9.	1985	04	17	06	00	10.17	30.59	78.41	13.1	-	U	-	-	U
10.	1985	04	20	07	17	01.29	30.71	78.56	11.6	-	D	-	-	D
11.	1985	04	20	15	28	57.42	30.82	78.47	14.5	D	D	U	D	D
12.	1985	04	25	15	59	47.32	30.57	78.39	02.8	-	-	D	-	D
13.	1985	04	25	21	45	15.30	30.70	78.67	10.3	-	U	U	D	-
14.	1985	04	26	20	44	05.90	30.66	78.80	05.3	-	U	U	D	-

							EPICENTRE LOCATION				FIRST P MOTION AT THE STATIONS						
S. NO.	DATE			ORIGIN TIME				LATITUDE	LONGITUDE	DEPTH		AKM	CHA	BNA	DAG	ODA	TIL	UKH
	Y	M	D	H	M	S		°N	°E	KM								
	1			2	3	4		5	6	7		8	9	10	11	12	13	14
15.	1985	10	31	17	41	40.62		30.51	79.35	04.9		-	-	-	-	-	D	D
16.	1985	11	01	17	25	56.61		30.38	78.53	02.8		U	U	-	U	-	-	-
17.	1985	11	05	22	08	33.76		30.65	78.86	10.1		-	-	U	-	-	D	-
18.	1985	11	06	05	42	02.06		30.45	79.30	15.7		-	-	D	-	-	D	-
19.	1985	11	06	10	17	34.18		30.46	79.10	7.2		-	-	D	-	-	-	U
20.	1985	11	10		2.29	49.53		30.77	79.25	13.1		D	-	D	-	-	-	D
21.	1985	11	18	05	26	31.17		30.64	78.89	05.8		-	-	-	-	D	-	D
22.	1985	11	18	14	47	06.48		30.59	78.86	16.5		-	-	D	-	U	D	D
23.	1985	11	19	21	21	30.80		30.50	78.91	08.6		-	-	-	D	D	-	D
24.	1985	11	28	02	32	19.20		30.66	78.75	07.0		-	U	D	-	D	-	-
25.	1985	11	29	17	24	06.66		30.41	78.50	07.7		U	D	-	U	-	-	-
26.	1985	12	04	17	13	36.07		30.43	78.54	04.6		-	D	D	D	-	-	-
27.	1985	12	08	04	40	13.00		30.46	79.03	07.4		-	-	D	U	D	-	U
28.	1985	12	18	14	20	14.29		30.50	79.17	10.7		-	-	D	-	D	D	D

TABLE II.1 RECORDED P AND S ARRIVAL TIMES FOR EARTHQUAKES WHOSE HYPOCENTRAL COORDINATES WERE DETERMINED.

ARRIVAL TIMES AT STATIONS

S. No.	DATE Y	M	D	NEAREST COMMON HOURS & MINUTES H	M	AKMUNDSAM P PHASE SECS	S PHASE SECS	CHAMIYALA P PHASE SECS	S PHASE SECS	LAMBGAON / LATASERA P PHASE SECS	S PHASE SECS	BEENAGAON P PHASE SECS	S PHASE SECS	DHONTRI P PHASE SECS	S PHASE SECS
(1)	(2)	(3)	(4)	(5)	(6)	(7)	(8)	(9)	(10)	(11)	(12)	(13)	(14)	(15)	(16)
1)	1984	12	12	12	25	35.0	39.7	32.4	35.6	33.8	37.1	—	—	—	—
2)	1984	12	18	17	59	39.1	—	36.5	38.5	37.2	40.1	—	—	—	—
3)	1984	12	19	12	27	11.9	13.6	12.6	14.0	13.5	15.3	—	—	—	—
4)	1984	12	24	04	17	23.0	28.0	20.2	23.0	21.6	24.6	—	—	—	—
5)	1985	01	01	16	40	60.7	65.6	57.6	60.2	59.6	63.5	—	—	—	—
6)	1985	02	03	15	55	54.8	59.7	54.1	57.3	53.9	56.7	—	—	51.2	52.8
7)	1985	02	06	05	53	58.3	66.2	55.1	60.5	57.5	63.1	53.1	56.8	—	—
8)	1985	02	10	20	57	27.2	30.5	23.6	25.6	—	—	20.5	21.5	—	—
9)	1985	02	14	03	40	8.2	24.8	7.4	22.0	7.5	21.4	6.3	21.1	5.5	17.3
10)	1985	02	15	21	01	24.7	29.6	21.8	25.8	24.6	28.8	19.7	22.2	29.2	31.4
11)	1985	03	01	18	49	18.2	24.0	17.7	21.9	16.3	19.8	17.7	—	14.6	17.7
12)	1985	03	02	04	47	27.7	32.5	27.1	31.3	26.1	29.9	26.8	30.5	24.9	28.5
13)	1985	03	28	05	57	36.2	39.0	—	—	—	—	35.3	37.3	32.9	—

TABLE III.1 : FIRST MOTION DATA, FOR EARTHQUAKES CONTRIBUTING STRIKE-SLIP TYPE COMPOSITE FAULT PLANE SOLUTIONS (U FOR COMPRESSION AND D FOR DILATATION)

S. NO.	DATE			ORIGIN TIME			EPICENTRE LOCATION			FIRST P MOTION AT THE STATIONS				
							LATITUDE	LONGITUDE	DEPTH					
	Y	M	D	H	M	S	^{0}N	^{0}E	KM	AKM	CHA	LAM / LAT	BNA	DHO
(1)	(2)	(3)	(4)	(5)	(6)	(7)	(8)	(9)	(10)	(11)	(12)	(13)	(14)	(15)
1.	1985	03	01	18	49	10.44	30.75	78.51	07.4	U	U	U	D	U
2.	1985	03	30	19	06	10.69	30.90	78.60	11.4	—	D	—	D	—
3.	1985	03	30	20	43	53.18	30.79	78.56	08.5	—	U	U	D	D
4.	1985	03	31	16	04	48.51	30.48	78.93	06.1	D	U	—	U	U
5.	1985	04	08	00	19	13.50	30.77	78.72	11.7	—	D	D	—	D
6.	1985	04	19	22	26	21.23	30.55	78.45	04.6	D	U	—	U	D
7.	1985	04	24	04	45	23.67	30.71	78.54	10.5	—	—	D	—	D
8.	1985	04	25	12	46	35.72	30.68	78.65	06.1	—	U	D	U	D
9.	1985	04	25	18	36	19.90	30.58	78.52	14.9	—	U	D	U	D

S. NO.	DATE			ORIGIN TIME			EPICENTRE LOCATION			FIRST P MOTION AT THE STATIONS						
	Y	M	D	H	M	S	LATITUDE °N	LONGITUDE °E	DEPTH KM	AKM	CHA	BNA	DAG	ODA	TIL	UKH
(1)	(2)	(3)	(4)	(5)	(6)	(7)	(8)	(9)	(10)	(11)	(12)	(13)	(14)	(15)	(16)	(17)
10.	1985	11	18	20	45	26.60	30.55	78.64	20.4	D	—	—	—	—	U	U
11.	1985	11	25	05	49	14.90	30.32	79.49	13.4	—	—	U	U	—	D	—
12.	1985	12	02	00	24	21.54	30.38	78.85	11.4	—	U	U	—	—	—	D
13.	1985	12	12	12	18	14.90	30.66	79.61	14.0	U	—	—	—	U	—	U
14.	1986	01	02	04	39	49.25	30.44	79.18	10.2	—	—	U	—	D	D	D
15.	1986	01	16	09	44	58.17	30.62	78.71	10.0	D	D	U	—	U	U	U
16.	1986	01	26	07	58	49.12	30.66	78.78	20.3	D	D	U	—	—	—	—
17.	1986	02	09	07	41	26.23	30.59	78.96	08.4	—	D	D	—	—	U	—
18.	1986	02	28	22	16	09.74	30.53	78.79	12.3	U	D	D	U	—	U	U
19.	1986	03	19	10	00	09.78	30.41	78.97	14.0	U	U	U	—	U	—	U

TABLE III.2 : FIRST MOTION DATA, FOR EARTHQUAKES CONTRIBUTING REVERSE/THRUST TYPE COMPOSITE FAULT PLANE SOLUTIONS

(U FOR COMPRESSION AND D FOR DILATATION)

S. NO.	DATE			ORIGIN TIME			EPICENTRE LOCATION			FIRST P MOTION AT THE STATIONS				
							LATITUDE	LONGITUDE	DEPTH					
	Y	M	D	H	M	S	°N	°E	KM	AKM	CHA	LAM/ LAT	BNA	DHO
1.	1984	12	18	17	59	33.73	30.59	78.68	09.6	D	-	D	-	-
2.	1985	02	06	05	53	50.14	30.57	78.87	07.2	D	-	D	-	-
3.	1985	02	15	21	01	17.74	30.59	78.81	02.4	D	D	-	U	-
4.	1985	04	02	01	49	24.67	30.58	78.42	12.8	D	D	U	D	D
5.	1985	04	03	21	23	33.95	30.58	78.44	12.1	-	U	U	D	D
6.	1985	04	07	22	21	46.62	30.68	78.67	07.7	-	D	D	U	U
7.	1985	04	08	06	50	58.07	30.44	78.60	12.7	-	U	-	U	U
8.	1985	04	08	17	55	06.19	30.68	78.80	13.6	-	U	D	U	U
9.	1985	04	17	06	00	10.17	30.59	78.41	13.1	-	U	-	-	U
10.	1985	04	20	07	17	01.29	30.71	78.56	11.6	-	D	-	-	D
11.	1985	04	20	15	28	57.42	30.82	78.47	14.5	D	D	U	D	D
12.	1985	04	25	15	59	47.32	30.57	78.39	02.8	-	-	D	-	D
13.	1985	04	25	21	45	15.30	30.70	78.67	10.3	-	U	U	D	-
14.	1985	04	26	20	44	05.90	30.66	78.80	05.3	-	U	U	D	-

EPICENTRE LOCATION

S. NO.	DATE			ORIGIN TIME			LATITUDE	LONGITUDE	DEPTH	FIRST P MOTION AT THE STATIONS						
	Y	M	D	H	M	S	°N	°E	KM	AKM	CHA	BNA	DAG	ODA	TIL	UKH
		1		2	3	4	5	6	7	8	9	10	11	12	13	14
15.	1985	10	31	17	41	40.62	30.51	79.35	04.9	-	-	-	-	-	D	D
16.	1985	11	01	17	25	56.61	30.38	78.53	02.8	U	U	-	U	-	-	-
17.	1985	11	05	22	08	33.76	30.65	78.86	10.1	-	-	U	-	-	D	-
18.	1985	11	06	05	42	02.06	30.45	79.30	15.7	-	-	D	-	-	D	-
19.	1985	11	06	10	17	34.18	30.46	79.10	7.2	-	-	D	-	-	-	U
20.	1985	11	10		2.29	49.53	30.77	79.25	13.1	D	-	D	-	-	-	D
21.	1985	11	18	05	26	31.17	30.64	78.89	05.8	-	-	-	-	D	-	D
22.	1985	11	18	14	47	06.48	30.59	78.86	16.5	-	-	D	-	U	D	D
23.	1985	11	19	21	21	30.80	30.50	78.91	08.6	-	-	-	D	D	-	D
24.	1985	11	28	02	32	19.20	30.66	78.75	07.0	-	U	D	-	D	-	-
25.	1985	11	29	17	24	06.66	30.41	78.50	07.7	U	D	-	U	-	-	-
26.	1985	12	04	17	13	36.07	30.43	78.54	04.6	-	D	D	D	-	-	-
27.	1985	12	08	04	40	13.00	30.46	79.03	07.4	-	-	D	U	D	-	U
28.	1985	12	18	14	20	14.29	30.50	79.17	10.7	-	-	D	-	D	D	D

	1	2	3	4	5	6	7	8	9	10	11	12	13	14
29.	1985 12 22	23	58	56.88	30.47	79.15	01.3	-	-	-	-	-	D	D
30.	1985 12 24	19	51	29.48	30.65	78.65	08.4	-	-	-	-	D	-	D
31.	1985 12 26	05	51	48.99	30.43	79.11	11.3	-	-	D	-	-	U	-
32.	1985 12 29	02	37	58.99	30.51	79.35	05.8	-	-	D	-	-	U	D
33.	1985 12 31	02	27	33.32	30.73	79.00	15.8	-	-	U	-	-	U	D
34.	1986 01 04	18	35	30.16	30.72	78.80	24.0	-	U	U	-	D	-	-
35.	1986 01 05	00	18	36.74	30.49	79.25	11.9	-	-	-	-	-	D	U
36.	1986 01 05	02	01	59.25	30.50	79.07	02.6	D	-	-	-	-	D	D
37.	1986 01 05	04	31	29.90	30.51	79.08	05.2	D	-	D	-	-	-	D
38.	1986 01 05	07	43	39.70	30.49	79.09	04.0	D	-	-	-	-	D	U
39.	1986 01 05	07	44	25.26	30.50	79.09	05.2	-	-	D	-	-	-	U
40.	1986 01 05	24	18	23.92	30.58	78.20	12.0	-	-	-	-	D	U	D
41.	1986 01 12	03	33	28.29	30.75	79.24	22.1	D	D	-	-	D	D	-
42.	1986 01 12	13	43	00.21	30.58	78.18	29.2	U	U	D	-	-	-	-
43.	1986 01 16	09	44	58.17	30.62	78.71	10.0	D	D	U	-	U	U	U
44.	1986 01 27	05	55	10.10	30.54	78.88	08.4	U	D	U	U	U	U	U
45.	1986 01 27	16	11	26.05	30.62	78.85	09.4	-	D	U	D	D	D	-
46.	1986 01 28	12	51	16.44	30.16	79.54	21.3	-	-	D	-	-	D	U

	1	2	3	4	5	6	7	8	9	10	11	12	13	14
29.	1985 12 22	23	58	56.88	30.47	79.15	01.3	-	-	-	-	-	D	D
30.	1985 12 24	19	51	29.48	30.65	78.65	08.4	-	-	-	-	D	-	D
31.	1985 12 26	05	51	48.99	30.43	79.11	11.3	-	-	D	-	-	U	-
32.	1985 12 29	02	37	58.99	30.51	79.35	05.8	-	-	D	-	-	U	D
33.	1985 12 31	02	27	33.32	30.73	79.00	15.8	-	-	U	-	-	U	D
34.	1986 01 04	18	35	30.16	30.72	78.80	24.0	-	U	U	-	D	-	-
35.	1986 01 05	00	18	36.74	30.49	79.25	11.9	-	-	-	-	-	D	U
36.	1986 01 05	02	01	59.25	30.50	79.07	02.6	D	-	-	-	-	D	D
37.	1986 01 05	04	31	29.90	30.51	79.08	05.2	D	-	D	-	-	-	D
38.	1986 01 05	07	43	39.70	30.49	79.09	04.0	D	-	-	-	-	D	U
39.	1986 01 05	07	44	25.26	30.50	79.09	05.2	-	-	D	-	-	-	U
40.	1986 01 05	24	18	23.92	30.58	78.20	12.0	-	-	-	-	D	U	D
41.	1986 01 12	03	33	28.29	30.75	79.24	22.1	D	D	-	-	D	D	-
42.	1986 01 12	13	43	00.21	30.58	78.18	29.2	U	U	D	-	-	-	-
43.	1986 01 16	09	44	58.17	30.62	78.71	10.0	D	D	U	-	U	U	U
44.	1986 01 27	05	55	10.10	30.54	78.88	08.4	U	D	U	U	U	U	U
45.	1986 01 27	16	11	26.05	30.62	78.85	09.4	-	D	U	D	D	D	-
46.	1986 01 28	12	51	16.44	30.16	79.54	21.3	-	-	D	-	-	D	U

	1	2	3	4	5	6	7	8	9	10	11	12	13	14
47.	1986 02 05	01	39	38.78	30.19	78.92	06.7	-	U	D	-	-	-	D
48.	1986 02 06	15	59	29.67	30.65	78.75	10.6	-	-	-	-	-	-	-
49.	1986 02 06	17	58	42.82	30.46	79.23	13.7	D	-	D	-	-	D	U
50.	1986 02 07	21	00	33.39	30.77	78.50	09.3	D	D	U	-	-	U	D
51.	1986 02 08	16	27	57.90	30.56	79.31	23.5	D	U	D	-	D	U	-
52.	1986 02 09	05	47	01.40	30.59	78.95	10.8	-	D	-	-	-	D	U
53.	1986 02 09	07	41	26.23	30.59	78.96	08.4	-	D	D	-	-	U	-
54.	1986 02 15	02	45	48.39	30.98	78.25	29.8	D	U	U	-	-	D	-
55.	1986 02 15	09	57	50.50	30.65	79.02	08.6	U	D	D	-	-	-	U
56.	1986 02 21	05	11	03.00	30.22	78.73	14.7	U	U	-	-	-	-	-
57.	1986 02 23	09	11	36.68	30.58	78.63	08.7	U	U	U	-	-	-	-
58.	1986 02 24	20	20	09.31	30.51	79.19	01.4	-	D	D	-	-	-	-
59.	1986 03 03	02	41	39.57	30.73	78.82	01.9	D	D	-	-	D	-	U
60.	1986 10 19	16	13	10.01	30.54	79.22	17.7	-	-	-	-	-	-	-

TABLE III.3 : FIRST MOTION DATA, FOR EARTHQUAKES CONTRIBUTING NORMAL TYPE COMPOSITE FAULT PLANE SOLUTIONS (U FOR COMPRESSION AND D FOR DILATATION

S. NO.	DATE			ORIGIN TIME			EPICENTRE LOCATION			FIRST P MOTION AT THE STATIONS				
							LATITUDE	LONGITUDE	DEPTH					
	Y	M	D	H	M	S	°N	°E	KM	AKM	CHA	LAM/LAT	BNA	DHO
(1)	(2)	(3)	(4)	(5)	(6)	(7)	(8)	(9)	(10)	(11)	(12)	(13)	(14)	(15)
1.	1984	12	24	04	17	16.06	30.60	78.73	11.8	U	D	U	—	—
2.	1985	02	03	15	55	47.90	30.69	78.54	09.1	U	D	U	—	—
3.	1985	03	02	04	47	20.32	30.70	78.55	18.6	U	U	D	U	U
4.	1985	03	30	20	33	18.36	30.78	78.48	14.7	—	U	U	D	D
5.	1985	04	01	14	15	27.03	30.38	78.53	03.2	D	—	—	U	U
6.	1985	04	06	06	52	14.24	30.41	78.51	00.5	U	U	—	U	U
7.	1985	04	08	00	36	26.22	30.63	78.87	10.2	—	U	D	U	U
8.	1985	04	10	22	04	43.35	30.66	78.72	03.1	D	—	—	—	U
9.	1985	04	13	07	07	02.08	30.39	78.51	07.2	—	U	U	U	U
10.	1985	04	14	07	35	40.26	30.64	78.44	03.2	—	—	U	D	U
11.	1985	04	16	04	16	14.17	30.58	79.12	06.9	—	U	—	U	U
12.	1985	04	16	19	03	58.59	30.88	78.94	23.1	D	D	D	D	U
13.	1985	04	17	02	18	09.47	30.29	78.42	14.5	U	U	—	U	U
14.	1985	04	19	21	25	44.70	30.24	78.66	11.6	—	D	U	—	—
15.	1985	04	25	12	47	28.14	30.35	78.52	07.1	U	U	D	U	U
16.	1985	04	26	21	06	46.10	30.79	78.52	10.4	—	U	D	D	D

S. NO.	DATE			ORIGIN TIME			EPICENTRE LOCATION LATITUDE °N	LONGITUDE °E	DEPTH KM	FIRST P MOTION AT THE STATIONS AKM	CHA	BNA	DAG	ODA	TIL	UKH
	Y	M	D	H	M	S										
(1)	(2)	(3)	(4)	(5)	(6)	(7)	(8)	(9)	(10)	(11)	(12)	(13)	(14)	(15)	(16)	(17)
17.	1985	11	01	23	06	15.48	30.76	79.17	12.0	U	—	—	—	—	U	U
18.	1985	11	07	18	03	44.37	30.42	78.57	12.7	—	—	U	U	U	—	—
19.	1985	11	09	01	31	27.42	30.59	78.44	05.2	D	—	D	—	—	—	U
20.	1985	11	18	23	30	16.89	30.65	78.64	11.8	—	U	D	—	—	—	D
21.	1985	11	19	06	50	03.69	30.55	78.62	20.2	U	D	U	—	—	—	U
22.	1985	11	24	15	52	30.99	30.38	78.57	02.3	—	—	—	—	U	—	—
23.	1985	11	26	22	22	25.41	30.66	78.56	27.0	D	D	U	—	—	—	U
24.	1985	12	06	17	33	32.87	30.43	79.23	07.4	—	U	D	—	U	—	D
25.	1985	12	18	11	09	16.31	30.58	79.12	05.1	U	U	U	—	—	U	—
26.	1985	12	22	04	15	52.89	30.50	79.32	06.6	—	—	—	—	—	—	U
27.	1985	12	22	13	25	25.40	30.58	78.49	14.1	D	D	D	U	—	D	D
28.	1985	12	23	00	51	57.97	30.44	78.61	06.7	U	—	U	U	—	U	—
29.	1985	12	23	13	36	23.05	30.46	79.15	03.5	—	—	—	—	—	—	D
30.	1986	01	07	20	49	32.38	30.59	79.05	07.3	—	—	—	—	U	—	U
31.	1986	01	08	05	47	45.65	30.57	79.26	12.1	—	—	U	—	—	—	U
32.	1986	01	09	13	15	50.41	30.23	78.87	04.2	—	—	U	—	—	—	—
33.	1986	02	09	13	19	12.88	30.52	78.89	05.1	—	—	—	—	—	—	U
34.	1986	02	15	02	09	41.56	30.58	78.45	24.2	D	U	U	—	—	—	—
35.	1986	02	07	00	07	32.31	30.50	79.44	08.0	—	U	—	—	—	U	U
36.	1986	02	26	04	16	55.58	29.75	78.59	07.1	—	U	U	U	U	—	—

APPENDIX - IV

RAY.F
MAIN PROGRAM FOR WAVE SPEED ESTIMATION 3-D RAY TRACING
IN FORTRAN CODE
DEVELOPED BY
SUSHIL KUMAR (R/S EARTH SCIENCES)
UNDER THE GUIDENCE OF
PROF. RAMESH CHANDER
PROFESSOR, DEPARTMENT OF EARTH SCIENCES
UNIVERSITY OF ROORKEE, ROORKEE.

```
C     NP- No. of planes, NST- No. of stations, NSO- No. of sources
C     DIPRO, AZR - Shooting angle and Azimuth of the Ray; X10,Y10,Z10 - Lat., Long and focal
                                                              depth of NSO
      COMMON/BLOCK1/ DIPP(100),AZP(100),XP(100),YP(100),ZP(100),
    1 V(100),T(100),D(100)

      DIMENSION H(100),DEL(10,10),TOBS(10,10),TCAL(10,10)

      DIMENSION DIPR0(20),AZR(20),X10(20),Y10(20),Z10(20)

      DIMENSION STX(20),STY(20),DELX(10,10),DELY(10,10)

      OPEN(1,FILE='R1.DAT',STATUS='OLD') OPEN(2,FILE='RESULTS01.RES')

      OPEN(3,FILE='RESULTS02.RES')

      READ(1,*)NP,NST,NSO

      READ(1,*)(DIPR0(I),AZR(I),X10(I),Y10(I),Z10(I),I=1,NSO)

      DO 4 I=1,NSO

      X10(I)=X10(I)*60.*1.848218

    4 Y10(I)=Y10(I)*60.*1.60168

      READ(1,*)(STX(J),STY(J),J=1,NST)

      DO 5 I=1,NST

      STX(I)=STX(I)*60.*1.848218

    5 STY(I)=STY(I)*60.*1.60168

      DO 1 I=1,NSO

    1 READ(1,*)(TOBS(I,J),J=1,NST)

C     TOBS - Observed time; DIPP, AZP - Dip and Azimuth of a plane
C     XP, YP, ZP, V(I) - Defining points (X,Y,Z) of plane and velocity in the
C     medium before the plane                                    221
```

```
C       NDEF - Layer no. for which velocity is to be findout
        READ(1,*)(DIPP(I),AZP(I),XP(I),YP(I),ZP(I),V(I),I=1,NP)

        READ(1,*)NDEF

        V(NP+1)=V(NP)

        DO 9 I=1,NP

        XP(I)=XP(I)*60.*1.848218

9       YP(I)=YP(I)*60.*1.60168

        TOL=0.05

        PI=4.*ATAN(1.)/180

        SUMNUM=0.0

        SUMDEN=0.0

        DO 2 I=1,NSO

        IF((Z10(I).GT.40).AND.(Z10(I).LT.70)) V(1)=6.4

        IF((Z10(I).GT.70).AND.(Z10(I).LT.110)) V(1)=8.05

        IF((Z10(I).GT.110).AND.(Z10(I).LT.160)) V(1)=8.5

        IF((Z10(I).GT.160).AND.(Z10(I).LT.185)) V(1)=8.3

        IF((Z10(I).GT.185).AND.(Z10(I).LT.230)) V(1)=9.11

        IF(Z10(I).GT.230) V(1)=9.11

        DIPR=DIPR0(I)

        DO 3 J=1,NST

        DELX(I,J)=STX(J)-X10(I)

        DELY(I,J)=STY(J)-Y10(I)

        WRITE(*,*)'ACTUAL DELX = ',DELX(I,J)

        WRITE(*,*)'ACTUAL DELY = ',DELY(I,J)

        DELTA=SQRT(DELX(I,J)**2+DELY(I,J)**2)

        THETA=ATAN2(DELY(I,J),DELX(I,J))/PI

        DIPR=DIPR0(I)

10      CALL RAYTIME (DIPR,DELX(I,J),DELY(I,J),TCAL(I,J),NP,DIPR0(I),
```

```
    1   AZR(I),X10(I),Y10(I),Z10(I),PI,DIPR2)

        WRITE(3,*)'TOBS= ',TOBS(I,J),'CALCULATED TIME= ',TCAL(I,J)

        WRITE(2,*)'TOBS= ',TOBS(I,J),'CALCULATED TIME= ',TCAL(I,J)

        DIFF1=TOBS(I,J)-TCAL(I,J)

        IF(ABS(DIFF1).LT.TOL) GO TO 20

        SUMDV=0.0

        DO 70 II=1,NP

   70   SUMDV=SUMDV+D(II)/V(II)

        ANUM=(TOBS(I,J)-SUMDV)

        DO 80 II=1,NP

        DEN=ANUM*2./V(II)-D(II)/(V(II)**2)

   80   H(II)=ANUM/DEN

        WRITE(3,*)'V(',NDEF,')= ',V(NDEF),'CORRECTION = ',H(NDEF)

        V(NDEF)=V(NDEF)+H(NDEF)

   C    WRITE(*,*)'H(',NDEF,')=',H(NDEF)

        GO TO 10

   20   SUMNUM=SUMNUM+D(NDEF)*D(NDEF)

        SUMDV=0.0

        DO 30 K=1,NP

        IF(K.EQ.NDEF)GOTO 30

        SUMDV=SUMDV+D(K)/V(K)

   30   CONTINUE

        SUMDEN=SUMDEN+D(NDEF)*(TOBS(I,J)-SUMDV)

        WRITE(3,*)'V(1)=',V(1),'V(2)=',V(2),'V(3)=',V(3),'V(4)=',V(4)

        WRITE(3,*)'DIPR=',DIPR,'AZR= ',AZR(I)

        WRITE(3,*)'CALCULATED TIME= T(',I,',',J,')=',TCAL(I,J)

        WRITE(3,*)'D(1)=',D(1),'D(2)=',D(2),'D(3)=',D(3),'D(4)=',D(4)
```

```
3      CONTINUE

2      CONTINUE

       AVERAGEV=SUMNUM/SUMDEN

       WRITE(2,*)'AVERAGE V(',NDEF,')=',AVERAGEV

       WRITE(3,*)'AVERAGE V(',NDEF,')=',AVERAGEV

       WRITE(*,*)'AVERAGE V(',NDEF,')=',AVERAGEV

       STOP

       END
```

--------------------------------SUBROUTINE RAYTIME-------——————————————————————

```
       THIS ROUTINE OPTIMIZES  THE DISTANCE TRAVELLED BY THE

       RAY DURING THE TOTAL PATH OF TRAVEL AND THE TIME TAKEN

       FOR TOTAL PATH

       SUBROUTINE RAYTIME (DIPR,DELX,DELY,STIME,NP,DIPR0,AZR,

1      X10,Y10,Z10,PI,DIPR2)
```

------------------------------------—————————————————————————————

```
       COMMON/BLOCK1/ DIPP(100),AZP(100),XP(100),YP(100),ZP(100),V(100)

1      ,T(100),D(100)

       TOL=0.025 899

       CALL RAYDEL(DIPR,DELX0,DELY0,DEL1,STIME,NP,DIPR0,AZR,

1      X10,Y10,Z10,PI,DIPR2)

       IF((ABS(DELX0-DELX).LT.TOL).AND.(ABS(DELY0-DELY).LT.TOL))THEN

       GOTO 999

       ENDIF

       IF(DEL1.EQ.0)THEN

       WRITE(*,*)'REFLECTION'

       DIPR=DIPR- 1

       GO TO 899
```

```
      ENDIF

      DIPR=DIPR+1

      CALL RAYDEL(DIPR,DELX1,DELY1,DEL1,STIME,NP,DIPR0,AZR,

   1  X10,Y10,Z10,PI,DIPR2)

      B1=(DELX1-DELX0)/1

      B2=(DELY1-DELY0)/1

      AZR=AZR+1

      DIPR=DIPR-1

      CALL RAYDEL(DIPR,DELX2,DELY2,DEL1,STIME,NP,DIPR0,AZR,

   1  X10,Y10,Z10,PI,DIPR2)

      C1=(DELX2-DELX0)/1

      C2=(DELY2-DELY0)/1

      A1=-DELX0+DELX

      A2=-DELY0+DELY

      DELI=(A1*C2-A2*C1)/(C2*B1-C1*B2)

      DELFI=(A1*B2-A2*B1)/(B2*C1-B1*C2)

      WRITE(*,*)'>> CORRECTION IN DIP=',DELI

      WRITE(*,*)'>> CORRECTION IN AZIMUTH=',DELFI

      DIPR=DIPR+DELI

      AZR=AZR+DELFI-1

      IF((DIPR.GT.180).OR.(DIPR.LT.90))THEN

      WRITE(*,*)'DIP > 180 OR DIP < 90 '

      WRITE(*,*)' PLEASE CHANGE INITIAL DIP IN THE DATA'

      STOP

      ELSE

      GOTO 899

      ENDIF
```

```
        CALL RAYDEL(DIPR,DELX3,DELY3,DEL1,STIME,NP,DIPR0,AZR,
    1  X10,Y10,Z10,PI,DIPR2)
999    WRITE(*,*)'DISTENCE CONVERGED'
       WRITE(*,*)'TIME TAKEN BY THE RAY=',STIME
102    FORMAT(2X,'DELTA =',E12.6,3X,'  TOTAL TIME. =',E10.5)
       RETURN
       END
```

-----------------------------------SUBROUTINE RAYDEL-----------------------------------

```
       THIS ROUTINE CALCULATES THE DISTENCE TRAVELLED BY THE RAY
       DURING ITS TOTAL PATH OF TRAVEL AND THE CORRESPONDING TIME
       SUBROUTINE RAYDEL(DIPR1,DELX,DELY,DELTA,STIME,NP,DIPR0,AZR1,
```

```
    1  X10,Y10,Z10,PI,DIPRR2)
       COMMON/BLOCK1/ DIPP(100),AZP(100),XP(100),YP(100),ZP(100),V(100)
    1  ,T(100),D(100)
       STIME=0.0
       DELX=0.0
       DELY=0.0
       X0=X10
       Y0=Y10
       Z0=Z10
       DIPR2=DIPR1
       WRITE(*,*)'INITIAL DIP AND AZIMUTH'
       WRITE(*,*)'DIP= ',DIPR1,'AZR= ',AZR1
       DIPR=DIPR1
       AZR=AZR1
       K=1
```

```
        IF(DIPP(2).EQ.90) K=2

        IF(K.EQ.1)THEN

        CALL STRIKE(X0,Y0,Z0,DIPR,AZR,XP(1),YP(1),ZP(1),DIPP(1),AZP(1),
1   V(1),V(2),PI,X1,Y1,Z1,DIPR2,AZR2,D(1),T(1),1)

        IF(Z1.LT.ZP(NP))THEN

        CALL SHIFT(NP,1)

        ENDIF

        ENDIF

        IF(K.EQ.2)THEN

        CALL STRIKE(X0,Y0,Z0,DIPR,AZR,XP(2),YP(2),ZP(2),DIPP(2),AZP(2),
1   V(2),V(3),PI,X1,Y1,Z1,DIPR2,AZR2,D(2),T(2),2)

        IF(Z1.GT.ZP(1)) CALL SHIFT(1,NP)

        ENDIF

        DO 10 I=1,NP

        CALL STRIKE (X0,Y0,Z0,DIPR,AZR,XP(I),YP(I),ZP(I),DIPP(I),AZP(I),
1   V(I),V(I+1),PI,X1,Y1,Z1,DIPR2,AZR2,D(I),T(I),I)

        STIME=STIME+T(I)

        DELX=DELX+(X1-X0)

        DELY=DELY+(Y1-Y0)

        WRITE(*,*)'DELX(',I,')=',DELX,'DELY(',I,')=',DELY

        IF(Z1.LE.0) GO TO 20

        X0=X1

        Y0=Y1

        Z0=Z1

        DIPR=DIPR2

        AZR=AZR2

        IF((XP(I).EQ.0.0).AND.(ZP(I).EQ.0.0))GOTO 20
```

```
10      CONTINUE

20      DELTA=SQRT(DELX**2+DELY**2)

        WRITE(*,*)'DELX=',DELX,'DELY=',DELY

30      RETURN

        END
```

--------------------------------------SUBROUTINE STRIKE--------------------------------------

```
        THIS ROUTINE CALCULATES THE CALCULATES THE CO-ORDINATES OF THE

        STRIKING POINT AND THE DIP AND AZIMUTH OF THE REFRECTING RAY

        SUBROUTINE STRIKE (X0,Y0,Z0,DIPR,AZR,XP,YP,ZP,DIPP,AZP,
```

```
     1  V1,V2,PI,X1,Y1,Z1,DIPR2,AZR2,D,T,I)

        PR1=SIN(DIPR*PI)*COS(AZR*PI)

        PR2=SIN(DIPR*PI)*SIN(AZR*PI)

        PR3=COS(DIPR*PI)

        DIPN=(180+DIPP)

        AZN=(180+AZP)

        PN1=SIN(DIPN*PI)*COS(AZN*PI)

        PN2=SIN(DIPN*PI)*SIN(AZN*PI)

        PN3=COS(DIPN*PI)

        SNUM=(XP-X0)*PN1+(YP-Y0)*PN2+(ZP-Z0)*PN3

        SDEN=PR1*PN1+PR2*PN2+PR3*PN3

        S=SNUM/SDEN

C       POINT OF INCIDENCE ON THE PLANE

        X1=X0+S*PR1

        Y1=Y0+S*PR2

        Z1=Z0+S*PR3

        WRITE(*,*)'X1,Y1,Z1=',X1,Y1,Z1
```

```
D=SQRT((X0-X1)**2+(Y0-Y1)**2+(Z0-Z1)**2)

T=D/V1

VT=((V2**2)-(V1**2))/(V2**2)

PN=SDEN PNV=(PN**2-VT)

IF (PNV.LT.0) THEN

DELTA=0.0

WRITE(*,*)'R E F L E C T I O N'

ENDIF

PNV=SQRT(PNV)

PNNV=(PN-PNV)

VV=V2/V1 PR21=VV*(PR1-(PNNV*PN1))

PR22=VV*(PR2-(PNNV*PN2))

PR23=VV*(PR3-(PNNV*PN3))

DIPR2=(ACOS(PR23))/PI

A=SIN(DIPR2*PI)

AZR2=(ACOS(PR21/A))/PI

AZR2=ATAN2(PR22,PR21)/PI

IF(AZR2.LT.0)AZR2=360+AZR2

WRITE(*,*)'DIP AND AZIMUTH AFTER STRIKING PLANE NO.',I

WRITE(*,*)DIPR2,AZR2

RETURN

END
```

---SUBROUTINE SHIFT---

THIS ROUTINE SHIFTS THE PLANES ACCORDING TO THE PATH OF THE TRAVELLING RAY

```
SUBROUTINE SHIFT(M,N)
```

```
        COMMON/BLOCK1/ DIPP(100),AZP(100),XP(100),YP(100),ZP(100),V(100)
1      ,T(100),D(100)
        DIMENSION XXP(100),YYP(100),ZZP(100),AAZP(100),ADIPP(100),AV(100)
        NP=MAX0(M,N)
        DO 10 I=1,NP
        XXP(I)=XP(I)
        YYP(I)=YP(I)
        ZZP(I)=ZP(I)
        AAZP(I)=AZP(I)
        ADIPP(I)=DIPP(I) 10
        AV(I)=V(I)
        XP(N)=XXP(M)
        YP(N)=YYP(M)
        ZP(N)=ZZP(M)
        AZP(N)=AAZP(M)
        DIPP(N)=ADIPP(M)
        V(N)=AV(M)
        IF((M.EQ.1).AND.(N.EQ.NP)) GO TO 40
        DO 20 I=1,NP-1
        XP(I+1)=XXP(I)
        YP(I+1)=YYP(I)
        ZP(I+1)=ZZP(I)
        AZP(I+1)=AAZP(I)
        DIPP(I+1)=ADIPP(I)
20      V(I+1)=AV(I)
        TEMP=V(2)
        V(2)=V(1)
```

```
         V(1)=TEMP

         GO TO 50

40       DO 30 I=1,NP-1

         XP(I)=XXP(I+1)

         YP(I)=YYP(I+1)

         ZP(I)=ZZP(I+1)

         AZP(I)=AAZP(I+1)

         DIPP(I)=ADIPP(I+1)

30       V(I)=AV(I+1)

         TEMP=V(NP)

         V(NP)=V(1)

         V(1)=TEMP

50       RETURN

         END
```